Supplementary Information

Rapid, Solvent-Minimized and Sustainable Access to Various Types of Ferroelectric-Fluid Molecules by Harnessing Mechano-Chemical Technology

Hiroya Nishikawa*, Motonobu Kuwayama, Atsuko Nihonyanagi, Barun Dhara and Fumito Araoka*

*To whom correspondence should be addressed.

E-mail: hiroya.nishikawa@riken.jp (H.N.) and fumito.araoka@riken.jp (F.A.)

Table of contents

Methods

1. General and materials

Materials: All reagents and solvents were purchased from Kanto Chemical Co., Inc., Tokyo Chemical Industry Co., Ltd., FUJIFILM Wako Pure Chemical Corporation, Sigma-Aldrich Co., LLC. and Combi-Blocks Inc. and used without further purification.

Mechanochemical (MC) reaction: All MC reactions were performed using a grinding jar used as a reaction jar, equipped with a Retsch MM400 milling machine. To avoid metal contamination, zirconia-type jars (15 mL and 30 mL, Smartsnap, FORMTECH) and one zirconia ball (12 mm, ~6 g) were used instead of a widely-used stainless steel-type (SUS) jar and a SUS ball. PTFE O-ring and PTFE sealing spacer were used for sealing the 15-mL and 30-mL jars, respectively. For the MC reaction under heating conditions, a heat gun with a temperature control (1450B, Takagi Co.) was used (Fig. S1a). To transfer solvent into the reaction jar, we employed an electronic micro-pipet (eVol, SGE Analytcical Science). A calibration curve regarding the preset temperature (T_{pre}) of the heat gun and the internal temperature (T_{int}) of the jar was obtained by monitoring T_{int} of the jar using a thermal imaging camera (F30w, Nippon Avionics). Analytical thin layer chromatography (TLC) was performed on silica gel layer glass plate (60 F254, Merck) and visualized by UV irradiation (254 nm). Column chromatography was performed on a Biotage Isolera™ Prime flash system (Biotage) using SNAP Ultra (particle size 25 μm; HP-spherical silica, Biotage) and FlashPure EcoFlex (Alumina Neutral, particle size 50–75 μm, BUCHI) column cartridges.

Nuclear magnetic resonance (NMR) spectroscopy: ^{1}H, ^{13}C, and ^{19}F NMR spectra were recorded on JNM-ECZ500 (JEOL) operating at 500 MHz, 126 MHz, and 471 MHz for ^{1}H [$^{1}H\{^{19}F\}$], $^{13}C\{^{1}H\}$ [$^{13}C\{^{1}H,^{19}F\}$] and ^{19}F [$^{19}F\{^{1}H\}$] NMR, respectively, using the TMS (trimethylsilane) as an internal standard for ^{1}H NMR and the deuterated solvent for ^{13}C NMR. The absolute values of the coupling constants are given in Hz, regardless of their signs. Signal multiplicities were abbreviated by s (singlet), d (doublet), t (triplet), q (quartet), quint (quintet), sext (sextet), and dd (double–doublet), respectively.

High-resolution mass (HRMS) spectroscopy: The quadrupole time-of-flight high-resolution mass spectrometry (QTOF-HRMS) was performed on COMPACT (BRUKER). The calibration was carried out using LC/MS tuning mix, for APCI/APPI (Agilent Technologies).

Density Functional Theory (DFT) Calculation: Calculations were performed using the Chem3D (pro, 22.2.0.3300) and Gaussian 16 (G16, C.01) softwares (installed at the RIKEN Hokusai GreatWave Supercomputing facility) for MM2 and DFT calculations, respectively. GaussView 6 (6.0.16) software was used to visually analyze the calculation results. Positions of hydrogens of molecules were optimized using the B3LYP/6-31G++ level Gaussian 16 program package. [S1] Dipole moments of molecules were calculated using b3lyp/6-311+g(d,p) and B3LYP-gd3bj which were added for empirical dispersion corrections to the standard B3LYP. The calculation method is as follows: opt=tight b3lyp/6-311+g(d,p) geom=connectivity empiricaldispersion=gd3bj int=ultrafine.

Polarized optical microscopy: Polarized optical microscopy was performed on a polarizing microscope (Eclipse LV100 POL, Nikon) with a hot stage (HSC402, INSTEC) on the rotation stage. Unless otherwise noted, the sample temperature was controlled using the INSTEC temperature controller and a liquid nitrogen cooling system pump (mk2000 and LN2-P/LN2-D2, INSTEC). We used homeotropic polyimide (PI) cells (rectangular electrode, cell gap: 9 μm, LCC), silanized cells (rectangular electrode, cell gap: 12.7 μm, homemade), and homogeneous non-rubbed PI cells (comb-type electrode, thickness: 17 and 4.8 μm, homemade).

Differential scanning calorimetry (DSC). Differential scanning calorimetry was performed on a calorimeter (DSC30, Mettler-Toledo). Rate, 5 K min^{-1}. Cooling/heating profiles were recorded and analyzed using the Mettler-Toledo STARe software system.

Dielectric spectroscopy. Dielectric relaxation spectroscopy was performed ranging between 1 Hz and 1 MHz using an impedance/gain-phase analyzer (SI 1260, Solartron Metrology) and a dielectric interface (SI 1296, Solartron Metrology). Prior to starting the measurement of the LC sample, the capacitance of the empty cell was determined as a reference. We used a homemade Au-coated cell [chloronium (Cr) bottom layer: 5 nm, Au top layer: 50 nm] without any alignment layers (13.0 μm) and a homemade silanized cell (thickness: 12.7 μm).

***PE* hysteresis measurement.** *PE* hysteresis measurements were performed in the temperature range of the N_F phase under a triangular-wave electric field (10 kV cm^{-1}, 200 Hz) using a ferroelectricity evaluation system (FCE 10, TOYO Corporation), which is composed of an arbitrary waveform generator (2411B), an IV/QV amplifier (model 6252) and a simultaneous A/D USB device (DT9832). We used a homemade Au-coated IPS cell

(thickness: 10 μm, electrode distance: 1 mm) with parallel rubbing conditions and a Cr-coated IPS cell (thickness: 17 μm, electrode distance: 500 μm).

SHG measurement. The SHG investigation was carried out using a Q-switched DPSS Nd: YAG laser (FQS-400-1-Y-1064, Elforlight) at λ = 1064 nm with a 5 ns pulse width (pulse energy: 400 μJ). The primary beam was incident on the LC cell followed by the detection of the SHG signal. The electric field was applied normally to the LC cell. We used a homemade Au-coated IPS cell (thickness: 10 μm, electrode distance: 1 mm) with parallel rubbing conditions. The experimental details are mentioned in Supplementary Note 1.

Wide-angle X-ray scattering (WAXD) analysis. Two-dimensional WAXD measurement was carried out using the NANOPIX system (Rigaku). The samples held in a glass capillary (1.5 mm in diameter) were measured under a magnetic field at a constant temperature using a temperature controller and a hot stage with temperature-resistant magnets (~0.5 T). The scattering vector q ($q = 4\pi\sin\theta\,\lambda^{-1}$; 2θ and λ = scattering angle and wavelength of an incident X-ray beam (1.54 Å) and position of an incident X-ray beam on the detector were calibrated using several orders of layer diffractions from silver behenate (d = 58.380 Å). The sample-to-detector distances were 71 mm, where acquired scattering 2D images were integrated along the Debye–Scherrer ring by using software (Igor Pro with Nika-plugin), affording the corresponding one-dimensional profiles.

Information of liquid crystalline (LC) cells:

IPS cells (homemade):

- Au-coated type (Cr bottom layer: 5 nm; Au top layer: 50 nm), electrode distance: 1 mm, electrode length: 13 mm, electrode width, 2 mm
- Alignment layer: AL1254
- Rubbing condition: parallel (rubbing depth: 100 μm, rubbing times: 10)
- Experiments: *P-E* hysteresis (thickness: 10 μm) and SHG (thickness: 5 μm) studies

Comb-type electrical cells (homemade):

- Cr-coated type, electrode distance: 500 μm, electrode length: 4 mm, electrode width, 500 μm
- Alignment layer: AL1254
- Rubbing condition: parallel (rubbing depth: 100 μm, rubbing times: 10)
- Experiments: *P-E* hysteresis

Non-alignment layer cells (homemade):

- Au-coated type (Cr bottom layer: 5 nm; Au top layer: 50 nm), electrode area: 5 × 5 mm
- Experiments: capacitance measurement

Silanized cells (homemade):

- ITO-coated type, electrode area: 5 × 10 mm
- Alignment layer: octadecyltrimethoxysilane (TCI), vapor adsorption at 120 °C (2 hrs)
- Experiments: POM (thickness: 12.7 μm) and DR (thickness: 12.7 μm) studies

Homeotropic-alignment PI layer cells (LCC):

- Alignment layer: NA
- Experiments: POM (thickness: 9.0 μm) studies

2. Synthesis and Characterization.

2.1. General setup and calibration curve for MC reaction.

In our experiment, we used an experimental system, which is similar to the setup reported by Ito et al. (Fig. S1a) [S2]. A pair of reaction jars were attached to the milling machine and hot air is blown down from the cramped heat guns (HG-1450, Takagi Co.) close to the top surface of the vibrating jars. The distance between the air nozzle and jar was set to be 10 mm. The internal temperature (T_{int}) was determined by a thermographic observation using a thermographic camera (F30w, Noppon Avionics). Since T_{int} and preset temperature (T_{pre}) of the heat gun were different, we prepared the calibration curve on T_{int} vs T_{pre} for every reaction jar (Fig. S1b). For example, for a 15-mL jar, when T_{pre} was set to 110 °C, T_{int} was given 80 °C. Fig. S1c and d show the time to reach the thermal equilibrium state. For both jars, the thermal equilibrium was achieved after about 10 min. Thus, note that in certain MC reactions where the reaction is complete within 10 minutes, we observe a chemical reaction with sequential internal temperature increases.

2.1.1. General protocol of MC-etherification.

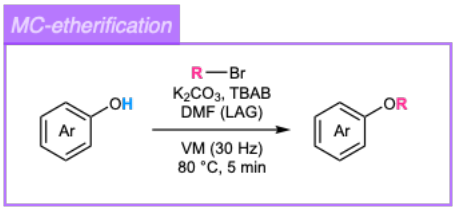

Aryl alcohol (6.59 mmol), alkyl bromide (9.88 mmol, 1.5 equiv), K_2CO_3 (13.2 mmol, 2.0 equiv), and TBAB (0.5 mmol, 5 mol %) were loaded in a reaction jar (30 mL) with one grinding ball. Then DMF (η ~ 0.2 mL/g, η_{tot} ~ 0.6–0.9 mL/g) was added via a micropipette. After closing the jars without purging, be equipped with MM400 (5 min, f = 30 Hz) and with a heat gun (T_{pre} = 110 °C, T_{int} = 80 °C). After 5 min, the jar was immediately transferred to the crushed ice and then opened. The reaction mixture was filtered off with DCM to remove inorganic salt and evaporated. The crude was purified by flash column chromatography (SiO_2, DCM/hexane, 0–100/0) to afford the target ether (Yield ~95%).

2.1.2. General protocol of MC-hydrolysis.

Methyl ester (5.8 mmol) and NaOH (granule, 11.6 mmol, 2.0 equiv) were loaded in a grinding jar (30 mL) with one grinding ball. Then DI water (522 μL) and DIOX (η ~ 10 mL/g) were added via a micropipette. After closing the jar without purging with inert gas, be equipped with MM400 (30 min, f = 30 Hz) and with a heat gun (T_{pre} = 140 °C, T_{int} = 100 °C). After 30 min, the jar was immediately transferred to the crushed ice and then opened. The reaction mixture was transferred to a flask, diluted with DI water, and then acidified with 1 M HCl to precipitate the crude. The precipitate was dissolved into Et_2O, dried off $MgSO_4$, evaporated, and dried in vacuo to afford the target carboxylic acid (Yield ~90%).

2.1.3. General protocol of MC-esterification. [S3]

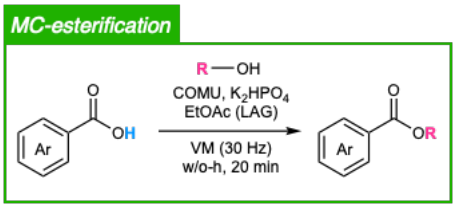

Carboxylic acid (3.17 mmol), alcohol (3.80 mmol, 1.2 equiv), COMU (3.49 mmol, 1.1 equiv), and K_2HPO_4 (9.51 mmol, 3.0 equiv) were loaded in a grinding jar (30 mL) with one grinding ball. Then EtOAc (η ~ 0.19 mL/g) was added via a micropipette. After closing the jar without purging with inert gas, be equipped with MM400 (20 min, f = 30 Hz). After 20 min, the reaction mixture was filtered off with DCM to remove inorganic salt. The resulting solution was washed with DI water thoroughly, dried off $MgSO_4$, evaporated, and purified by flash

column chromatography (SiO_2, EtOAc/DCM, 0–10/90) to afford the target ester (Yield ~82%). *Note: in the workup process, not enough washing with DI water causes an ester exchange reaction between the product and COMU during separation by chromatography.*

2.1.4. General protocol of MC-oxidation.

Aldehyde (1.23 mmol) and Oxone (2.45 mmol, 2.0 equiv) were loaded in a grinding jar (15 mL) with one grinding ball. Then DMF (η ~ 1.0 mL/g) was added via a micropipette. After closing the jar without purging with inert gas, be equipped with MM400 (30 min, f = 30 Hz). After 30 min, the mixing was stopped to suppress the heat of the reaction for 10 min. After additional mixing for 30 min, the jar was opened. The resulting slurry was transferred to the flask and DI water was added to afford precipitation. The precipitate was dissolved into Et_2O, dried off $MgSO_4$, evaporated, and dried in vacuo to afford the target carboxylic acid (Yield ~80–90%).

2.1.5. General protocol of MC-acetalization

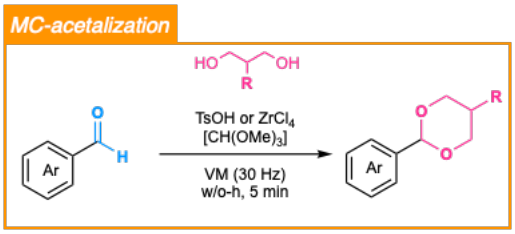

Aldehyde (14.1 mmol), diol (23.9 mmol, 1.7 equiv), PTSA (12.7 mmol, 0.9 equiv), or $ZrCl_4$ (0.9 equiv) were loaded in a grinding jar (30 mL) with one grinding ball. After closing the jar without purging with inert gas, be equipped with MM400 (5 min, f = 30 Hz). After 5 min, the reaction mixture was filtered off with DCM to remove inorganic salt and evaporated. The resulting crude was washed with *cold* DI water, and extracted with DCM. The collected organic layer was dried off $MgSO_4$, evaporated, and purified by flash column chromatography (SiO_2, DCM) to afford the target 1,3-dioxane (Yield ~95%). *Note: 1) Transfer and washing of the reaction mixture using not-cold DI water cause an opening cyclic aldehyde (backreaction) due to local thermal heating. 2) For gram-scale synthesis of methyl 4-(1,3-dioxan-2-yl)benzoate (**23**),we employed $CH(OMe)_3$ (η ~ 0.1 mL/g) for the effective reaction.*

2.1.6. General protocol of MC-SMC

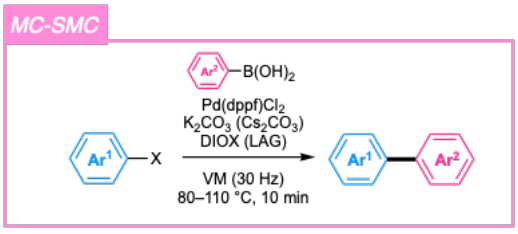

Aryl bromide (0.46 mmol), aryl boronic acid (0.50 mmol, 1.5 equiv) [or aryl dioxaborolane (0.50 mmol, 1.1 equiv)], $Pd(dppf)_2Cl_2$ (0.049 mmol, 3 mol%), K_2CO_3 (1.40 mmol, 3.0 equiv) [or Cs_2CO_3], [and BHT (0.046 mmol, 10 mol%)] were loaded in a grinding jar (15 mL) with one grinding ball. Then DIOX ($\eta \sim 0.3$ mL/g) and DI water (27 μL, 1.50 mmol, 3.0 equiv) were added via a micropipette. After closing the jar without purging with inert gas, be equipped with MM400 (15 min, $f = 30$ Hz) and with a heat gun (T_{pre} = 110–140 °C, T_{int} = 80–110 °C). After 15 min, the jar was immediately transferred to the crushed ice and then opened. The reaction mixture was filtered off with DCM to remove inorganic salt and catalyst and then was evaporated. The resulting crude was purified by flash column chromatography (SiO_2, DCM/hexane, 50/50–100/0) to afford the target compound. *Note: see detailed protocols below.*

2.1.6.1 example #1: Synthesis of 4'-pentyl-[1,1'-biphenyl]-4-carbonitrile (5CB).

4-bromobenzonitrile (2.00 g, 11.0 mmol), (4-pentylphenyl)boronic acid (3.17 g, 16.5 mmol, 1.5 equiv), $Pd(dppf)_2Cl_2$ (269.2 mg, 0.330 mmol, 3 mol%), and K_2CO_3 (4.56 g, 33.0 mmol, 3.0 equiv) were loaded in a grinding jar (30 mL) with one grinding ball. Then DIOX ($\eta \sim 0.3$ mL/g, 2.99 mL) and DI water (0.89 mL, 33.0 mmol, 3.0 equiv) were added via a micropipette. Same dosage of chemicals was added into the other jar. After closing the jars without purging with inert gas, be equipped with MM400 (5 min, $f = 30$ Hz) and with a heat gun (T_{pre} = 140 °C, T_{int} = 110 °C). After 5 min, the jars were immediately transferred to the crushed ice and then opened. The reaction mixtures were combined, filtered off with DCM to remove inorganic salt and catalyst, and then was evaporated. The resulting crude was purified by flash column chromatography (SiO_2, DCM/hexane, 50/50–100/0) to afford the target compound (5CB) (5.20 g, yield ~95%).

2.1.6.2 example #2: Synthesis of 3',4',5'-trifluoro-2-nitro-[1,1'-biphenyl]-4-ol (9b)

4-Bromo-3-nitrophenol (500 mg, 2.29 mmol), 4,4,5,5-tetramethyl-2-(3,4,5-trifluorophenyl)-1,3,2-dioxaborolane (651 mg, 2.52 mmol, 1.1 equiv), $Pd(dppf)_2Cl_2$ (50.3 mmol, 3 mol%), K_2CO_3 (951 mg, 6.90 mmol, 3.0 equiv), and BHT (50.5 mg, 0.229 mmol, 10 mol%) were loaded in a grinding jar (30 mL) with one grinding ball. Then DIOX ($\eta \sim 0.5$ mL/g, 1.1 mL) and DI water (136 μL, 7.6 mmol, 3.0 equiv) were added via a micropipette. After closing the jar without purging with inert gas, be equipped with MM400 (15 min, $f = 30$ Hz) and with a heat gun (T_{pre} = 140 °C, T_{int} = 110 °C). After 15 min, the jar was immediately transferred to the crushed ice and then opened. The reaction mixture was filtered off with DCM to remove inorganic salt and catalyst and then was evaporated. The resulting crude was purified by flash column chromatography (SiO_2, DCM/hexane, 50/50–100/0) to afford the target compound

(Yield ~70%). The resulting crystal was recrystallized from DCM to yield a yellow needle crystal.

2.1.6.3 example #3: Synthesis of 4-ethyl-2,3',5',6-tetrafluoro-1,1'-biphenyl (12a)

5-Ethyl-1,3-difluoro-2-iodobenzene (3.00 g, 11.2 mmol), (3,5-difluorophenyl)boronic acid (2.12 g, 13.4 mmol, 1.2 equiv), $Pd(dppf)_2Cl_2$ (50.3 mg, 0.069 mmol, 3 mol%), and Cs_2CO_3 (10.9 g, 33.6 mmol) were loaded in a grinding jar (30 mL) with one grinding ball. Then DIOX (η ~ 0.5 mL/g) was added via a micropipette. After closing the jar without purging with inert gas, be equipped with MM400 (15 min, f = 30 Hz) and with a heat gun (T_{pre} = 150 °C, T_{int} = 110 °C). After 15 min, the jar was immediately transferred to the crushed ice and then opened. The reaction mixture was filtered off with DCM to remove inorganic salt and catalyst and then was evaporated. The resulting crude was purified by flash column chromatography (SiO_2, hexane) to afford the target compound (**12a**) (Yield ~90%). Note: *the addition of DI water accelerates reaction time from 15 min to 10 min, but the yield tends to reduce to ~80–85%.*

2.1.7. General protocol of MC-MIC

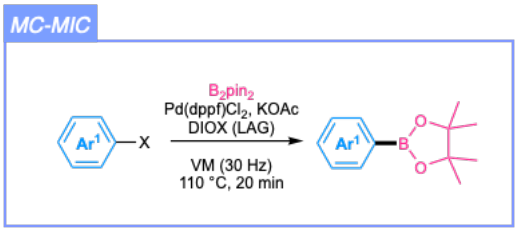

Aryl bromide (8.26 mmol), B_2pin_2 (9.91 mmol, 1.2 equiv), KOAc (24.8 mmol, 3.0 equiv), and $Pd(dppf)_2Cl_2$ (0.248 mmol, 3 mol%) were loaded in a grinding jar (30 mL) with one grinding ball. Then DIOX (η ~ 0.3 mL/g) was added via a micropipette. After closing the jar without purging with inert gas, be equipped with MM400 (20 min, f = 30 Hz) and with a heat gun (T_{pre} = 110 °C, T_{int} = 80 °C). After 20 min, the jar was immediately transferred to the crushed ice and then opened. The reaction mixture was filtered off with DCM to remove inorganic salt and catalyst and evaporated. The resulting crude was purified by flash column chromatography (SiO_2, DCM/hexane, 0–50/50) to afford the target compound (Yield ~88%).

2.8. General protocol of MC-SHC

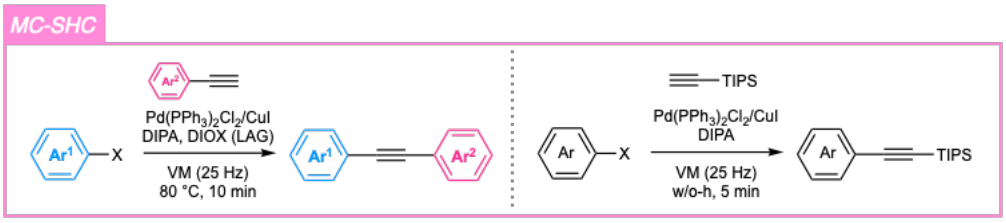

2.1.8.1 example #1: Synthesis of ((4-bromo-3,5-difluorophenyl)ethynyl)triisopropylsilane (18)

2-Bromo-1,3-difluoro-5-iodobenzene (1.50 g, 4.70 mmol), ethynyltriisopropylsilane (1.26 mL, 5.64 mmol, 1.2 equiv), DIPA (0.98 mL, 7.10 mmol, 1.5 equiv), $Pd(dppf)_2Cl_2$ (99 mg, 0.141 mmol, 3 mol%), and CuI (9.0 mg, 0.047 mmol, 1 mol%) were loaded in a grinding jar (30 mL) with one grinding ball. After closing the jar without purging with inert gas, be equipped with MM400 (5 min, f = 25 Hz). After 5 min, the jar was opened and then the reaction mixture was filtered off with DCM to remove catalyst, and evaporated. The resulting crude was purified by flash column chromatography (SiO_2, DCM/hexane, 50/50–100/0) to afford the target compound (**18**) (Yield ~95%). Note: η_{tot} ~ 1.4 mL/g.

2.1.8.2 example #2: Synthesis of BIOTN1 (22a)

1-(3,5-Difluoro-4-iodophenyl)-4-methyl-2,6,7-trioxabicyclo[2.2.2]octane (**17a**) (300 mg, 0.81 mmol), 4'-ethynyl-2',3,5,6'-tetrafluoro-[1,1'-biphenyl]-4-carbonitrile (**21**) (224 mg, 0.81 mmol, 1.0 equiv), DIPA (0.17 mL, 1.2 mmol, 1.5 equiv), $Pd(dppf)_2Cl_2$ (17.2 mg, 0.024 mmol, 3 mol%), and CuI (1.6 mg, 0.008 mmol, 1 mol%) were loaded in a grinding jar (15 mL) with one grinding ball. Then DIOX (η ~ 0.5 mL/g) was added via a micropipette. After closing the jar without purging with inert gas, be equipped with MM400 (20 min, f = 25 Hz) and with a heat gun (T_{pre} = 110 °C, T_{int} = 80 °C). After 20 min, the jar was immediately transferred to the crushed ice and then opened. The reaction mixture was filtered off with DCM to remove catalyst and evaporated. The resulting crude was purified by flash column chromatography (Al_2O_3, neutral, DCM/hexane, 50/50–100/0) to afford the target compound (**22a**) (Yield ~80%). The resulting crystal was recrystallized from DCM/hexane to yield a white powder.

2.2 Protocol of SC reaction

2.2.1. General protocol of SC-carboxylation

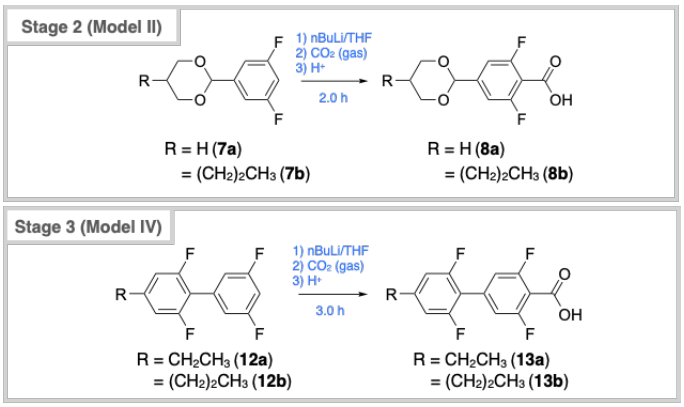

2.2.1.1 example #1: Synthesis of 2,6-difluoro-4-(5-propyl-1,3-dioxan-2-yl)benzoic acid (8b)

To **7b** (13.4 g, 55.4 mmol) in THF (200 mL) was added dropwise a solution of *n*-butyllithium (40.1 mL of 1.52 M in *n*-hexane, 61.0 mmol) at −78°C under Ar atmosphere. After stirring for 1 hour at the temperature, the balloon with CO_2 gas was equipped with the flask, and the reaction was stirred under CO_2 atmosphere for 1 hour at −78 °C. The reaction solution was quenched with 2N HCl *aq*., and extracted with EtOAc. The organic layer was dried over Na_2SO_4, evaporated, and purified by reprecipitation with *n*-hexane and a small amount of AcOEt. After filtration, the filter cake was dried in vacuo to give **8b** in 88% yield (13.9 g) as a white solid.

2.2.1.2 example #2: Synthesis of 2,6-difluoro-4-(5-propyl-1,3-dioxan-2-yl)benzoic acid (13a)

To **12a** (1.92 g, 7.55 mmol) in THF (20 mL) was added dropwise a solution of *n*-butyllithium (5.30 mL of 1.58 M in *n*-hexane, 8.31 mmol) at −78 °C under Ar atmosphere. After stirring for 1.5 hours at the temperature, the balloon with CO_2 gas was equipped with the flask, and the reaction was stirred under CO_2 atmosphere for 1.5 hours at −78 °C. The reaction solution was quenched with 1N HCl *aq*., and extracted with EtOAc. The organic layer was dried over Na_2SO_4 and dried in vacuo to give **13a** in 98.4% yield (2.22 g) as a white solid.

2.2.2. General protocol of SC-Iodization

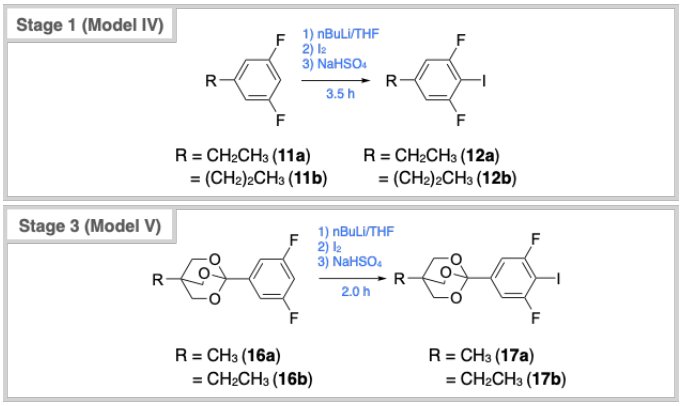

2.2.2.1 example #1: Synthesis of 5-ethyl-1,3-difluoro-2-iodobenzene (12a)

To **11a** (2.8 mL, 21.5 mmol) in THF (25 mL) was added dropwise a solution of *n*-butyllithium (14.9 mL of 1.59 M in *n*-hexane, 23.6 mmol) at −78 °C under Ar atmosphere. After stirring for 1 hour at the temperature, iodine (5.40 g, 21.5 mmol) was added at the temperature, and the reaction was stirred for 2 hours at −78 °C and then for 30 minutes at 0 °C. The reaction solution was quenched with saturated $NaHSO_3$ *aq*., and extracted with *n*-hexane. The organic extracts were purified by column chromatography on silica gel using *n*-hexane as eluent to give **12a** in 91 % yield (5.23 g) as a colorless oil.

2.2.2.2 example #2: Synthesis of 1-(3,5-difluoro-4-iodophenyl)-4-methyl-2,6,7-trioxabicyclo[2.2.2]octane (17a)

To **16a** (1.24 g, 5.12 mmol) in THF (10 mL) was added dropwise a solution of *n*-butyllithium (3.54 mL of 1.59 M in *n*-hexane, 5.63 mmol) at −78 °C under Ar atmosphere. After stirring for 1 hour at the temperature, iodine (1.30 g, 5.12 mmol) was added at the temperature, and the reaction was stirred for 1 hour at −78 °C. The reaction solution was quenched with ice water and extracted with DCM. The organic extracts were purified by neutral alumina column chromatography using DCM /*n*-hexane (gradient from 20 % to 50 % DCM) as an eluent followed by recrystallization from hexane to give **17a** in 66.1 % yield (1.25 g) as a white solid.

2.2.3. General protocol of SC-orthoesterification

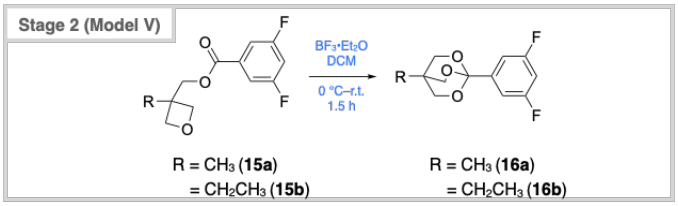

2.2.3.1 example #1: Synthesis of 1-(3,5-difluorophenyl)-4-methyl-2,6,7-trioxabicyclo[2.2.2]octane (16a)

To a solution of **15a** (1.62 g, 6.69 mmol) in DCM (10 mL) was added BF_3-OEt_2 (47% solution, 213 μL, 0.81 mmol) at room temperature, and the resulting solution was stirred for 1.5 hours.

The reaction mixture was quenched with Et_3N (233 μL, 1.67 mmol) and H_2O, and extracted with DCM. The organic extracts were purified by neutral alumina column chromatography using DCM as an eluent to give **16a** in 77 % yield (1.24 g) as a white powder.

2.2.3. General protocol of SC-deprotection

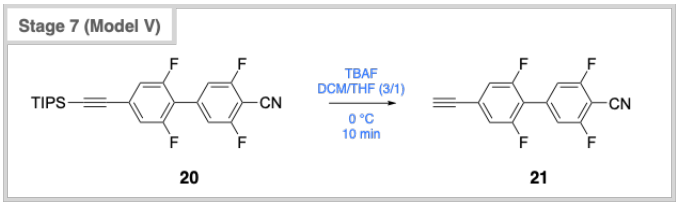

20 21

2.2.2.1 example #1: Synthesis of 4'-ethynyl-2',3,5,6'-tetrafluoro-[1,1'-biphenyl]-4-carbonitrile (21)

To a solution of **20** (1.03 g, 2.39 mmol) in DCM/THF (3/1 = 15/5 mL) was added a 1M solution of tetrabutylammonium fluoride in THF (2.86 mL, 2.86 mmol) at 0 °C. The resulting reaction solution was stirred for 10 minutes, quenched with H_2O at 0 °C, and extracted with DCM. The organic extracts were purified by column chromatography on silica gel using AcOEt/*n*-hexane (gradient from 1 % to 7 % AcOEt) as an eluent to give **21** in 91 % yield (597 mg) as a white solid.

2.3. Material database

RM series:

methyl 4-methoxy-2-propoxybenzoate (**1a**)

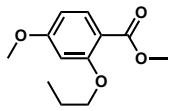

^{1}H-NMR (500 MHz, $CDCl_3$) δ 7.85 (d, J = 8.7 Hz, 1H), 6.48 (dd, J = 8.6, 2.3 Hz, 1H), 6.46 (d, J = 2.3 Hz, 1H), 3.97 (t, J = 6.4 Hz, 2H), 3.86 (s, 3H), 3.84 (s, 3H), 1.87 (td, J = 14.0, 7.0 Hz, 2H), 1.08 (t, J = 7.4 Hz, 3H).

^{13}C{^{1}H}-NMR (126 MHz, $CDCl_3$) δ 166.5, 164.2, 160.9, 133.9, 112.6, 104.6, 99.9, 70.4, 55.5, 51.7, 22.6, 10.6.

QTOF-HRMS (*m*/*z*, $[M+H]^+$) Calcd for $C_{12}H_{16}O_4$: 225.1127; found: 225.1129

methyl 2-(hexyloxy)-4-methoxybenzoate (**1b**)

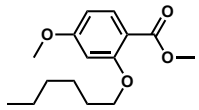

^{1}H-NMR (500 MHz, $CDCl_3$) δ 7.85 (d, J = 8.6 Hz, 1H), 6.49-6.46 (m, 2H), 4.00 (t, J = 6.6 Hz, 2H), 3.85 (s, 3H), 3.84 (s, 3H), 1.87-1.81 (m, 2H), 1.53-1.47 (m, 2H), 1.35 (td, J = 7.2, 3.7 Hz, 4H), 0.91 (t, J = 6.9 Hz, 3H)

^{13}C{^{1}H}-NMR (126 MHz, $CDCl_3$) δ 166.5, 164.2, 160.9, 133.9, 112.6, 104.6, 99.9, 69.0, 55.5, 51.7, 31.6, 29.1, 25.7, 22.7, 14.1

QTOF-HRMS (*m*/*z*, $[M+H]^+$) Calcd for $C_{15}H_{23}O_4$: 267.1596; found: 267.1612

4-methoxy-2-propoxybenzoic acid (**2a**)

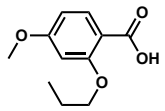

^{1}H-NMR (500 MHz, methonal-d4) δ 7.86 (d, J = 8.7 Hz, 1H), 6.62-6.59 (m, 2H), 4.10-3.98 (m, 2H), 3.89-3.71 (m, 3H), 1.87 (td, J = 14.1, 6.9 Hz, 2H), 1.07 (t, J = 7.4 Hz, 3H)

^{13}C{^{1}H}-NMR (126 MHz, methanol-d4) δ 169.1, 166.4, 161.9, 135.2, 112.7, 106.9, 100.5, 72.0, 56.1, 23.4, 10.8

QTOF-HRMS (*m*/*z*, $[M]^-$) Calcd for $C_{11}H_{13}O_4^{\bullet-}$: 209.0819; found: 209.0912

2-(hexyloxy)-4-methoxybenzoic acid (**2b**)

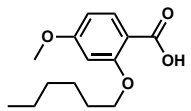

^{1}H-NMR (500 MHz, acetone-d6) δ 7.94 (d, J = 8.7 Hz, 1H), 6.74 (d, J = 2.3 Hz, 1H), 6.68 (dd, J = 8.7, 2.3 Hz, 1H), 4.29 (t, J = 6.5 Hz, 2H), 3.90 (s, 3H), 1.92-1.87 (m, 2H), 1.56-1.50 (m, 2H), 1.41-1.32 (m, 4H), 0.91 (t, J = 7.1 Hz, 3H)

^{13}C{^{1}H}-NMR (126 MHz, acetone-d6) δ 165.9, 165.8, 160.8, 135.2, 112.2, 107.5, 100.3, 70.6, 56.2, 32.2, 26.4, 23.3, 14.3, 0.1

QTOF-HRMS (*m*/*z*, [M+H]$^{+}$) Calcd for $C_{14}H_{21}O_4$: 253.1440; found: 253.1448

4-formylphenyl 4-methoxy-2-propoxybenzoate (**3a**)

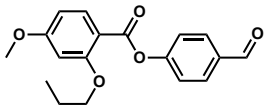

^{1}H-NMR (500 MHz, $CDCl_3$) δ 10.01 (s, 1H), 8.06 (d, J = 8.9 Hz, 1H), 7.95 (d, J = 8.3 Hz, 2H), 7.39 (d, J = 8.4 Hz, 2H), 6.56 (dd, J = 8.7, 2.1 Hz, 1H), 6.52 (d, J = 2.1 Hz, 1H), 4.02 (t, J = 6.4 Hz, 2H), 3.89 (s, 3H), 1.88 (m, 2H), 1.07 (t, J = 7.4 Hz, 3H)

^{13}C{^{1}H}-NMR (126 MHz, $CDCl_3$) δ 191.1, 165.3, 163.3, 162.0, 156.2, 134.7, 133.8, 131.3, 122.8, 110.8, 105.1, 99.8, 70.5, 55.7, 22.6, 10.7

QTOF-HRMS (*m*/*z*, [M+H]$^{+}$) Calcd for $C_{18}H_{19}O_5$: 315.1232; found: 315.1243

4-formylphenyl 2-(hexyloxy)-4-methoxybenzoate (**3b**)

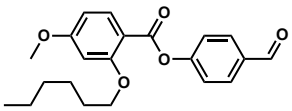

^{1}H-NMR (500 MHz, $CDCl_3$) δ 10.01 (s, 1H), 8.05 (d, J = 8.9 Hz, 1H), 7.95 (d, J = 8.3 Hz, 2H), 7.39 (d, J = 8.4 Hz, 2H), 6.57-6.55 (m, 1H), 6.52 (d, J = 2.1 Hz, 1H), 4.05 (d, J = 6.4 Hz, 2H), 3.89 (s, 3H), 1.87-1.81 (m, 2H), 1.52-1.46 (m, 2H), 1.33-1.25 (m, 4H), 0.85 (t, J = 6.9 Hz, 3H)

^{13}C{^{1}H}-NMR (126 MHz, $CDCl_3$) δ 191.2, 165.3, 163.3, 162.0, 156.2, 134.7, 133.8, 131.3, 122.8, 110.8, 105.0, 99.8, 69.0, 55.7, 31.6, 29.2, 25.7, 22.6, 14.1

QTOF-HRMS (*m*/*z*, [M+H]$^{+}$) Calcd for $C_{21}H_{25}O_5$: 357.1702; found: 357.1708

4-formylphenyl 2,4-dimethoxybenzoate (**3c**)

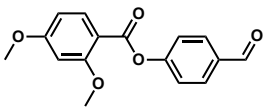

^{1}H-NMR (500 MHz, $CDCl_3$) δ 10.01 (s, 1H), 8.09 (d, J = 8.7 Hz, 1H), 7.95 (d, J = 8.4 Hz, 2H), 7.39 (d, J = 8.4 Hz, 2H), 6.58 (dd, J = 8.9, 2.3 Hz, 1H), 6.54 (d, J = 2.3 Hz, 1H), 3.94 (s, 3H), 3.91 (s, 3H)

^{13}C{^{1}H}-NMR (126 MHz, $CDCl_3$) δ 191.2, 165.4, 162.9, 162.6, 156.1, 134.7, 133.8, 131.2, 122.9, 110.5, 105.0, 99.1, 56.1, 55.7

QTOF-HRMS (*m*/*z*, $[M+H]^+$) Calcd for $C_{16}H_{15}O_5$: 287.0919; found: 287.0918

4-((4-methoxy-2-propoxybenzoyl)oxy)benzoic acid (**4a**)

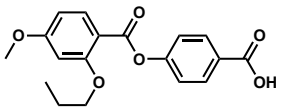

^{1}H-NMR (500 MHz, $CDCl_3$) δ 10.01 (s, 1H), 8.09 (d, J = 8.7 Hz, 1H), 7.95 (d, J = 8.4 Hz, 2H), 7.39 (d, J = 8.4 Hz, 2H), 6.58 (dd, J = 8.9, 2.3 Hz, 1H), 6.54 (d, J = 2.3 Hz, 1H), 3.94 (s, 3H), 3.91 (s, 3H)

^{13}C{^{1}H}-NMR (126 MHz, $CDCl_3$) δ 191.2, 165.4, 162.9, 162.6, 156.1, 134.7, 133.8, 131.2, 122.9, 110.5, 105.0, 99.1, 56.1, 55.7

QTOF-HRMS (*m*/*z*, $[M+H]^+$) Calcd for $C_{18}H_{19}O_6$: 331.1182; found: 331.1191

4-((2-(hexyloxy)-4-methoxybenzoyl)oxy)benzoic acid (**4b**)

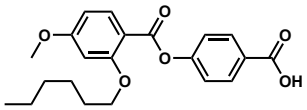

^{1}H-NMR (500 MHz, DMSO-d6) δ 8.02 (d, J = 8.7 Hz, 2H), 7.93 (d, J = 8.7 Hz, 1H), 7.33 (d, J = 8.7 Hz, 2H), 6.69 (d, J = 2.3 Hz, 1H), 6.66 (dd, J = 8.7, 2.3 Hz, 1H), 4.04 (t, J = 6.0 Hz, 2H), 1.74 (td, J = 13.7, 7.3 Hz, 2H), 0.99 (t, J = 7.4 Hz, 3H)

^{13}C{^{1}H}-NMR (126 MHz, acetone-d6) δ 167.0, 166.1, 163.9, 162.5, 156.1, 135.0, 131.9, 128.6, 123.0, 111.8, 106.3, 100.3, 70.9, 56.1, 23.2, 10.9

QTOF-HRMS (*m*/*z*, $[M+H]^+$) Calcd for $C_{21}H_{25}O_6$: 373.1651; found: 373.1661

4-((2,4-dimethoxybenzoyl)oxy)benzoic acid (**4c**)

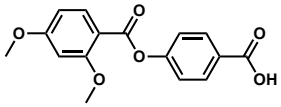

^{1}H-NMR (500 MHz, methanol-d4) δ 8.11-8.08 (m, 2H), 8.05 (d, J = 8.7 Hz, 1H), 7.30-7.28 (m, 2H), 6.68 (d, J = 2.3 Hz, 1H), 6.65 (dd, J = 8.7, 2.3 Hz, 1H), 3.91 (d, J = 3.3 Hz, 6H)

^{13}C{^{1}H}-NMR (126 MHz, methanol-d4) δ 167.8, 165.8, 163.6, 162.6, 155.0, 134.1, 130.9, 128.1, 121.8, 110.0, 105.3, 98.5, 55.1, 54.9

QTOF-HRMS (*m*/*z*, $[M+H]^+$) Calcd for $C_{16}H_{15}O_6$: 303.0869; found: 303.0881

4-((4-nitrophenoxy)carbonyl)phenyl 4-methoxy-2-propoxybenzoate (**5a**), C3RM

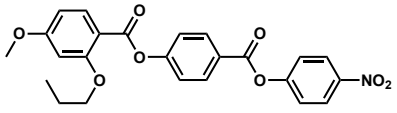

^{1}H-NMR (500 MHz, $CDCl_3$) δ 8.34 (d, J = 8.9 Hz, 2H), 8.26 (d, J = 8.6 Hz, 2H), 8.07 (d, J = 8.7 Hz, 1H), 7.43 (d, J = 9.0 Hz, 2H), 7.39 (d, J = 8.6 Hz, 2H), 6.57 (dd, J = 8.7, 2.3 Hz, 1H), 6.52 (s, 1H), 4.03 (t, J = 6.4 Hz, 2H), 3.90 (s, 3H), 1.89 (m, 2H), 1.08 (t, J = 7.4 Hz, 3H)
^{13}C{^{1}H}-NMR (126 MHz, $CDCl_3$) δ 165.2, 163.6, 163.3, 161.9, 156.1, 155.7, 145.4, 134.6, 131.9, 125.5, 125.3, 122.7, 122.5, 110.7, 105.0, 99.7, 69.0, 55.6, 31.5, 29.1, 25.7, 22.6, 14.0
QTOF-HRMS (*m*/*z*, $[M+H]^+$) Calcd for $C_{24}H_{22}NO_8$: 452.1345; found: 452.1353

4-((4-nitrophenoxy)carbonyl)phenyl 2-(hexyloxy)-4-methoxybenzoate (**5b**), C6RM

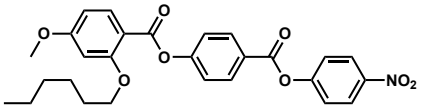

^{1}H-NMR (500 MHz, $CDCl_3$) δ 8.34 (d, J = 9.2 Hz, 2H), 8.26 (d, J = 8.9 Hz, 2H), 8.06 (d, J = 8.7 Hz, 1H), 7.43 (d, J = 9.2 Hz, 2H), 7.39 (d, J = 8.9 Hz, 2H), 6.57 (dd, J = 8.8, 2.4 Hz, 1H), 6.52 (d, J = 2.3 Hz, 1H), 4.07 (d, J = 6.4 Hz, 2H), 3.89 (s, 3H), 1.88-1.82 (m, 2H), 1.53-1.47 (m, 2H), 1.35-1.26 (m, 4H), 0.87 (t, J = 7.1 Hz, 3H)
^{13}C{^{1}H}-NMR (126 MHz, $CDCl_3$) δ 165.3, 163.6, 163.2, 161.9, 156.1, 155.7, 145.4, 134.6, 131.9, 125.5, 125.3, 122.7, 122.5, 110.6, 105.0, 99.7, 70.4, 55.6, 22.5, 10.6
QTOF-HRMS (*m*/*z*, $[M+H]^+$) Calcd for $C_{27}H_{27}NO_8$: 494.1815; found: 494.1829

4-((4-nitrophenoxy)carbonyl)phenyl 2,4-dimethoxybenzoate (**5c**), RM734

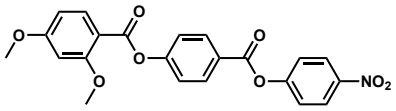

^{1}H-NMR (500 MHz, $CDCl_3$) δ 8.34 (d, J = 9.0 Hz, 2H), 8.26 (d, J = 8.6 Hz, 2H), 8.11 (d, J = 8.7 Hz, 1H), 7.44 (d, J = 9.0 Hz, 2H), 7.40 (d, J = 8.6 Hz, 2H), 6.59 (d, J = 8.7 Hz, 1H), 6.55 (d, J = 2.3 Hz, 1H), 3.95 (s, 3H), 3.91 (s, 3H)
^{13}C{^{1}H}-NMR (126 MHz, $CDCl_3$) δ 165.5, 163.8, 162.9, 162.7, 156.1, 155.8, 145.5, 134.8, 132.0, 125.7, 125.4, 122.8, 122.6, 110.4, 105.1, 99.1, 56.2, 55.8
QTOF-HRMS (*m*/*z*, $[M+H]^+$) Calcd for $C_{22}H_{18}NO_8$: 424.1032; found: 424.1036

DIO series:

2-(3,5-difluorophenyl)-1,3-dioxane (**7a**)

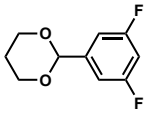

$^{1}H\{^{19}F\}$-NMR (500 MHz, $CDCl_3$) δ 7.02 (d, J = 2.4 Hz, 2H), 6.76 (t, J = 2.4 Hz, 1H), 5.45 (s, 1H), 4.27 (ddd, J = 12.0, 4.9, 1.3 Hz, 2H), 3.97 (td, J = 12.3, 2.4 Hz, 2H), 2.26-2.16 (m, 1H), 1.48-1.44 (m, 1H)

$^{13}C\{^{1}H,^{19}F\}$-NMR (126 MHz, $CDCl_3$) δ 162.9, 142.3, 109.2, 103.9, 99.7, 67.3, 25.6

$^{19}F\{^{1}H\}$-NMR (471 MHz, $CDCl_3$) δ −109.7

QTOF-HRMS (*m*/*z*, $[M]^+$) Calcd for $C_{10}H_9F_2O_2^{\bullet+}$: 199.0565; found: 199.0603

4-(1,3-dioxan-2-yl)-2,6-difluorobenzoic acid (**8a**)

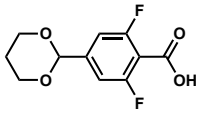

$^{1}H\{^{19}F\}$-NMR (500 MHz, DMSO-d6) δ 7.16 (s, 2H), 5.55 (s, 1H), 4.14 (dd, J = 10.7, 5.0 Hz, 2H), 3.93 (td, J = 12.2, 2.4 Hz, 2H), 1.98 (m, 1H), 1.45 (d, J = 12.3 Hz, 1H)

$^{13}C\{^{1}H,^{19}F\}$-NMR (126 MHz, DMSO-d6) δ 161.9, 159.0, 144.1, 112.0, 109.8, 98.3, 66.7, 25.2

$^{19}F\{^{1}H\}$-NMR (471 MHz, DMSO-d6) δ −111.6

QTOF-HRMS (*m*/*z*, $[M+H]^+$) Calcd for $C_{11}H_{11}F_2O_4$: 245.0625; found: 245.0625

methyl 4-(1,3-dioxan-2-yl)benzoate (**23**)

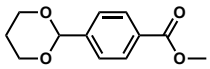

^{1}H-NMR (500 MHz, $CDCl_3$) δ 8.04 (dd, J = 6.7, 1.8 Hz, 2H), 7.56 (d, J = 8.2 Hz, 2H), 5.54 (s, 1H), 4.29 (ddd, J = 11.9, 5.0, 1.3 Hz, 2H), 4.03-3.98 (m, 2H), 3.87-3.94 (3H), 2.29-2.19 (m, 1H), 1.49-1.45 (m, 1H)

$^{13}C\{^{1}H\}$-NMR (126 MHz, $CDCl_3$) δ 167.0, 143.3, 130.5, 129.7, 126.2, 100.9, 67.5, 52.2, 25.8

QTOF-HRMS (*m*/*z*, $[M+H]^+$) Calcd for $C_{12}H_{15}O_4$: 223.0970; found: 222.0892

4-(1,3-dioxan-2-yl)benzoic acid (**24**)

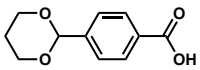

^{1}H-NMR (500 MHz, DMSO-d6) δ 7.93 (d, J = 8.0 Hz, 2H), 7.52 (d, J = 8.2 Hz, 2H), 5.59 (s, 1H), 4.16 (dd, J = 11.2, 4.9 Hz, 2H), 3.96 (td, J = 12.2, 2.1 Hz, 2H), 2.05-1.96 (m, 1H), 1.46 (d, J = 13.5 Hz, 1H)

^{13}C-NMR (126 MHz, DMSO-d6) δ 167.6, 143.8, 131.4, 129.6, 126.8, 100.4, 67.2, 25.9

QTOF-HRMS (*m*/*z*, $[M]^-$) Calcd for $C_{11}H_{12}O_4$: 207.0663; found: 207.0725

2,3',4',5'-tetrafluoro-[1,1'-biphenyl]-4-ol (**9a**)

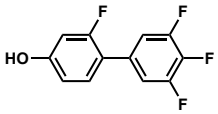

$^{1}H\{^{19}F\}$-NMR (500 MHz, $CDCl_3$) δ 7.21-7.25 (1H), 7.09-7.15 (2H), 6.68-6.74 (1H), 6.66-6.68 (1H), 4.99-5.13 (1H)

$^{13}C\{^{1}H,^{19}F\}$-NMR (126 MHz, DMSO-d6) 160.1, 160.0, 150.7, 138.3, 132.6, 131.7, 116.3, 113.4, 112.8, 103.6

$^{19}F\{^{1}H\}$-NMR (471 MHz, $CDCl_3$) δ −115.2 (s, 1F), −134.6 (d, J = 18.3 Hz, 2F), −162.3 (t, J = 20.2 Hz, 1F)

QTOF-HRMS (*m*/*z*, $[M]^+$) Calcd for $C_{12}H_6F_4O$: 242.0355; found: 242.0360

3',4',5'-trifluoro-2-nitro-[1,1'-biphenyl]-4-ol (**9b**)

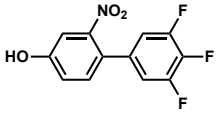

$^{1}H\{^{19}F\}$-NMR (500 MHz, DMSO-d6) δ 10.63 (s, 1H), 7.36 (d, J = 2.4 Hz, 1H), 7.33 (d, J = 8.4 Hz, 1H), 7.31 (d, J = 6.4 Hz, 2H), 7.13 (dd, J = 8.4, 2.6 Hz, 1H)

$^{13}C\{^{1}H,^{19}F\}$-NMR (126 MHz, DMSO-d6) δ 162.0, 158.9, 148.2, 147.1, 133.0, 123.0, 120.5, 112.8, 111.3, 109.5, 89.9

$^{19}F\{^{1}H\}$-NMR (471 MHz, DMSO-d6) δ −135.2 (d, J = 22.0 Hz, 2F), −163.0 (t, J = 22.0 Hz, 1F)

QTOF-HRMS (*m*/*z*, $[M+H]^+$) Calcd for $C_{12}H_7F_3NO_3$: 270.0378; found: 270.0388

3,5-difluoro-4'-hydroxy-2'-nitro-[1,1'-biphenyl]-4-carbonitrile (**9c**)

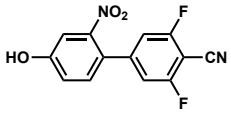

$^{1}H\{^{19}F\}$-NMR (500 MHz, DMSO-D6) δ 10.86 (s, 1H), 7.51 (s, 2H), 7.47 (d, J = 2.6 Hz, 1H), 7.41 (d, J = 8.4 Hz, 1H), 7.21 (dd, J = 8.4, 2.4 Hz, 1H)

$^{13}C\{^{1}H,^{19}F\}$-NMR (126 MHz, DMSO-d6) δ 162.0, 158.9, 148.2, 147.1, 133.0, 123.0, 120.5, 112.8, 111.3, 109.5, 89.9

$^{19}F\{^{1}H\}$-NMR (471 MHz, $CDCl_3$) δ −102.9

QTOF-HRMS (*m*/*z*, $[M+H]^+$) Calcd for $C_{13}H_7F_2N_2O_3$: 277.0425; found: 277.0370

2,3',4',5'-tetrafluoro-[1,1'-biphenyl]-4-yl 2,6-difluoro-4-((2r,5r)-5-propyl-1,3-dioxan-2-yl)benzoate (**10a**), *trans*DIO

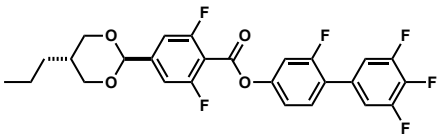

$^{1}H\{^{19}F\}$-NMR (500 MHz, $CDCl_3$) δ 7.43 (dd, J = 7.8, 0.9 Hz, 1H), 7.19-7.16 (m, 6H), 5.40 (s, 1H), 4.26 (dd, J = 11.7, 4.6 Hz, 2H), 3.54 (t, J = 11.5 Hz, 2H), 2.19-2.10 (m, 1H), 1.39-1.31 (m, 2H), 1.10 (q, J = 15.5, 7.3 Hz, 2H), 0.94 (t, J = 7.3 Hz, 3H)

$^{13}C\{^{1}H,^{19}F\}$-NMR (126 MHz, $CDCl_3$) δ 161.0, 159.4, 159.3, 151.3, 151.0, 145.7, 139.6, 130.9, 130.7, 124.4, 118.2, 113.3, 110.7, 110.4, 109.5, 98.9, 72.7, 34.0, 30.3, 19.6, 14.3

$^{19}F\{^{1}H\}$-NMR (471 MHz, $CDCl_3$) δ −108.4 (s, 2F), −114.2 (s, 1F), −134.1 (d, J = 18.3 Hz, 2F), -161.0 (t, J = 20.2 Hz, 1F)

QTOF-HRMS (*m*/*z*, $[M+H]^+$) Calcd for $C_{26}H_{21}F_6O_4$: 511.1344; found: 511.1341

2,3',4',5'-tetrafluoro-[1,1'-biphenyl]-4-yl 4-(1,3-dioxan-2-yl)-2,6-difluorobenzoate (**10b**), C0F2F1F3

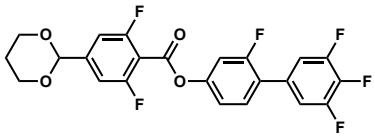

$^{1}H\{^{19}F\}$-NMR (500 MHz, $CDCl_3$) δ 7.43 (dd, J = 7.8, 1.1 Hz, 1H), 7.19-7.16 (m, 6H), 5.50 (s, 1H), 4.30 (ddd, J = 11.9, 4.9, 1.2 Hz, 2H), 4.03-3.97 (m, 2H), 2.27-2.18 (m, 1H), 1.52-1.48 (m, 1H)

$^{13}C\{^{1}H,^{19}F\}$-NMR (126 MHz, $CDCl_3$) δ 161.0, 159.4, 159.4, 151.2, 151.0, 145.9, 139.6, 130.9, 130.7, 124.4, 118.2, 113.3, 110.7, 110.3, 109.5, 99.0, 67.5, 25.6

$^{19}F\{^{1}H\}$-NMR (471 MHz, $CDCl_3$) δ −108.4 (s, 2F), −114.2 (s, 1F), −134.1 (d, J = 25.7 Hz, 2F), −161.0 (t, J = 20.2 Hz, 1F)

QTOF-HRMS (*m*/*z*, $[M+H]^+$) Calcd for $C_{23}H_{15}F_6O_4$: 469.0875; found: 469.0887

3',4',5'-trifluoro-2-nitro-[1,1'-biphenyl]-4-yl 4-(1,3-dioxan-2-yl)-2,6-difluorobenzoate (**10c**), C0F2NO2F3

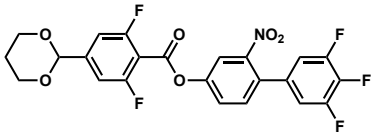

$^{1}H\{^{19}F\}$-NMR (500 MHz, $CDCl_3$) δ 7.91 (d, J = 2.3 Hz, 1H), 7.60 (dd, J = 8.4, 2.4 Hz, 1H), 7.45 (d, J = 8.4 Hz, 1H), 7.21 (d, J = 0.4 Hz, 2H), 6.96 (d, J = 6.0 Hz, 2H), 5.50 (s, 1H), 4.32-4.28 (m, 2H), 4.03-3.98 (m, 2H), 2.15-2.30 (1H), 1.46-1.53 (1H)

$^{13}C\{^{1}H,^{19}F\}$-NMR (126 MHz, $CDCl_3$) δ 161.1, 159.1, 151.3, 150.3, 148.9, 146.4, 140.1, 132.8, 132.7, 131.5, 126.4, 118.4, 112.8, 110.4, 108.8, 98.9, 67.5, 25.6

$^{19}F\{^{1}H\}$-NMR (471 MHz, $CDCl_3$) δ −107.8 (s, 2F), −133.0 (d, J = 18.3 Hz, 2F), −159.9 (t, J = 20.2 Hz, 1F)

QTOF-HRMS (*m*/*z*, $[M+H]^+$) Calcd for $C_{23}H_{15}F_5NO_6$: 496.0820; found: 496.0832

4'-cyano-3',5'-difluoro-2-nitro-[1,1'-biphenyl]-4-yl 4-(1,3-dioxan-2-yl)-2,6-difluorobenzoate (**10d**). C0F2NO2CN

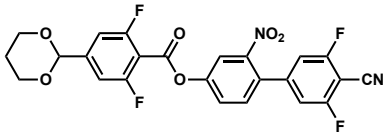

$^{1}H\{^{19}F\}$-NMR (500 MHz, $CDCl_3$) δ 8.02 (d, J = 2.3 Hz, 1H), 7.66 (dd, J = 8.4, 2.4 Hz, 1H), 7.46 (d, J = 8.3 Hz, 1H), 7.22 (d, J = 0.6 Hz, 2H), 7.03 (s, 2H), 5.51 (s, 1H), 4.30 (dd, J = 10.7, 5.0 Hz, 2H), 4.01 (td, J = 12.2, 2.5 Hz, 2H), 2.28-2.17 (m, 1H), 1.52-1.49 (m, 1H)

$^{13}C\{^{1}H,^{19}F\}$-NMR (126 MHz, $CDCl_3$) δ 162.9, 161.1, 158.9, 151.0, 148.2, 146.5, 145.3, 132.2, 130.8, 126.8, 118.9, 112.3, 110.4, 108.8, 108.6, 98.8, 92.4, 77.3, 77.0, 76.8, 67.4, 25.5

$^{19}F\{^{1}H\}$-NMR (471 MHz, $CDCl_3$) δ −102.4, −107.7

QTOF-HRMS (*m*/*z*, $[M+H]^+$) Calcd for $C_{24}H_{17}F_2N_2O_6$: 467.1055; found: 467.1052

2,3',4',5'-tetrafluoro-[1,1'-biphenyl]-4-yl 2,6-difluoro-4-((2s,5s)-5-propyl-1,3-dioxan-2-yl)benzoate (**10e**), *cis*DIO

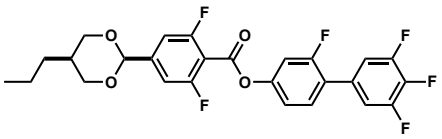

$^{1}H\{^{19}F\}$-NMR (500 MHz, $CDCl_3$) δ 7.43 (dd, J = 7.8, 1.1 Hz, 1H), 7.19-7.16 (m, 6H), 5.50 (s, 1H), 4.12-4.06 (m, 4H), 1.74 (dd, J = 15.6, 7.4 Hz, 2H), 1.51-1.47 (m, 1H), 1.43 (dt, J = 22.9, 7.5 Hz, 2H), 0.96 (t, J = 7.3 Hz, 3H)

$^{13}C\{^{1}H,^{19}F\}$-NMR (126 MHz, $CDCl_3$) δ 161.0, 159.4, 159.3, 151.3, 151.1, 145.9, 139.6, 130.9, 130.7, 124.4, 118.2, 113.3, 110.7, 110.3, 109.5, 99.2, 70.8, 34.0, 31.6, 20.6, 14.1

$^{19}F\{^{1}H\}$-NMR (471 MHz, $CDCl_3$) δ −108.4 (s, 2F), −114.2 (s, 1F), −134.1 (d, J = 22.0 Hz, 2F), −161.0 (t, J = 22.0 Hz, 1F)

QTOF-HRMS (*m*/*z*, $[M+H]^+$) Calcd for $C_{26}H_{21}F_6O_4$: 511.1344; found: 511.1341

4'-cyano-3',5'-difluoro-2-nitro-[1,1'-biphenyl]-4-yl 4-(1,3-dioxan-2-yl)benzoate (**10f**), C0F0F1F3

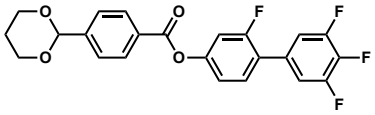

$^{1}H\{^{19}F\}$-NMR (500 MHz, $CDCl_3$) δ 8.20 (d, J = 8.3 Hz, 2H), 7.66 (d, J = 8.4 Hz, 2H), 7.43 (dd, J = 7.7, 1.6 Hz, 1H), 7.19 (d, J = 6.2 Hz, 2H), 7.16-7.13 (m, 2H), 5.59 (s, 1H), 4.31 (dd, J = 10.7, 4.9 Hz, 2H), 4.03 (td, J = 12.3, 2.4 Hz, 2H), 2.26 (ddt, J = 25.9, 12.5, 5.0 Hz, 1H), 1.52-1.48 (m, 1H)

$^{13}C\{^{1}H,^{19}F\}$-NMR (126 MHz, $CDCl_3$) δ 164.5, 159.5, 151.8, 151.2, 144.5, 139.6, 131.0, 130.6, 130.3, 129.1, 126.5, 123.9, 118.4, 113.3, 110.8, 100.7, 67.6, 25.8

$^{19}F\{^{1}H\}$-NMR (471 MHz, $CDCl_3$) δ −114.5 (s, 1F), −134.1 (d, J = 22.0 Hz, 2F), −161.2 (t, J = 20.2 Hz, 1F)

QTOF-HRMS (*m*/*z*, $[M+H]^+$) Calcd for $C_{23}H_{17}F_4O_4$: 433.1063; found: 433.1081

UUZU series:

5-ethyl-1,3-difluoro-2-iodobenzene (**11a**)

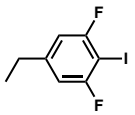

$^{1}H\{^{19}F\}$-NMR (500 MHz, $CDCl_3$) δ 6.75 (s, 2H), 2.64 (q, J = 7.6 Hz, 2H), 1.23 (t, J = 7.6 Hz, 3H)

$^{13}C\{^{1}H,^{19}F\}$-NMR (126 MHz, $CDCl_3$) δ 162.6, 148.3, 76.8, 66.9, 28.5, 14.9

$^{19}F\{^{1}H\}$-NMR (471 MHz, $CDCl_3$) δ −93.7

QTOF-HRMS (*m*/*z*, $[M]^+$) Calcd for $C_8H_7F_2I$: 267.9560; found: 267.9572

1,3-difluoro-2-iodo-5-propylbenzene (**11b**)

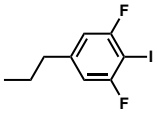

$^{1}H\{^{19}F\}$-NMR (500 MHz, $CDCl_3$) δ 6.72 (s, 2H), 2.57 (t, J = 7.6 Hz, 2H), 1.63 (m, 2H), 0.94 (t, J = 7.4 Hz, 3H)

$^{13}C\{^{1}H,^{19}F\}$-NMR (126 MHz, $CDCl_3$) δ 162.5, 146.8, 111.5, 66.9, 37.5, 24.0, 13.6

$^{19}F\{^{1}H\}$-NMR (471 MHz, $CDCl_3$) δ −93.9

QTOF-HRMS (*m*/*z*, $[M]^+$) Calcd for $C_9H_9F_2I$: 281.9717; found: 281.9734

4-ethyl-2,3',5',6-tetrafluoro-1,1'-biphenyl (**12a**)

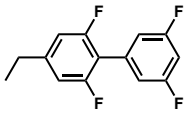

$^{1}H\{^{19}F\}$-NMR (500 MHz, $CDCl_3$) δ 7.00 (d, J = 2.4 Hz, 2H), 6.84 (q, J = 2.4 Hz, 3H), 2.68 (q, J = 7.6 Hz, 2H), 1.27 (t, J = 7.7 Hz, 3H)

$^{13}C\{^{1}H,^{19}F\}$-NMR (126 MHz, $CDCl_3$) δ 162.7, 159.6, 147.5, 132.4, 113.45, 113.4, 111.2, 103.5, 28.6, 14.8

$^{19}F\{^{1}H\}$-NMR (471 MHz, $CDCl_3$) δ −110.2, −115.1

QTOF-HRMS (*m*/*z*, $[M]^+$) Calcd for $C_{14}H_{11}F_4$: 254.0719; found: 254.0785

2,3',5',6-tetrafluoro-4-propyl-1,1'-biphenyl (**12b**)

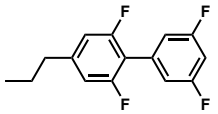

$^{1}H\{^{19}F\}$-NMR (500 MHz, $CDCl_3$) δ 7.00 (d, J = 2.4 Hz, 2H), 6.84-6.82 (m, 3H), 2.61 (t, J = 7.7 Hz, 2H), 1.67 (td, J = 15.0, 7.5 Hz, 2H), 0.98 (t, J = 7.4 Hz, 3H)

$^{13}C\{^{1}H,^{19}F\}$-NMR (126 MHz, $CDCl_3$) δ 162.7, 159.5, 146.1, 132.4, 113.5, 113.4, 111.7, 103.4, 37.6, 23.9, 13.6

$^{19}F\{^{1}H\}$-NMR (471 MHz, $CDCl_3$) δ −110.3, −115.2

QTOF-HRMS (*m*/*z*, $[M+H]^+$) Calcd for $C_{15}H_{13}F_4$: 269.0953; found: 269.0975

4'-ethyl-2',3,5,6'-tetrafluoro-[1,1'-biphenyl]-4-carboxylic acid (**13a**)

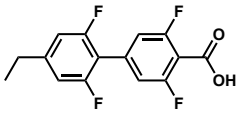

$^{1}H\{^{19}F\}$-NMR (500 MHz, DMSO-d6) δ 7.38 (s, 2H), 7.15 (s, 2H), 2.63 (t, J = 7.6 Hz, 2H), 1.63 (td, J = 14.9, 7.4 Hz, 2H), 0.92 (t, J = 7.3 Hz, 3H)

$^{13}C\{^{1}H,^{19}F\}$-NMR (126 MHz, $CDCl_3$) δ 165.7, 161.0, 159.5, 148.6, 136.0, 114.4, 112.4, 111.4, 108.6, 28.6, 14.8

$^{19}F\{^{1}H\}$-NMR (471 MHz, $CDCl_3$) δ −108.5 (s, 2F), −114.7 (s, 2F)

QTOF-HRMS (*m*/*z*, $[M+H]^+$) Calcd for $C_{15}H_{11}F_4O_2$: 299.0695; found: 299.0698

2',3,5,6'-tetrafluoro-4'-propyl-[1,1'-biphenyl]-4-carboxylic acid (**13b**)

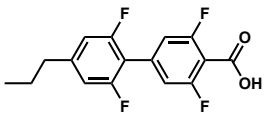

$^{1}H\{^{19}F\}$-NMR (500 MHz, DMSO-d6) δ 7.38 (s, 2H), 7.15 (s, 2H), 2.63 (t, J = 7.6 Hz, 2H), 1.63 (td, J = 14.9, 7.4 Hz, 2H), 0.92 (t, J = 7.3 Hz, 3H)

$^{13}C\{^{1}H,^{19}F\}$-NMR (126 MHz, $CDCl_3$) δ 166.1, 161.0, 159.4, 147.1, 136.0, 114.4, 112.4, 111.9, 108.6, 37.6, 23.8, 13.6

$^{19}F\{^{1}H\}$-NMR (471 MHz, $CDCl_3$) δ −108.5 (s, 2F), −114.8 (s, 2F)

QTOF-HRMS (*m*/*z*, $[M+H]^+$) Calcd for $C_{16}H_{13}F_4O_2$: 313.0852; found: 313.0856

4-cyano-3,5-difluorophenyl 4'-ethyl-2',3,5,6'-tetrafluoro-[1,1'-biphenyl]-4-carboxylate (**14a**), UUZU-2-N

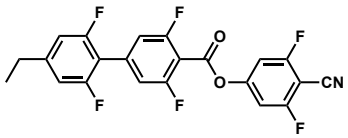

$^{1}H\{^{19}F\}$-NMR (500 MHz, $CDCl_3$) δ 7.21 (s, 2H), 7.12 (s, 2H), 6.89 (s, 2H), 2.71 (q, J = 7.6 Hz, 2H), 1.28 (t, J = 7.7 Hz, 3H)

$^{13}C\{^{1}H,^{19}F\}$-NMR (126 MHz, $CDCl_3$) δ 163.5, 160.9, 159.5, 157.9, 155.1, 149.0, 137.1, 114.6, 112.2, 111.5, 108.6, 107.6, 106.9, 90.6, 28.7, 14.7

$^{19}F\{^{1}H\}$-NMR (471 MHz, $CDCl_3$) δ −101.4 (s, 2F), −108.3 (s, 2F), −114.7 (s, 2F)

QTOF-HRMS (*m*/*z*, $[M+H]^+$) Calcd for $C_{22}H_{12}F_6NO_2$: 436.0772; found: 436.0774

4-cyano-3,5-difluorophenyl 2',3,5,6'-tetrafluoro-4'-propyl-[1,1'-biphenyl]-4-carboxylate (**14b**), UUZU-3-N

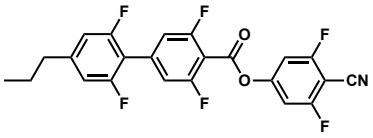

$^{1}H\{^{19}F\}$-NMR (500 MHz, $CDCl_3$) δ 7.21 (s, 2H), 7.12 (s, 2H), 6.87 (s, 2H), 2.64 (t, J = 7.6 Hz, 2H), 1.69 (m, 2H), 0.98 (t, J = 7.3 Hz, 3H)

$^{13}C\{^{1}H,^{19}F\}$-NMR (126 MHz, $CDCl_3$) δ 163.6, 160.9, 159.4, 157.9, 155.1, 147.5, 137.1, 114.6, 112.2, 112.0, 108.6, 107.6, 106.9, 90.6, 37.7, 23.8, 13.6

$^{19}F\{^{1}H\}$-NMR (471 MHz, $CDCl_3$) δ −101.4 (s, 2F), −108.3 (s, 2F), −114.8 (s, 2F)

QTOF-HRMS (*m*/*z*, $[M+H]^+$) Calcd for $C_{23}H_{14}F_6NO_2$: 450.0929; found: 450.0939

BIOTN series:

(3-methyloxetan-3-yl)methyl 3,5-difluorobenzoate (**15a**)

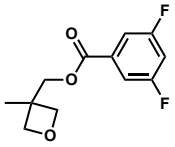

$^{1}H\{^{19}F\}$-NMR (500 MHz, $CDCl_3$) δ 7.56 (d, J = 2.3 Hz, 2H), 7.04 (t, J = 2.4 Hz, 1H), 4.61 (d, J = 6.0 Hz, 2H), 4.48 (d, J = 6.0 Hz, 2H), 4.43 (s, 2H), 1.43 (s, 3H)

$^{13}C\{^{1}H,^{19}F\}$-NMR (126 MHz, $CDCl_3$) δ 164.3, 162.8, 133.0, 112.6, 108.6, 79.4, 69.8, 39.3, 21.2

$^{19}F\{^{1}H\}$-NMR (471 MHz, $CDCl_3$) δ −108.1

QTOF-HRMS (*m*/*z*, $[M+H]^+$) Calcd for $C_{12}H_{13}F_2O_3$: 243.0833; found: 243.0853

(3-methyloxetan-3-yl)methyl 3,5-difluorobenzoate (**15b**)

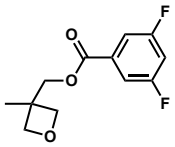

$^{1}H\{^{19}F\}$-NMR (500 MHz, $CDCl_3$) δ 7.55 (d, J = 2.4 Hz, 2H), 7.04 (t, J = 2.4 Hz, 1H), 4.56 (d, J = 6.2 Hz, 2H), 4.50-4.48 (m, 4H), 1.84 (q, J = 7.5 Hz, 2H), 0.97 (t, J = 7.5 Hz, 3H)

$^{13}C\{^{1}H,^{19}F\}$-NMR (126 MHz, $CDCl_3$) δ 164.3, 162.8, 133.1, 112.6, 108.6, 77.8, 67.6, 42.8, 26.9, 8.2

$^{19}F\{^{1}H\}$-NMR (471 MHz, $CDCl_3$) δ −108.1

QTOF-HRMS (*m*/*z*, $[M+H]^+$) Calcd for $C_{13}H_{15}F_2O_3$: 257.0989; found: 257.0993

1-(3,5-difluorophenyl)-4-methyl-2,6,7-trioxabicyclo[2.2.2]octane (**16a**)

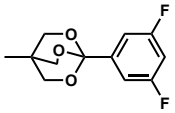

$^{1}H\{^{19}F\}$-NMR (500 MHz, $CDCl_3$) δ 7.15 (d, J = 2.4 Hz, 2H), 6.78 (t, J = 2.4 Hz, 1H), 4.08 (s, 6H), 0.89 (s, 3H)

$^{13}C\{^{1}H,^{19}F\}$-NMR (126 MHz, $CDCl_3$) δ 162.6, 141.0, 109.3, 106.5, 104.4, 73.3, 30.6, 14.3

$^{19}F\{^{1}H\}$-NMR (471 MHz, $CDCl_3$) δ −109.7

QTOF-HRMS (*m*/*z*, $[M+H]^+$) Calcd for $C_{12}H_{13}F_2O_3$: 243.0833; found: 243.0865

1-(3,5-difluorophenyl)-4-ethyl-2,6,7-trioxabicyclo[2.2.2]octane (**16b**)

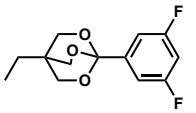

$^{1}H\{^{19}F\}$-NMR (500 MHz, $CDCl_3$) δ 7.15 (d, J = 2.4 Hz, 2H), 6.78 (t, J = 2.4 Hz, 1H), 4.10 (s, 6H), 1.33 (q, J = 7.7 Hz, 2H), 0.89 (t, J = 7.7 Hz, 3H)

$^{13}C\{^{1}H,^{19}F\}$-NMR (126 MHz, $CDCl_3$) δ 162.6, 141.1, 109.3, 106.6, 104.4, 71.8, 33.5, 22.4, 7.6

$^{19}F\{^{1}H\}$-NMR (471 MHz, $CDCl_3$) δ −109.7

QTOF-HRMS (*m*/*z*, $[M+H]^+$) Calcd for $C_{13}H_{15}F_2O_3$: 257.0989; found: 257.0993

1-(3,5-difluoro-4-iodophenyl)-4-methyl-2,6,7-trioxabicyclo[2.2.2]octane (**17a**)

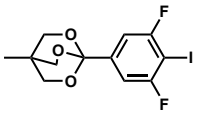

We used **17a** without further purification in the next step because of its high instability.

1-(3,5-difluoro-4-iodophenyl)-4-ethyl-2,6,7-trioxabicyclo[2.2.2]octane (**17b**)

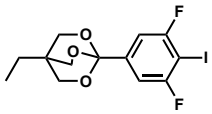

We used **17b** without further purification in the next step because of its high instability.

((4-bromo-3,5-difluorophenyl)ethynyl)triisopropylsilane (**18**)

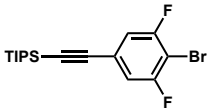

$^{1}H\{^{19}F\}$-NMR (500 MHz, $CDCl_3$) δ 7.03 (s, 2H), 1.10 (s, 18H)

$^{13}C\{^{1}H,^{19}F\}$-NMR (126 MHz, $CDCl_3$) δ 159.6, 124.5, 115.5, 103.8, 98.8, 94.7, 18.7, 11.3

$^{19}F\{^{1}H\}$-NMR (471 MHz, $CDCl_3$) δ −105.2

HRMS could not be found.

2,6-difluoro-4-(4,4,5,5-tetramethyl-1,3,2-dioxaborolan-2-yl)benzonitrile (**19**)

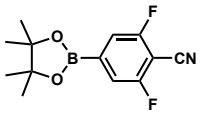

$^{1}H\{^{19}F\}$-NMR (500 MHz, $CDCl_3$) δ 7.41 (s, 2H), 1.33 (s, 12H)

$^{13}C\{^{1}H,^{19}F\}$-NMR (126 MHz, $CDCl_3$) δ 162.6, 117.3, 109.3, 94.2, 85.2, 24.8

$^{19}F\{^{1}H\}$-NMR (471 MHz, $CDCl_3$) δ −105.2

QTOF-HRMS (*m*/*z*, $[M+H]^+$) Calcd for $C_{13}H_{15}BF_2NO_2$: 266.1164; found: 266.1102

2',3,5,6'-tetrafluoro-4'-((triisopropylsilyl)ethynyl)-[1,1'-biphenyl]-4-carbonitrile (**20**)

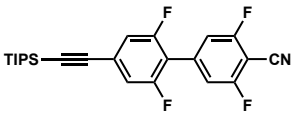

$^{1}H\{^{19}F\}$-NMR (500 MHz, $CDCl_3$) δ 7.19 (s, 1H), 7.14 (s, 1H), 1.13 (s, 12H)

$^{13}C\{^{1}H,^{19}F\}$-NMR (126 MHz, $CDCl_3$) δ 162.8, 159.1, 136.7, 127.0, 115.7, 115.1, 114.1, 108.9, 103.6, 96.1, 92.2, 18.6, 11.2

$^{19}F\{^{1}H\}$-NMR (471 MHz, $CDCl_3$) δ -103.7 (s, 2F), -113.7 (s, 2F)

HRMS could not be found.

4'-ethynyl-2',3,5,6'-tetrafluoro-[1,1'-biphenyl]-4-carbonitrile (**21**)

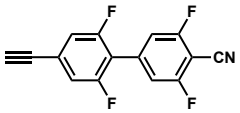

$^{1}H\{^{19}F\}$-NMR (500 MHz, $CDCl_3$) δ 7.20 (s, 2H), 7.17 (s, 2H), 3.27 (s, 1H)

$^{13}C\{^{1}H,^{19}F\}$-NMR (126 MHz, $CDCl_3$) δ 162.9, 159.2, 136.6, 125.7, 116.0, 115.9, 114.3, 109.0, 92.5, 81.2, 80.6

$^{19}F\{^{1}H\}$-NMR (471 MHz, $CDCl_3$) δ −103.4 (s, 2F), −113.2 (s, 2F)

QTOF-HRMS (*m*/*z*, $[M+H]^+$) Calcd for $C_{15}H_6F_4N$: 276.0436; found: 276.0440

4'-((2,6-difluoro-4-(4-methyl-2,6,7-trioxabicyclo[2.2.2]octan-1-yl)phenyl)ethynyl)-2',3,5,6'-tetrafluoro-[1,1'-biphenyl]-4-carbonitrile (**22a**)

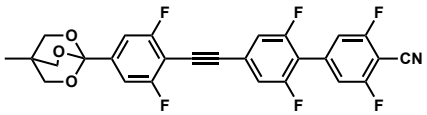

$^{1}H\{^{19}F\}$-NMR (500 MHz, $CDCl_3$) δ 7.24-7.21 (m, 6H), 4.08 (s, 6H), 0.90 (s, 3H)

$^{13}C\{^{1}H,^{19}F\}$-NMR (126 MHz, $CDCl_3$) δ 162.9, 162.6, 159.2, 141.2, 136.7, 126.0, 115.7, 115.6, 114.3, 109.6, 109.0, 106.4, 101.7, 96.1, 92.4, 80.2, 73.5, 30.7, 14.4

$^{19}F\{^{1}H\}$-NMR (471 MHz, $CDCl_3$) δ −103.5 (s, 2F), −106.3 (s, 2F), −113.2 (s, 2F)

QTOF-HRMS (*m*/*z*, $[M+H]^+$) Calcd for $C_{27}H_{16}F_6NO_3$: 516.1034; found: 516.1033

4'-((4-(4-ethyl-2,6,7-trioxabicyclo[2.2.2]octan-1-yl)-2,6-difluorophenyl)ethynyl)-2',3,5,6'-tetrafluoro-[1,1'-biphenyl]-4-carbonitrile (**22b**)

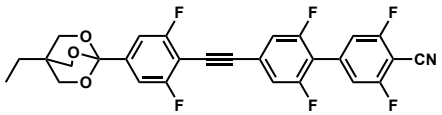

$^{1}H\{^{19}F\}$-NMR (500 MHz, $CDCl_3$) δ 7.25-7.22 (m, 6H), 4.11 (s, 6H), 1.34 (q, J = 7.7 Hz, 2H), 0.90 (t, J = 7.7 Hz, 3H)

$^{13}C\{^{1}H,^{19}F\}$-NMR (126 MHz, $CDCl_3$) δ 162.9, 162.6, 159.2, 141.3, 136.7, 126.0, 115.7, 115.6, 114.3, 109.6, 109.0, 106.5, 101.7, 96.1, 92.4, 80.2, 72.0, 33.6, 22.4, 7.7

$^{19}F\{^{1}H\}$-NMR (471 MHz, $CDCl_3$) δ −115.2 (s, 2F), −134.7 (s, 2F), −162.3 (s, 2F)

QTOF-HRMS (*m*/*z*, $[M+H]^+$) Calcd for $C_{28}H_{18}F_6NO_3$: 530.1191; found: 530.1187

Supplementary Note

Supplementary Note 1 | Calibration of SHG hysteresis loops

In all cases, the center position of the SHG hysteresis loop was shifted to left or right by ~5% of the maximum applied *E*-field (Fig. S18a), which would be due to the floating ground of the electrical system. This effect always appears like the charge-up behavior, i.e., the surface is electrically charged by the very first *E*-field. It remains almost permanently, because it is not easy to rip such a charge off the surface just by applying high reversal *E*-field. Therefore, once the field is applied, the SHG hysteresis loop becomes off-centered to the same direction but depending on the polarity of the first *E*-field. Compared in Fig. S18b-d is typical time evolution profiles of SHG, which happens in this situation. Such an effect looks to add or reduce the net *E*-field and induces a certain shift of the applied *E*-field. Thus, we assumed $E_{real} = E_{app} + E_{surface}$, where E_{real}, E_{app} and $E_{surface}$ are the effective *E*-field applied on the sample, the *E*-field applied to the whole cell, and the surface contribution, respectively. If this hypothesis is correct, the shift due to $E_{surface}$ can be eliminated simply by introducing an offset in E_{app} to cancel out the surface contribution $E_{surface}$. In order to verify this point, a positive DC *E*-field was first applied and examined the behavior under the influence of the offset in E_{app}. This DC *E*-field initially poled the surface polarization which induces negative $E_{surface}$. When a triangular waveform *E*-field of 200 V_{pp} without an offset was applied to this state, the SHG signal curve was asymmetric and the resulted hysteresis loop was off-centered as mentioned above (Fig. S18c). Next, −10 V_{DC} of offset was added to the triangular wave. Then, the SHG curve became further asymmetric, and the obtained SHG hysteresis loop shifted further away from the origin (Fig. S18b). Conversely, when +10 V_{DC} of offset was introduced, the SHG signal curve became symmetric, and a point-oriented SHG hysteresis loop appears with respect to the origin (Fig. S18d). Hence, this hypothesis would be correct, so that SHG hysteresis loop can be calibrated by using the *E*-field consisting of a triangular wave with a DC component.

Supplementary Figs. (Figs. S1–26)

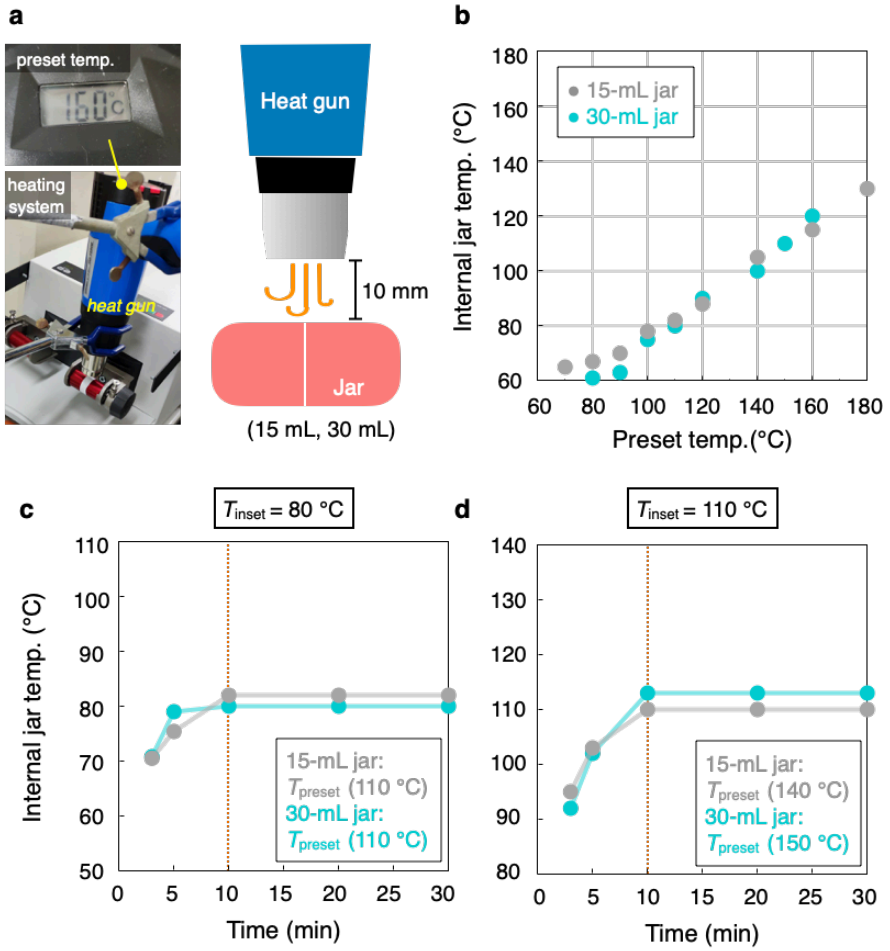

Fig. S1. a) Experimental setup, (b) T_{pre} vs T_{int}. T_{int} vs time for 15-mL (c) and 30-mL (d) jars.

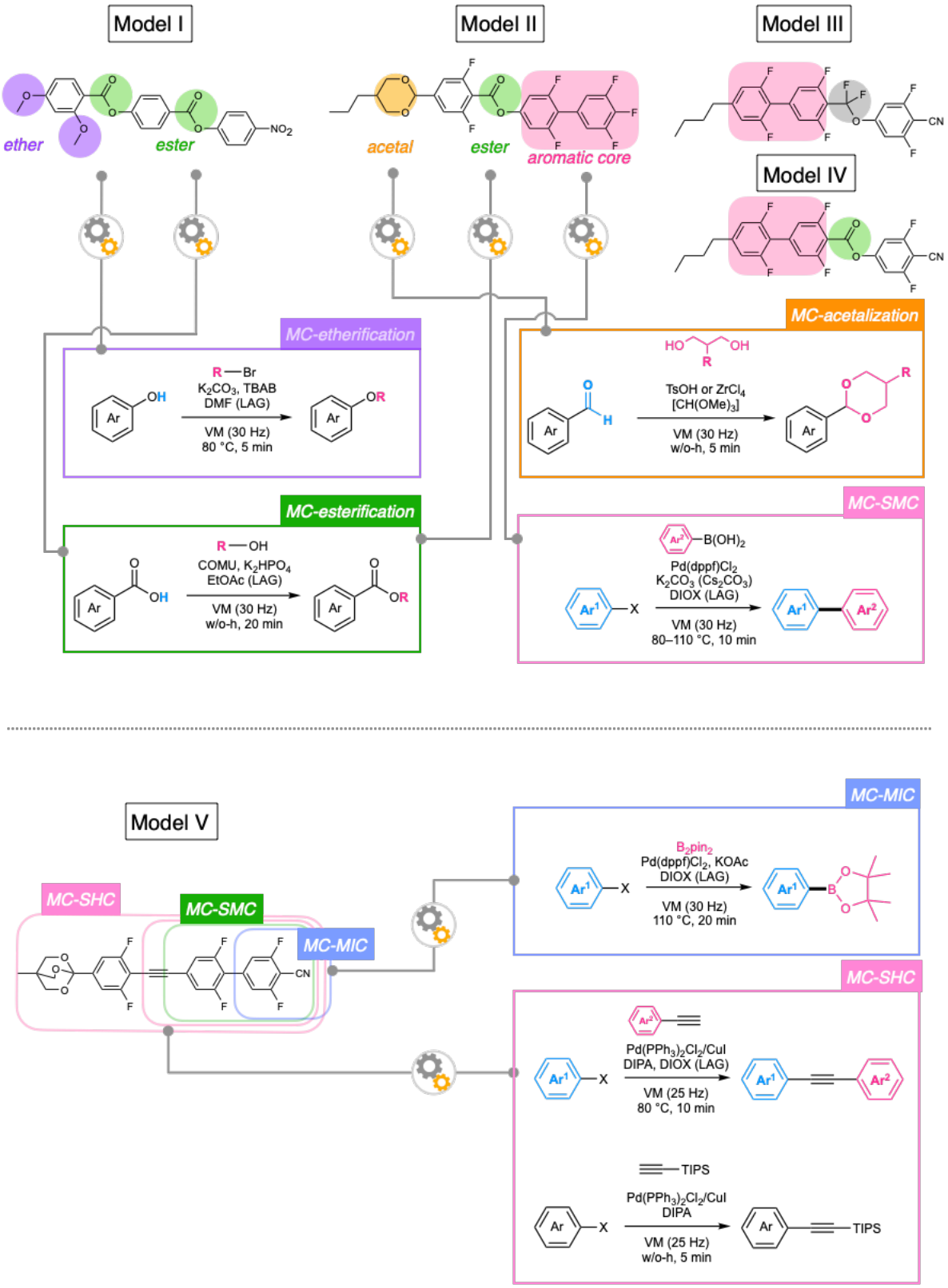

Fig. S2. MC synthetic strategy for the production of N_F/SmA_FLC molecules using the key MC reactions such as MC-etherification, MC-esterification, MC-acetalization, and MC-cross-coupling.

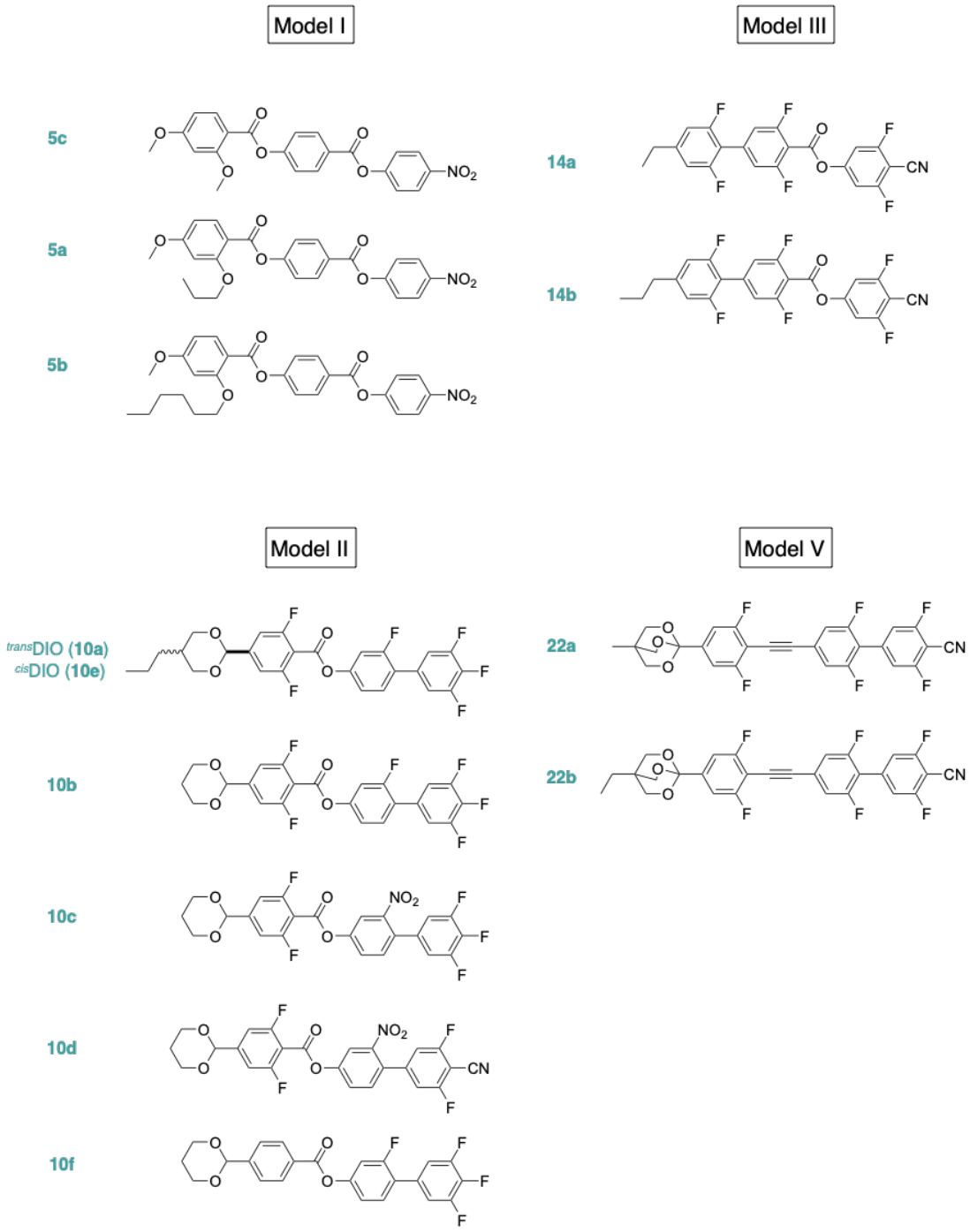

Fig. S3. The molecular libraries were synthesized by the MC technique.

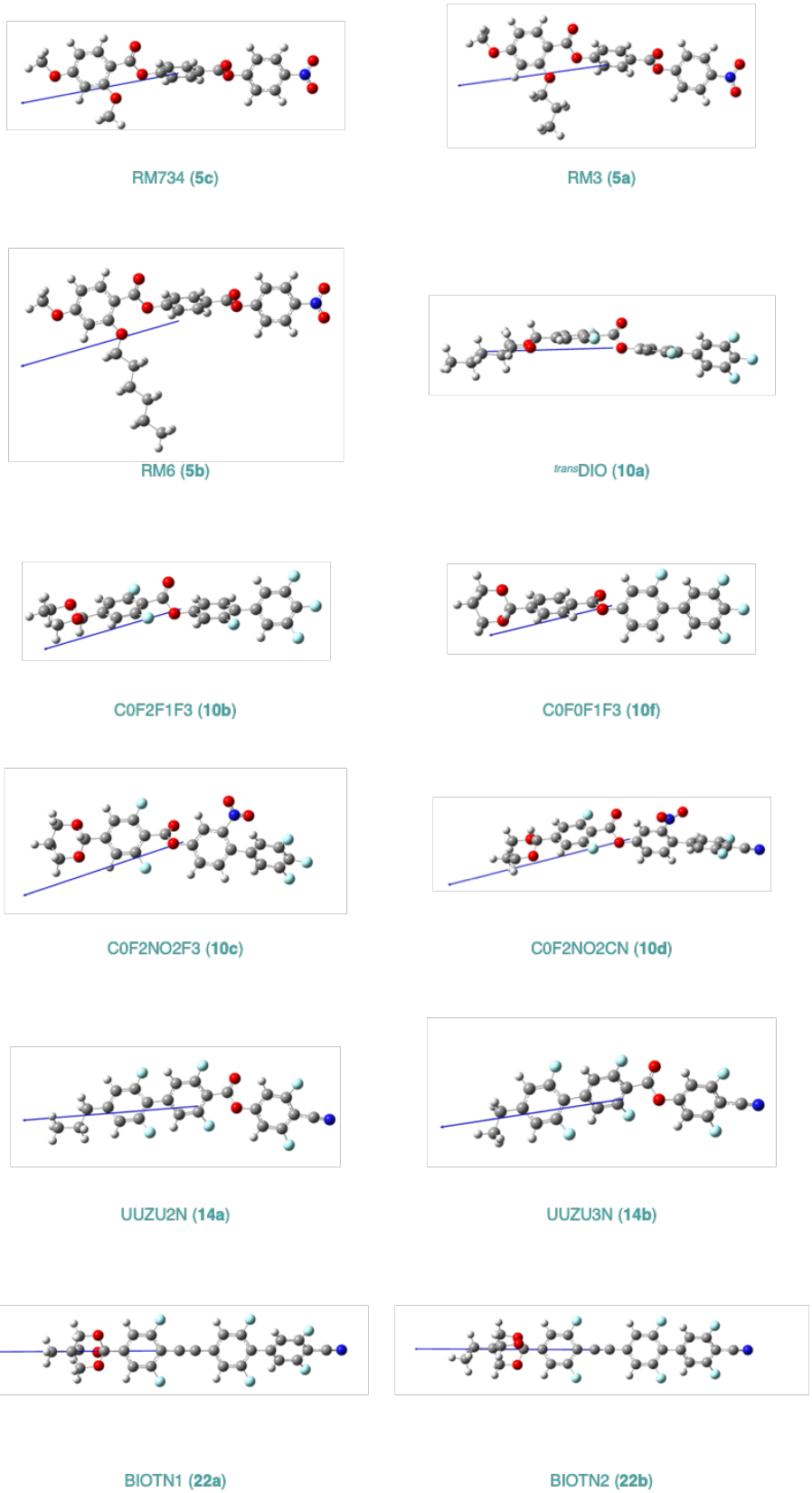

Fig. S4 The molecular structures optimized by MM2/DFT calculation.

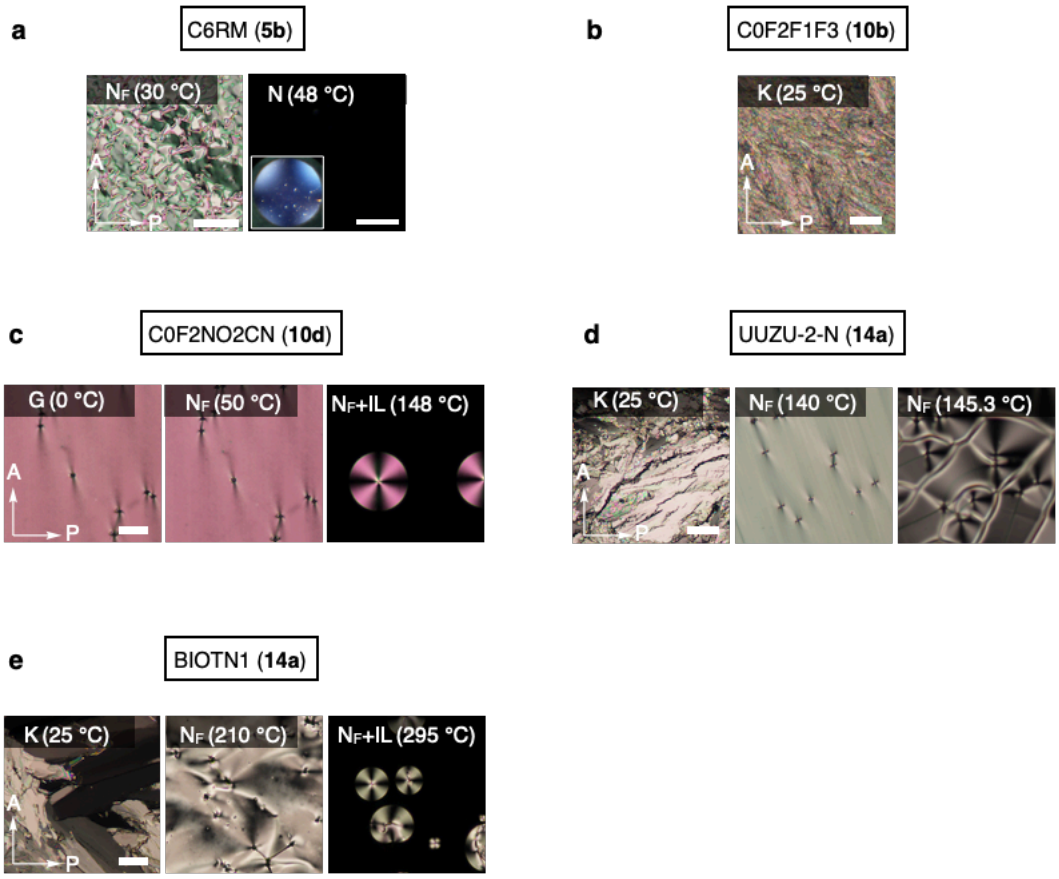

Fig. S5 Additional POM images. (a) C6RM (**5b**), (b) C0F2F1F3 (**10b**), (c) C0F2NO2CN (**10d**), (d) UUZU-2-N (**14a**) and (e) BIOTN2 (**14a**). Bar: 100 μm.

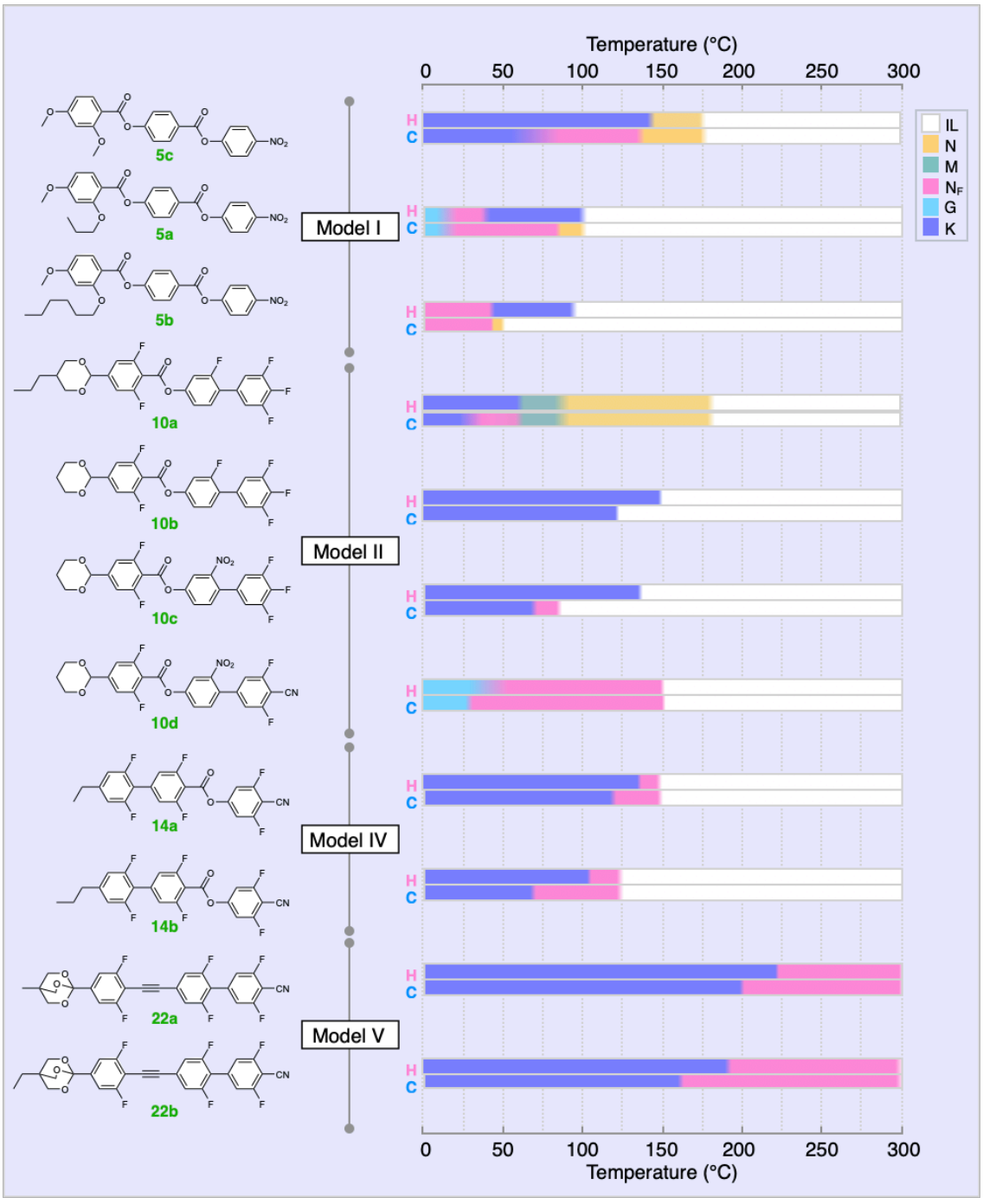

Fig. S6 Complete data of phase transition behavior for Models I, II, IV, and V.

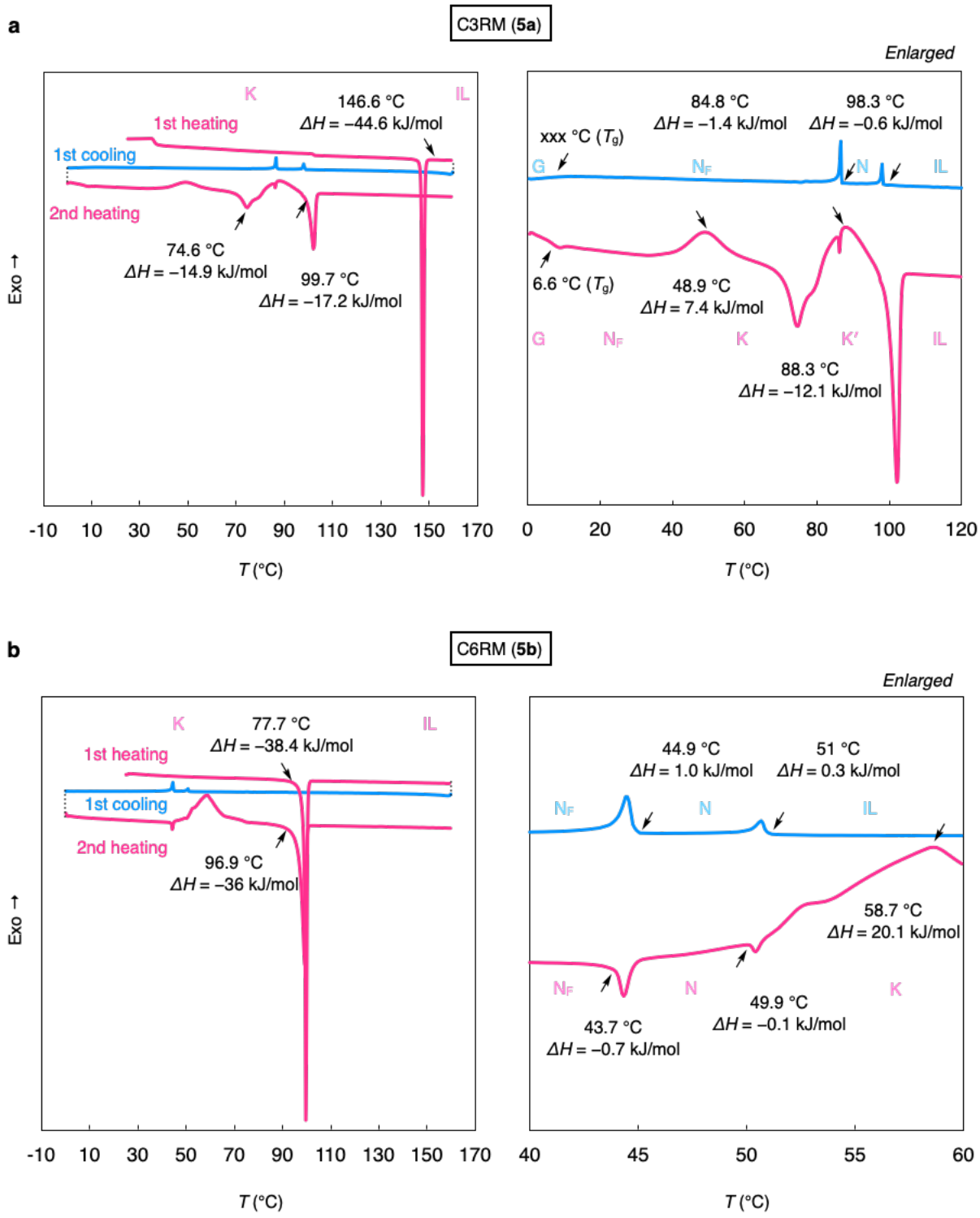

Fig. S7 DSC curves. (a) C3RM (**5a**) and (b) C6RM (**5b**). Scan rate: 5 K min^{-1}.

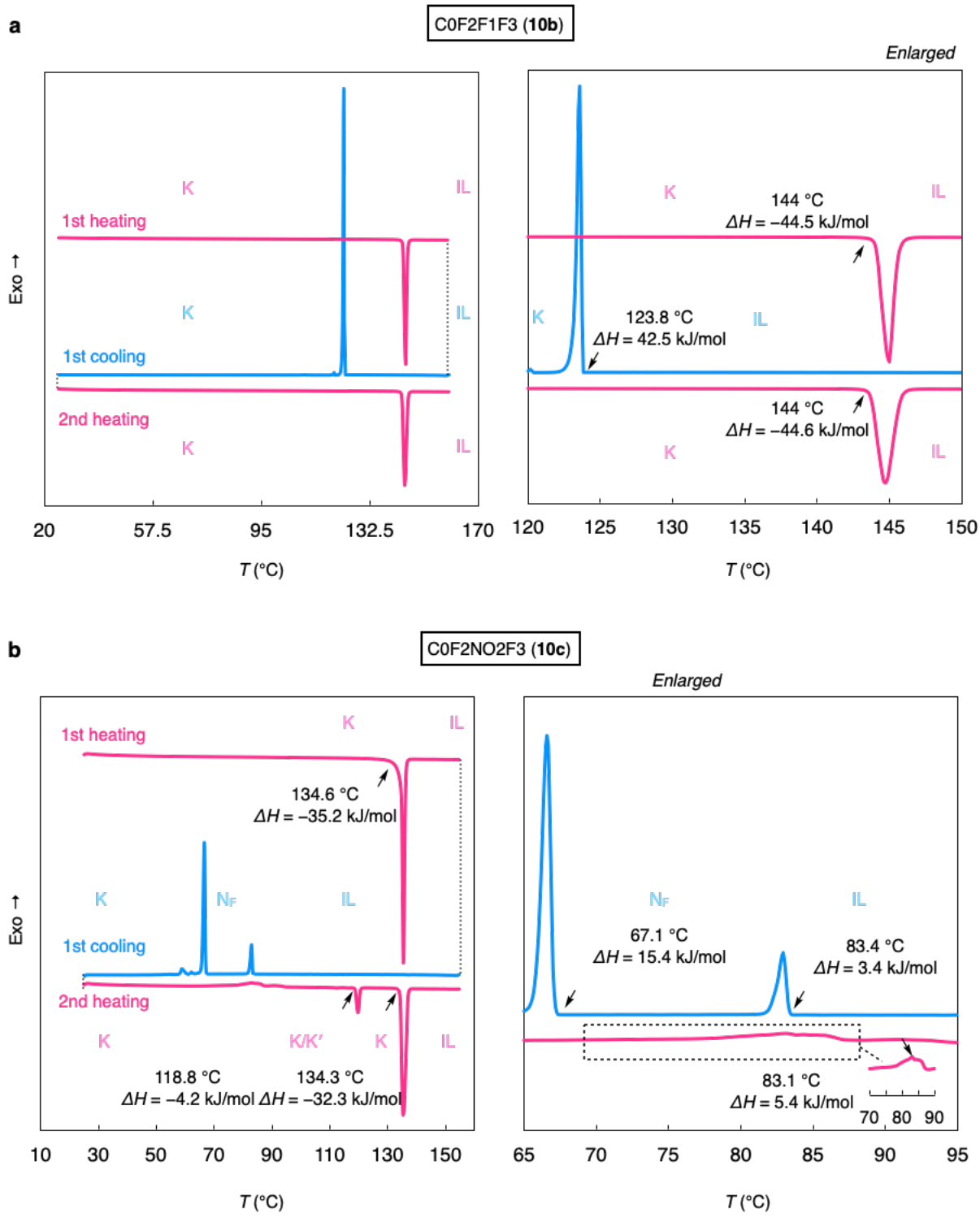

Fig. S8 DSC curves. (a) C0F2F1F3 (**10b**) and (b) C0F2NO2F3 (**10c**). Scan rate: 5 K min^{-1}.

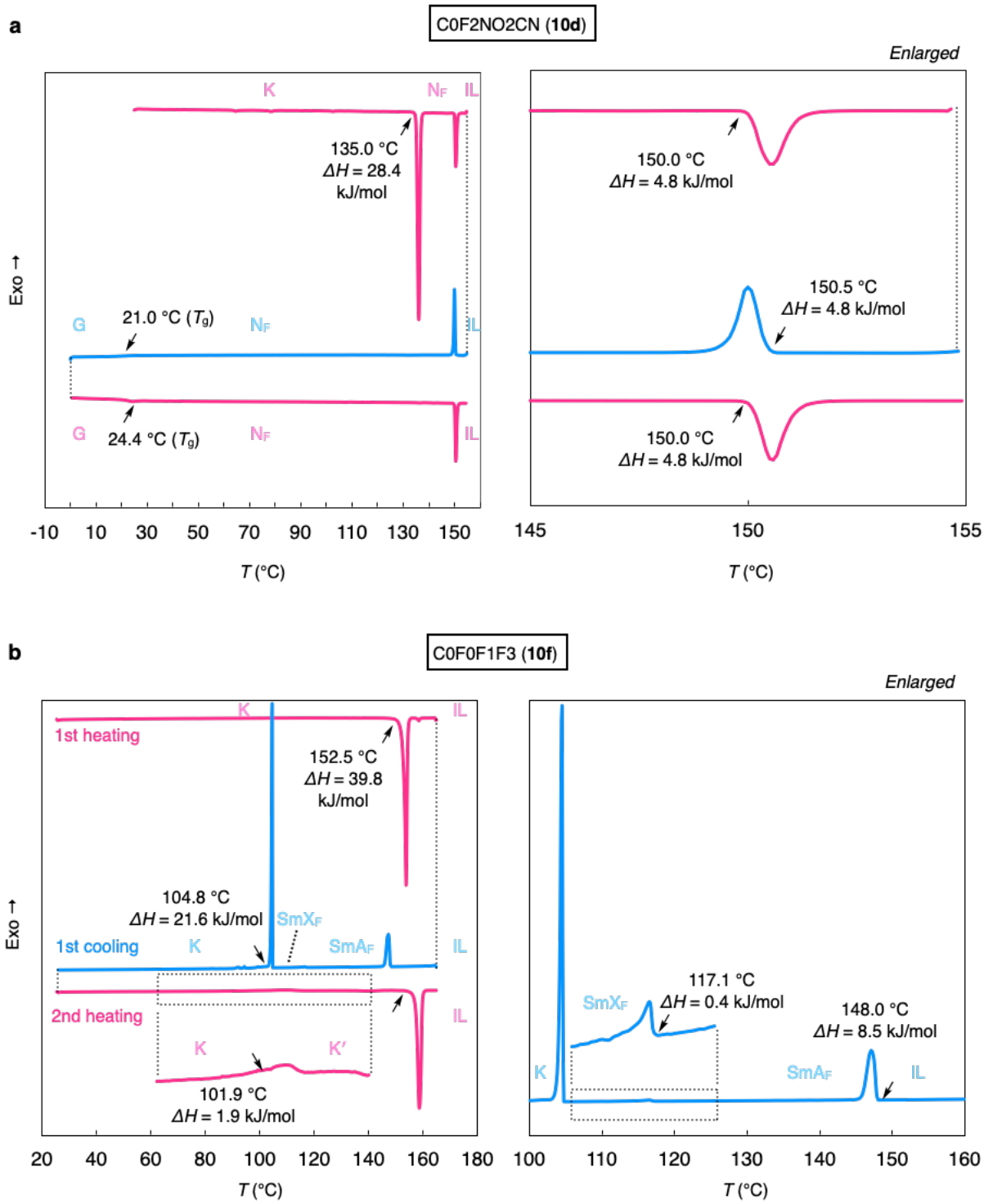

Fig. S9 DSC curves. (a) C0F2NO2CN (**10d**) and (b) C0F0F1F3 (**10f**). Scan rate: 5 K min^{-1}.

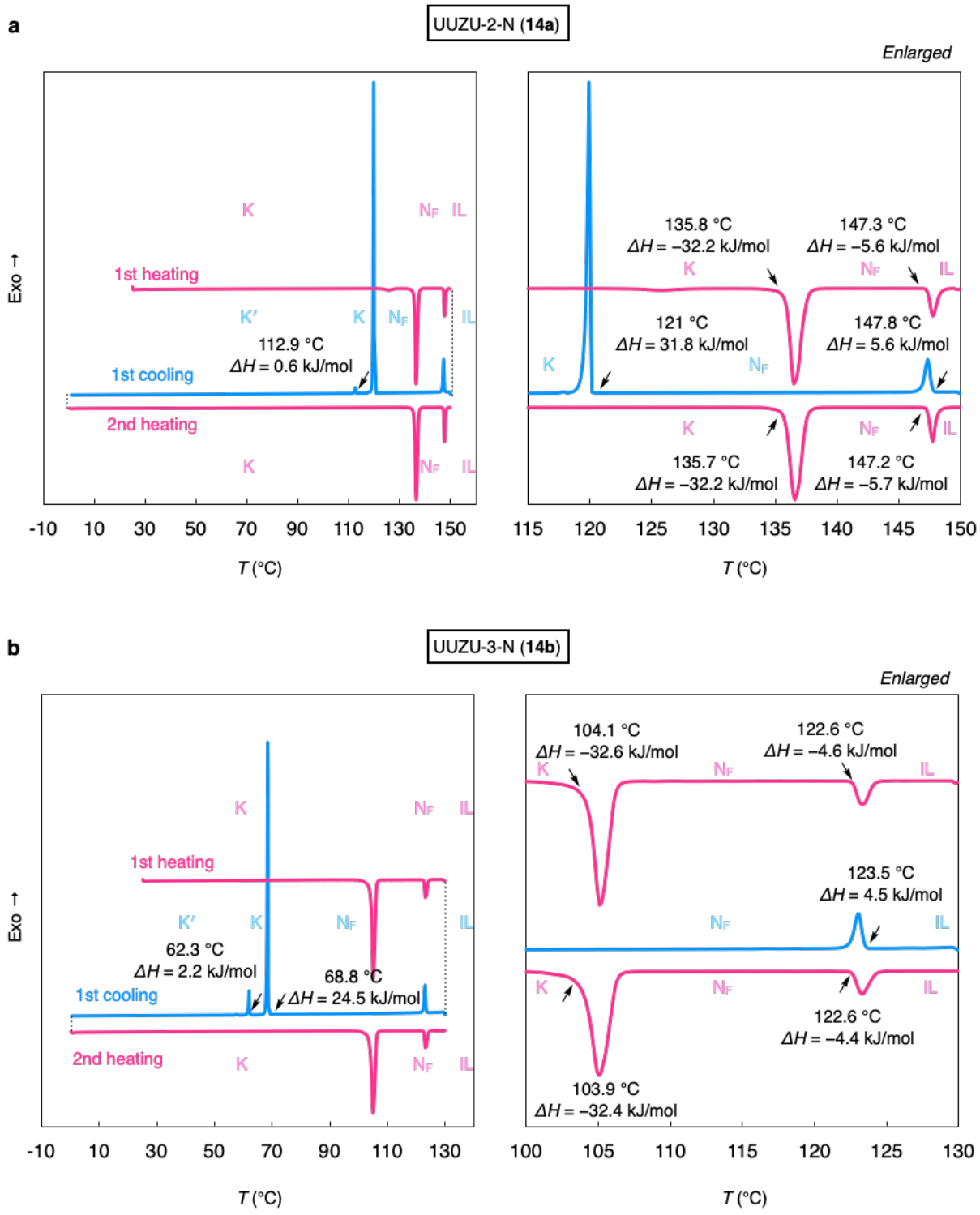

Fig. S10 DSC curves. (a) UUZU-2-N (**14a**) and (b) UUZU-3-N (**14b**). Scan rate: 5 K min^{-1}.

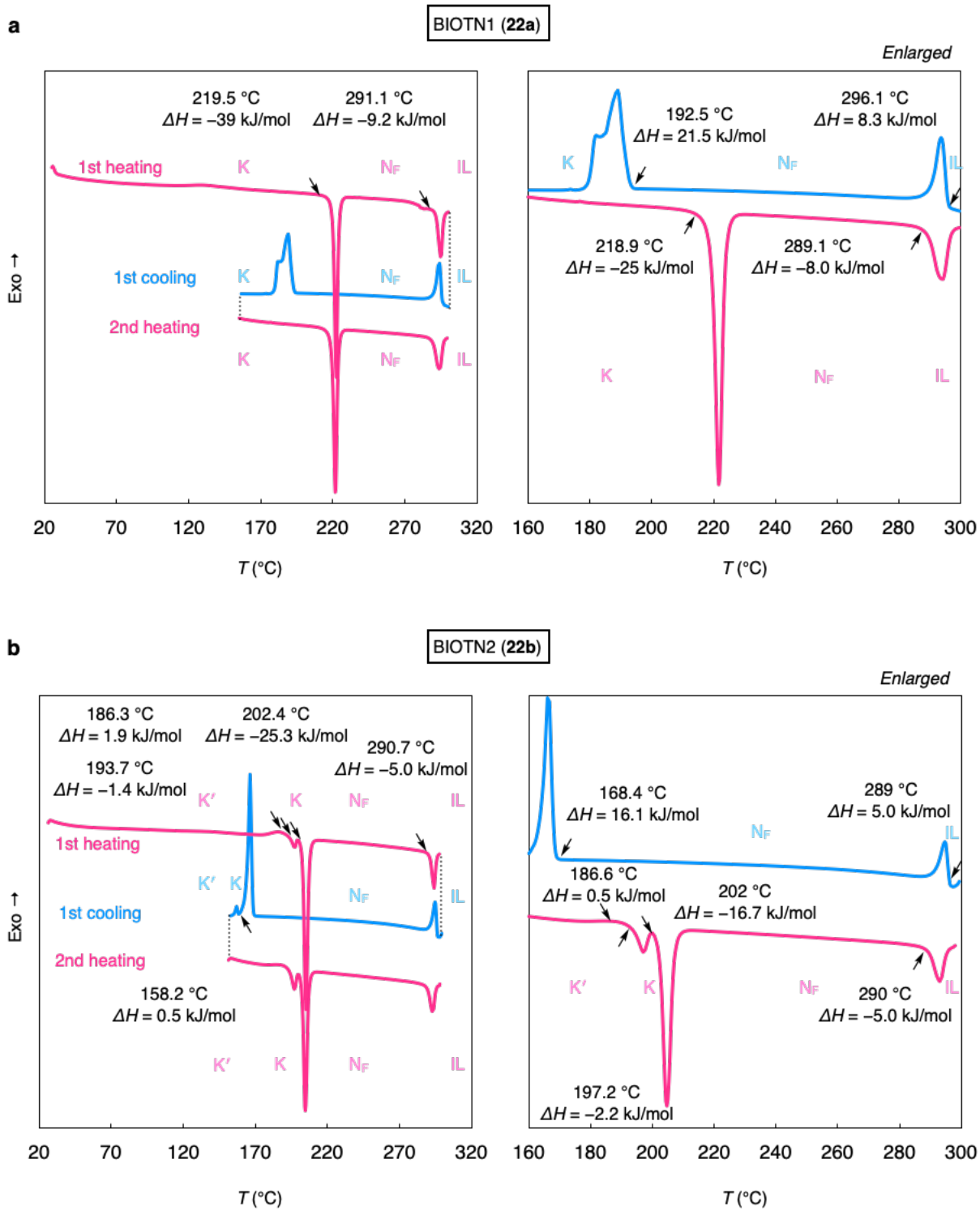

Fig. S11 DSC curves. (a) BIOTN1 (**22a**) and (b) BIOTN2 (**22b**). Scan rate: 20 K min^{-1}.

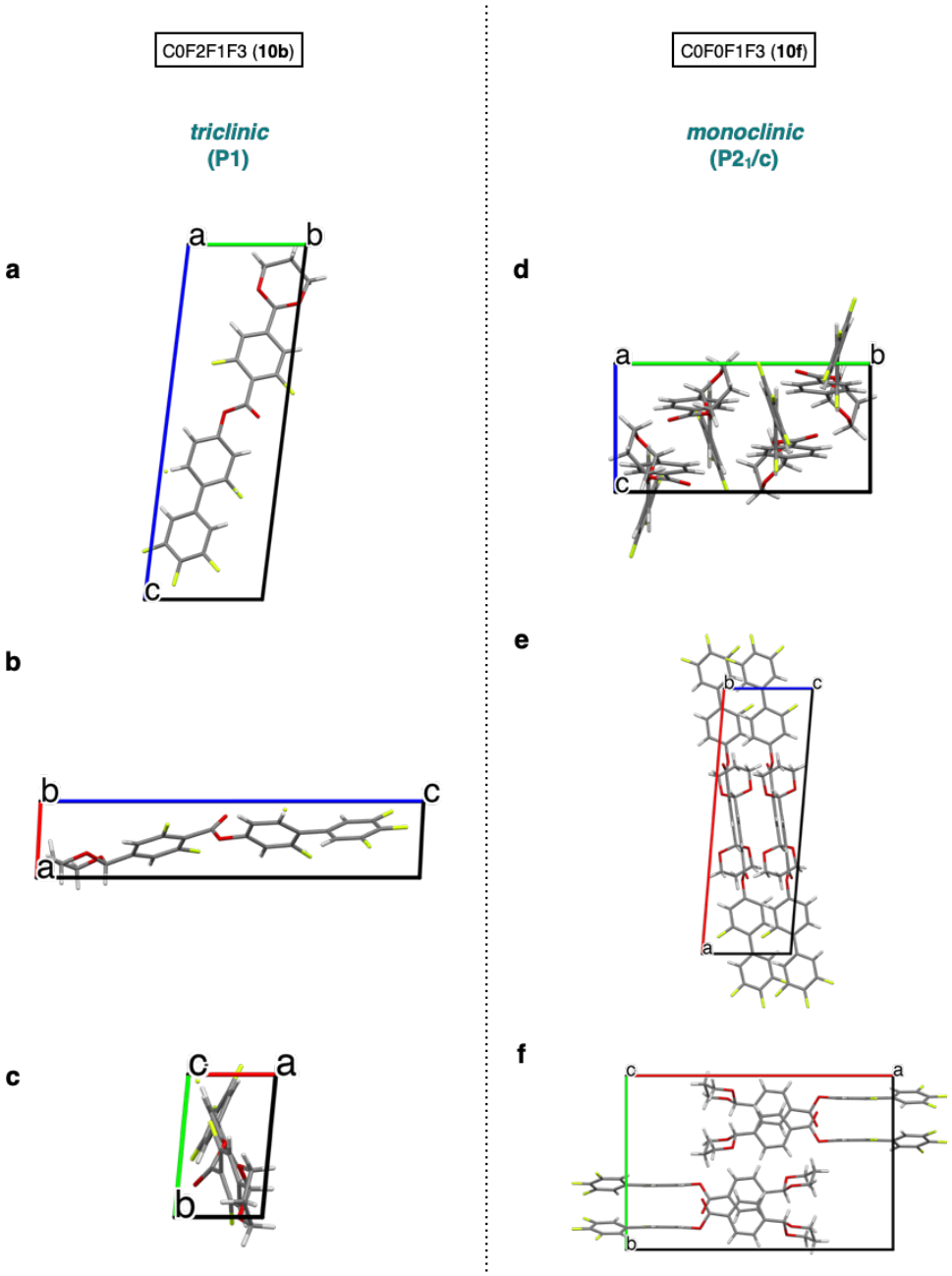

Fig. S12 SC-XRD data for 10b (left) and 10f (right). Panels a/d, b/e, and c/f donate the crystal structure viewed along the a-, b-, and c-axis, respectively. For **10b**, crystal system: triclinic, space group: *P*1, cell length: **a** = 3.88600(10) Å, **b** = 6.4109(2) Å, **c** = 19.4561(3) Å, cell angle: **α** = 96.797(2)°, **β** = 92.292(2)°, **γ** = 95.142(2)°, cell volume: **V** = 478.734 Å^3, **Z** = 1, **Z′** = 1, R-factor = 3.4 %; for **10f**, crystal system: monoclinic, space group: $P2_1/c$, cell length: **a** = 20.4308(2) Å, **b** = 13.35610(16) Å, **c** = 6.75589(7) Å, cell angle: **α** = 90°, **β** = 94.6910(11)°, **γ** = 90°, cell volume: **V** = 1837.34 Å^3, **Z** = 4, **Z′** = 1 R-factor = 3.44 %.

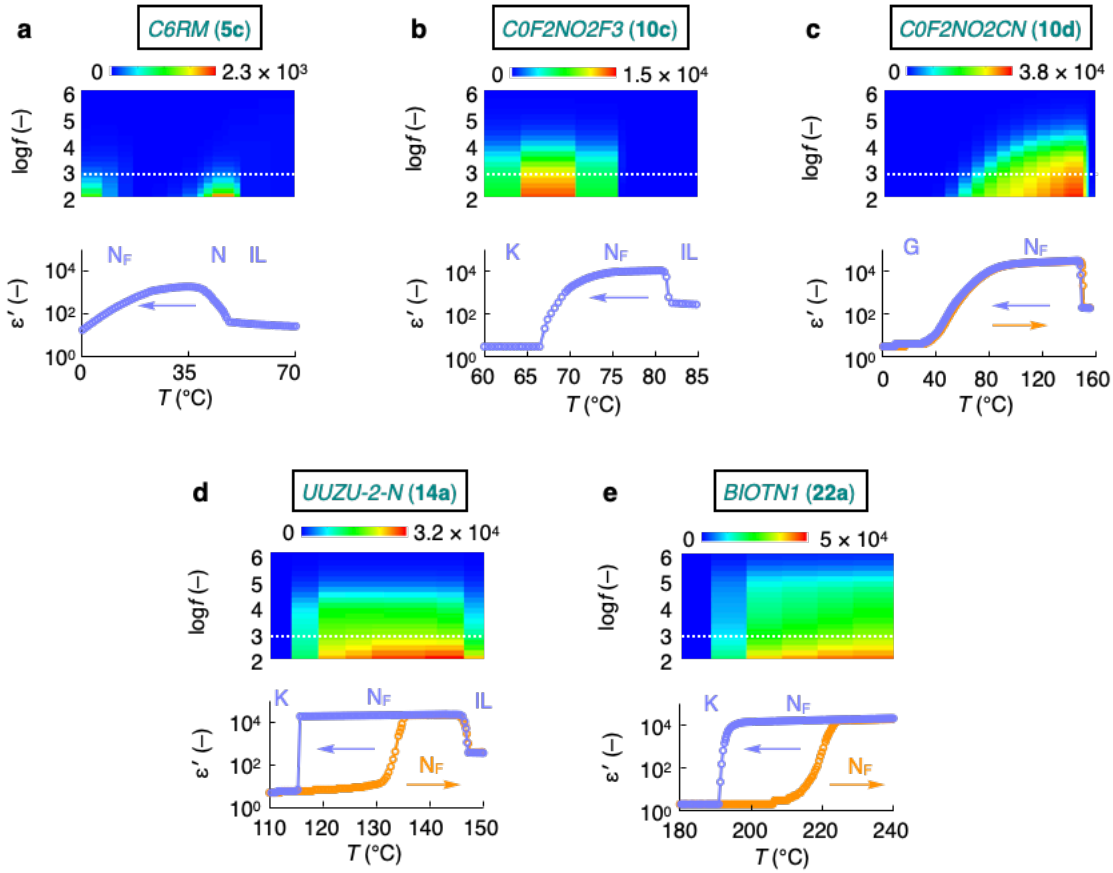

Fig. S13 Additional dielectric properties for N_FLC molecules. a) C6RM (**5b**), (b) C0F2NO2F3 (**10c**), (c) C0F2NO2CN (**10d**), (d) UUZU-2-N (**14a**) and (e) BIOTN1 (**22a**).

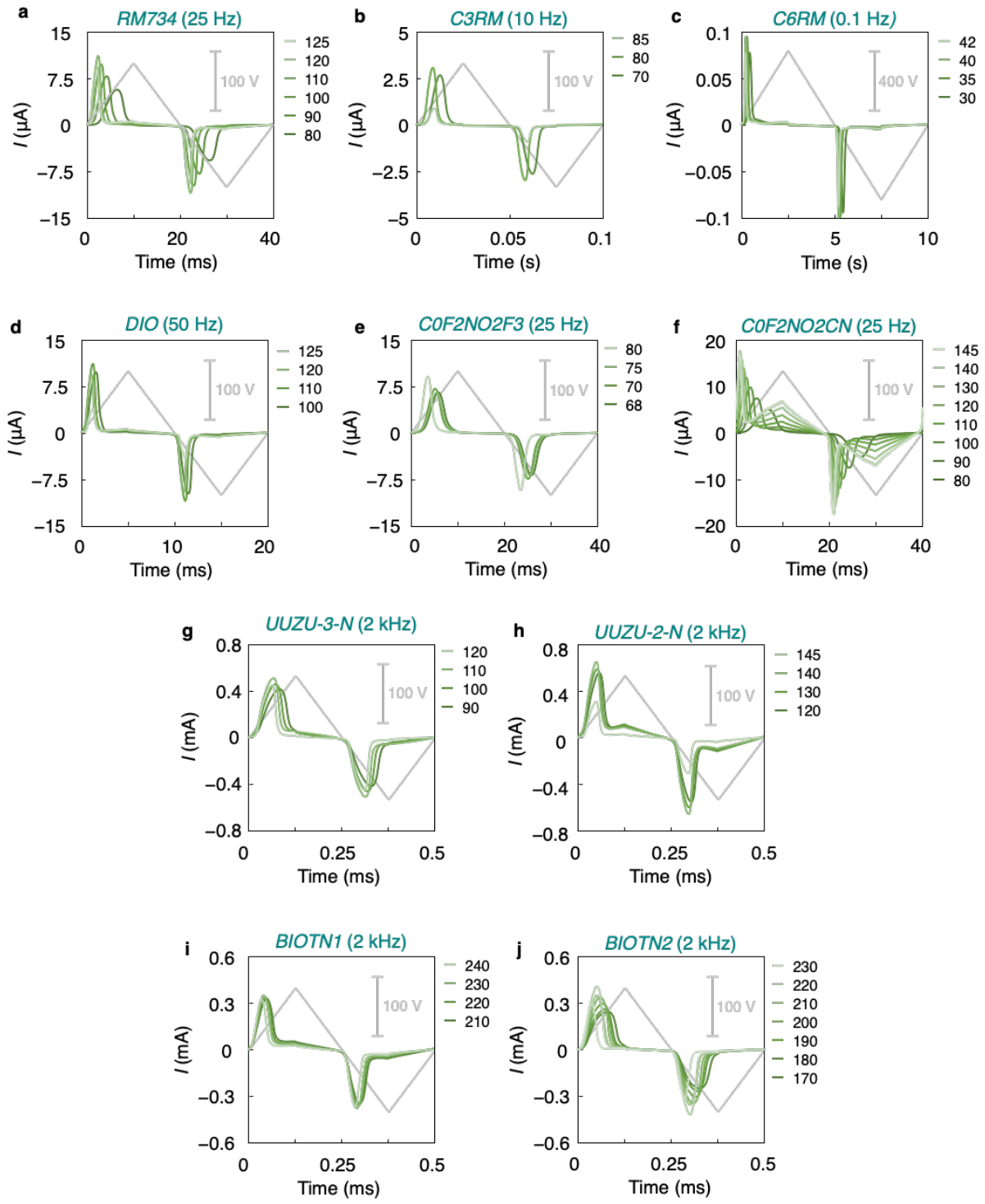

Fig. S14 Temperature dependence of reversal polarization current for the N_FLC molecules. a) RM734 (**5c**), (b) C3RM (**5a**), (c), C6RM (**5b**), (d) ^{trans}DIO (**10a**), (e) C0F2NO2F3 (**10c**), (f) C0F2NO2CN (**10d**), (g) UUZU-2-N (**14a**), (h) UUZU-3-N (**14b**), (i) BIOTN1 (**22a**) and (j) BIOTN2 (**22b**). V_{pp} = 200 V (for **5b**, V_{pp} = 800 V).

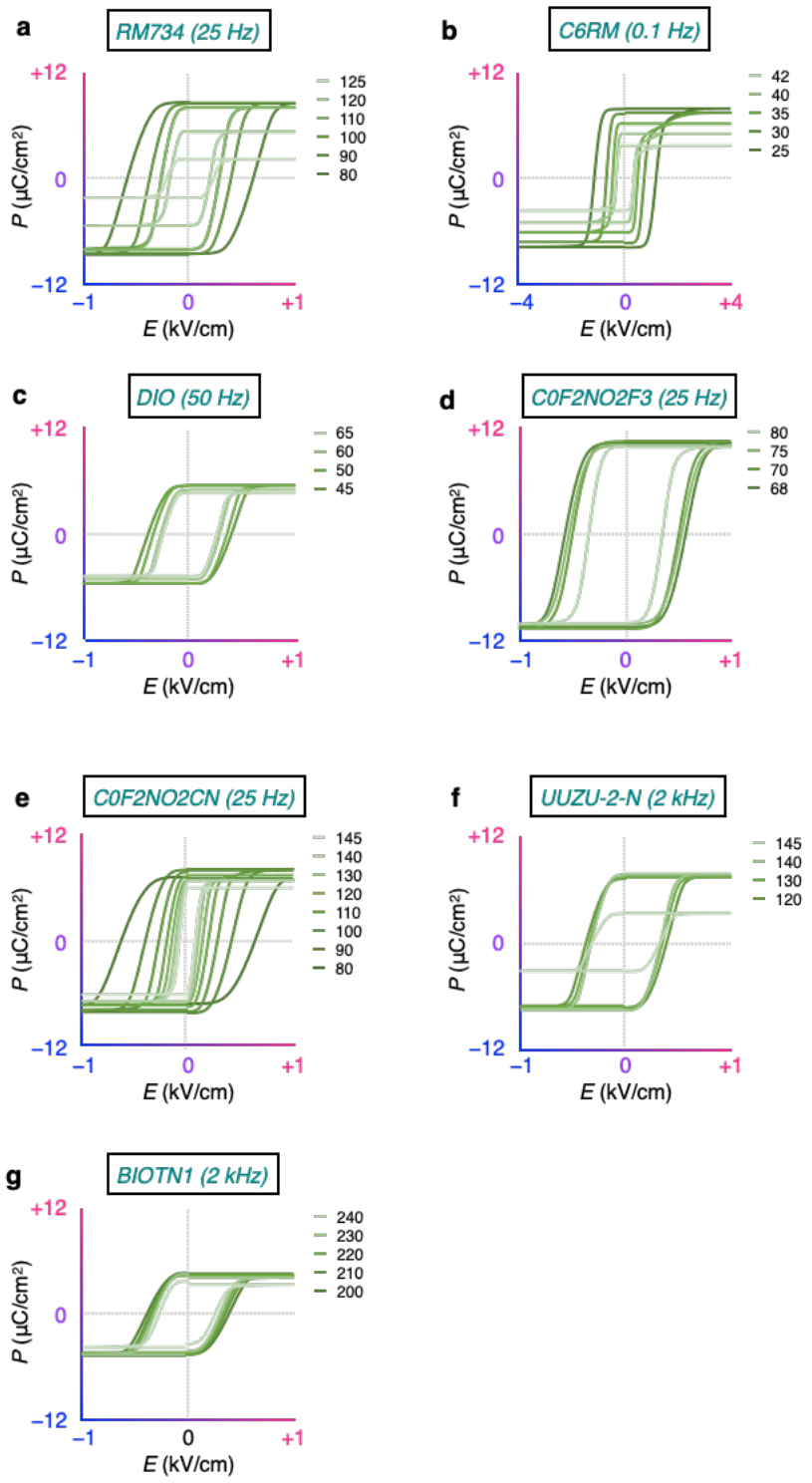

Fig. S15 Additional PE-HLs. a) RM734 (**5c**), (b) C6RM (**5b**), (c) *trans*DIO (**10a**), (d) C0F2NO2F3 (**10c**), (e) C0F2NO2CN (**10d**), (f) UUZU-2-N (**14a**) and (g) BIOTN1 (**22a**). The frequencies of input triangular wave voltage were 25 (a), 0.1 (b), 50 (c), 25 (d), 25 (e), 2000 (f), and 2000 Hz (g).

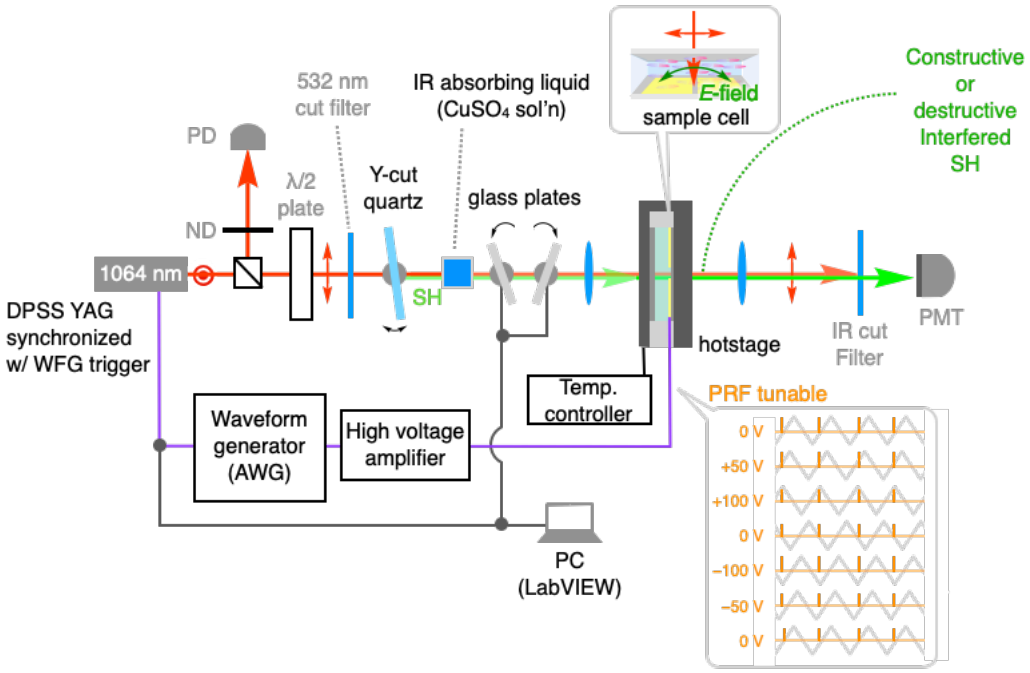

Fig. S16 Optical setup for SHG studies. The electric field (*E*-field) was applied normally to the sample cell (thickness: 5 μm).

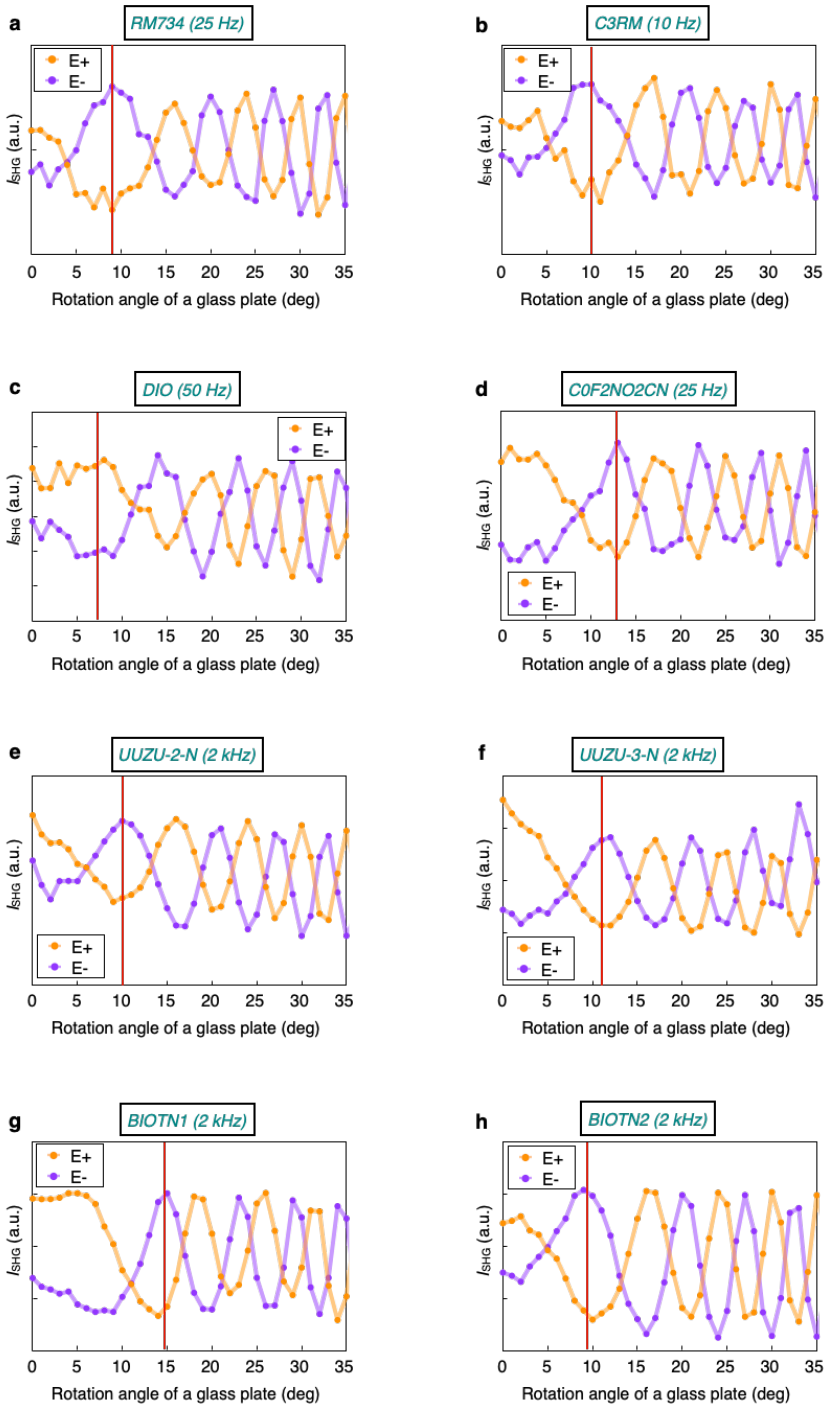

Fig. S17 Complete data of SHG interferograms. a) RM734 (**5c**), (b) C3RM (**5a**), (c) *trans*DIO (**10a**), (d) C0F2NO2CN (**10d**), (e) UUZU-2-N (**14a**), (f) UUZU-3-N (**14b**), (g) BIOTN1 (**22a**) and (h) BIOTN2 (**22b**). The mirror interferograms were generated by the application of *E*-field with + (orange line) and – (purple line) polarities. At the fixed angle marked by a red line, the SHG-HL was created.

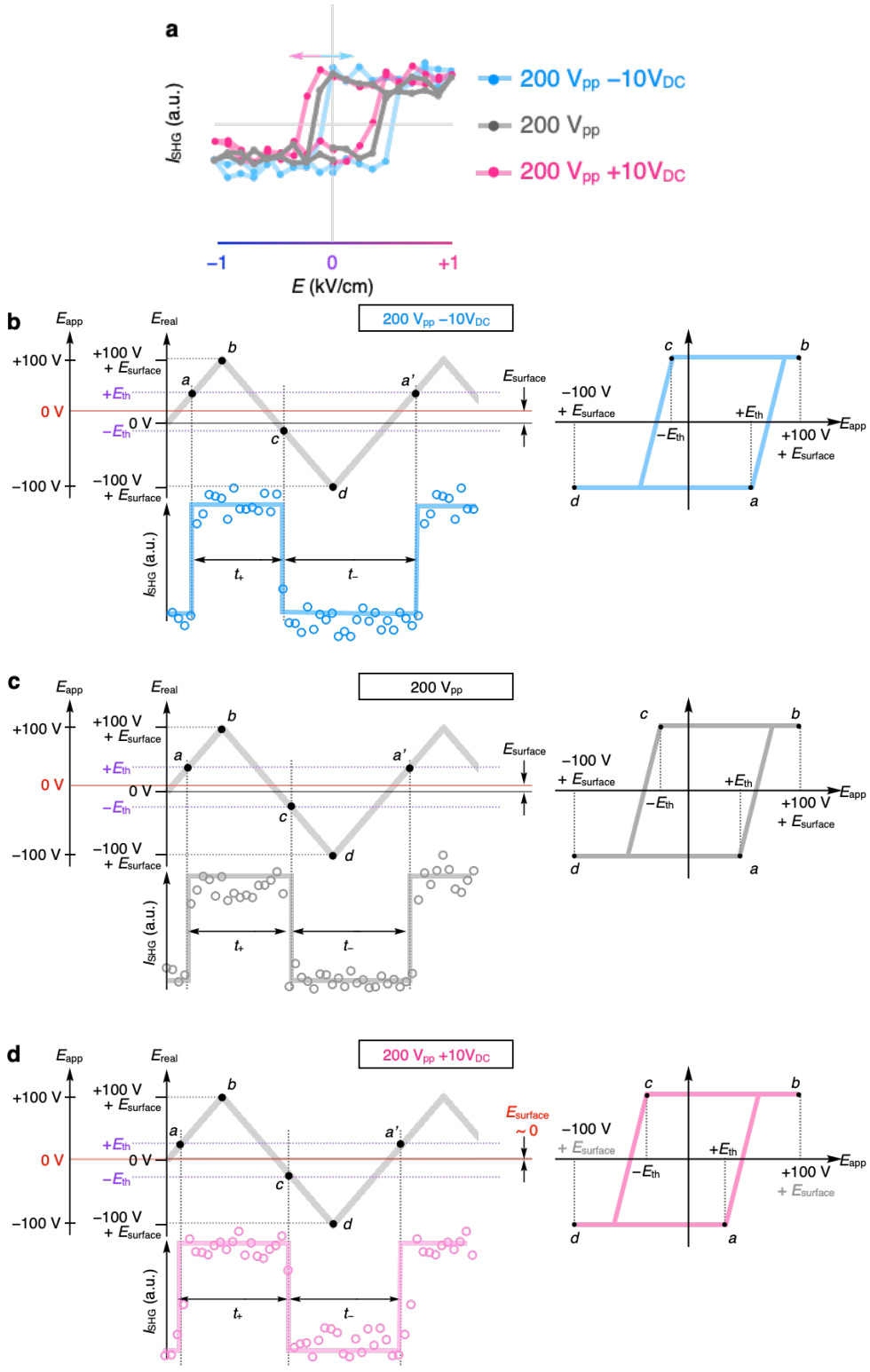

Fig. S18. **On the offset of the SHG hysteresis loops.** a) Typical appearance of the off-centered SHG hysteresis loops, b-d) time dependent SHG signal curves and the applied triangular field, where the *E*-field is shifted upper (b) or lower (c) due to the surface charge, resulting in the unbalancing of t_+ and t_- regions of SHG.

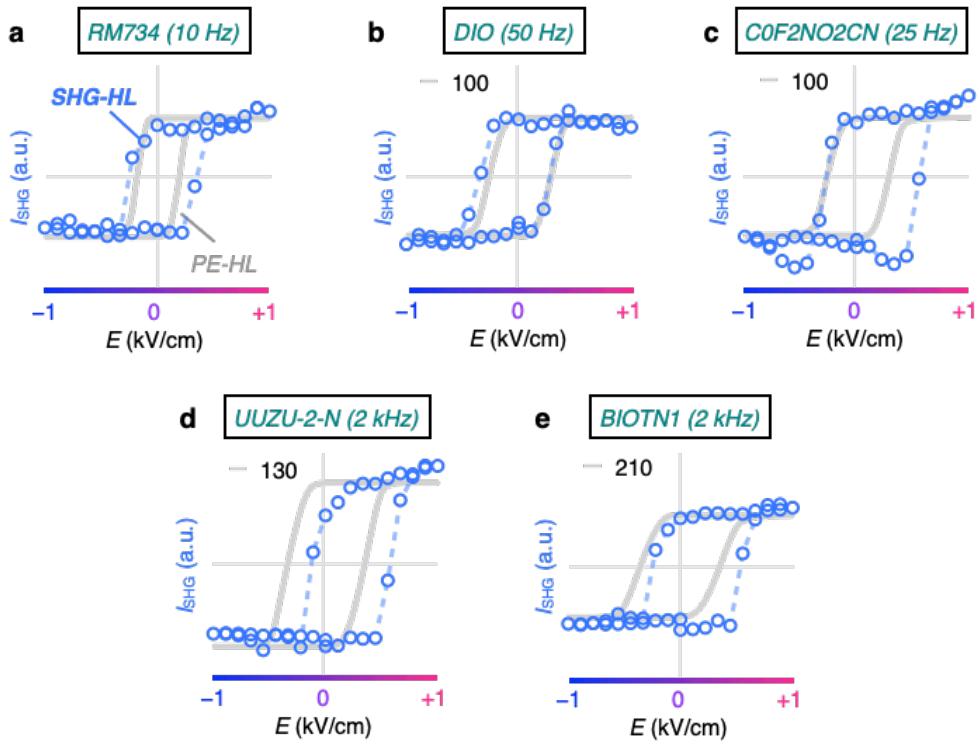

Fig. S19 Additional SHG-HL data. a) RM734 (**5c**), (b) DIO (**10a**), (c) C0F2NO2CN (**10d**), (d) UUZU-2-N (**14a**) and (e) BIOTN1 (**14a**). Note: the SHG-HL for C6RM (**5c**) and C0F2NO2F3 (**10c**) were not recorded because of their instability.

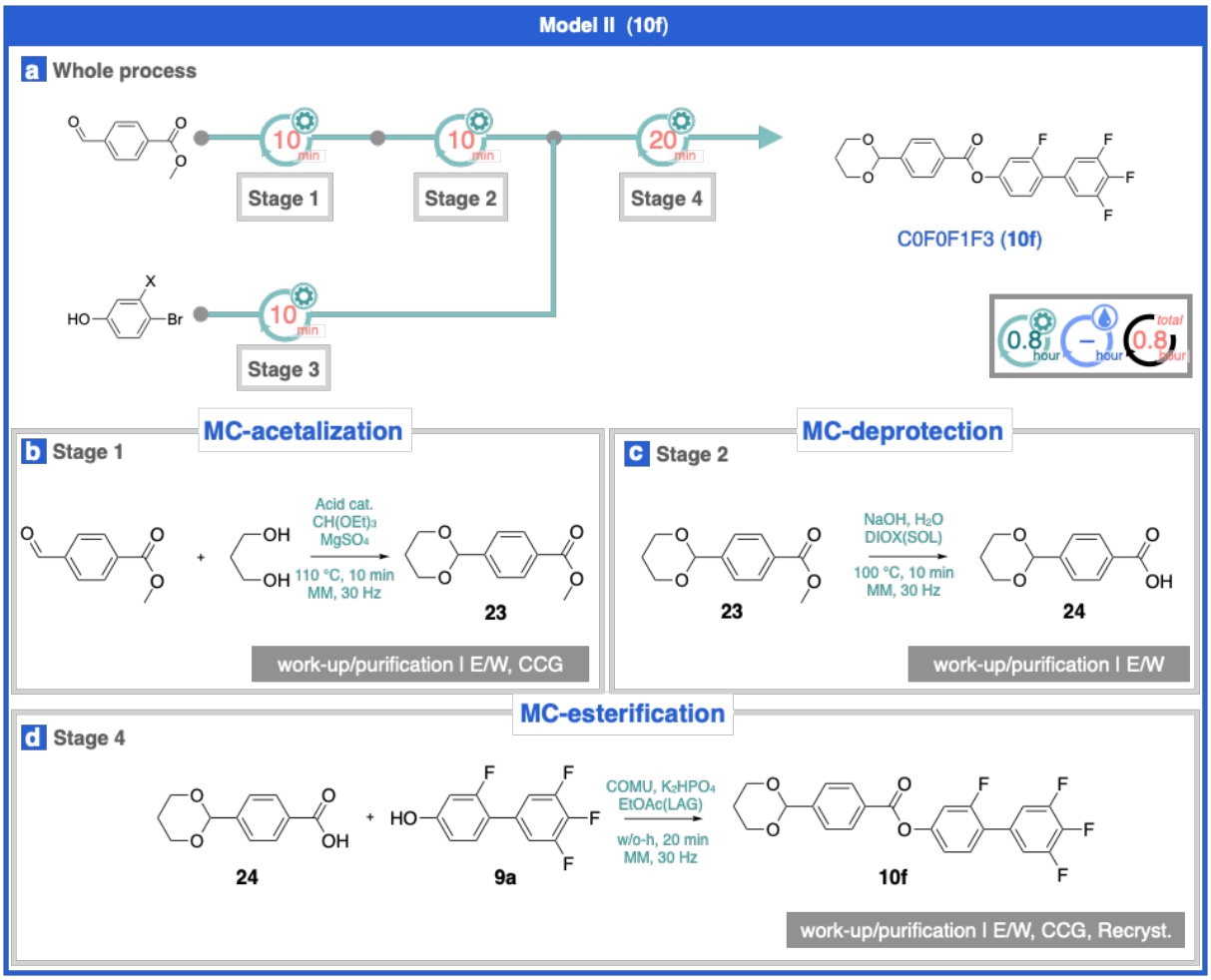

Fig. S20 The MC-synthesis pathway for **Model II** (**10f**).

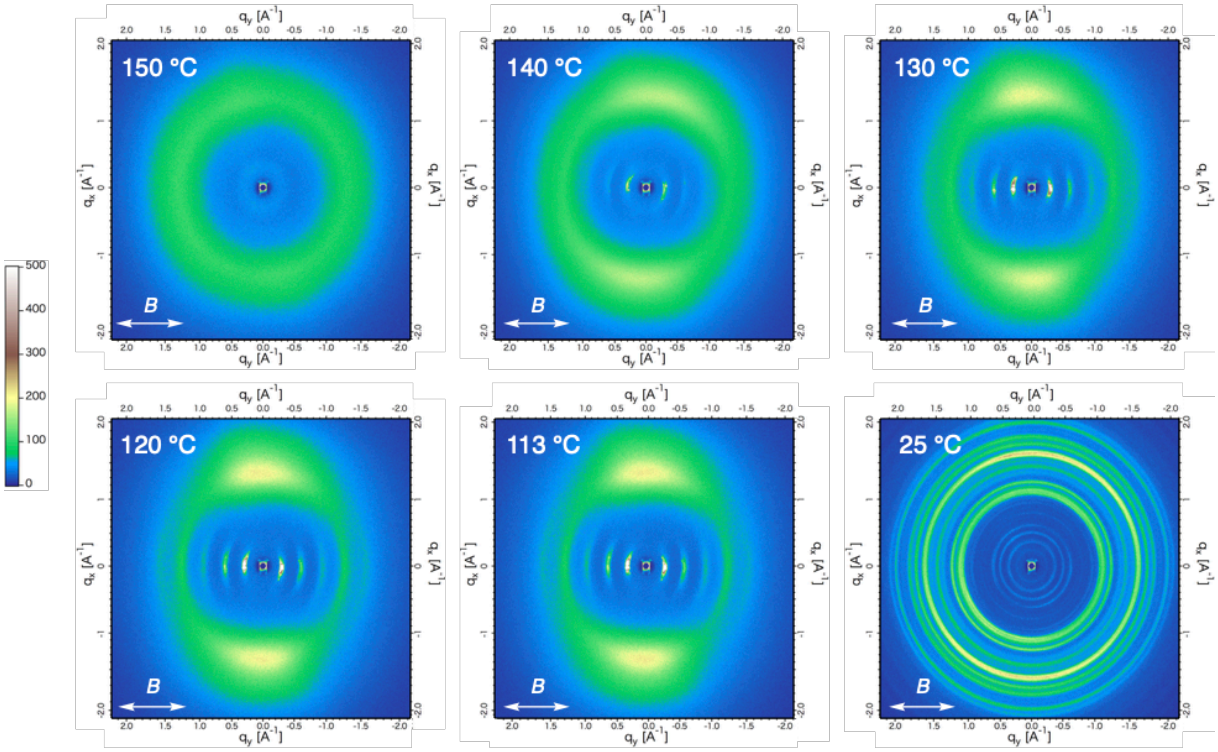

Fig. S21 Additional WAXD data in various temperatures for 10f.

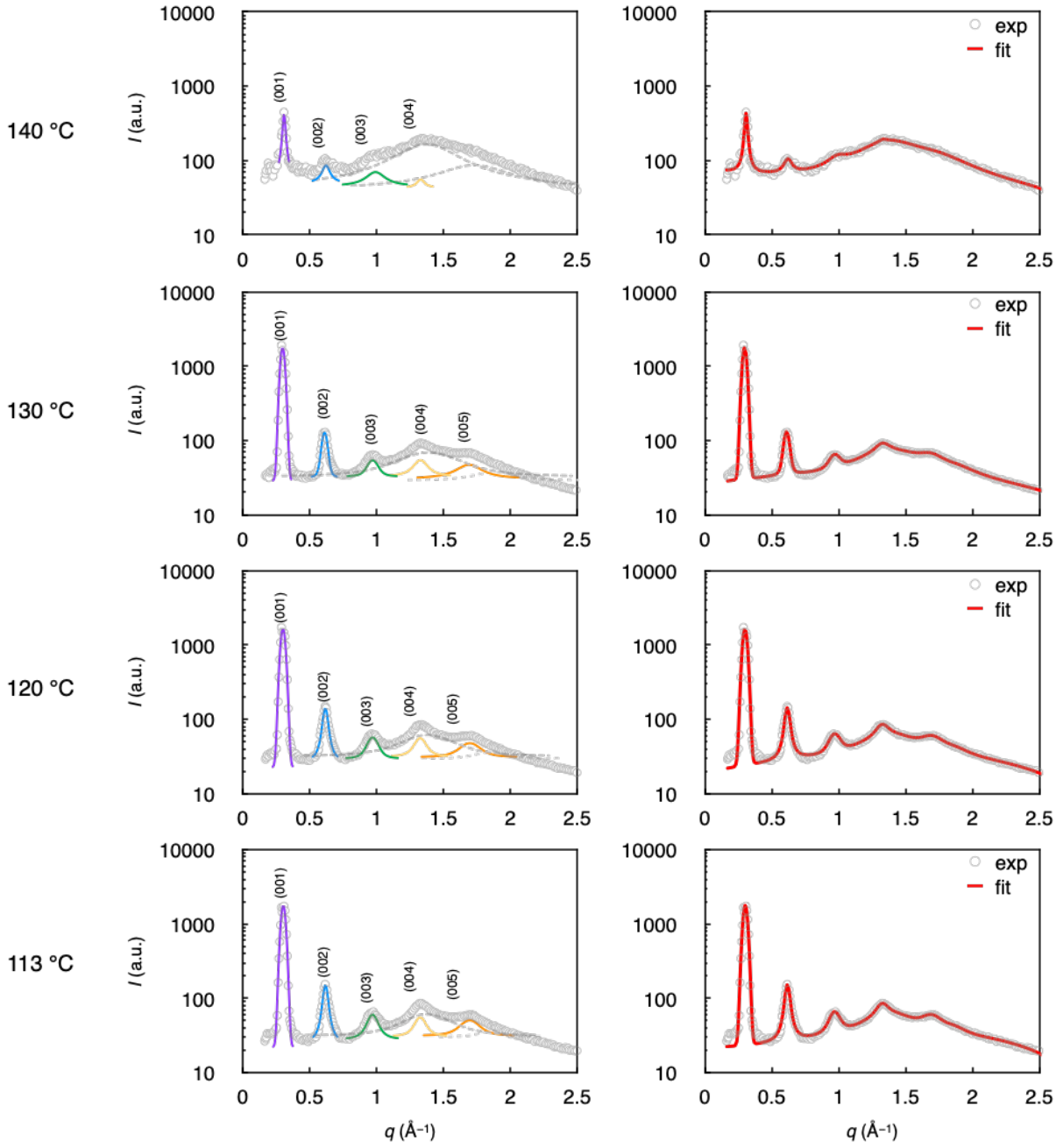

Fig. S22 1D WAXD profiles analyzed at φ_1 = 60° in various temperatures for 10f.

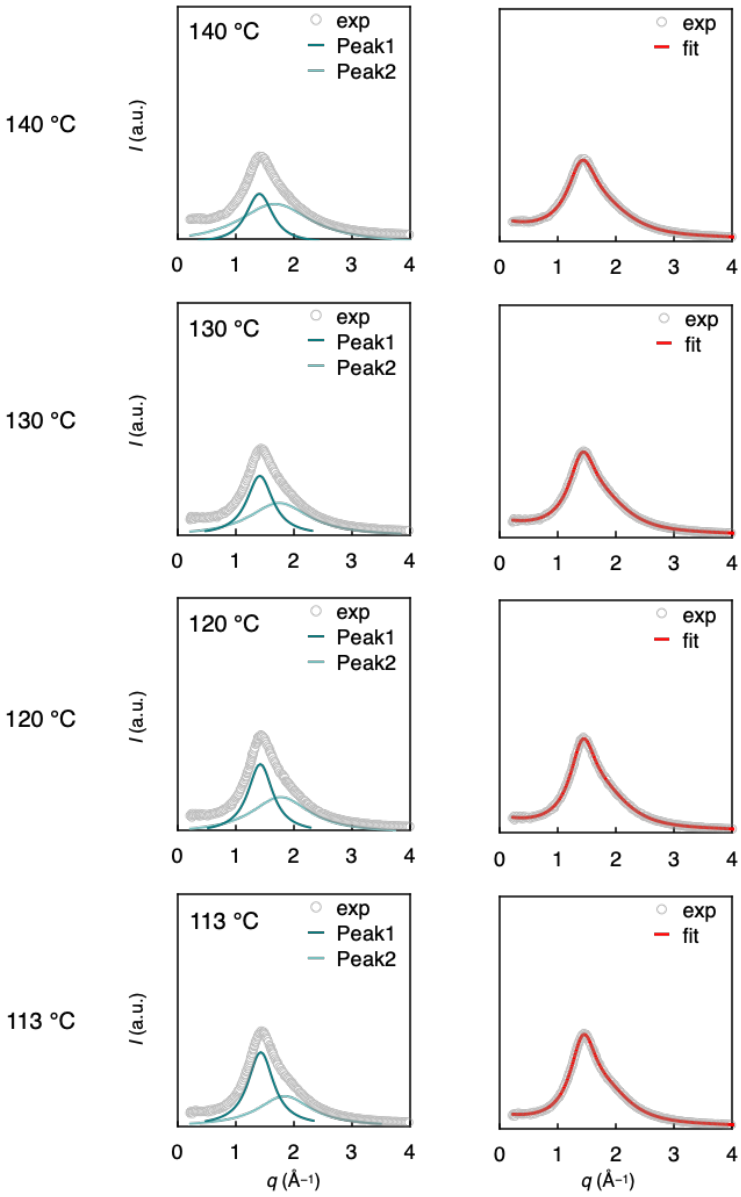

Fig. S23 1D WAXD profiles analyzed at φ_2 = 80° in various temperatures for 10f.

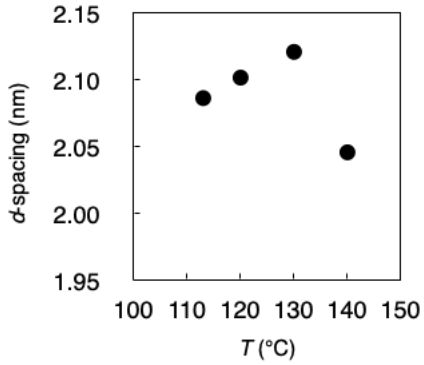

Fig. S24 *d*-spacing vs Temperature for 10f.

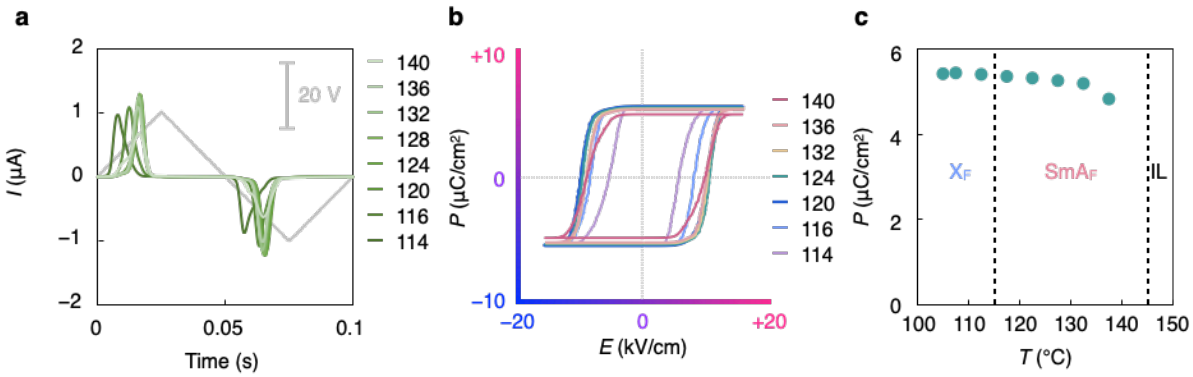

Fig. S25 PE-HL data in various temperatures (OPS) for 10f. a) reversal polarization current (V_{pp} = 40 V, 10 Hz), b) PE-HLs, c) polarization density vs temperature.

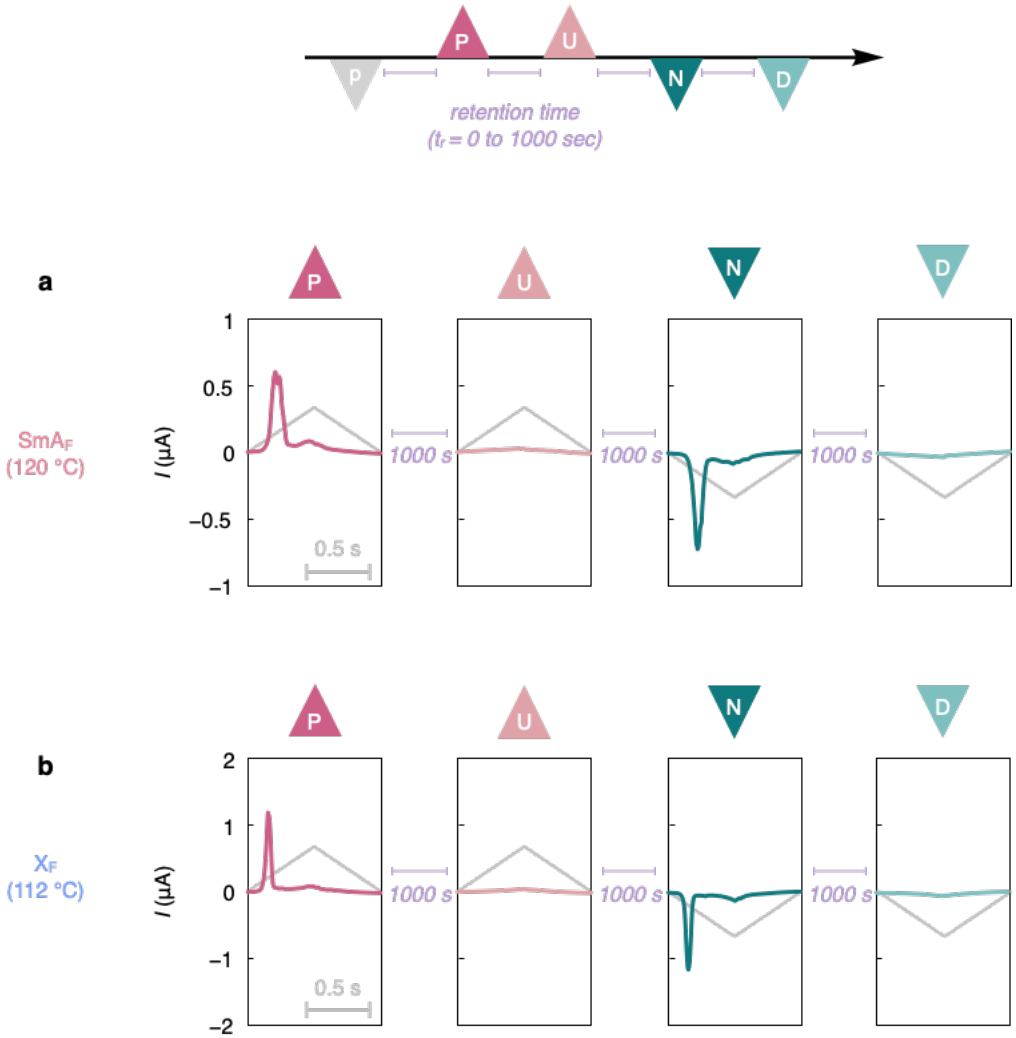

Fig. S26 Reversal polarization current under applied *E*-field with P, U, N and D waves (V_{pp} = 800 V, 0.5 Hz) in the SmA_F (a) and X_F (b) phases for **10f**. Retention time = 1000 s.

Supplementary Table (Table S1–S3)

Table S1 The molecular parameters of energy-minimized conformations calculated by MM2/DFT.

Entry	X	Y	Z	μ (D)	β (°)†
RM734 (**5c**)	11.4058	2.8278	–1.0036	11.8	14.7
RM3 (**5a**)	11.2184	2.4468	–1.5292	11.6	14.4
RM6 (**5b**)	11.354	1.7884	–1.7506	11.6	12.4
*trans*DIO (**10a**)	10.0829	0.3079	–0.5899	10.1	3.8
*cis*DIO (**10e**)	9.255	1.1777	2.7013	9.7	17.7
C0F2F1F3 (**10b**)	9.4917	1.1707	–2.5183	9.9	16.3
C0F0F1F3 (**10f**)	8.2852	–1.4955	–3.0914	9.0	22.5
C0F2NO2F3 (**10c**)	10.932	–4.4853	–3.1284	12.2	26.6
C0F2NO2CN (**10d**)	14.4588	0.516	3.6987	14.9	14.5
UUZU2N (**14a**)	–12.4749	–1.2162	0.6858	12.6	6.4
UUZU3N (**14b**)	–12.5979	–1.0173	0.6037	12.7	5.4
BIOTN1 (**22a**)	14.9672	–0.0374	0.0803	15.0	0.3
BIOTN2 (**22b**)	–15.1732	0.0613	0.0475	15.2	0.3

†, an angle between the permanent dipole moment (μ) and long molecular axis.

Table S2 The scattering vector (q) and the corresponding observed/calculated d-spacing of integrated WAXD patterns in various temperatures (φ_1 = 60°, under the magnetic field) for **10f**.

	140 °C			130 °C			120 °C			113 °C		
hkl	q (Å^{-1})	$d_{obs.}$ (nm)	$d_{calc.}$ (nm)	q (Å^{-1})	$d_{obs.}$ (nm)	$d_{calc.}$ (nm)	q (Å^{-1})	$d_{obs.}$ (nm)	$d_{calc.}$ (nm)	q (Å^{-1})	$d_{obs.}$ (nm)	$d_{calc.}$ (nm)
001	0.31	2.05	–	0.30	2.12	–	0.30	2.10	–	0.30	2.09	–
002	0.62	1.01	1.02	0.61	1.03	1.06	0.62	1.02	1.05	0.62	1.02	1.04
003	0.99	0.63	0.68	0.97	0.65	0.71	0.97	0.65	0.70	0.97	0.64	0.70
004	1.33	0.47	0.51	1.33	0.47	0.53	1.33	0.47	0.53	1.33	0.47	0.52
005	1.73	–	–	1.69	0.37	0.42	1.69	0.37	0.42	1.70	0.37	0.42

Table S3 The scattering vector (q) and the corresponding observed d-spacing of integrated WAXD patterns in various temperatures (φ_2 = 80°, under the magnetic field) for **10f**.

T (°C)	q_{peak1} (Å^{-1})	q_{peak2} (Å^{-1})	d_{peak1} (nm)	d_{peak2} (nm)
140	1.41	1.68	0.45	0.37
130	1.42	1.75	0.44	0.36
120	1.43	1.78	0.44	0.35
113	1.44	1.85	0.44	0.34

Supplementary References

S1 M. J. Frisch, G. W. Trucks, H. B. Schlegel, G. E. Scuseria, M. A. Robb, J. R. Cheeseman, G. Scalmani, V. Barone, B. Mennucci, G. A. Petersson, H. Nakatsuji, M. Caricato, X. Li, H. P. Hratchian, A. F. Izmaylov, J. Bloino, G. Zheng, J. L. Sonnenberg, M. Hada et al. Gaussian 09, revision E.01; Gaussian, Inc.: Wallingford, CT, 2009.

S2 T. Seo, N. Toyoshima, K. Kubota and H. Ito, *J. Am. Chem. Soc.* 2021, **143**, 6165–6175.

S3 T. Dalidovich, K. A. Mishra, T. Shalima, M. Kudrjašova, D. G. Kananovich and R. Aav, *ACS Sustainable Chem. Eng.*, 2020, **8**, 15703–15715.

Supplementary Spectra

*^{1}H NMR (a) and $^{13}C\{^{1}H\}$ NMR (b) spectra of compound **1a***

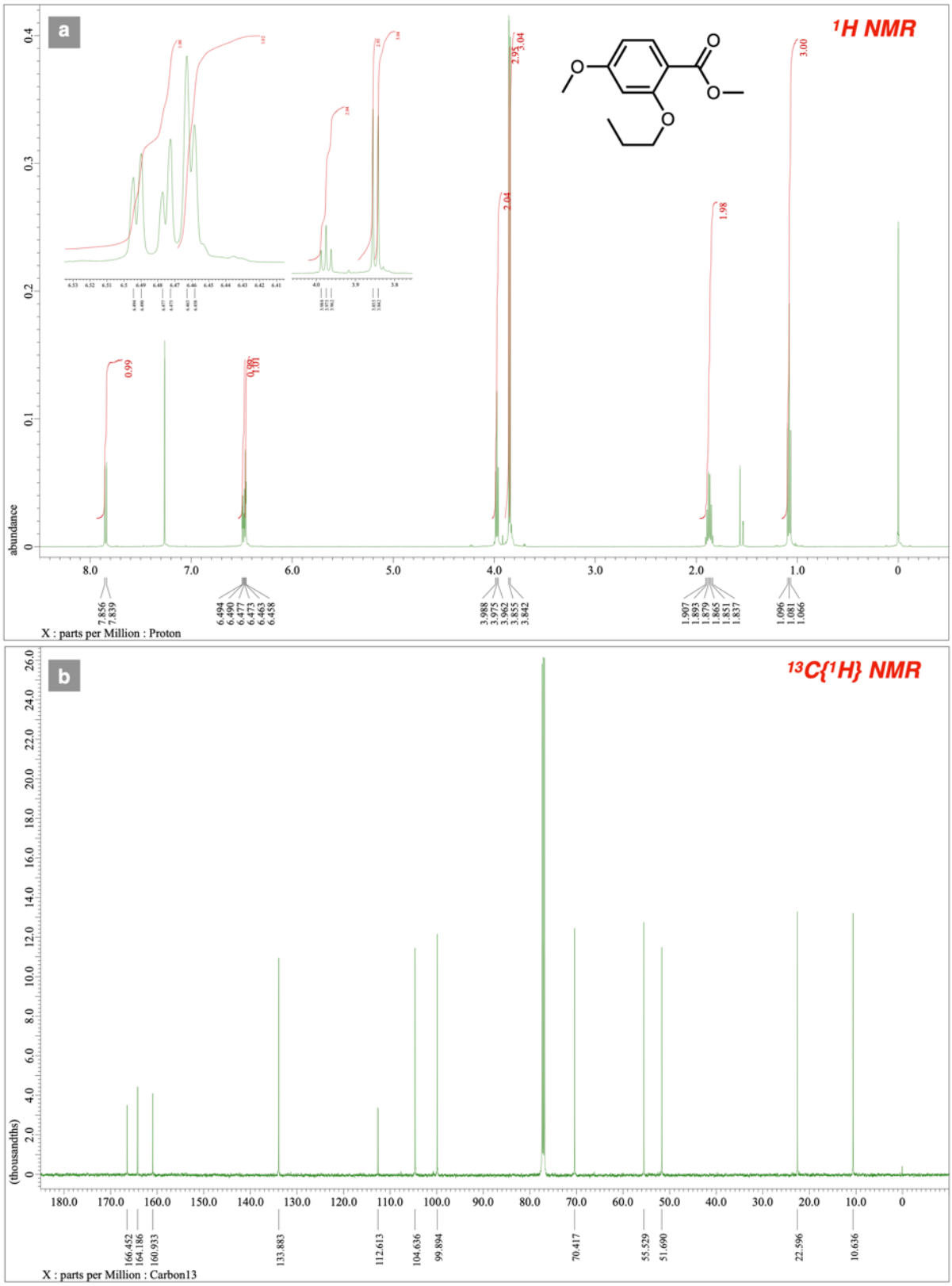

QTOF-HRMS spectra of compound ***1a***

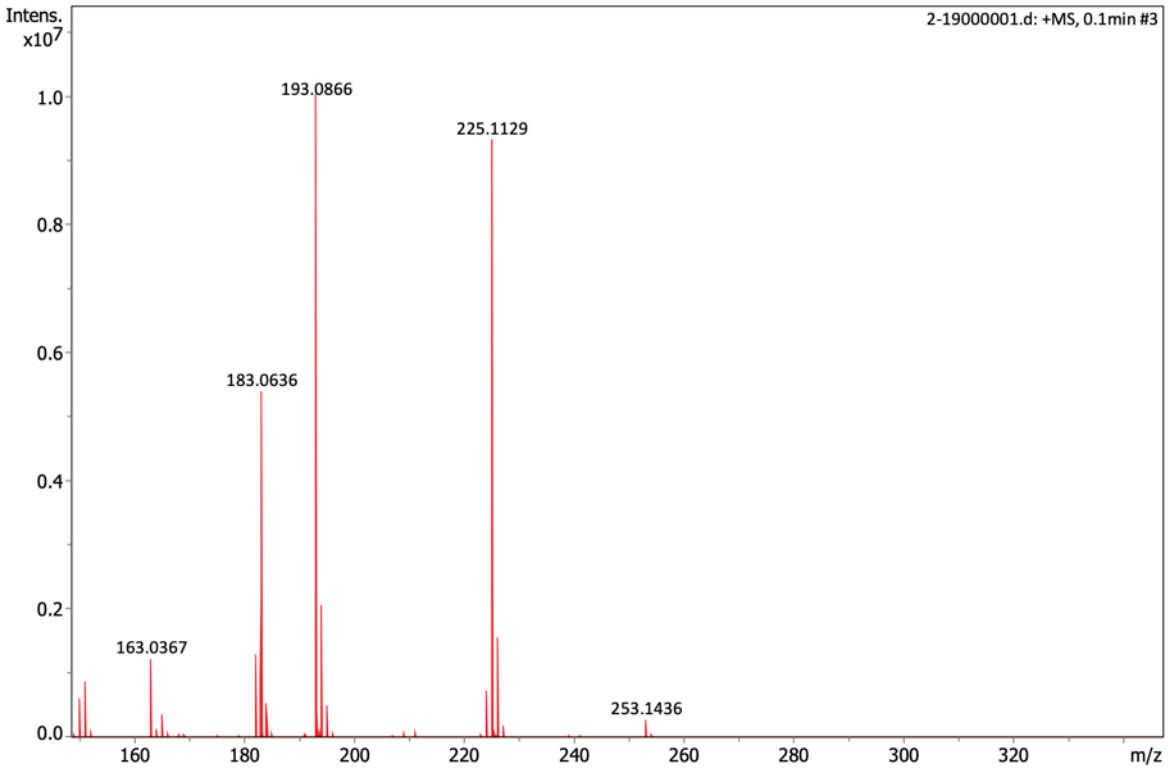

^{1}H NMR (a) and $^{13}C\{^{1}H\}$ NMR (b) spectra of compound ***1b***

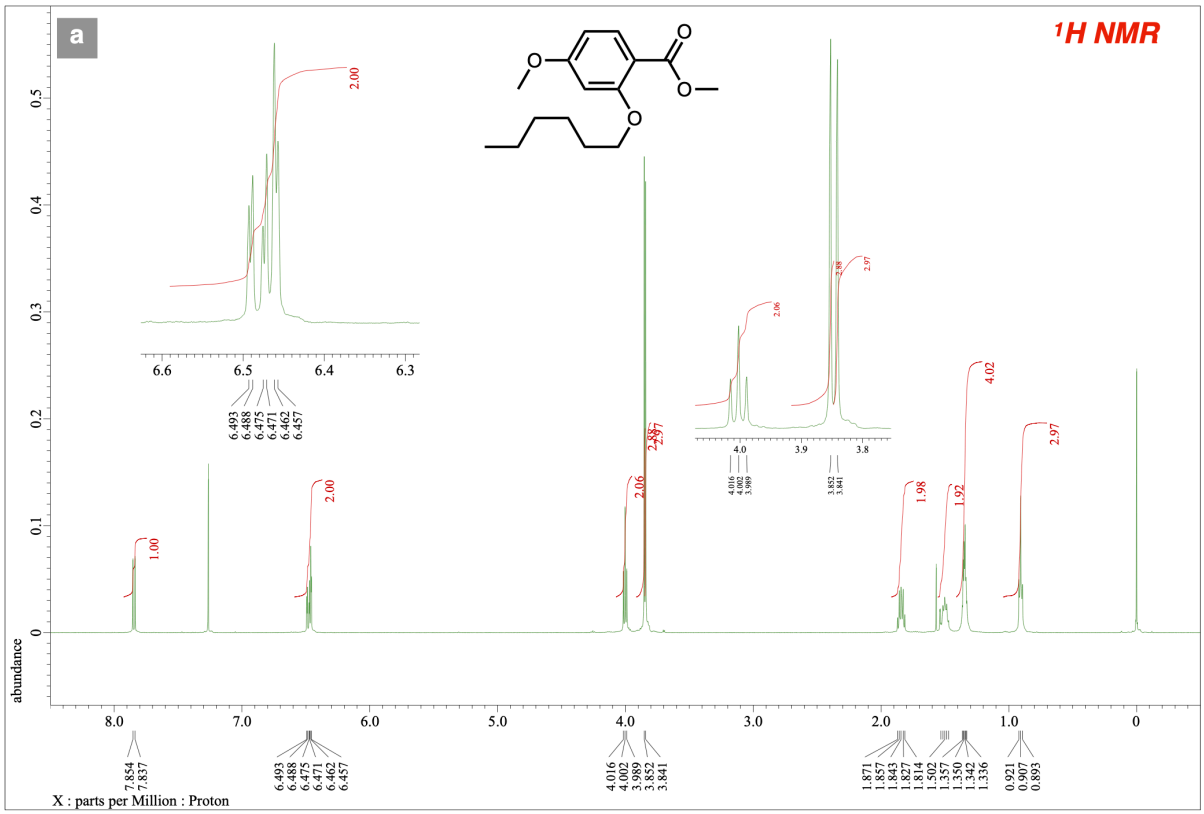

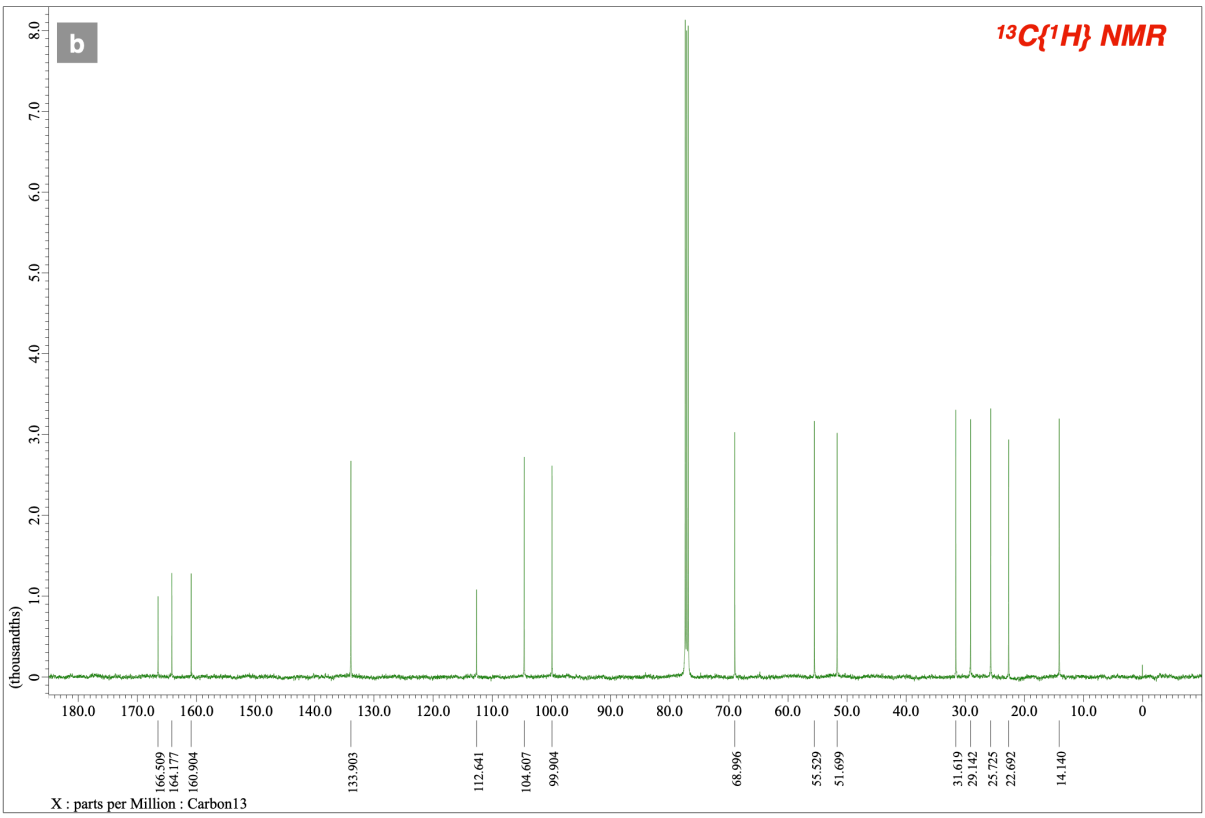

QTOF-HRMS spectra of compound ***1b***

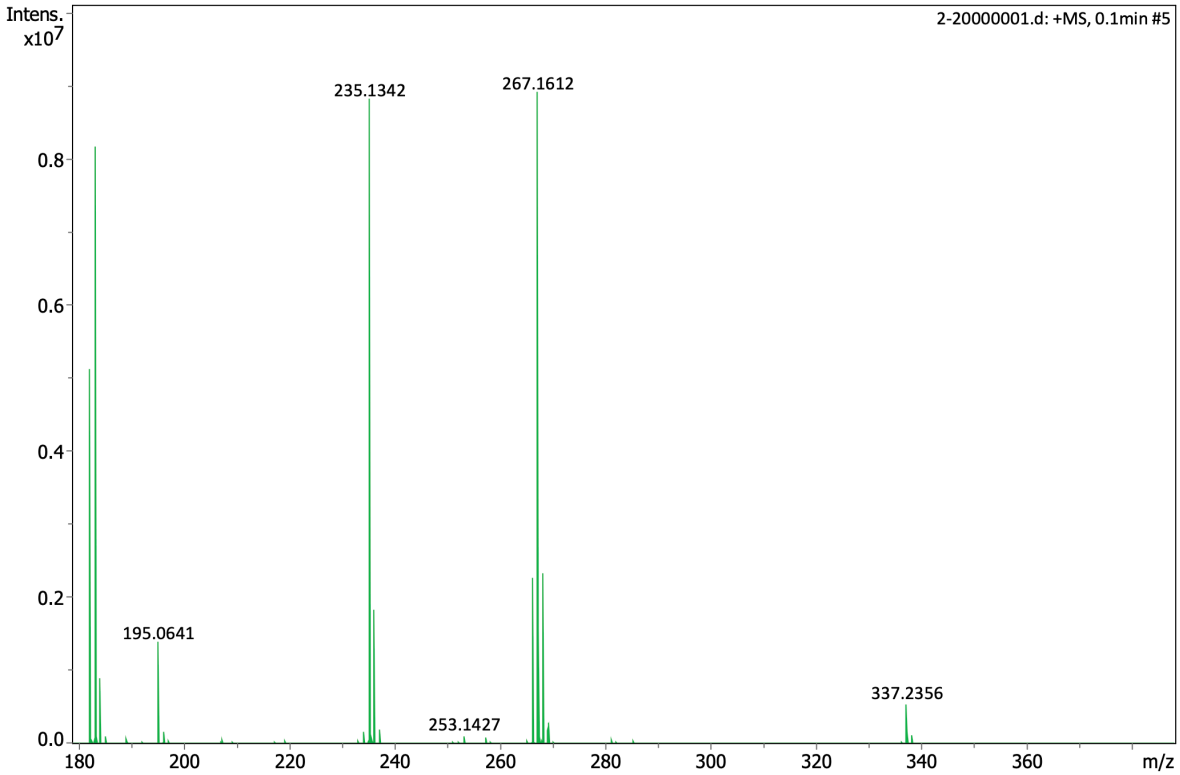

*^{1}H NMR (a) and $^{13}C\{^{1}H\}$ NMR (b) spectra of compound **2a***

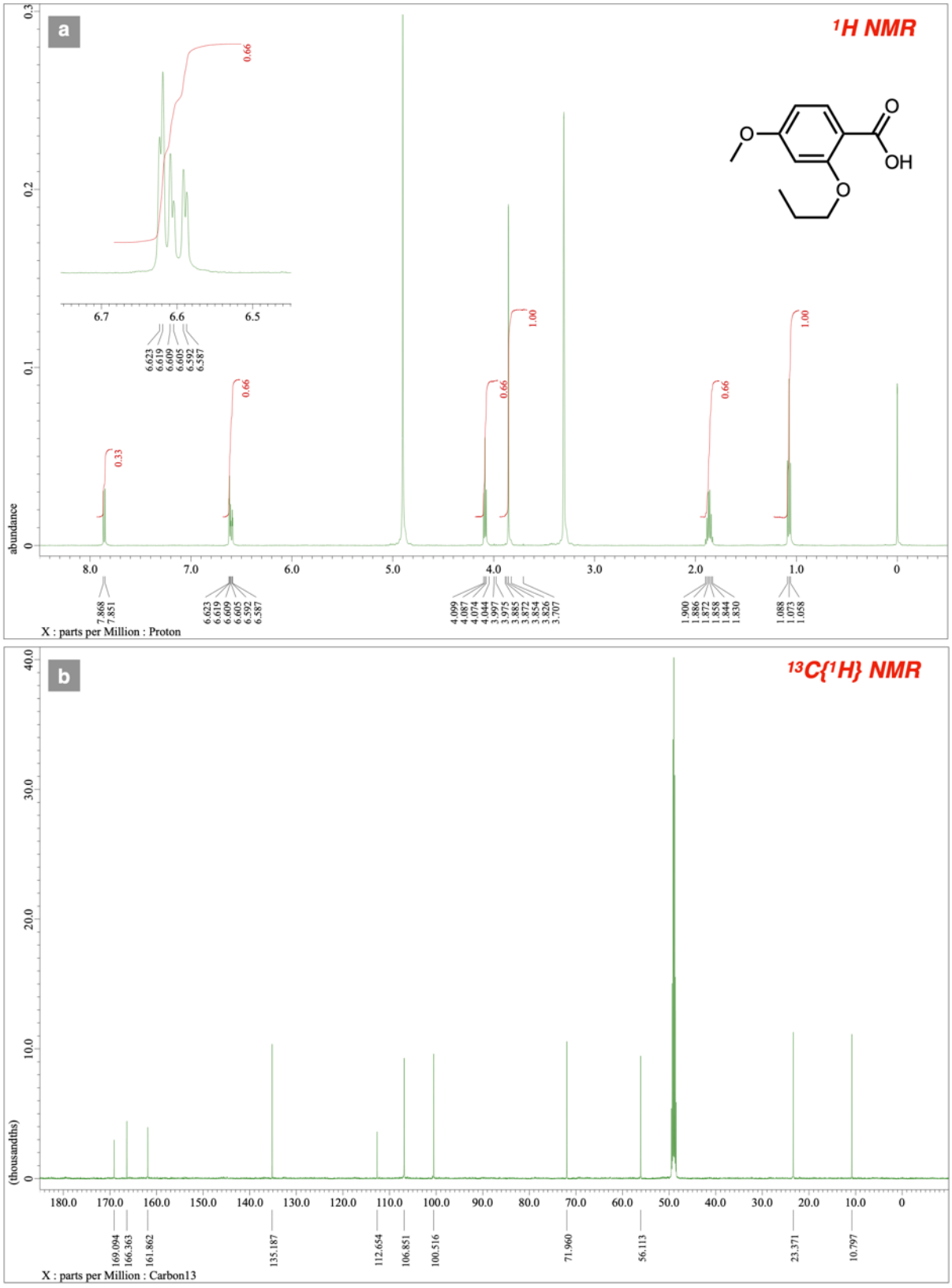

QTOF-HRMS spectra of compound ***2a***

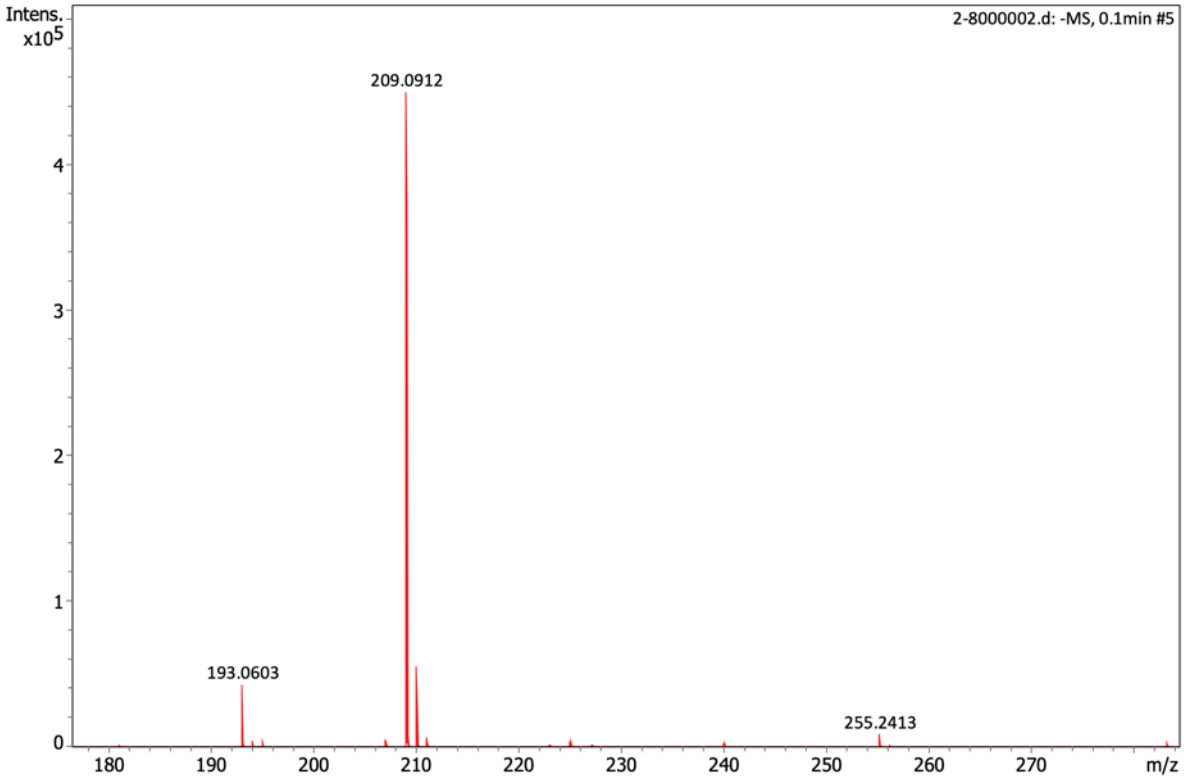

^{1}H NMR (a) and $^{13}C\{^{1}H\}$ NMR (b) spectra of compound ***2b***

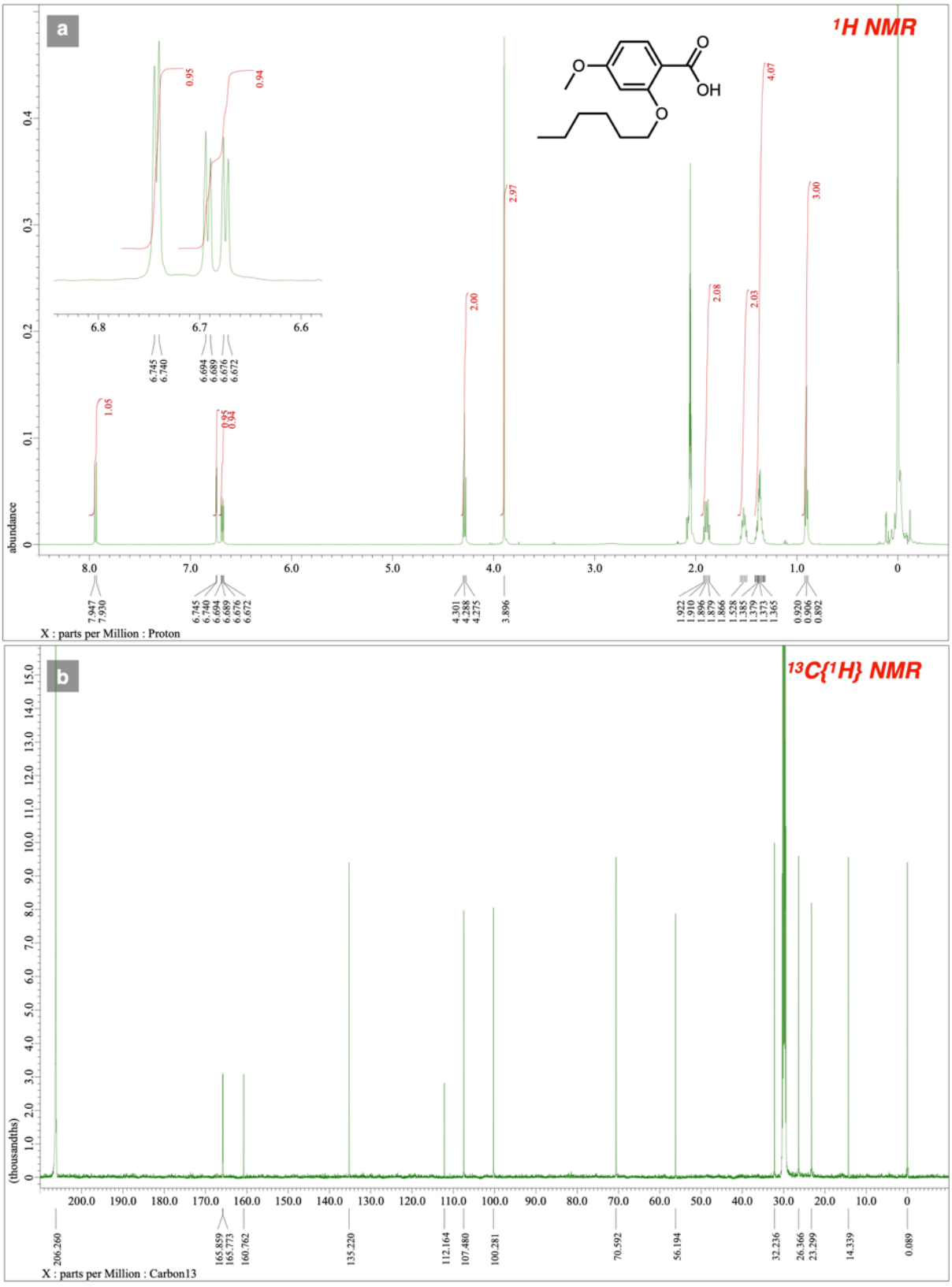

QTOF-HRMS spectra of compound ***2b***

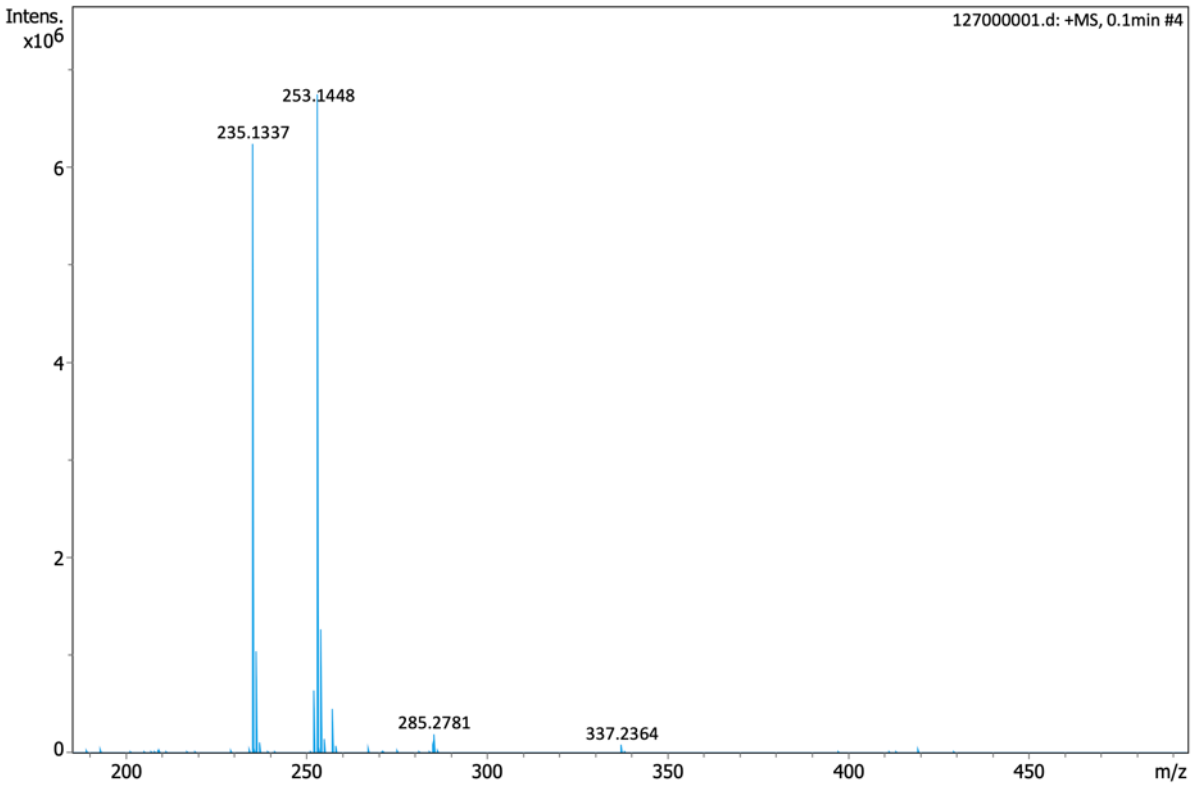

*^{1}H NMR (a) and ^{13}C{^{1}H} NMR (b) spectra of compound **3a***

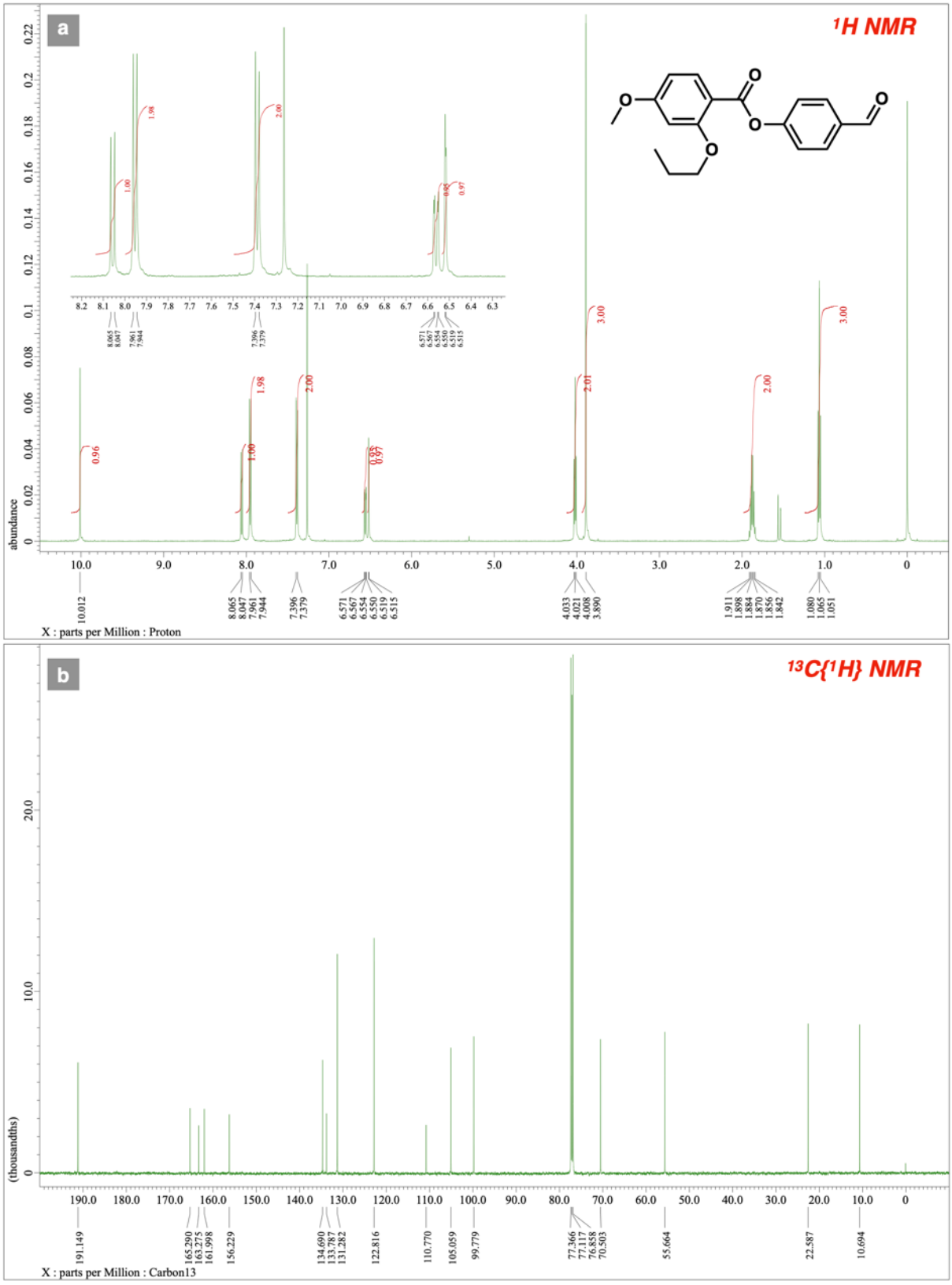

*QTOF-HRMS spectra of compound **3a***

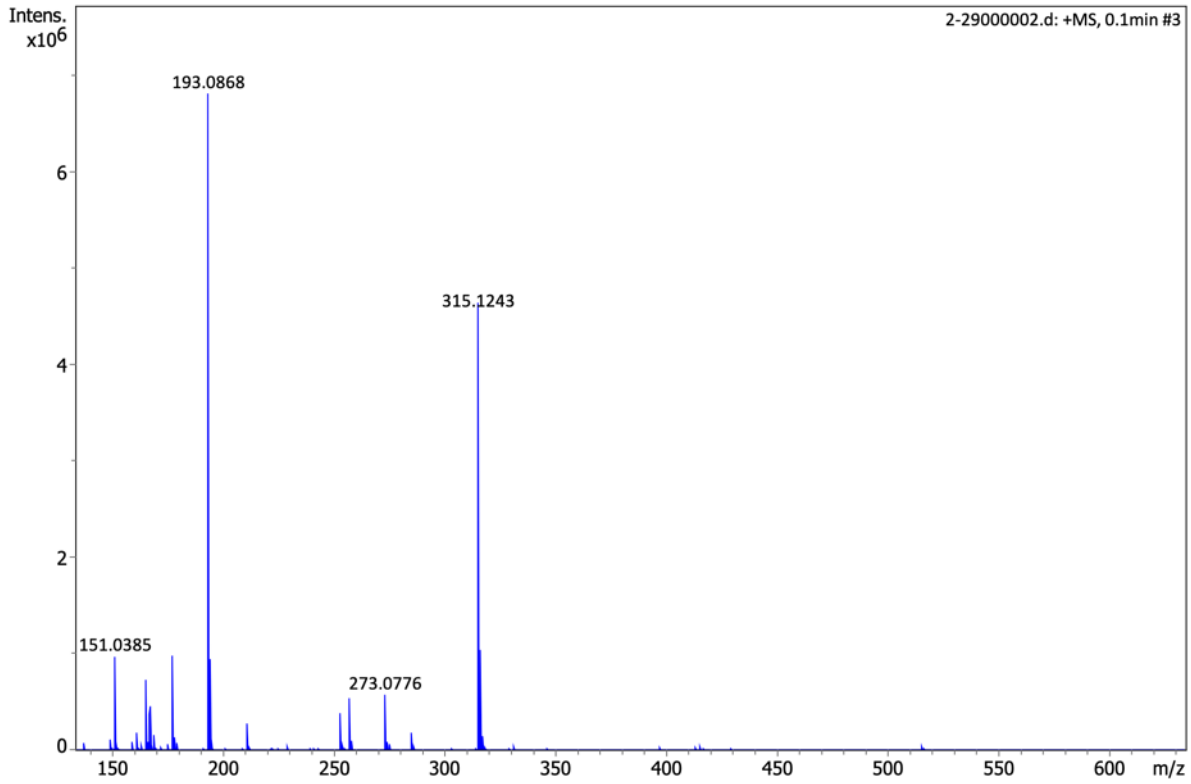

*^{1}H NMR (a) and $^{13}C\{^{1}H\}$ NMR (b) spectra of compound **3b***

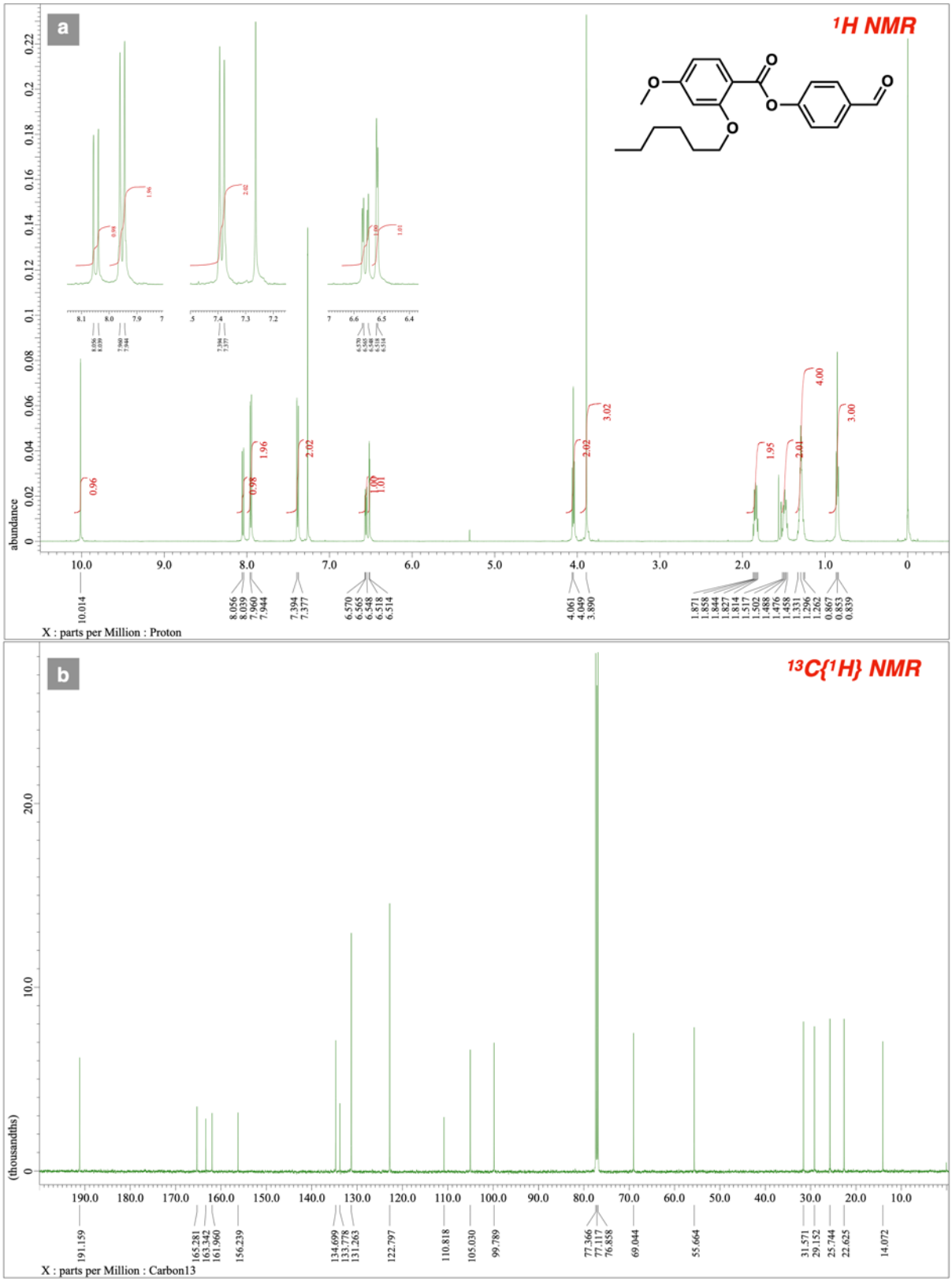

*QTOF-HRMS spectra of compound **3b***

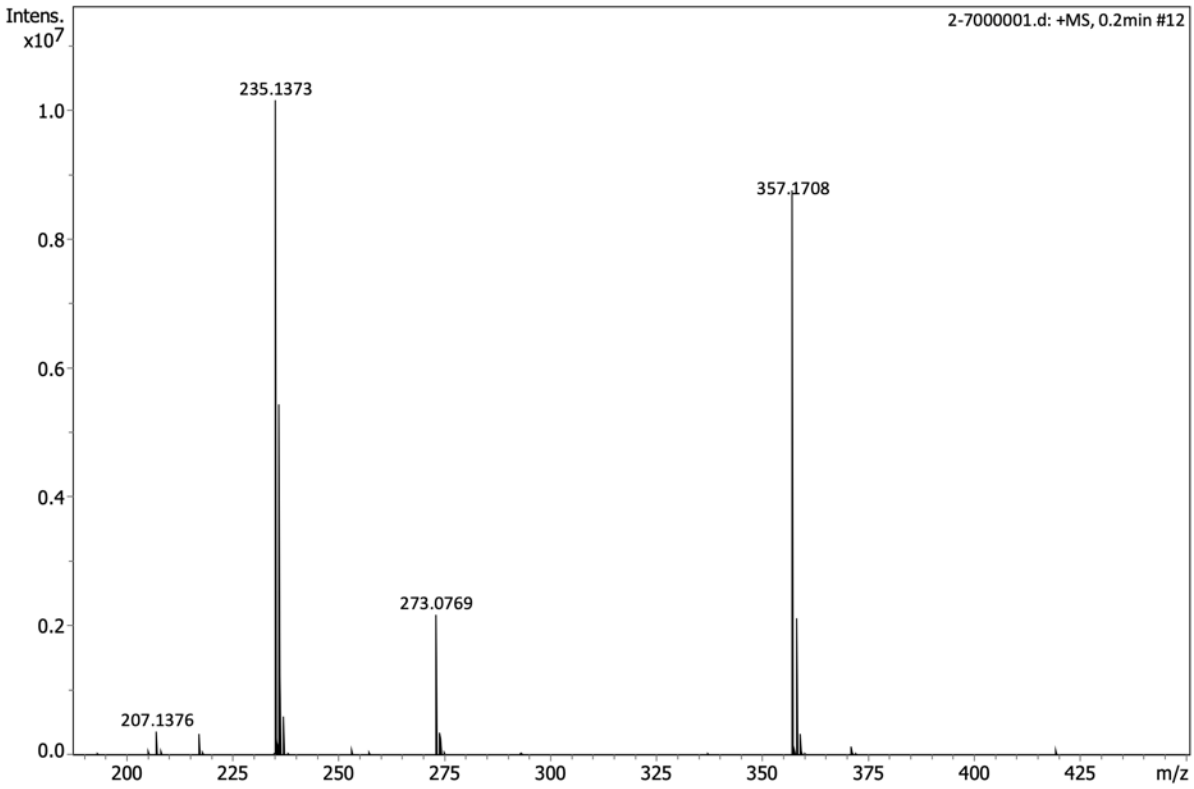

^{1}H NMR (a) and $^{13}C\{^{1}H\}$ NMR (b) spectra of compound ***3c***

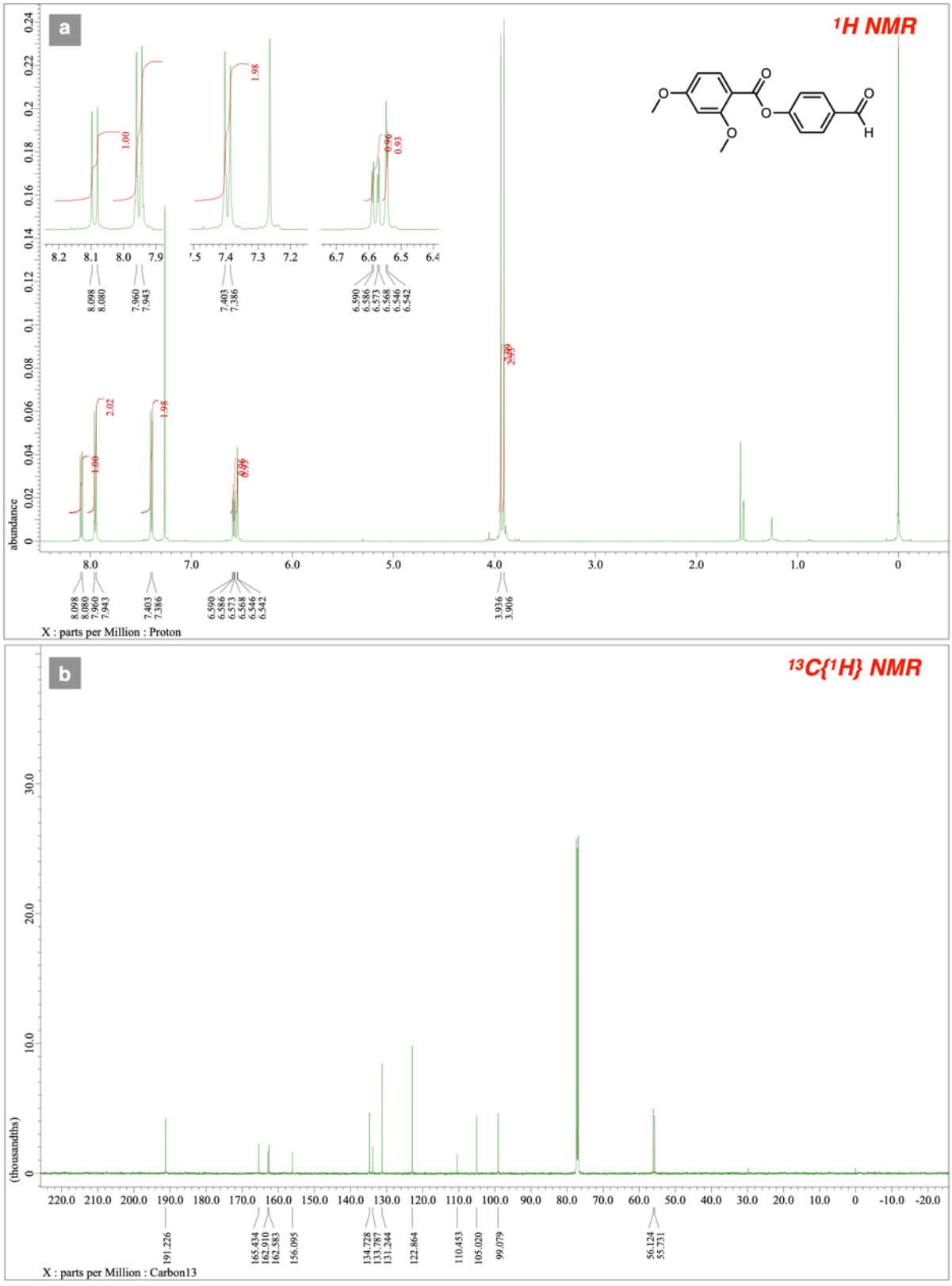

*QTOF-HRMS spectra of compound **3c***

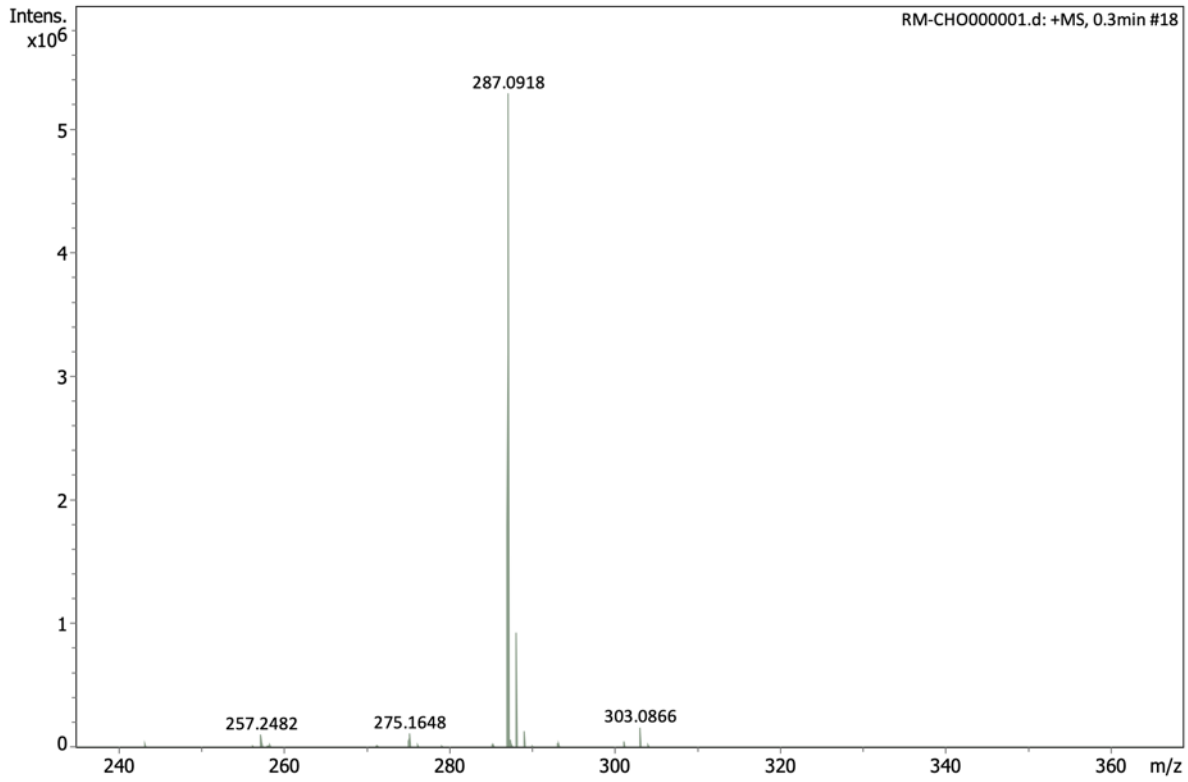

*^{1}H NMR (a) and $^{13}C\{^{1}H\}$ NMR (b) spectra of compound **4a***

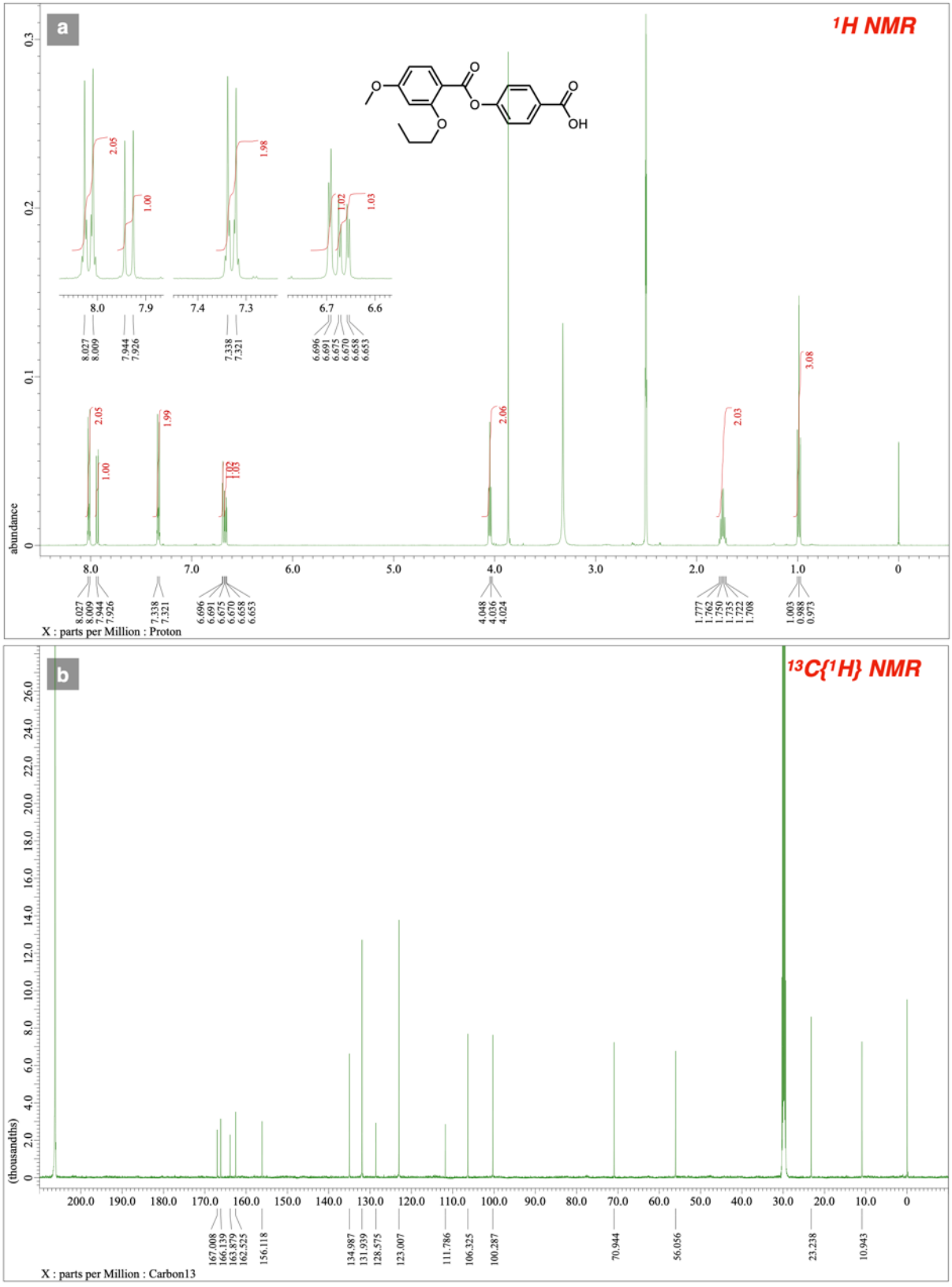

*QTOF-HRMS spectra of compound **4a***

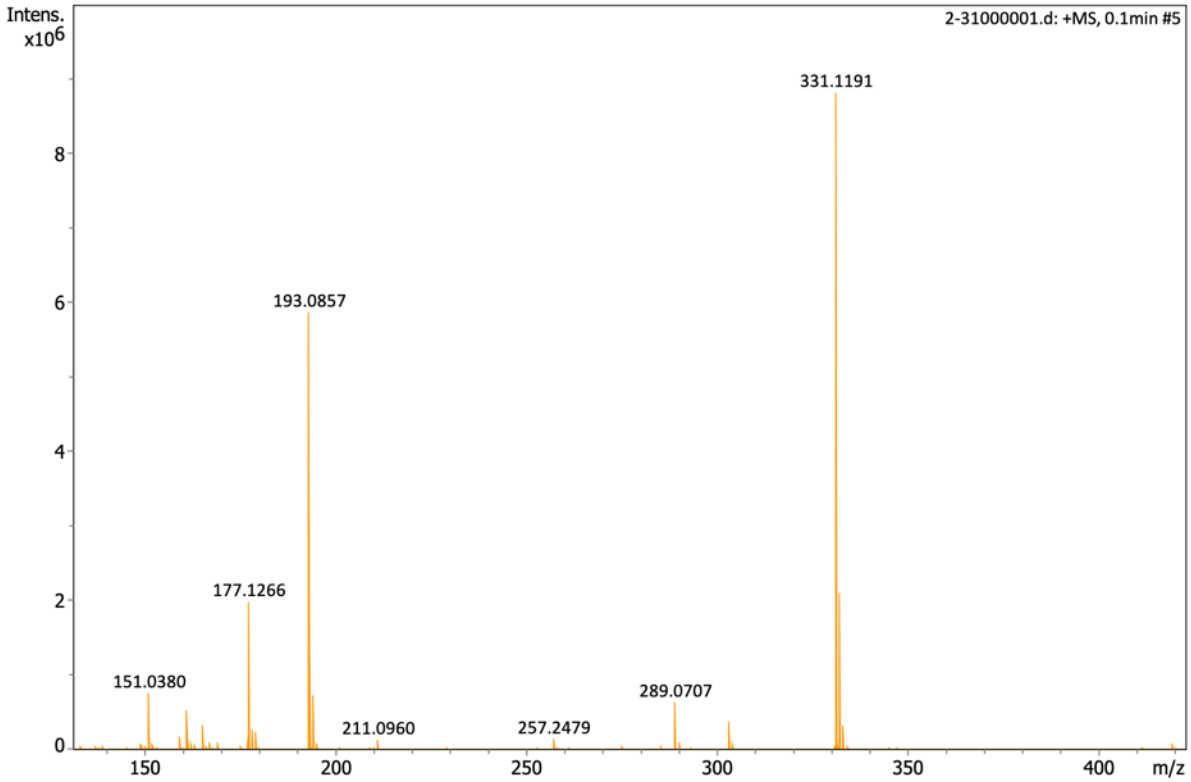

*^{1}H NMR (a) and $^{13}C\{^{1}H\}$ NMR (b) spectra of compound **4b***

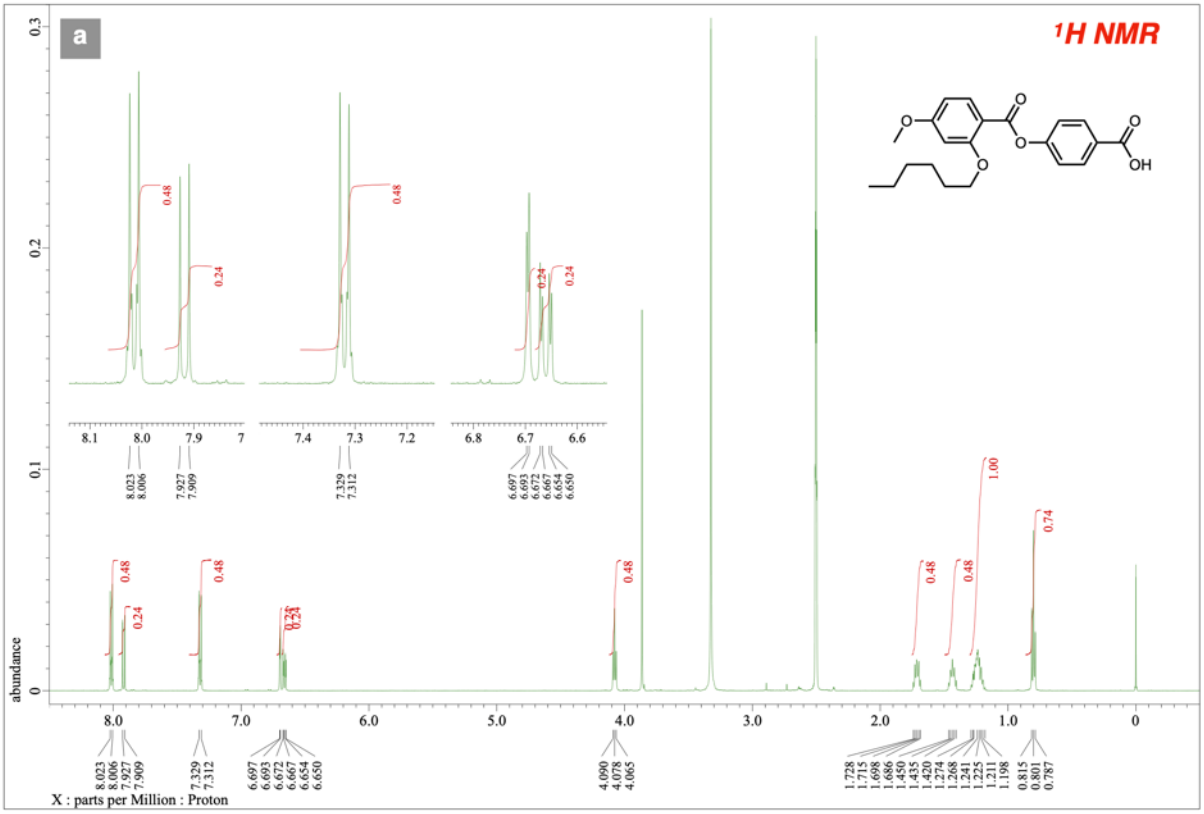

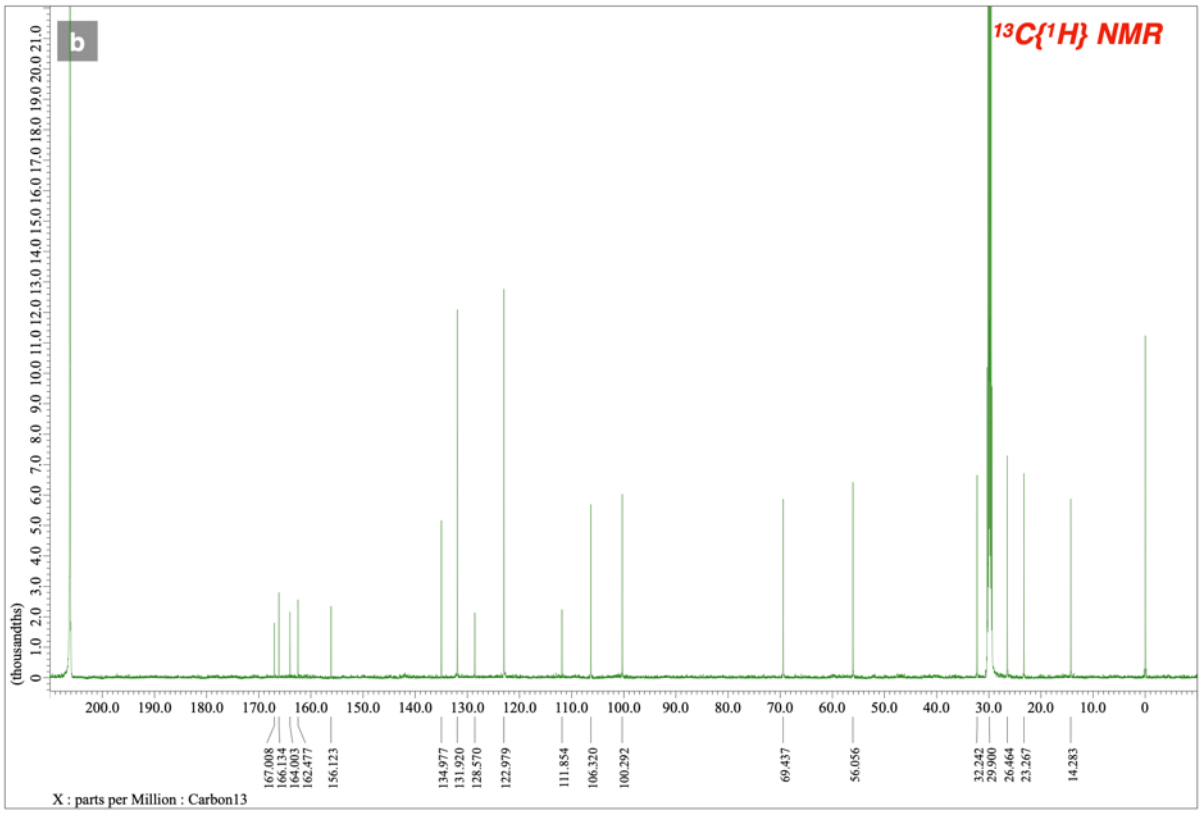

*QTOF-HRMS spectra of compound **4b***

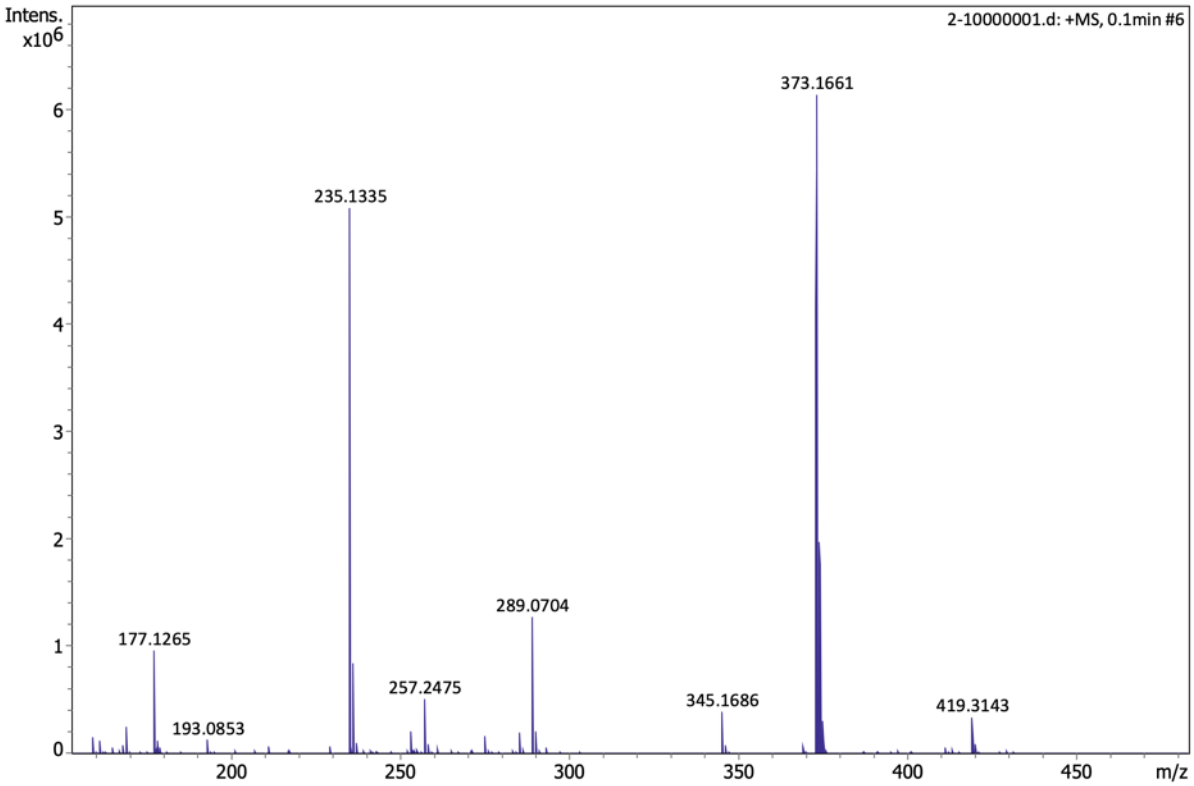

*^{1}H NMR (a) and $^{13}C\{^{1}H\}$ NMR (b) spectra of compound **4c***

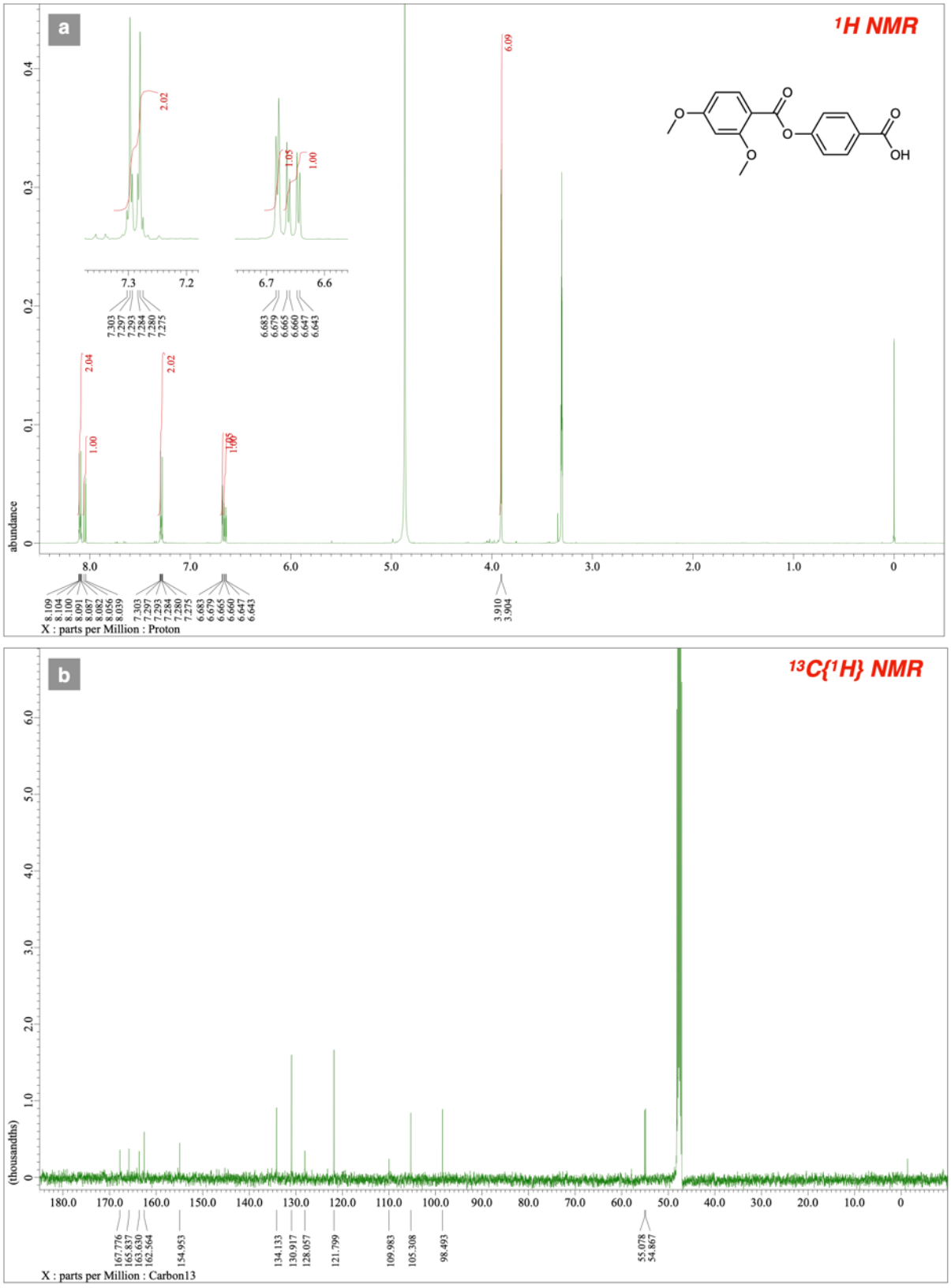

*QTOF-HRMS spectra of compound **4c**.*

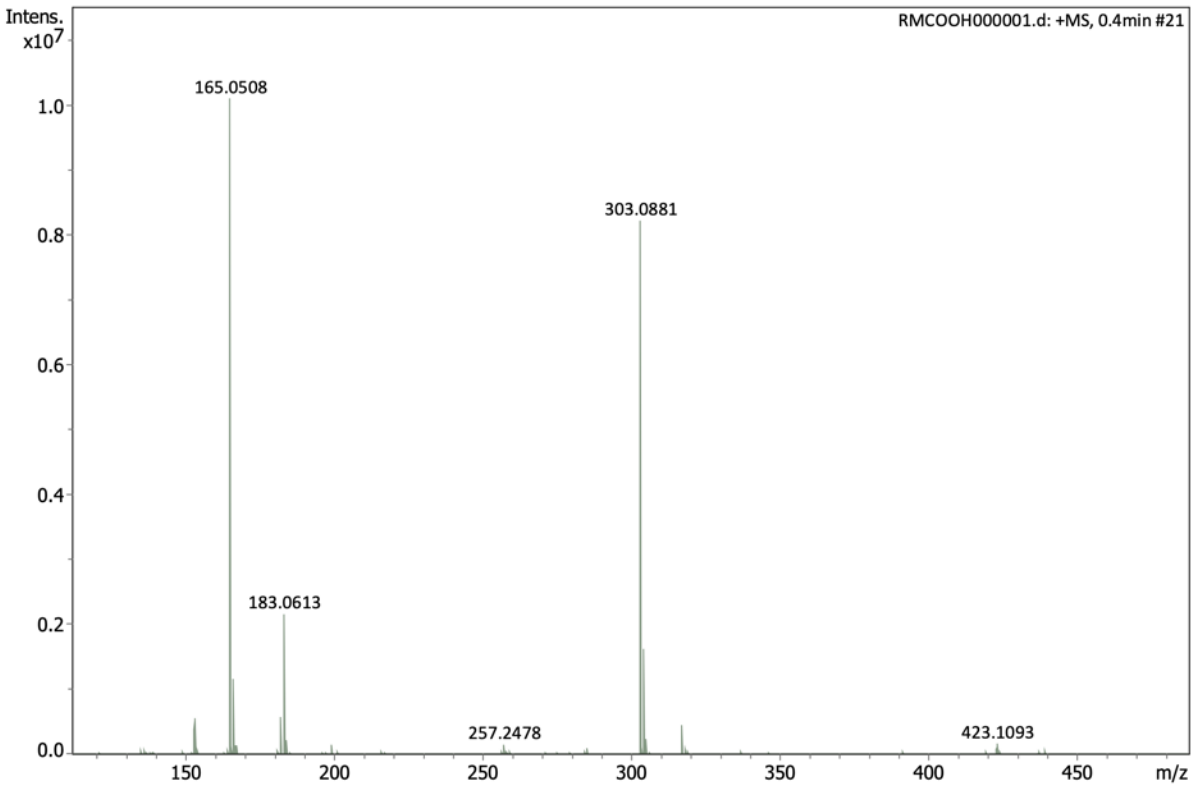

^{1}H NMR (a) and ^{13}C{^{1}H} NMR (b) spectra of compound ***5a***

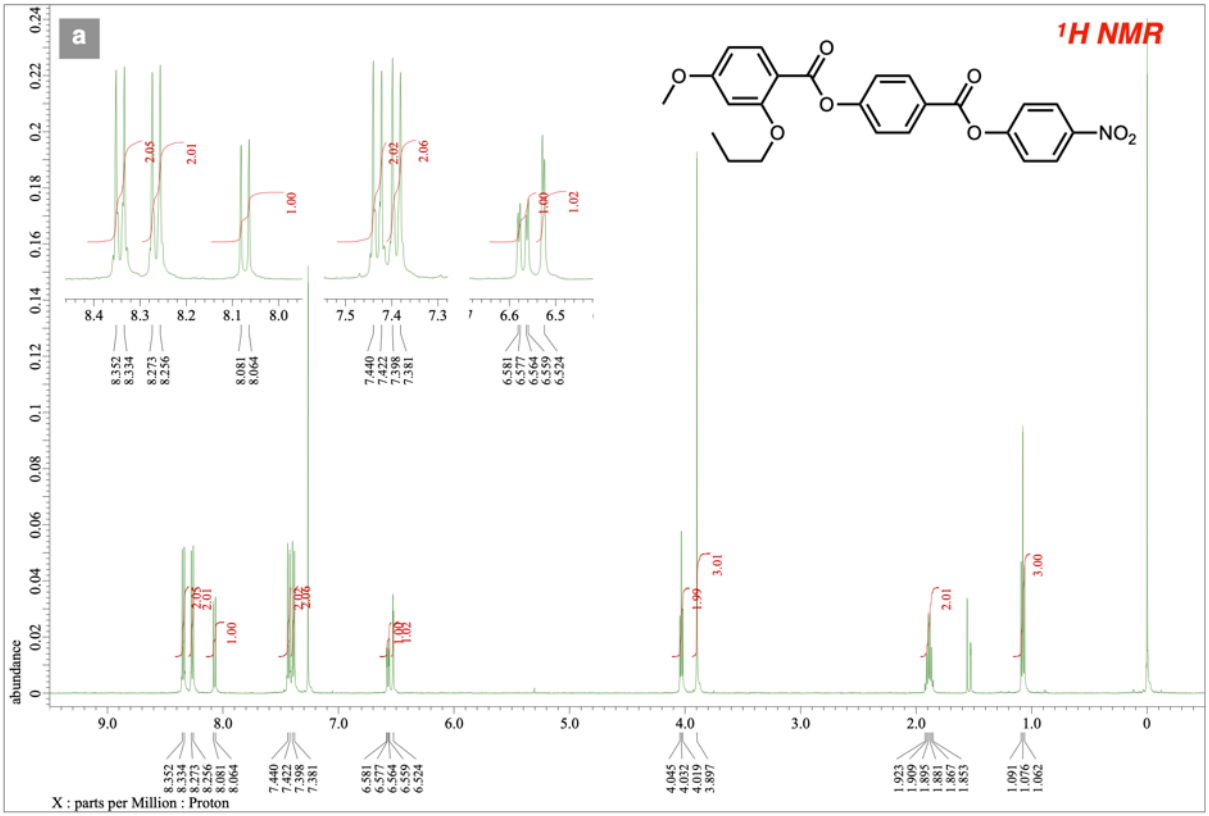

QTOF-HRMS spectra of compound ***5a***

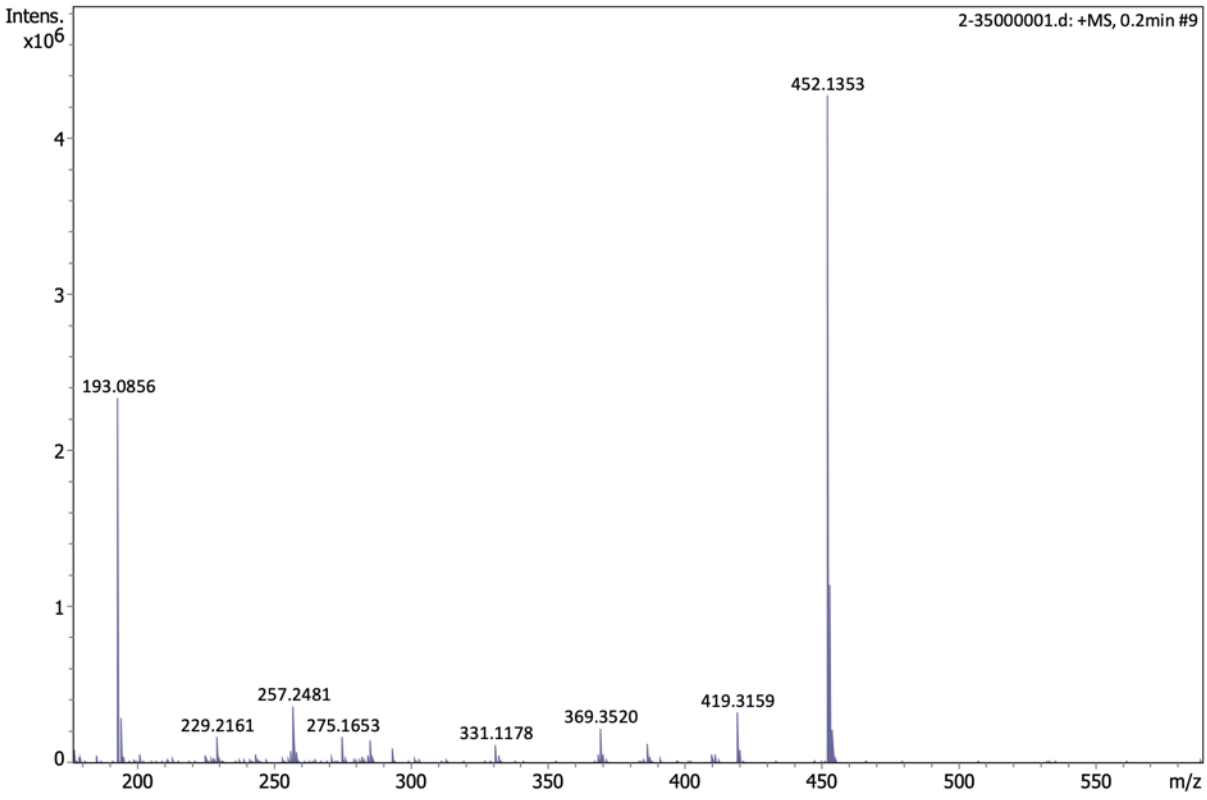

^{1}H NMR (a) and $^{13}C\{^{1}H\}$ NMR (b) spectra of compound ***5b***

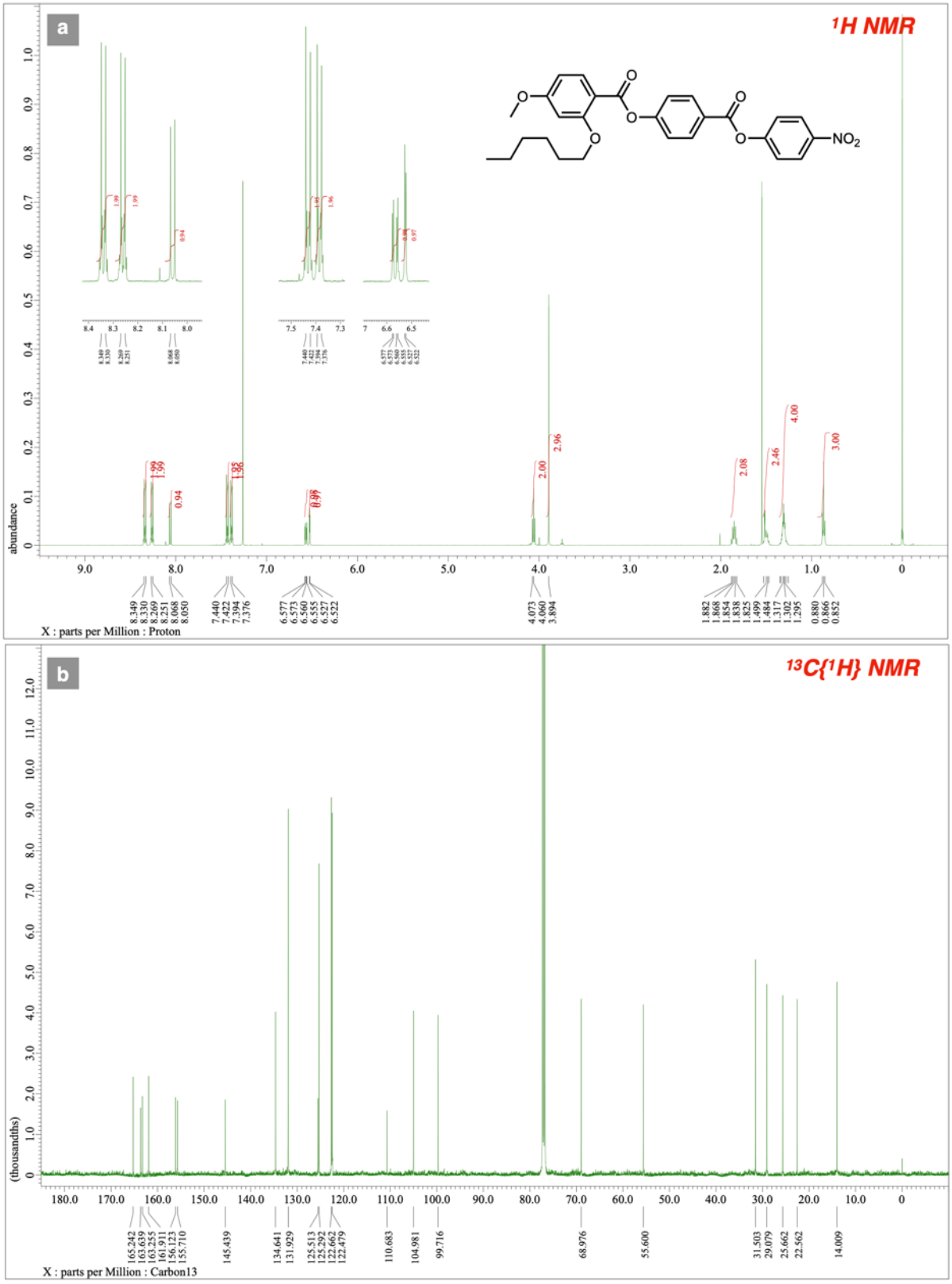

QTOF-HRMS spectra of compound ***5b***

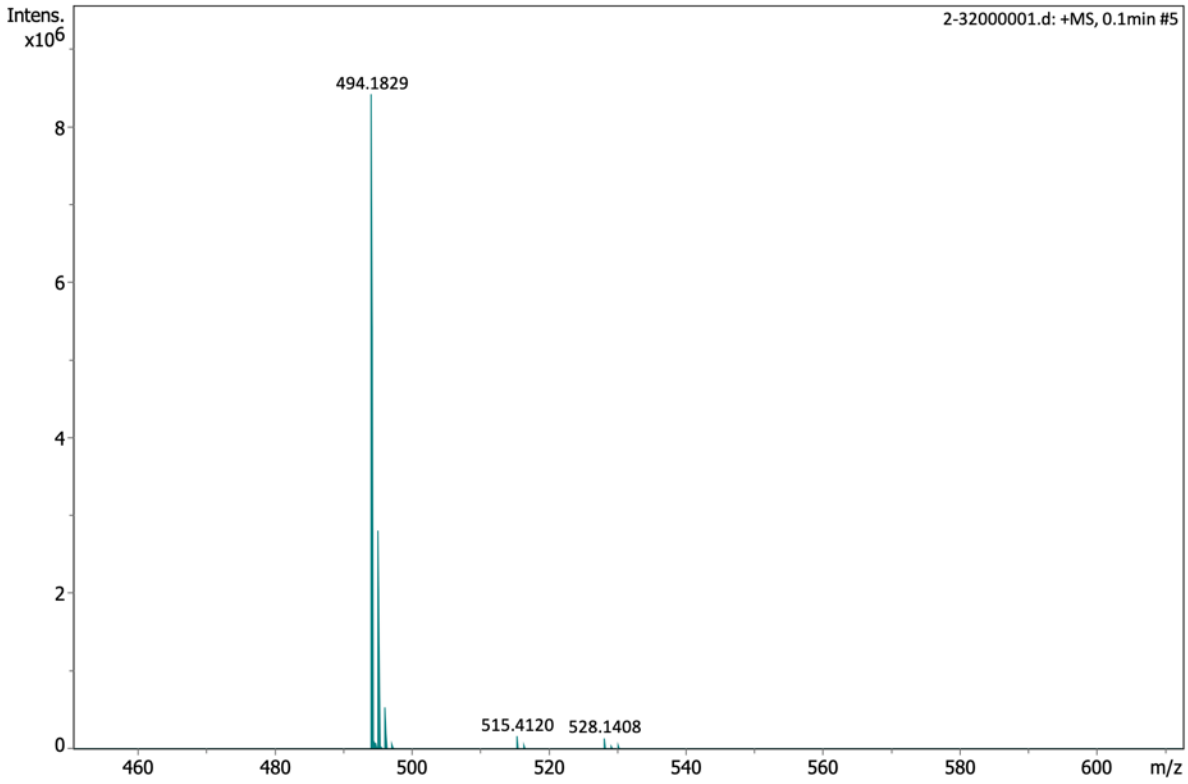

^{1}H NMR (a) and ^{13}C{^{1}H} NMR (b) spectra of compound ***5c***

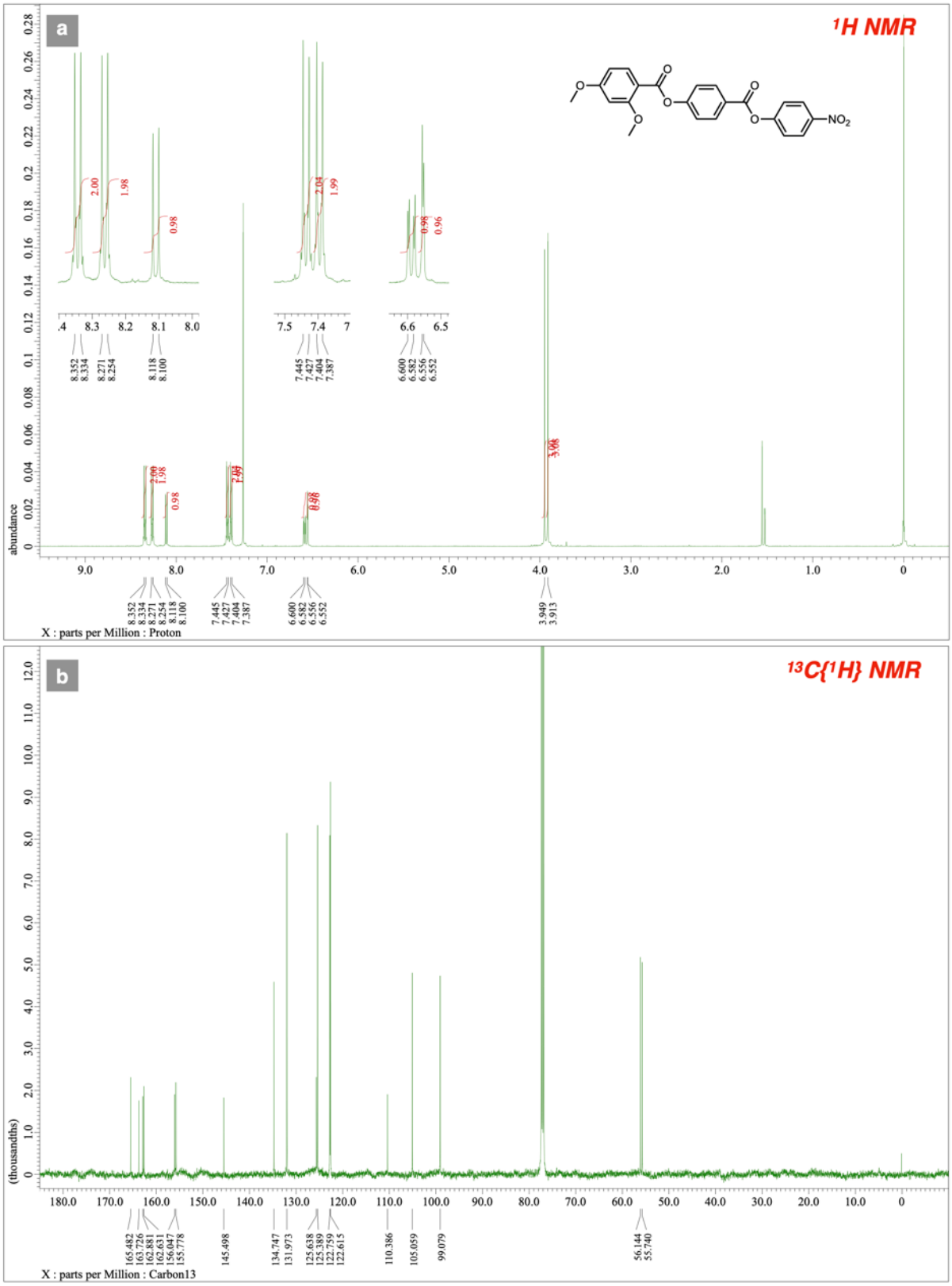

QTOF-HRMS spectra of compound ***5c***

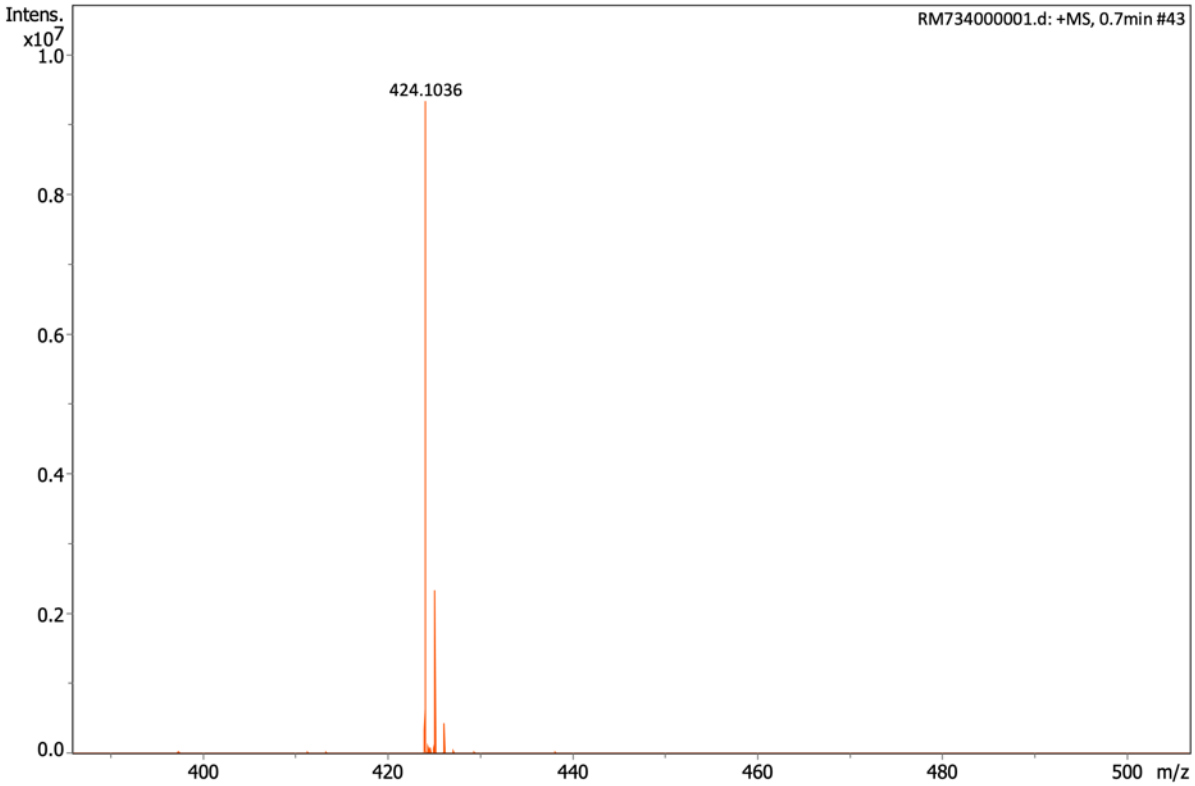

*^{1}H NMR (a) and $^{13}C\{^{1}H\}$ NMR (b) spectra of compound **7a***

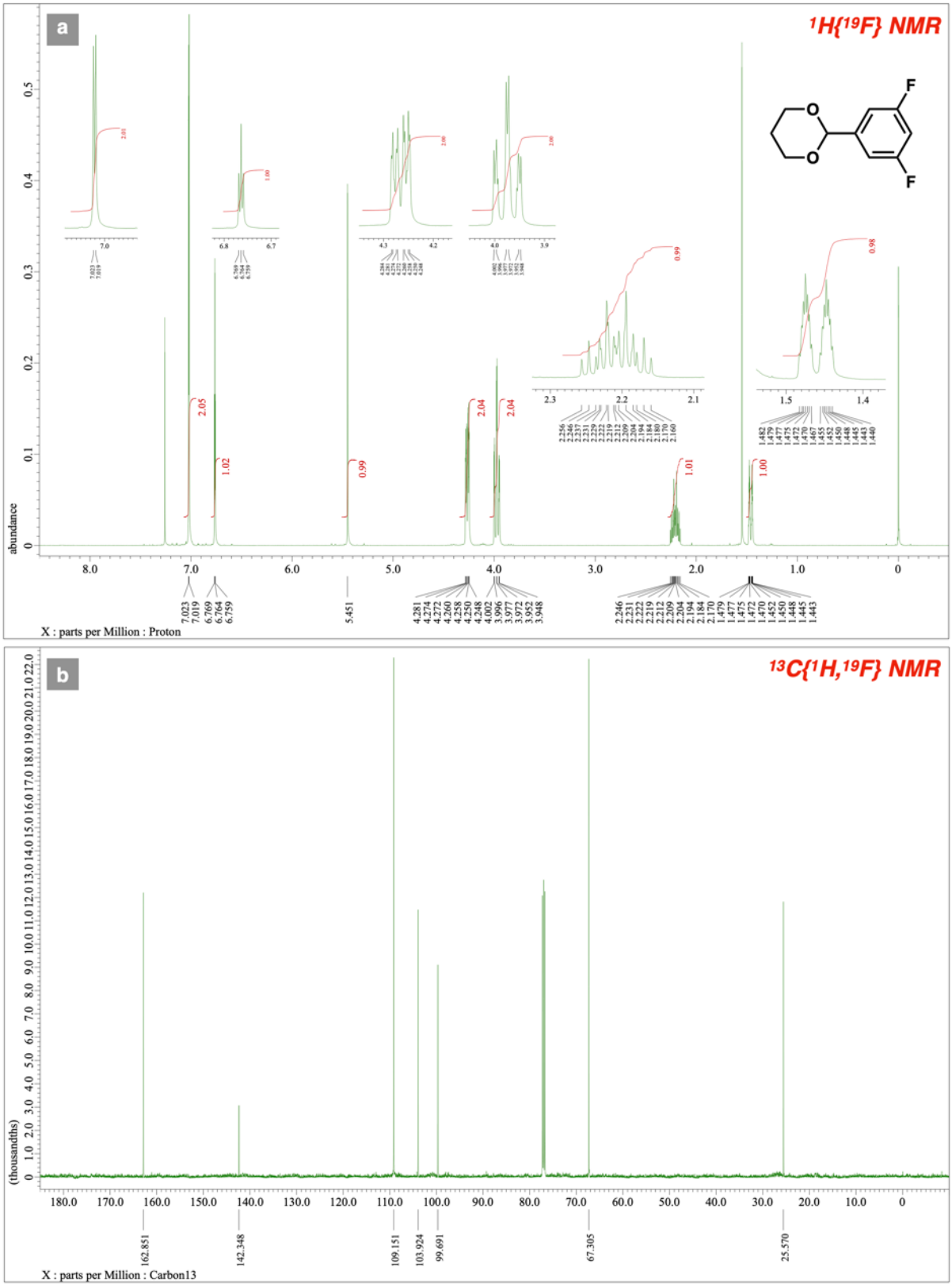

*^{19}F NMR (a) and QTOF-HRMS (b) spectra of compound **7a***

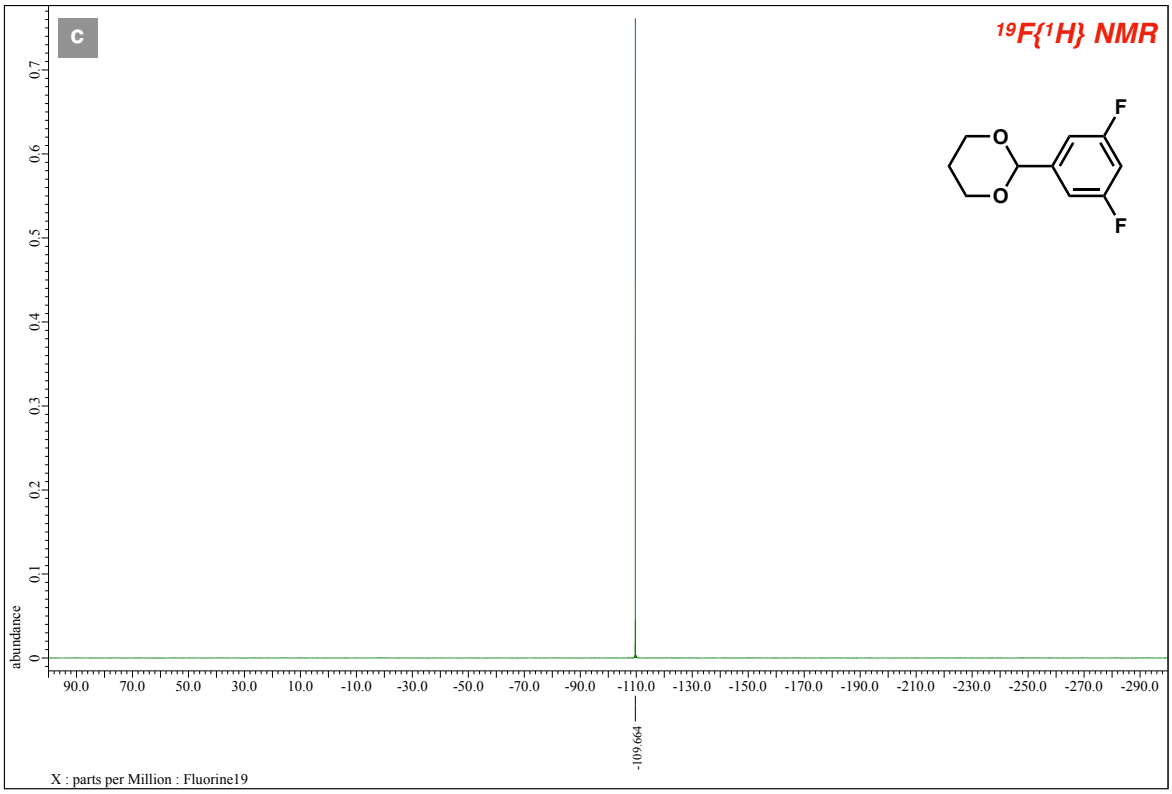

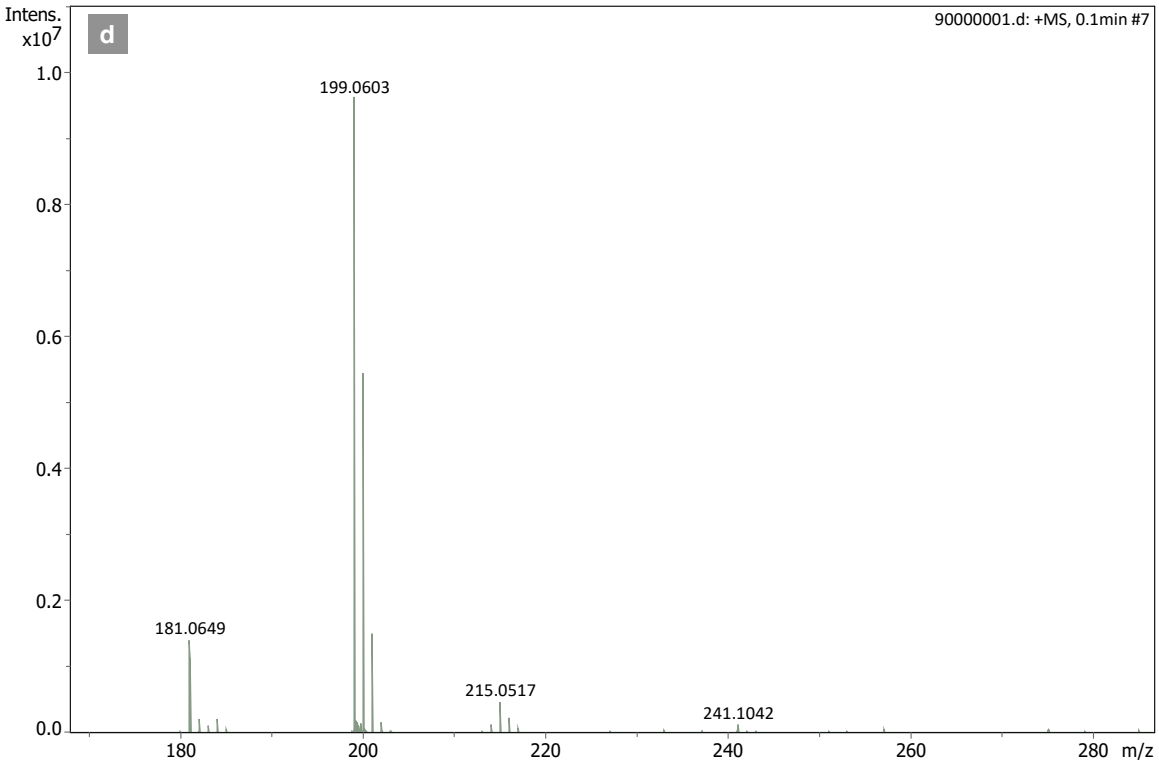

$^{1}H\{^{19}F\}$ NMR (a) and $^{13}C\{^{1}H,^{19}F\}$ NMR (b) spectra of compound ***23***

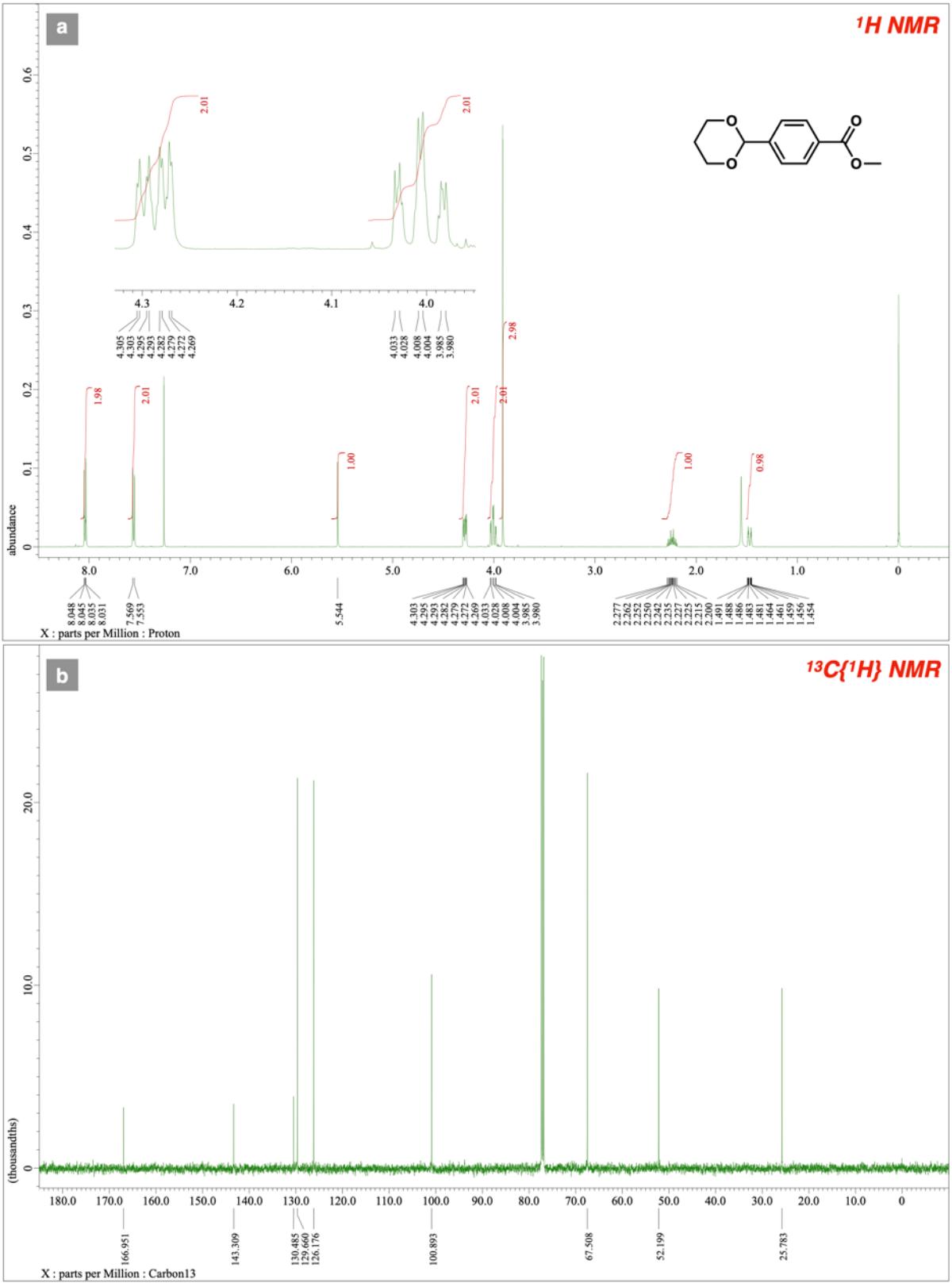

*$^{19}F\{^{1}H\}$ NMR (a) and QTOF-HRMS (b) spectra of compound **23***

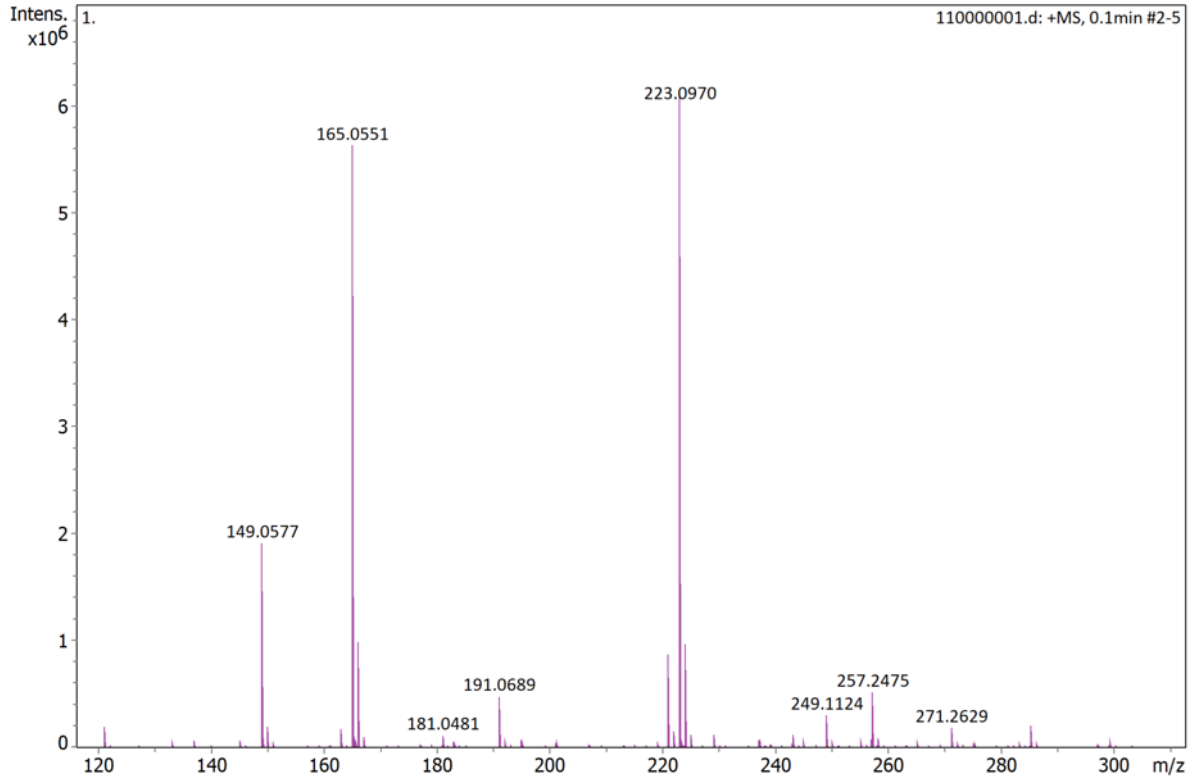

^{1}H NMR (a) and $^{13}C\{^{1}H\}$ NMR (b) spectra of compound ***8a***

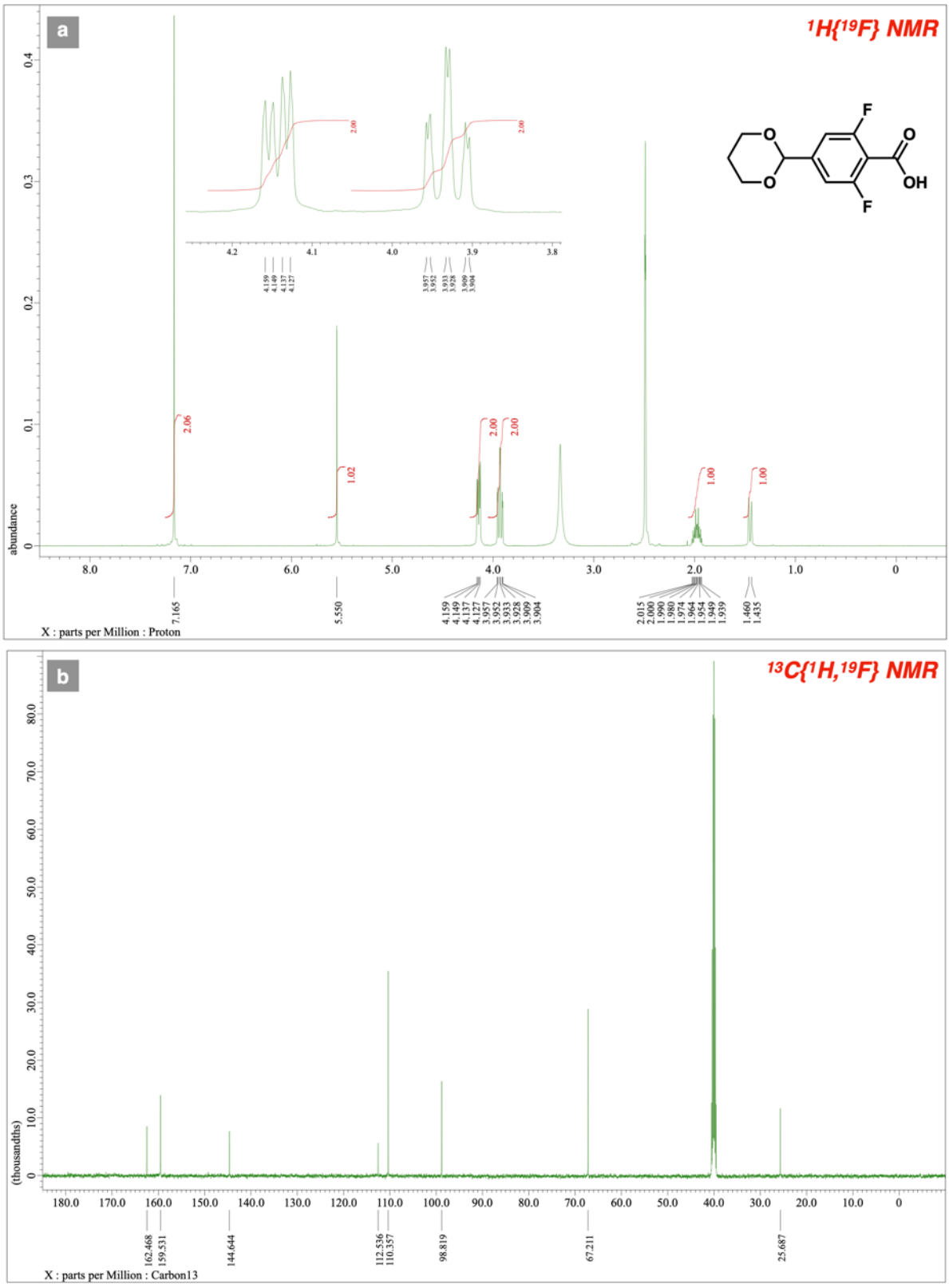

$^{19}F\{^{1}H\}$ NMR (a) and QTOF-HRMS (b) spectra of compound ***8a***

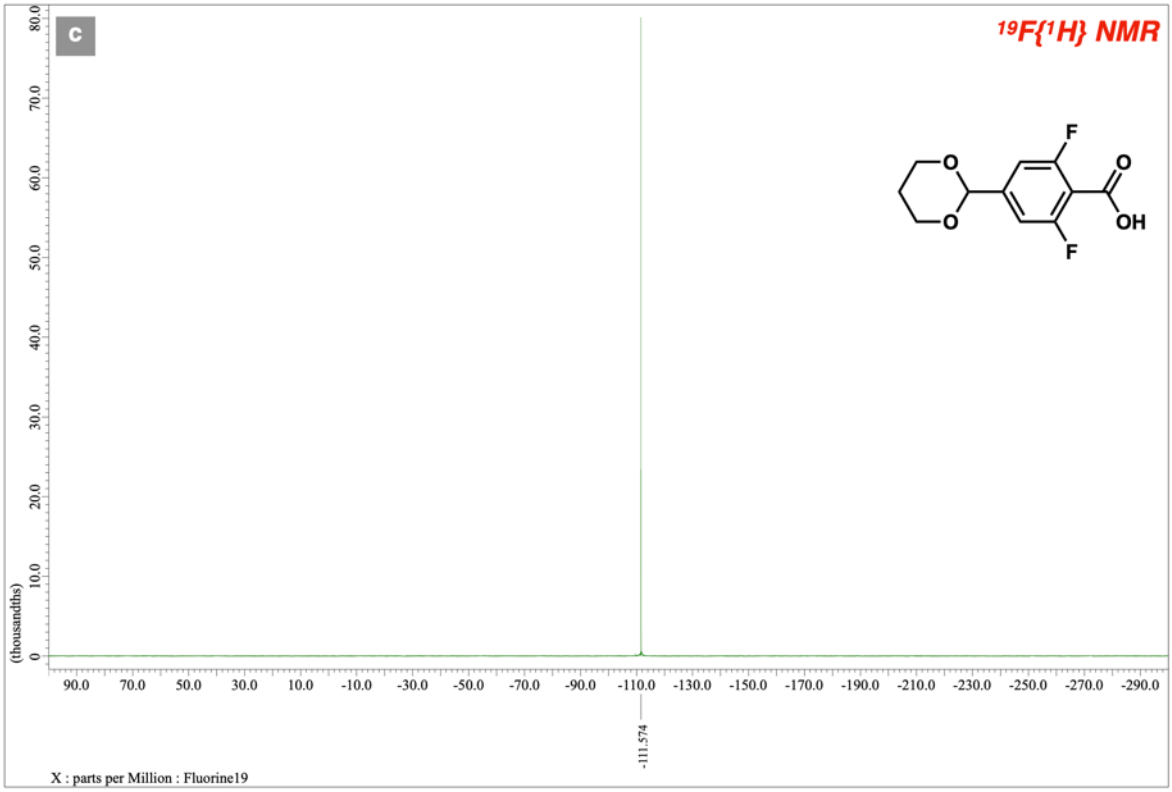

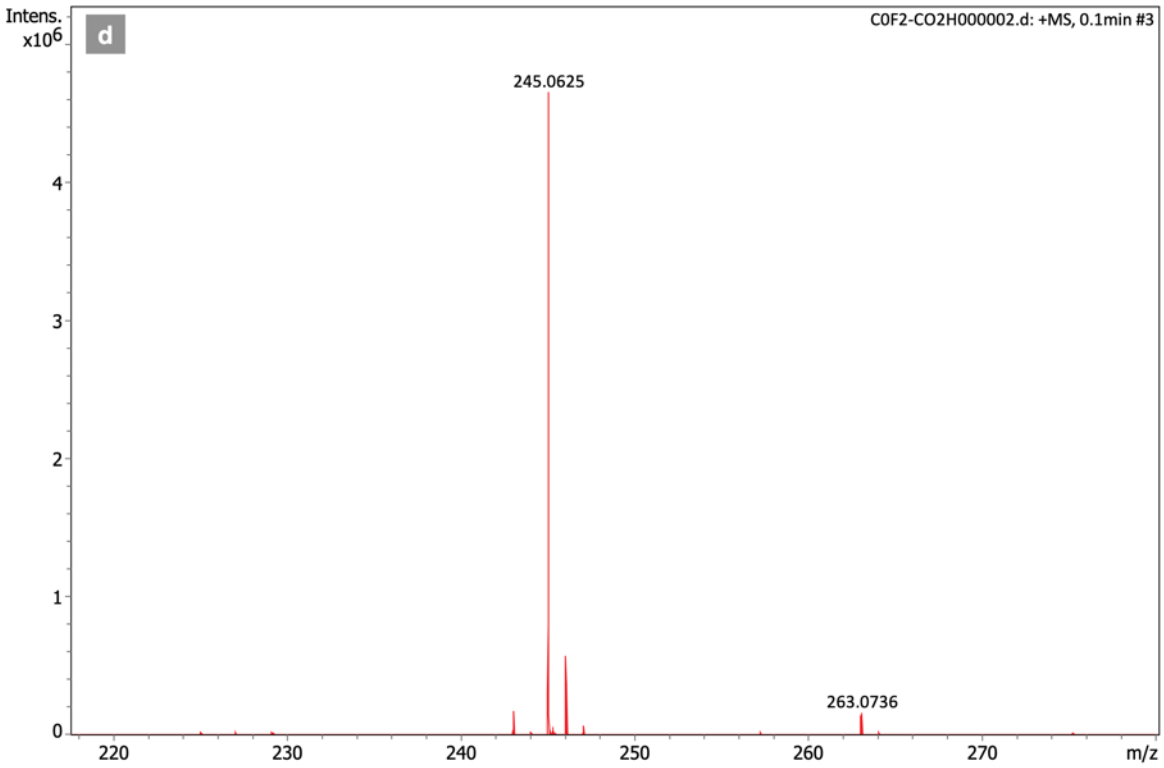

$^{1}H\{^{19}F\}$ NMR (a) and $^{13}C\{^{1}H,^{19}F\}$ NMR (b) spectra of compound ***24***

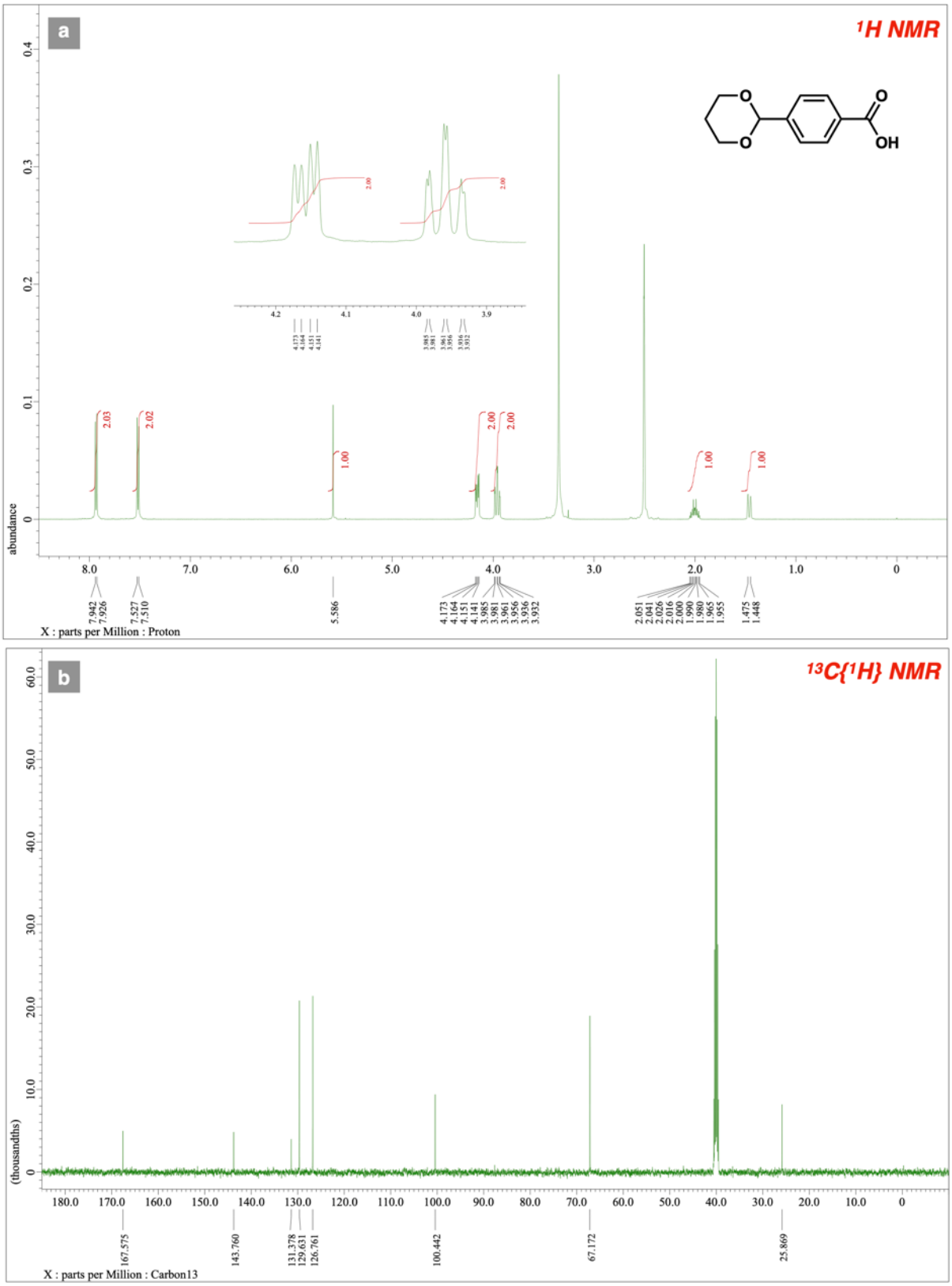

*$^{19}F\{^{1}H\}$ NMR (a) and QTOF-HRMS (b) spectra of compound **24***

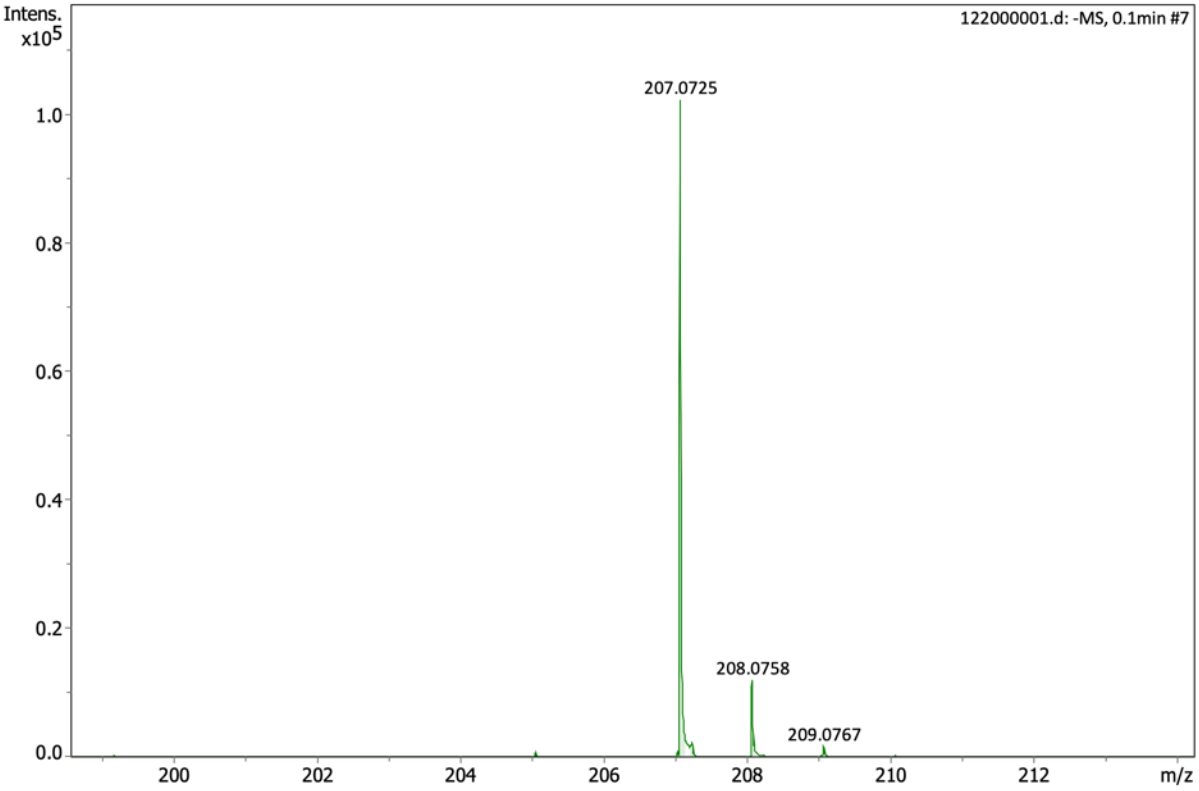

$^{1}H\{^{19}F\}$ NMR (a) and $^{13}C\{^{1}H,^{19}F\}$ NMR (b) spectra of compound ***9a***

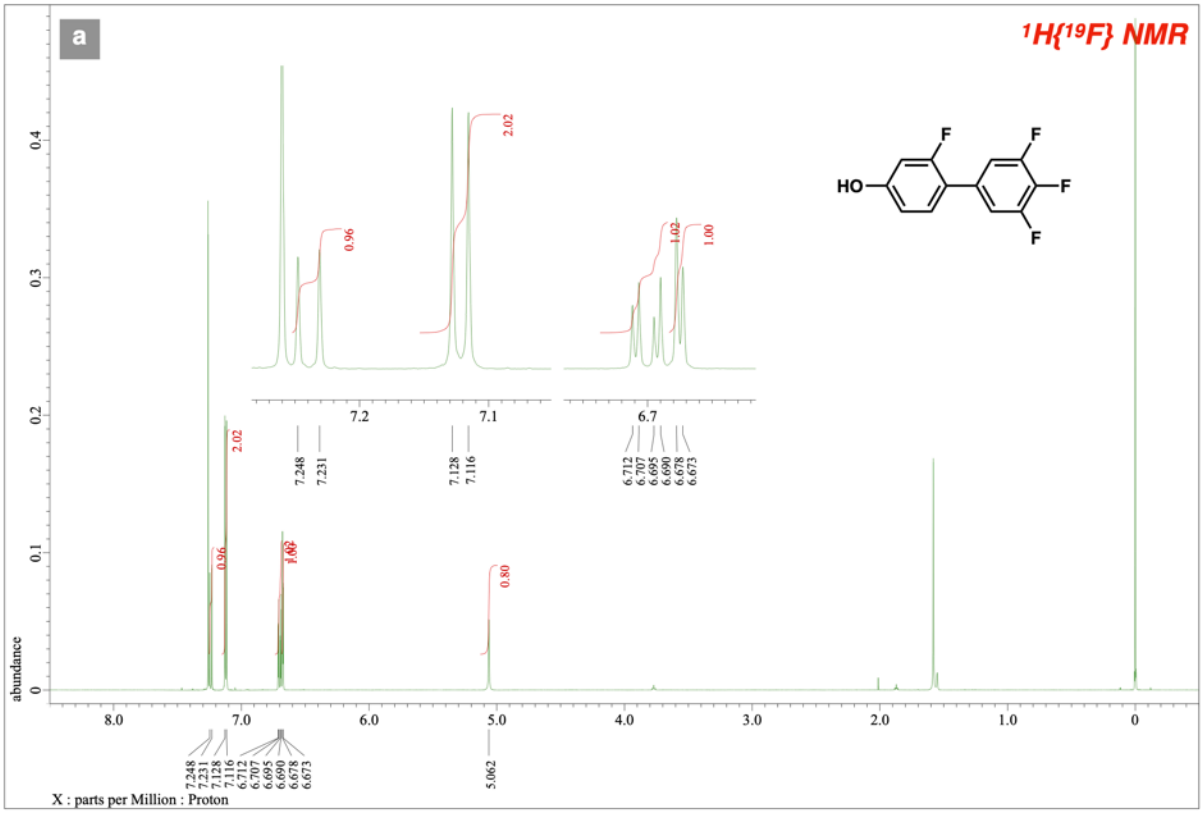

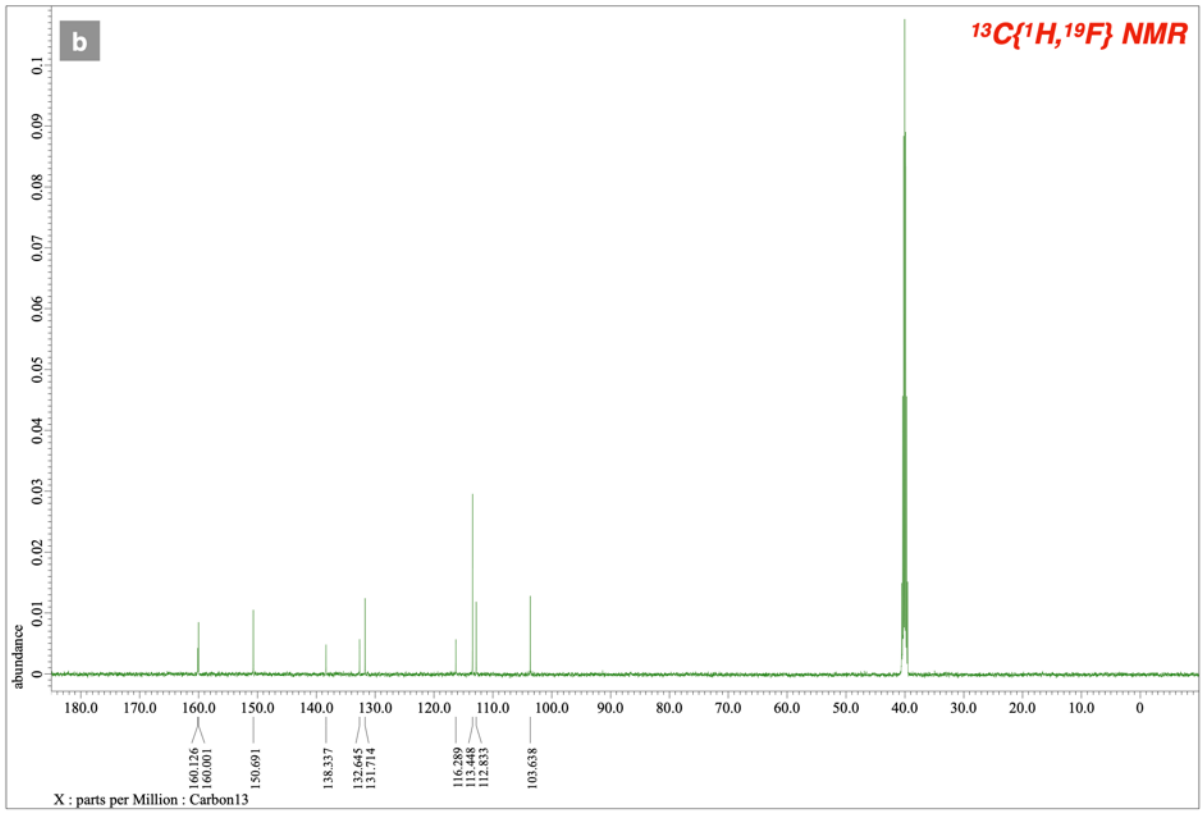

$^{19}F\{^{1}H\}$ NMR (a) and QTOF-HRMS (b) spectra of compound ***9a***

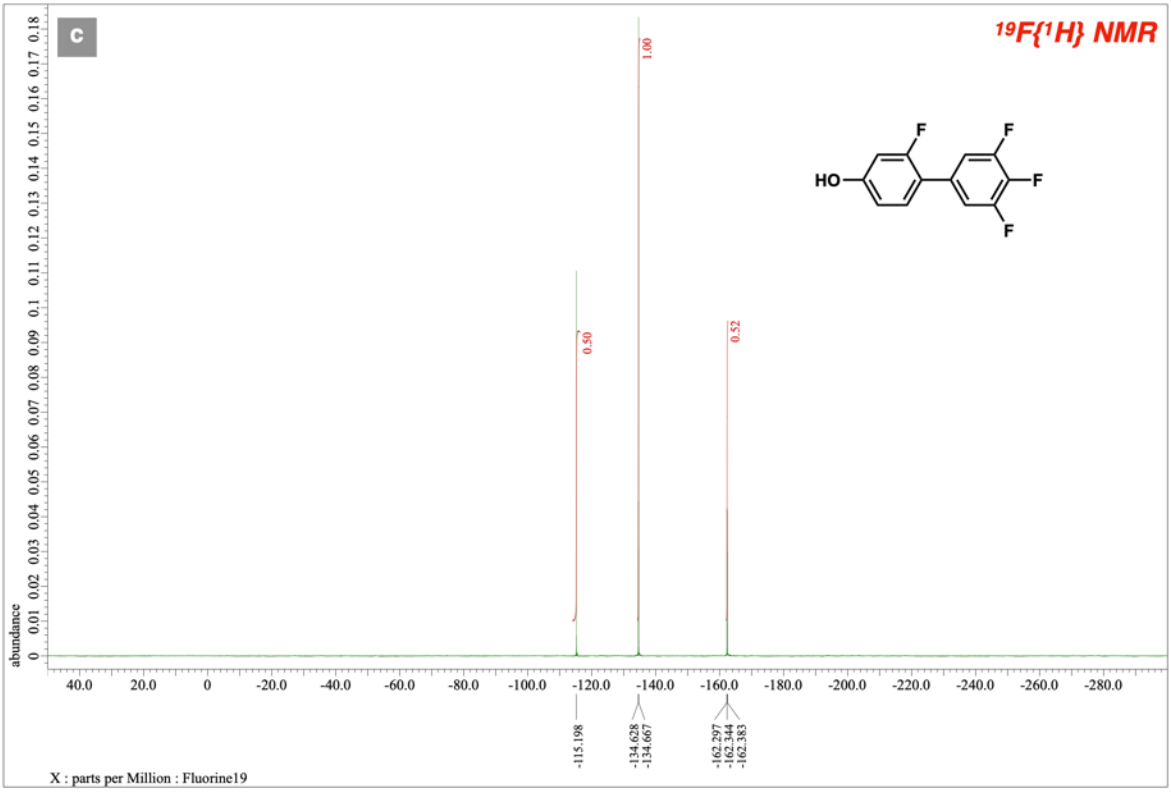

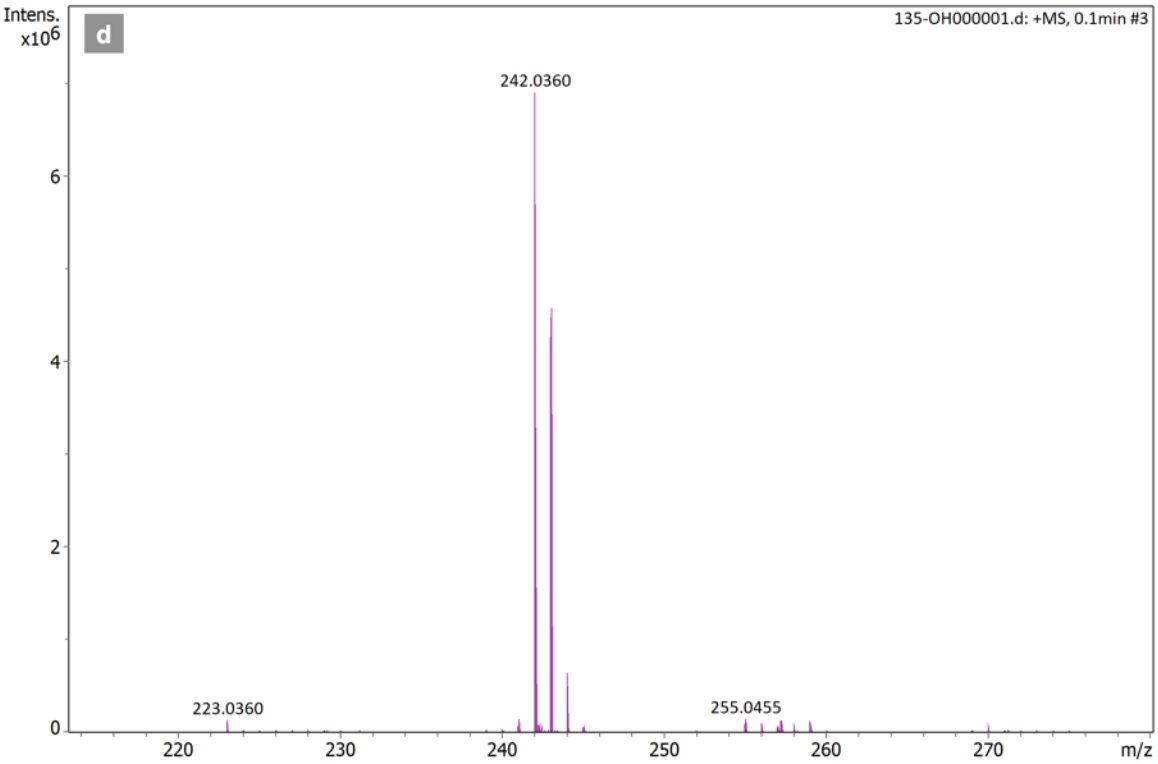

^{19}F NMR (a) and QTOF-HRMS (b) spectra of compound ***9b***

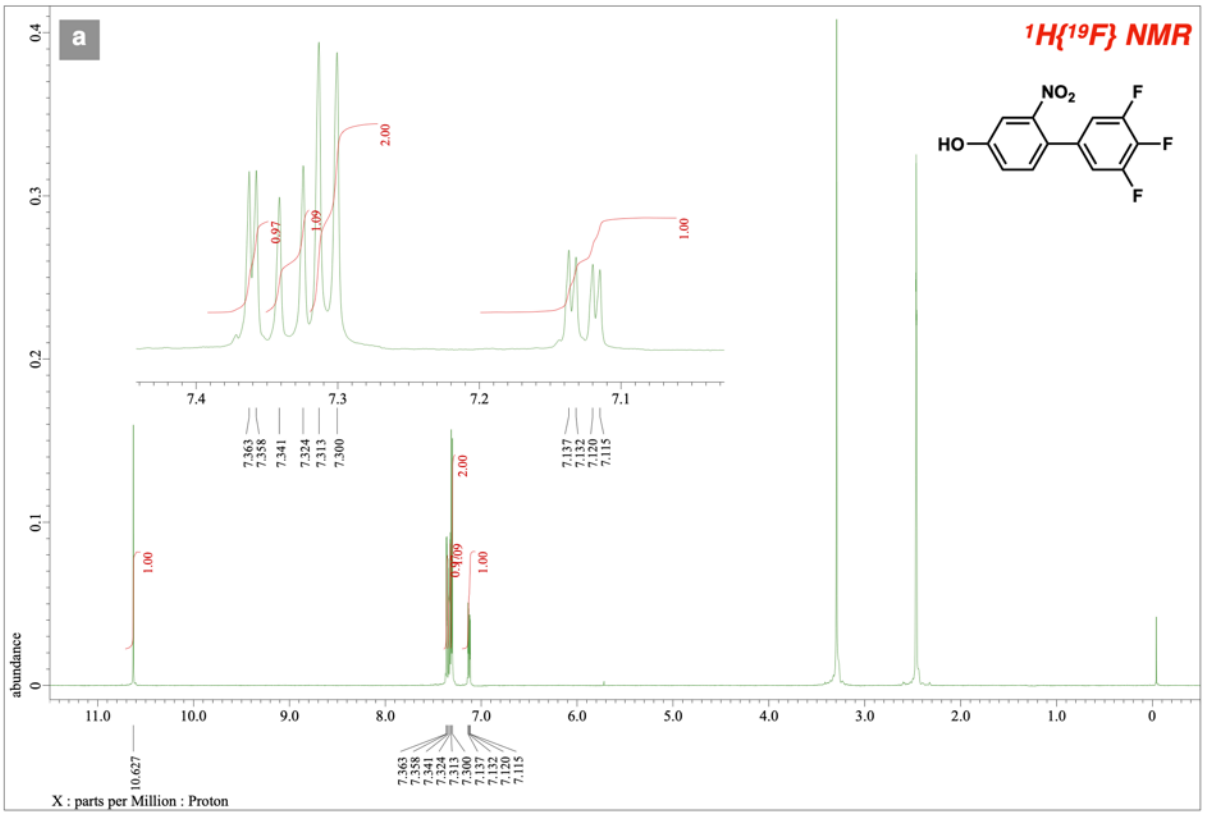

$^{19}F\{^{1}H\}$ NMR (a) and QTOF-HRMS (b) spectra of compound ***9b***

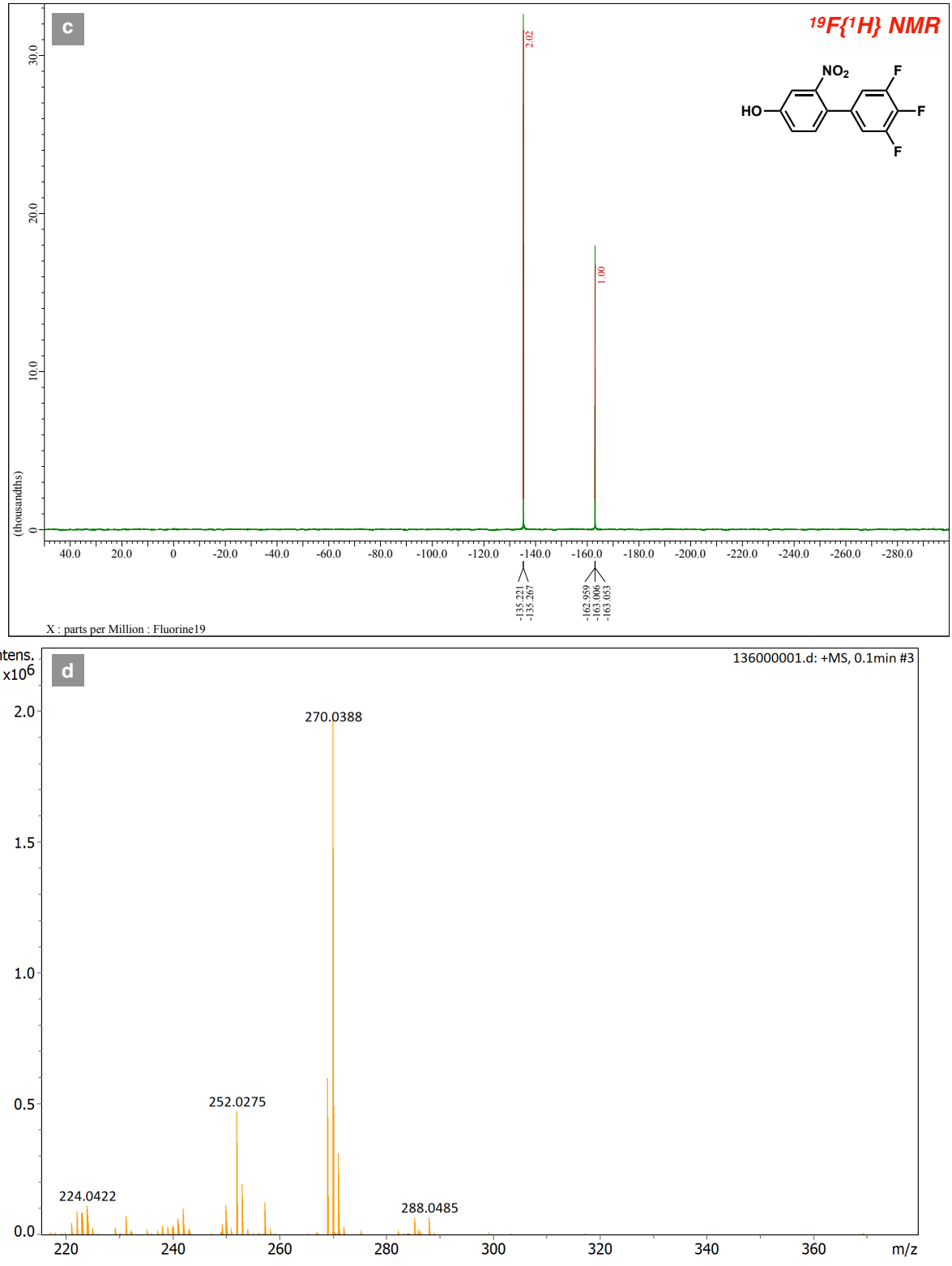

$^{1}H\{^{19}F\}$ NMR (a) and $^{13}C\{^{1}H,^{19}F\}$ NMR (b) spectra of compound ***9c***

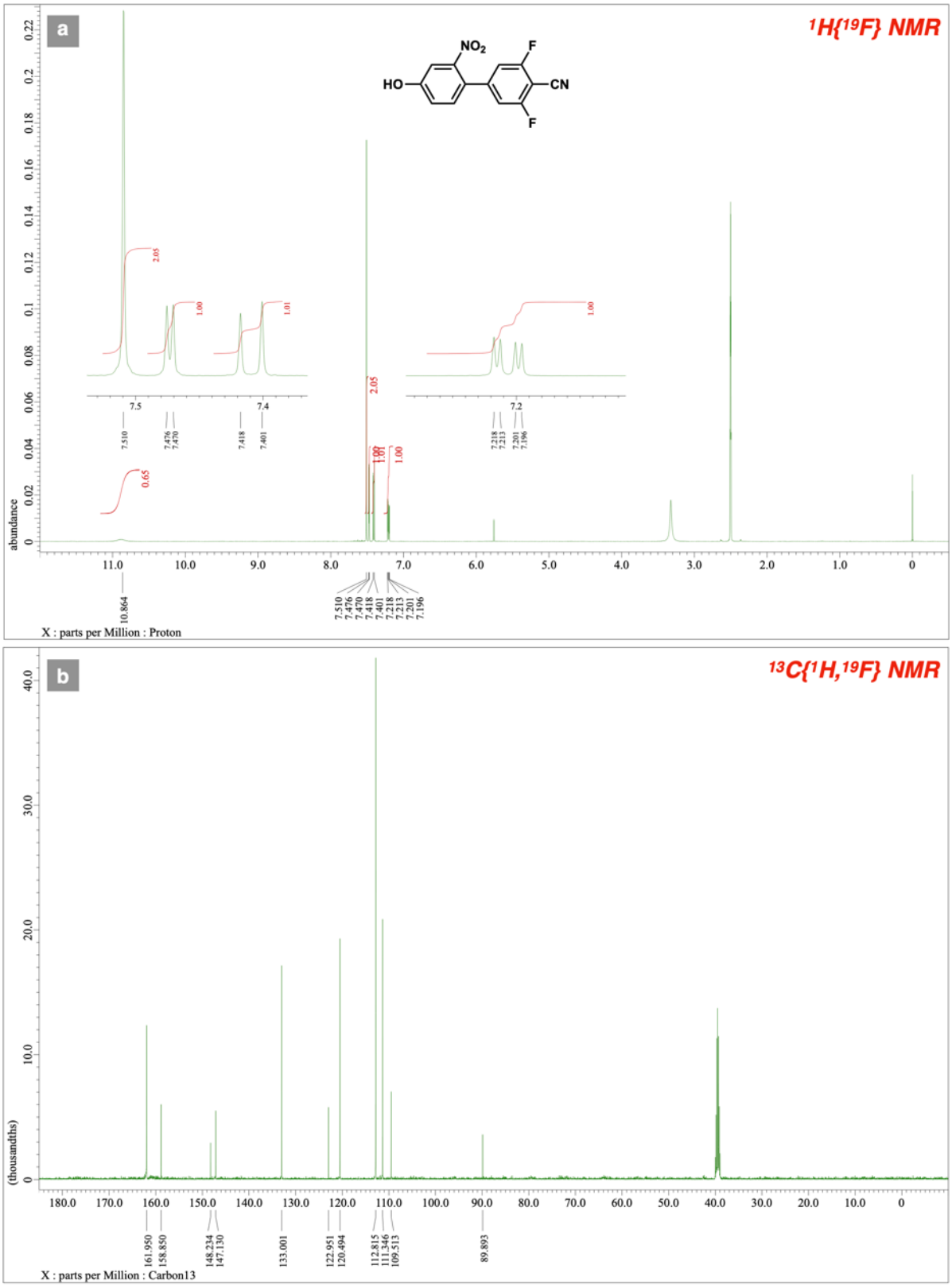

$^{19}F\{^{1}H\}$ NMR (a) and QTOF-HRMS (b) spectra of compound ***9c***

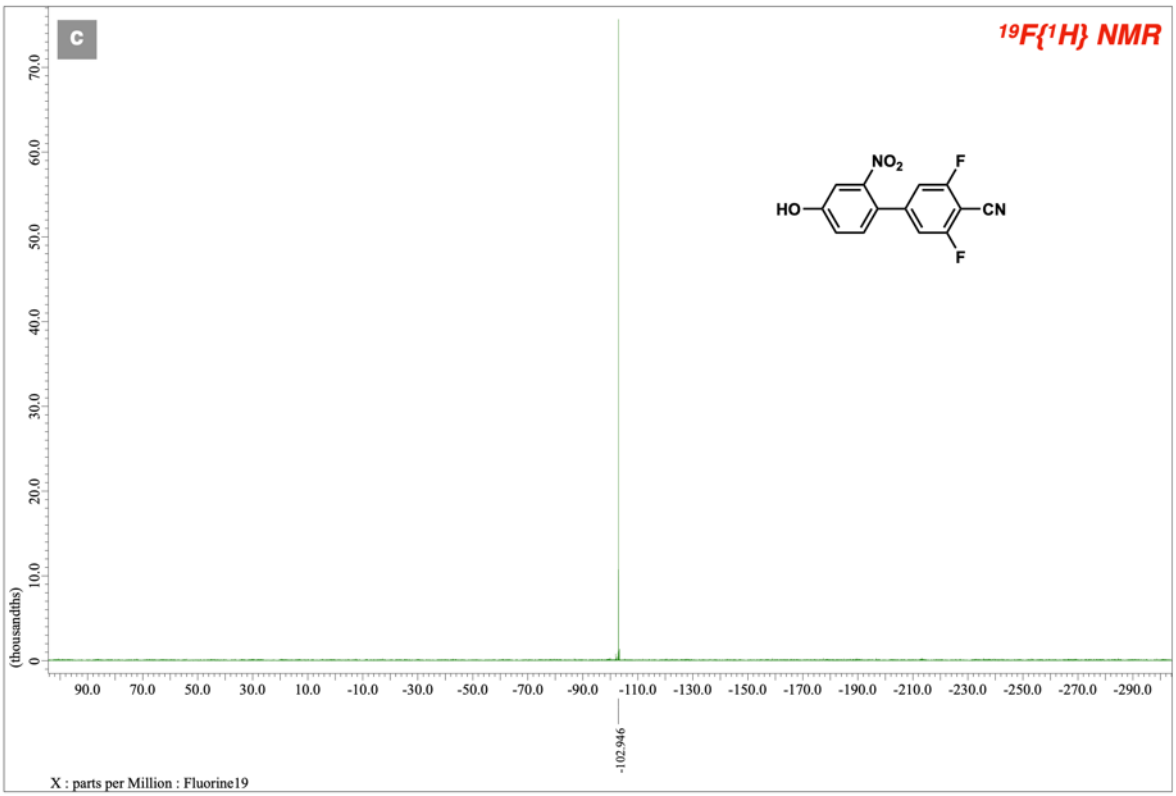

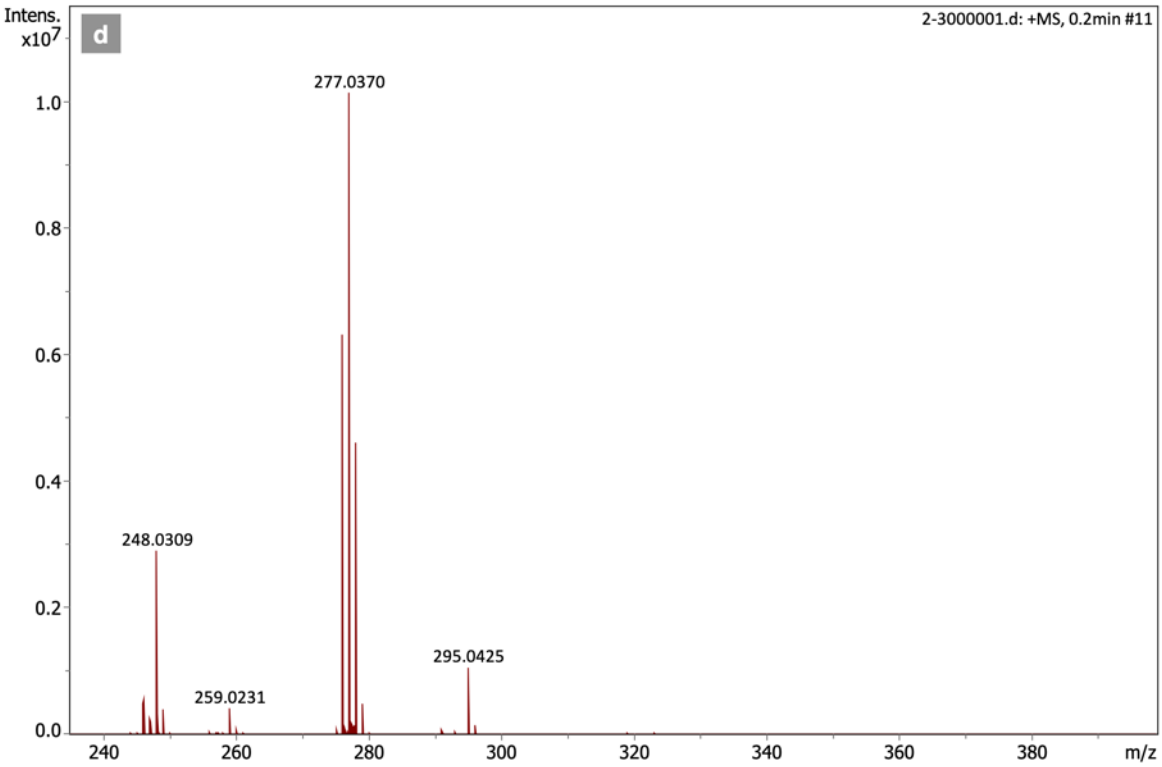

$^{1}H\{^{19}F\}$ NMR (a) and $^{13}C\{^{1}H,^{19}F\}$ NMR (b) spectra of compound ***10a***

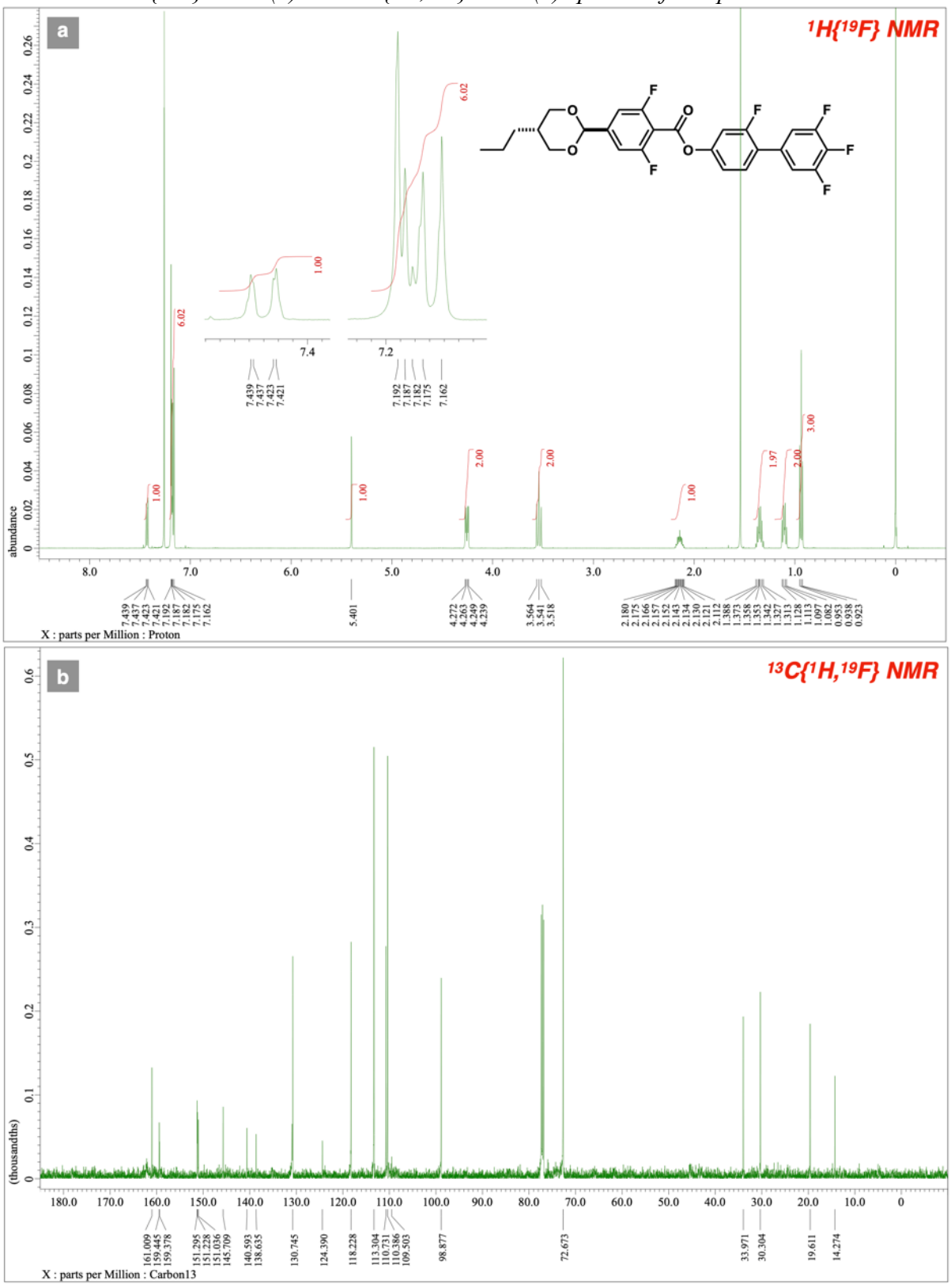

*$^{19}F\{^{1}H\}$ NMR (a) and QTOF-HRMS (b) spectra of compound **10a***

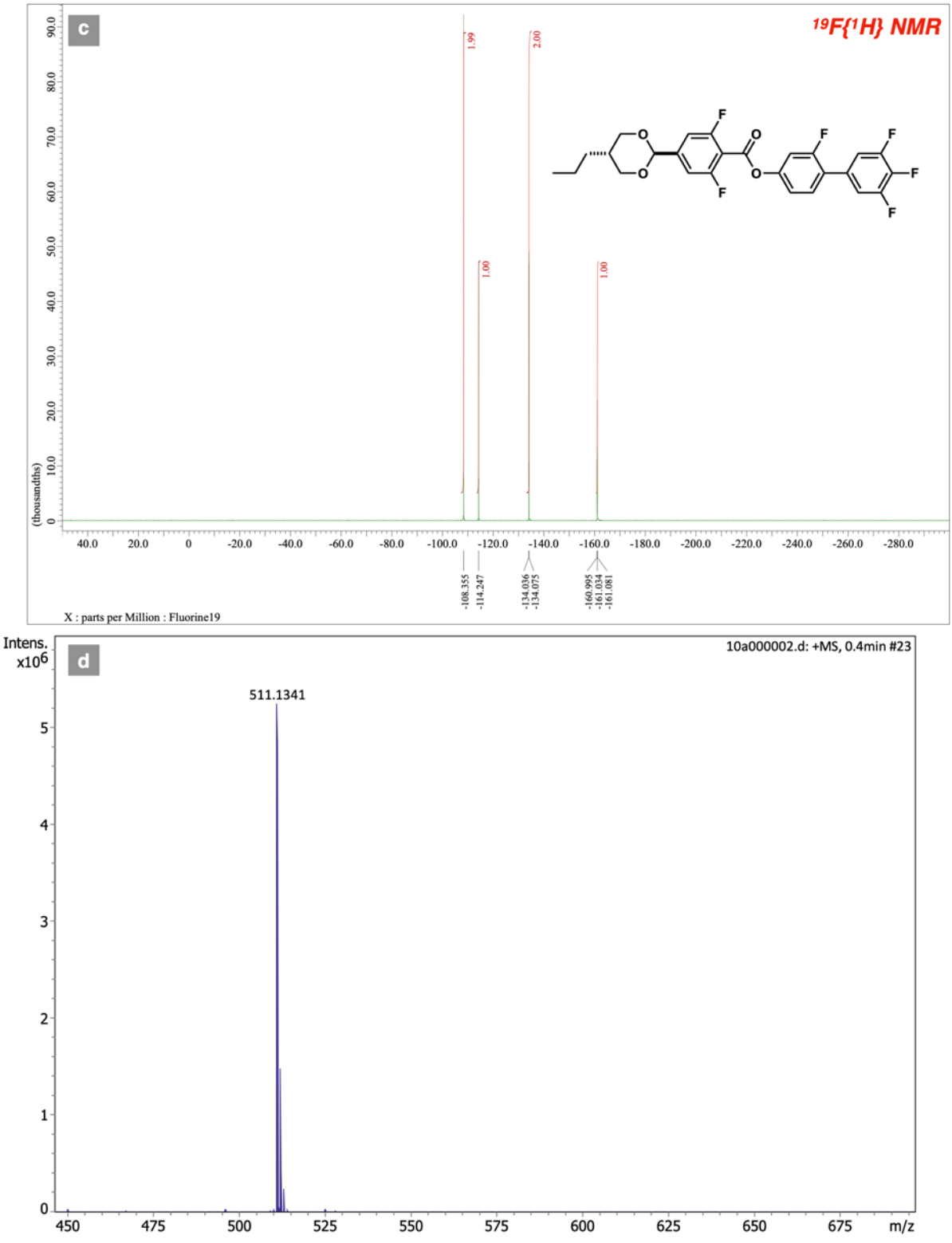

$^{1}H\{^{19}F\}$ NMR (a) and $^{13}C\{^{1}H,^{19}F\}$ NMR (b) spectra of compound ***10b***

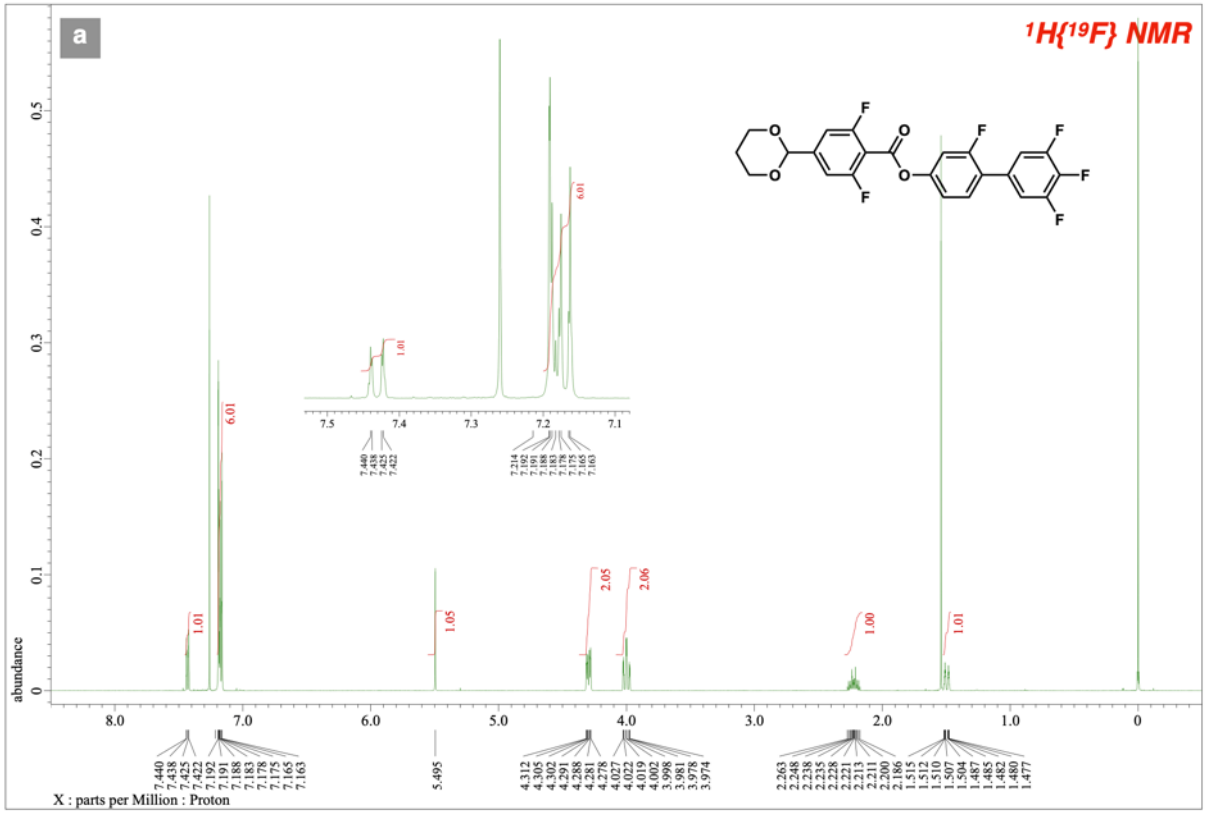

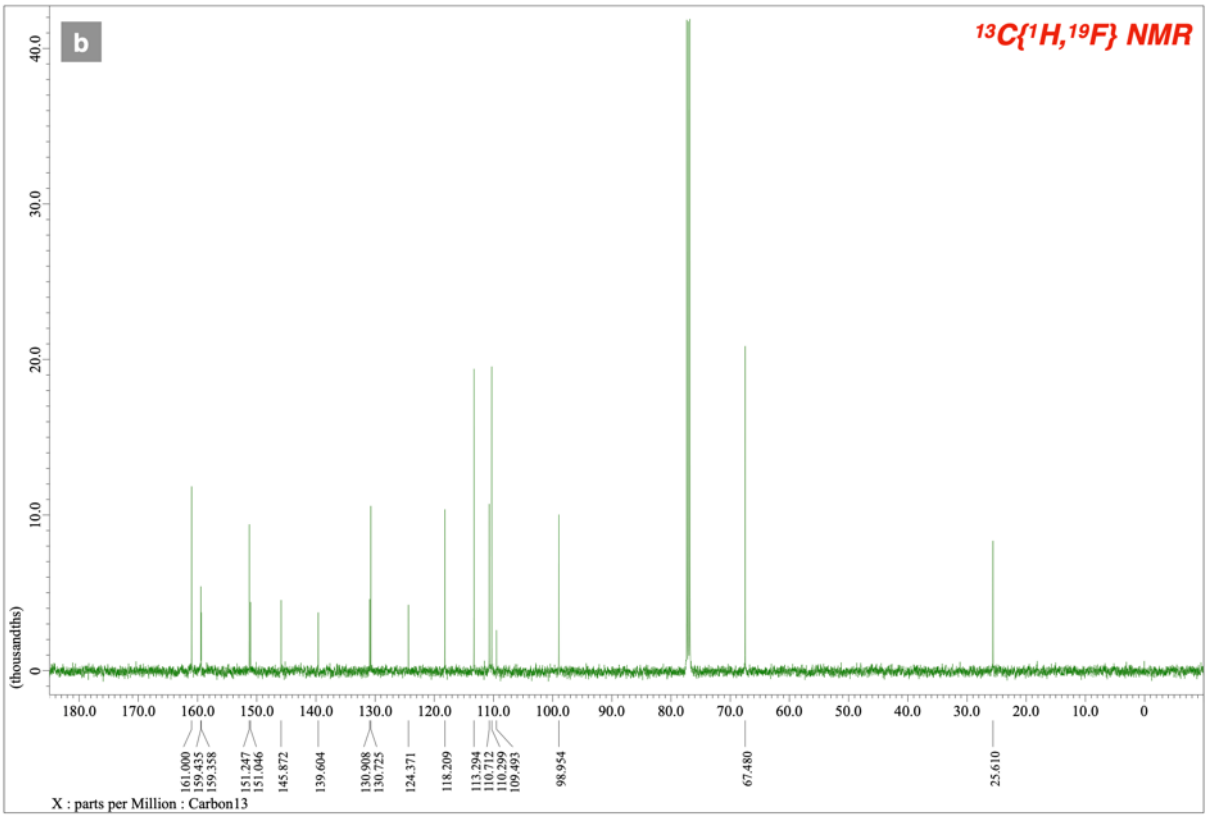

*$^{19}F\{^{1}H\}$ NMR (a) and QTOF-HRMS (b) spectra of compound **10b***

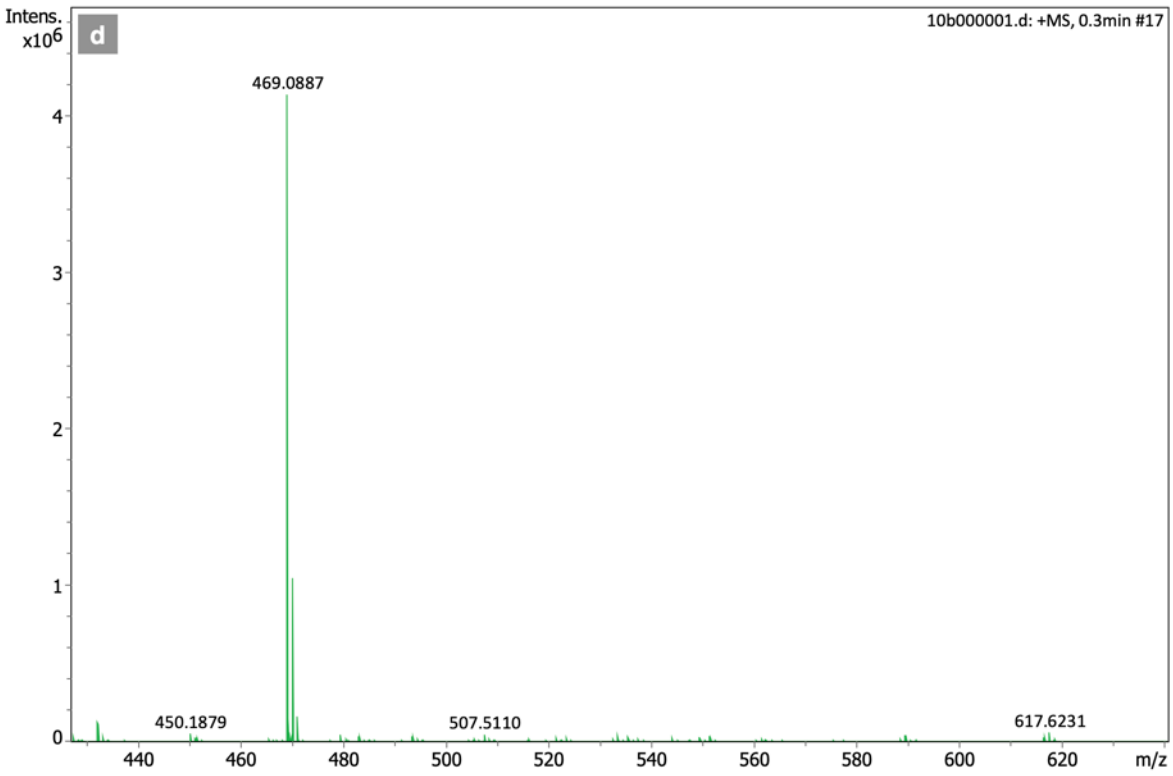

$^{1}H\{^{19}F\}$ NMR (a) and $^{13}C\{^{1}H,^{19}F\}$ NMR (b) spectra of compound ***10c***

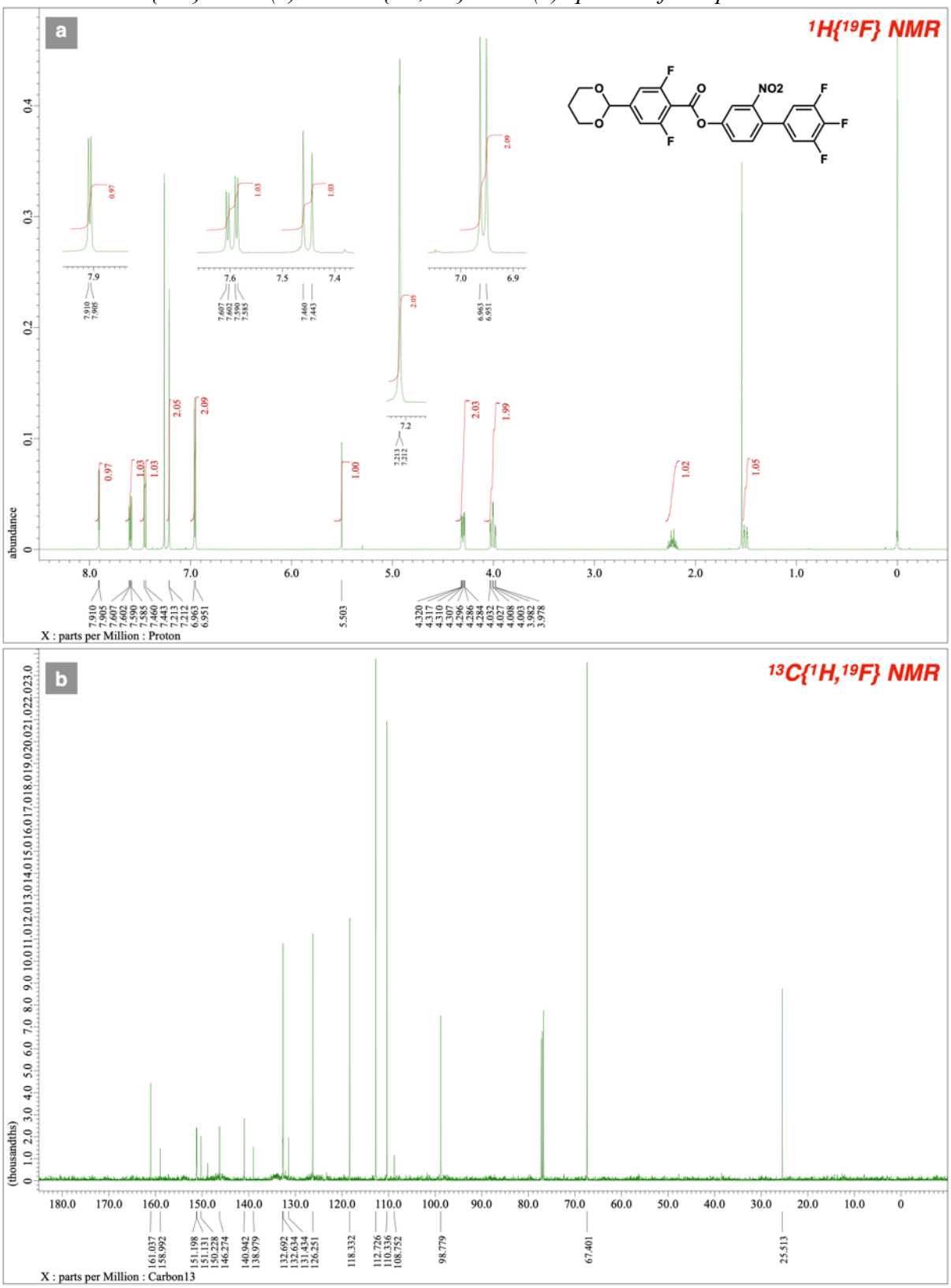

$^{19}F\{^{1}H\}$ NMR (a) and QTOF-HRMS (b) spectra of compound ***10c***

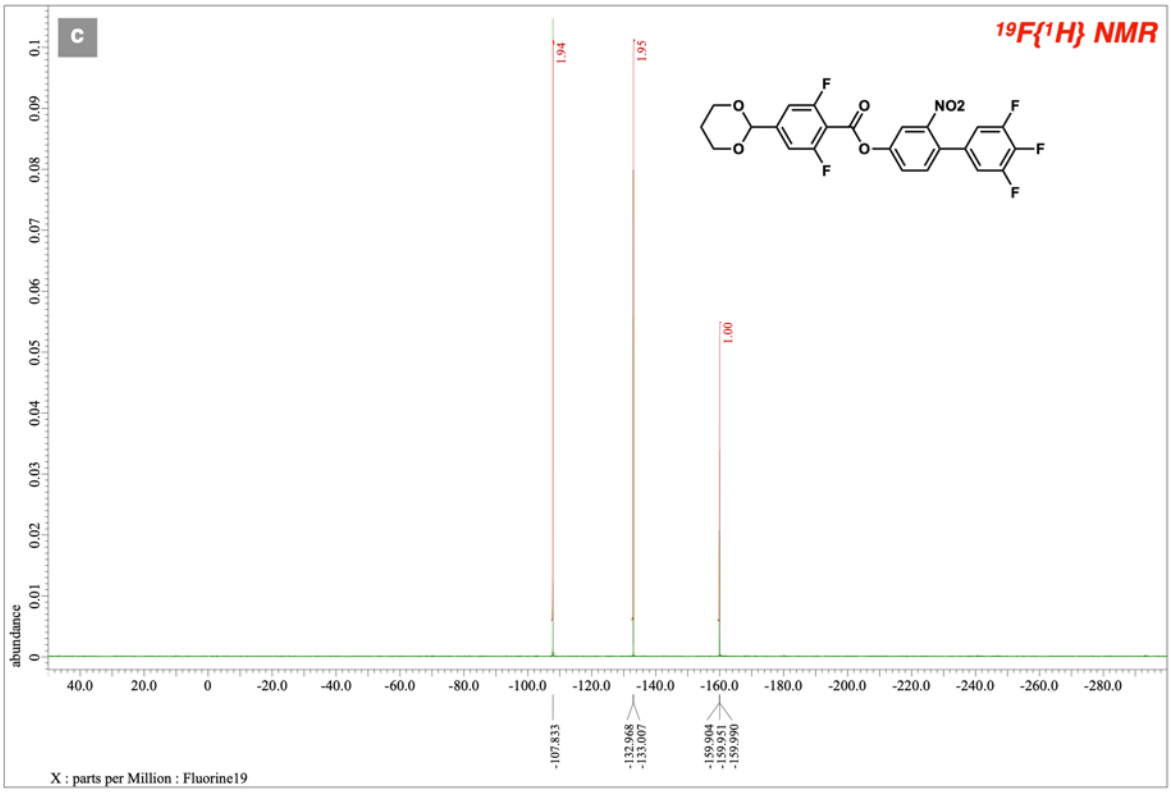

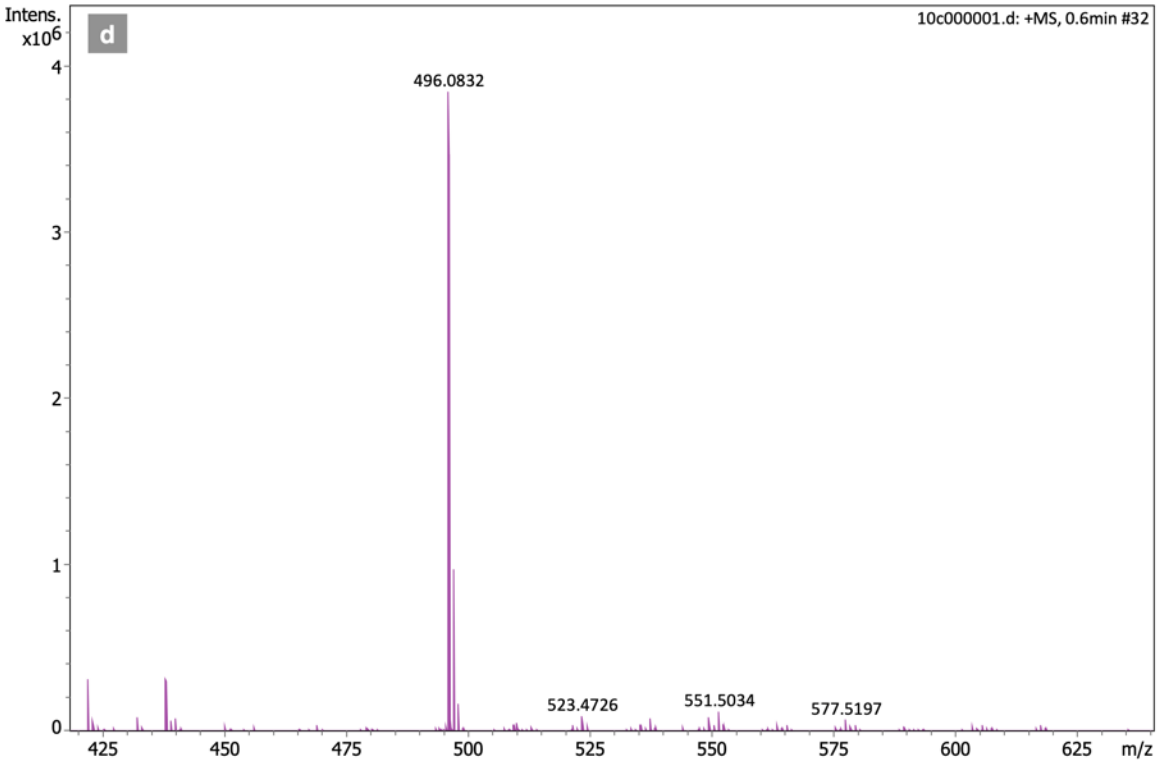

$^{1}H\{^{19}F\}$ NMR (a) and $^{13}C\{^{1}H,^{19}F\}$ NMR (b) spectra of compound ***10d***

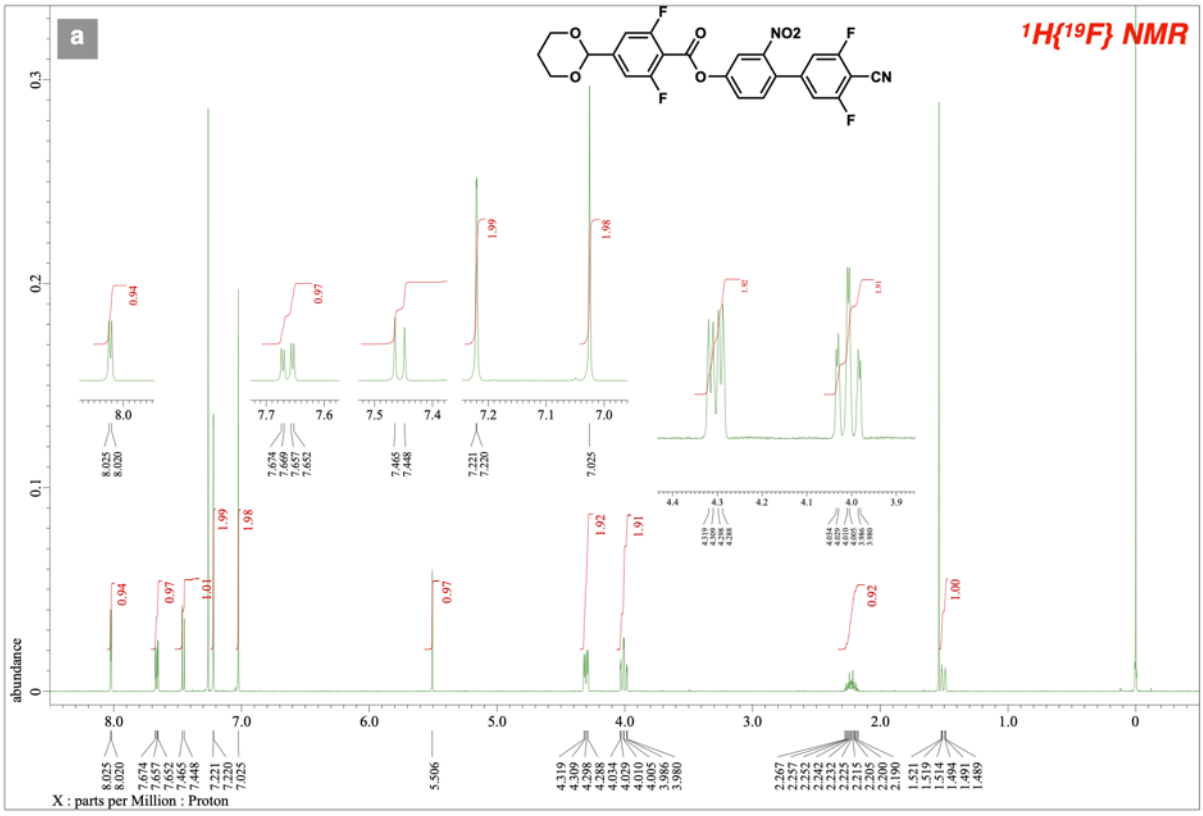

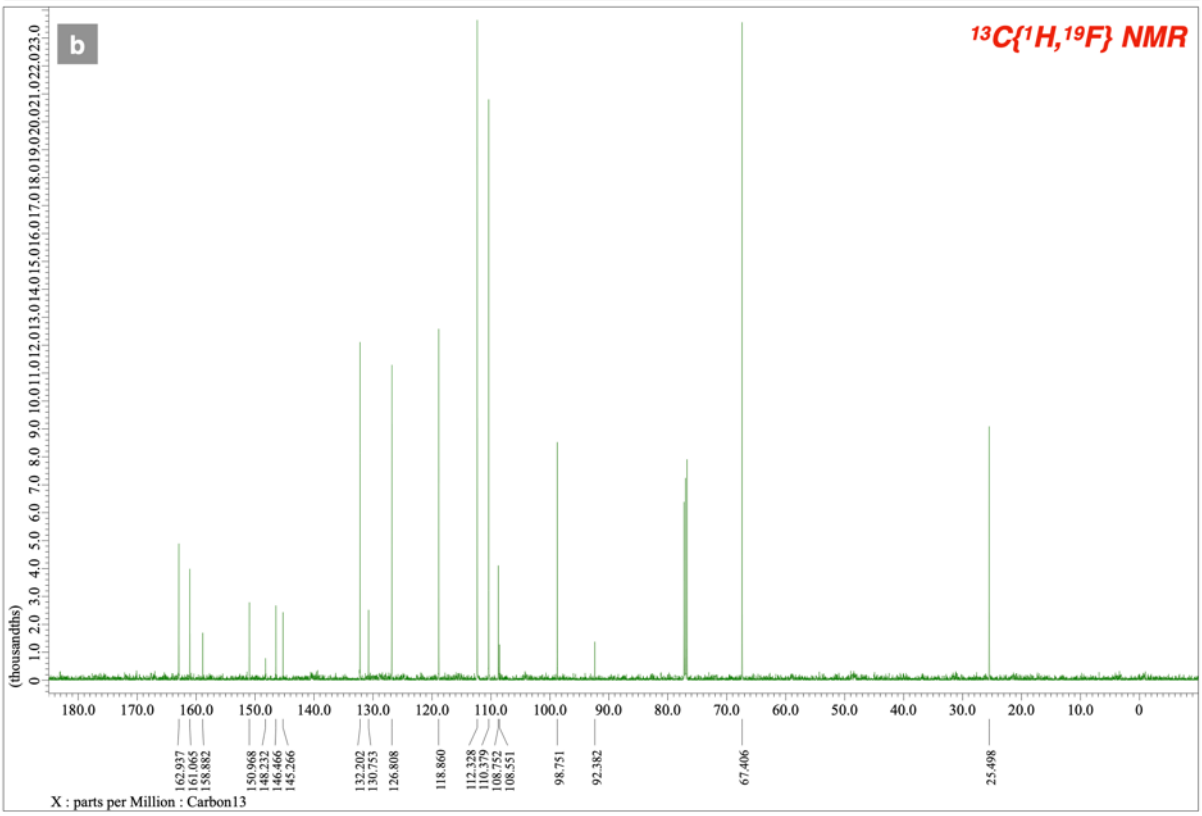

*$^{19}F\{^{1}H\}$ NMR (a) and QTOF-HRMS (b) spectra of compound **10d***

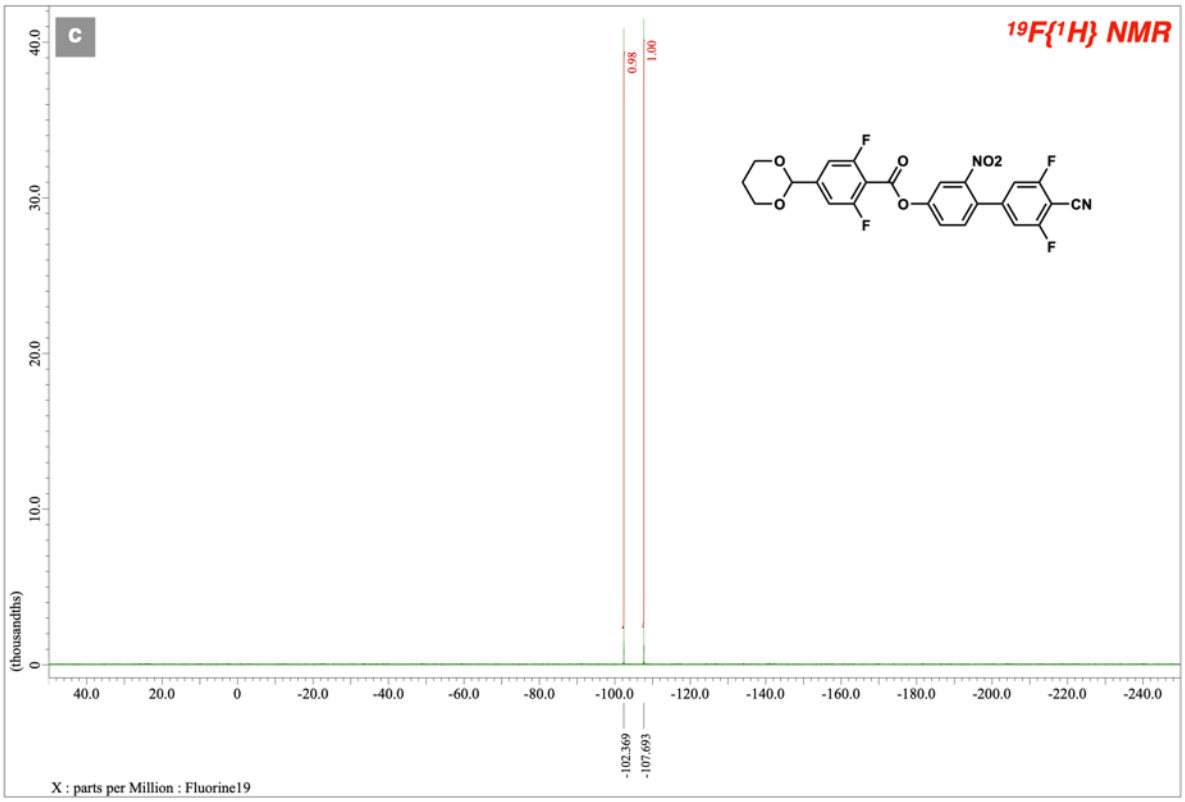

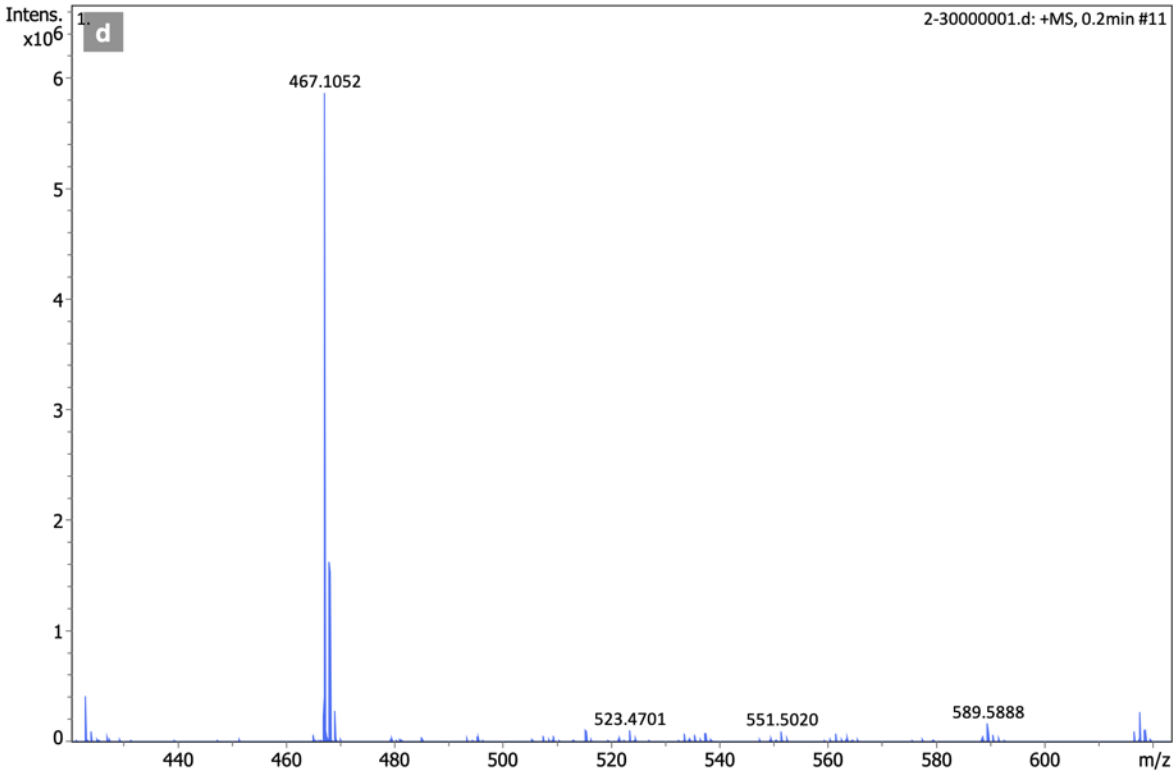

*$^{1}H\{^{19}F\}$ NMR (a) and $^{13}C\{^{1}H,^{19}F\}$ NMR (b) spectra of compound **10e***

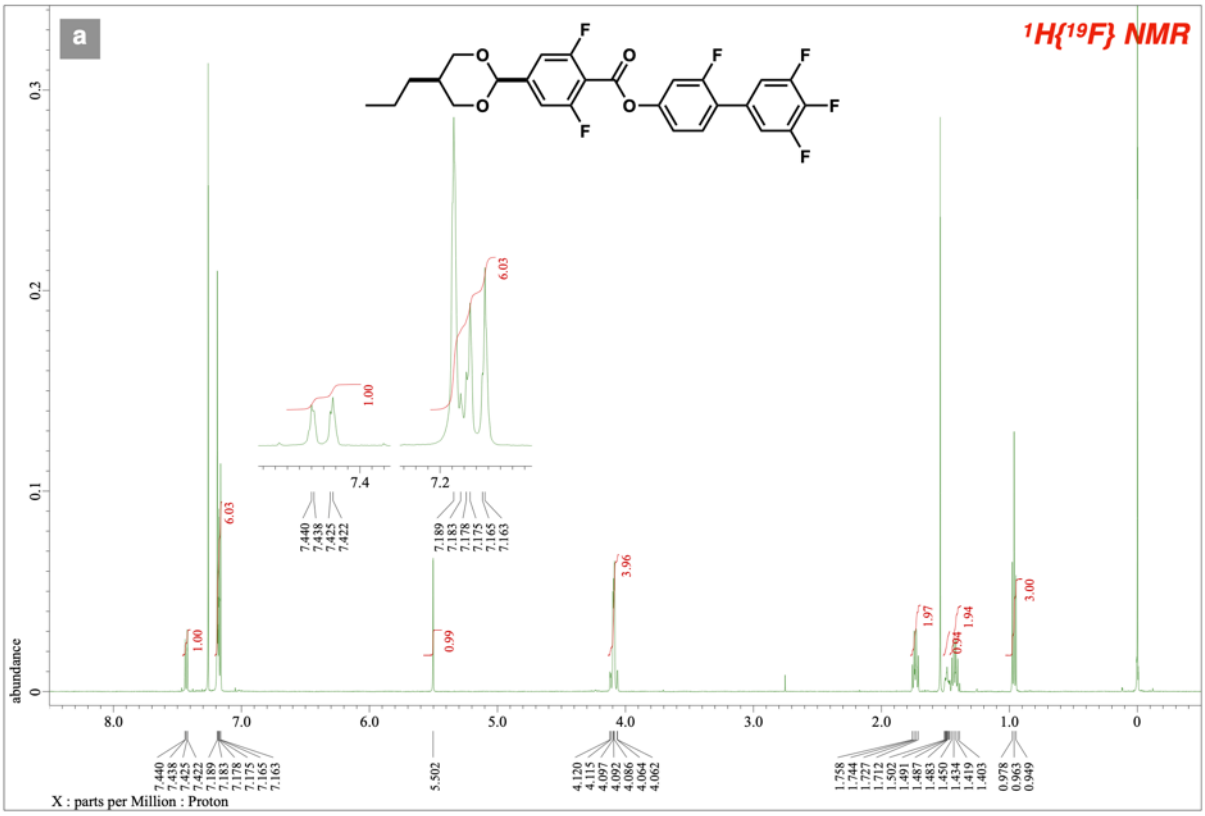

*$^{19}F\{^{1}H\}$ NMR (a) and QTOF-HRMS (b) spectra of compound **10e***

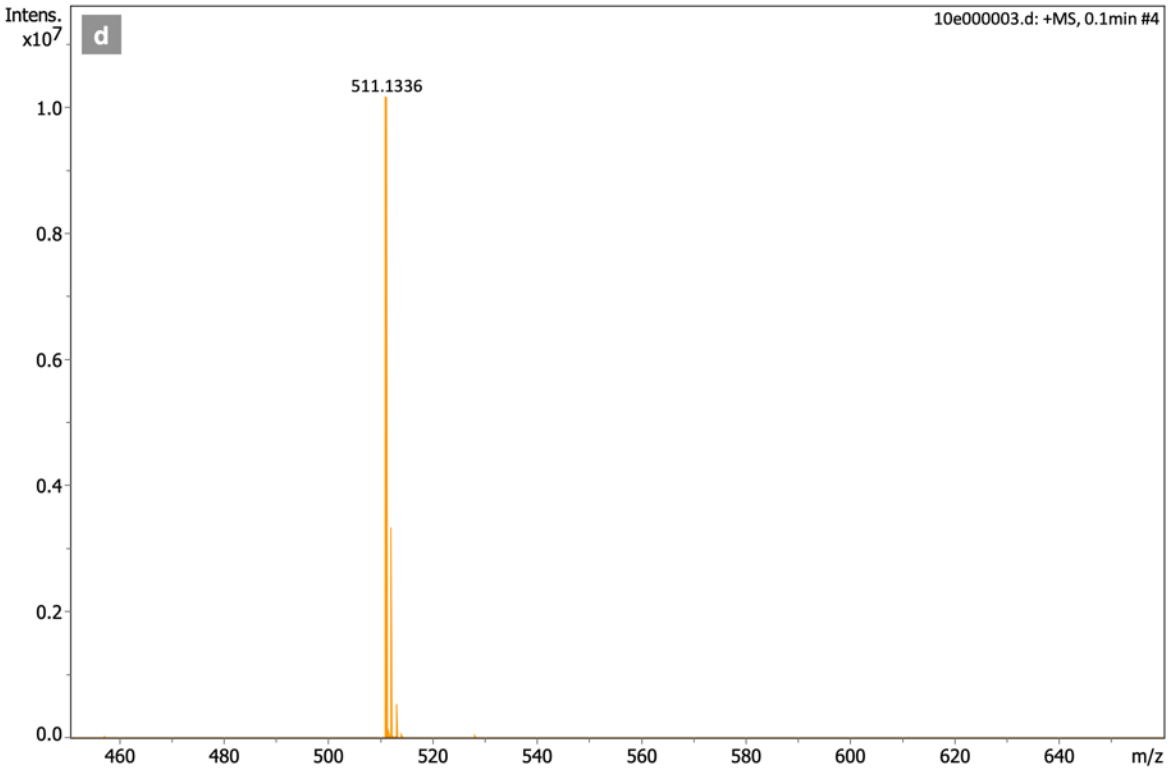

*$^{1}H\{^{19}F\}$ NMR (a) and $^{13}C\{^{1}H,^{19}F\}$ NMR (b) spectra of compound **10f***

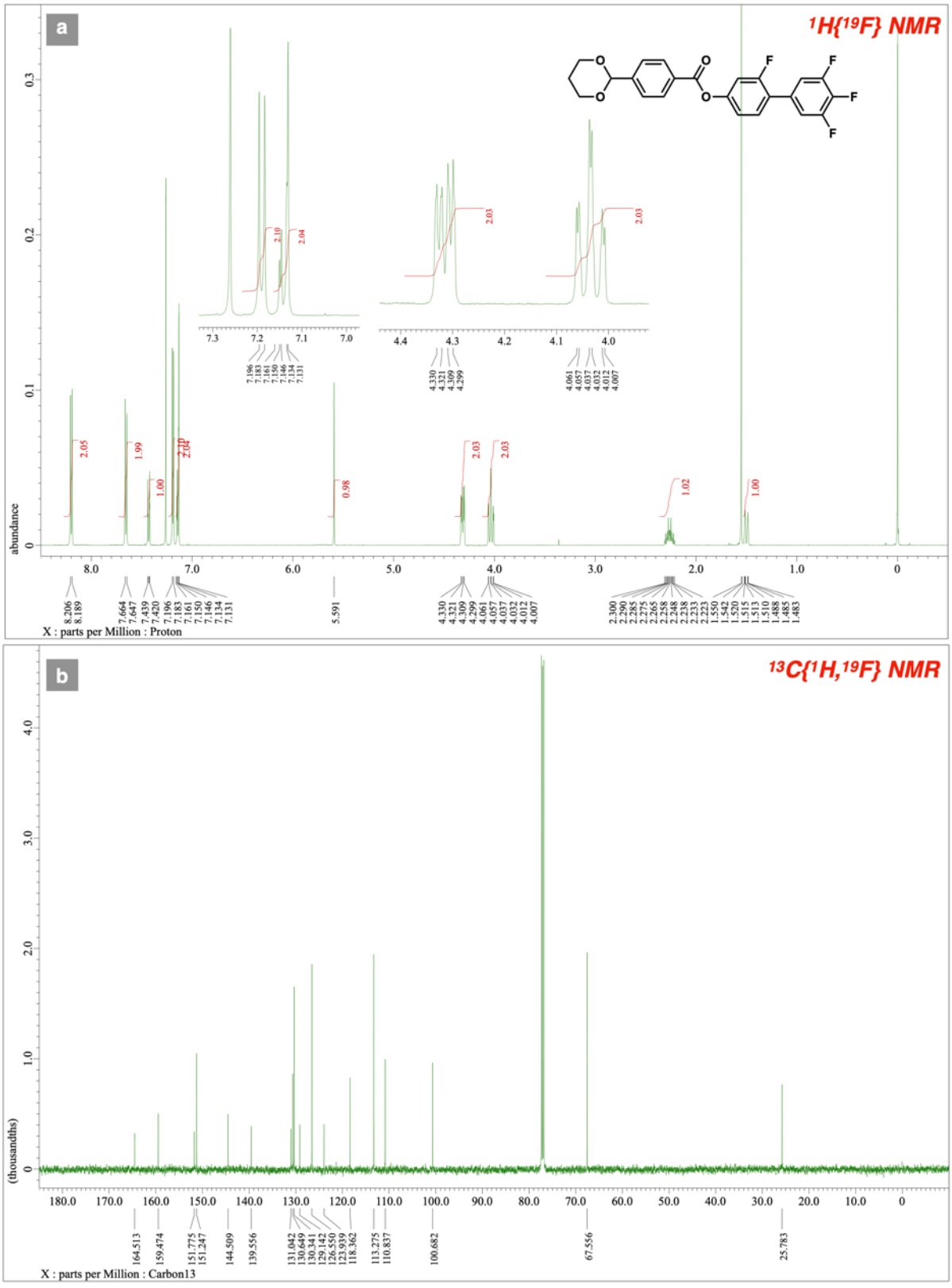

*$^{19}F\{^1H\}$ NMR (a) and QTOF-HRMS (b) spectra of compound **10f***

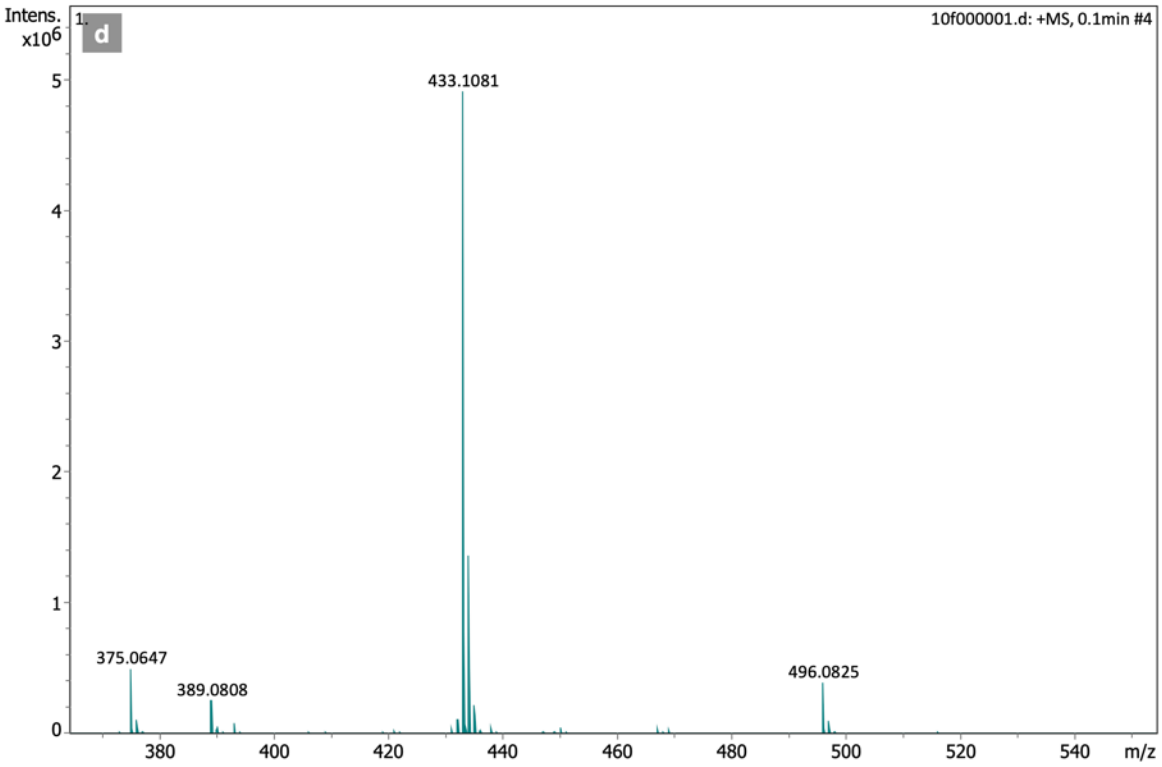

$^{1}H\{^{19}F\}$ NMR (a) and $^{13}C\{^{1}H,^{19}F\}$ NMR (b) spectra of compound ***11a***

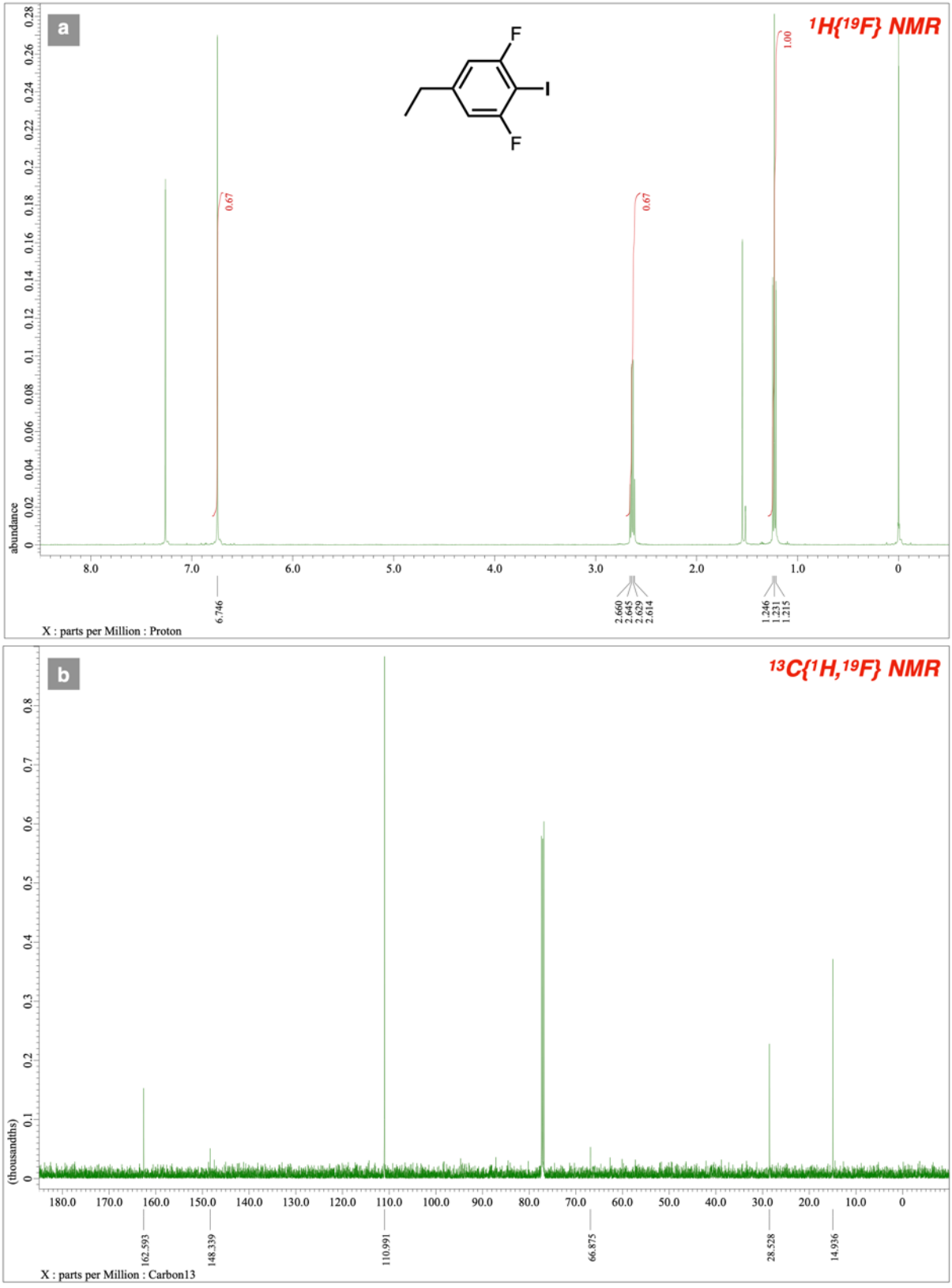

*$^{19}F\{^{1}H\}$ NMR (a) and QTOF-HRMS (b) spectra of compound **11a***

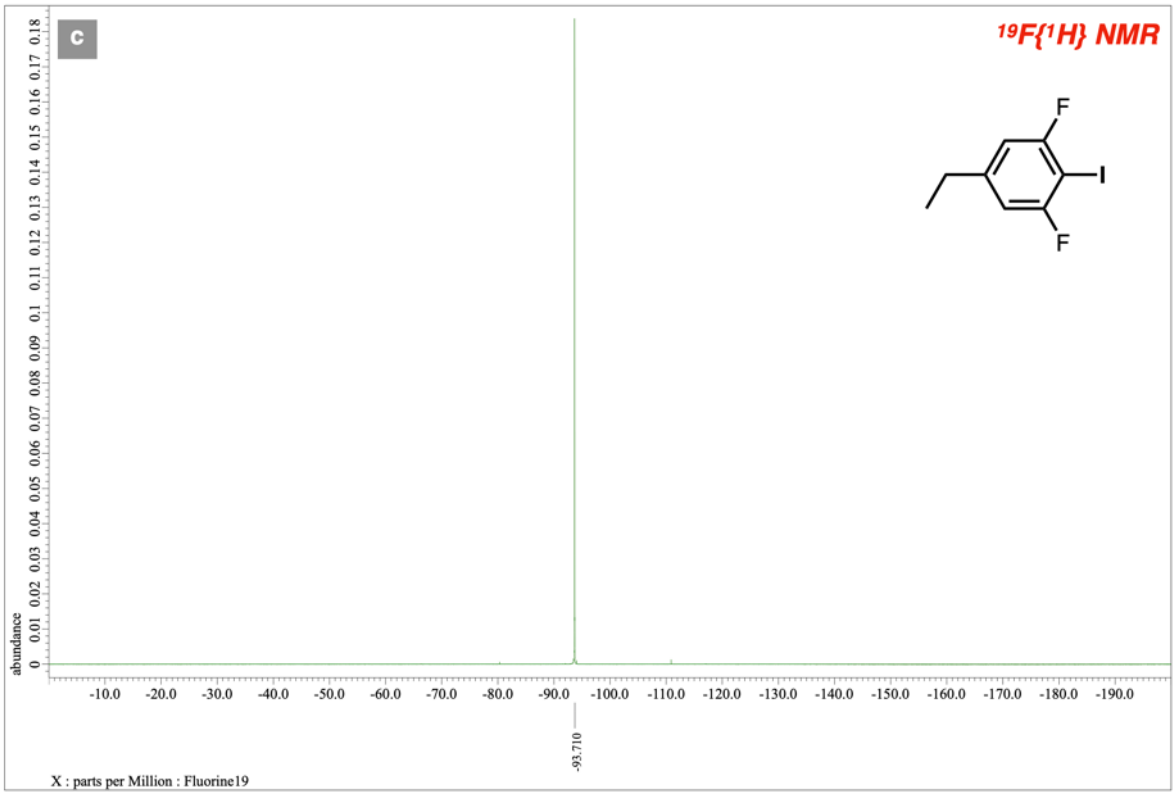

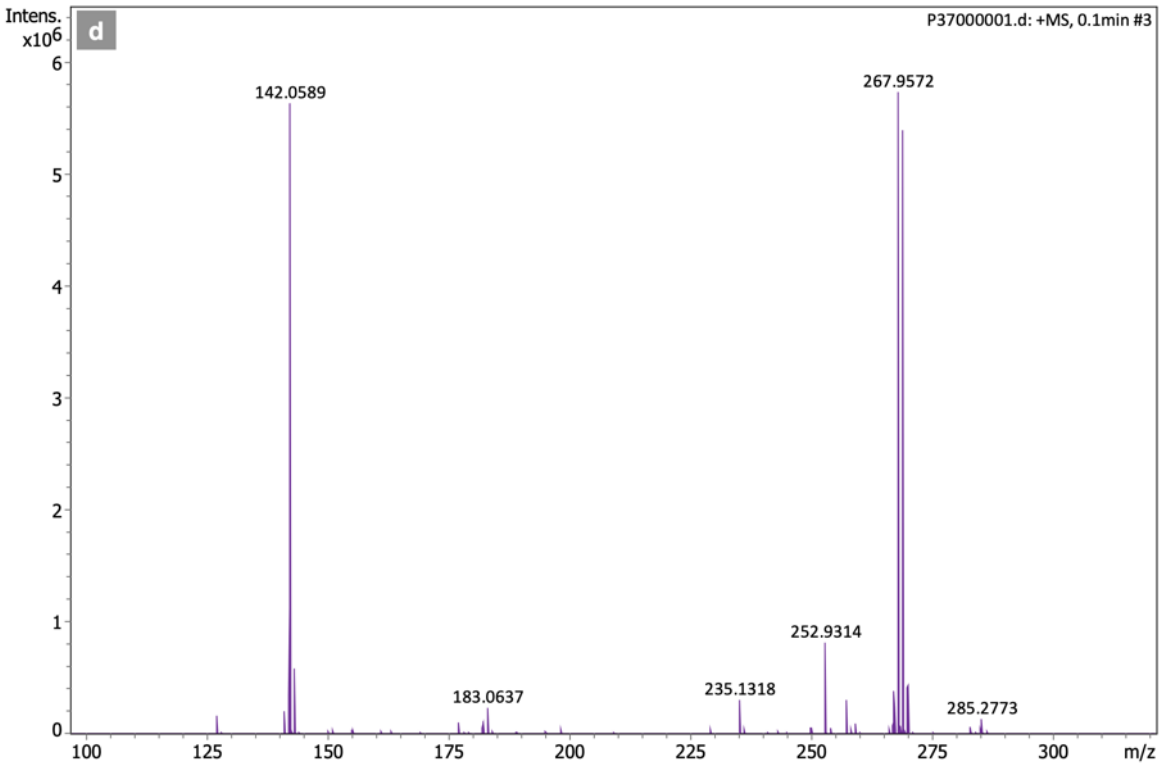

$^{1}H\{^{19}F\}$ NMR (a) and $^{13}C\{^{1}H,^{19}F\}$ NMR (b) spectra of compound ***11b***

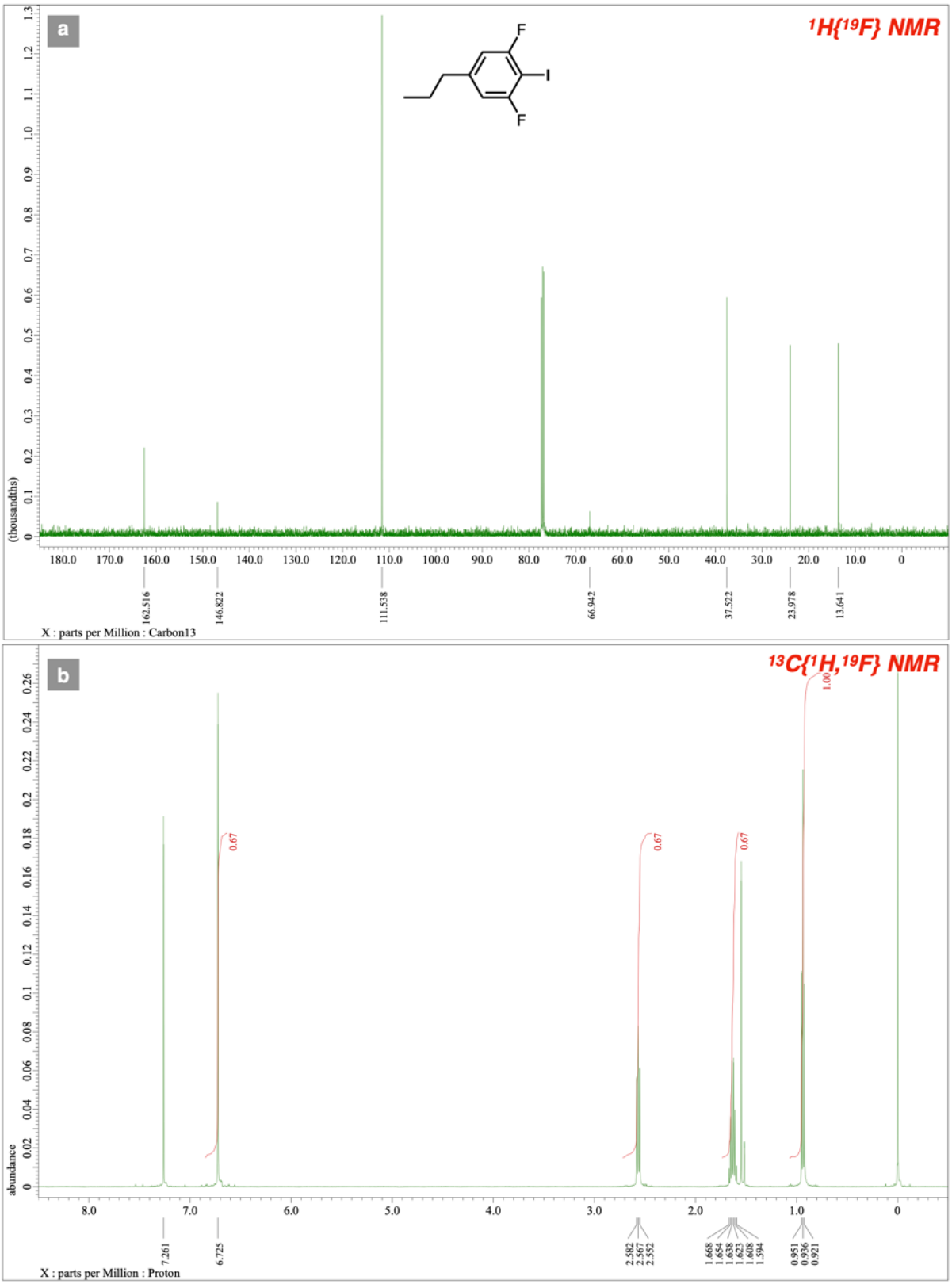

*$^{19}F\{^{1}H\}$ NMR (a) and QTOF-HRMS (b) spectra of compound **11b***

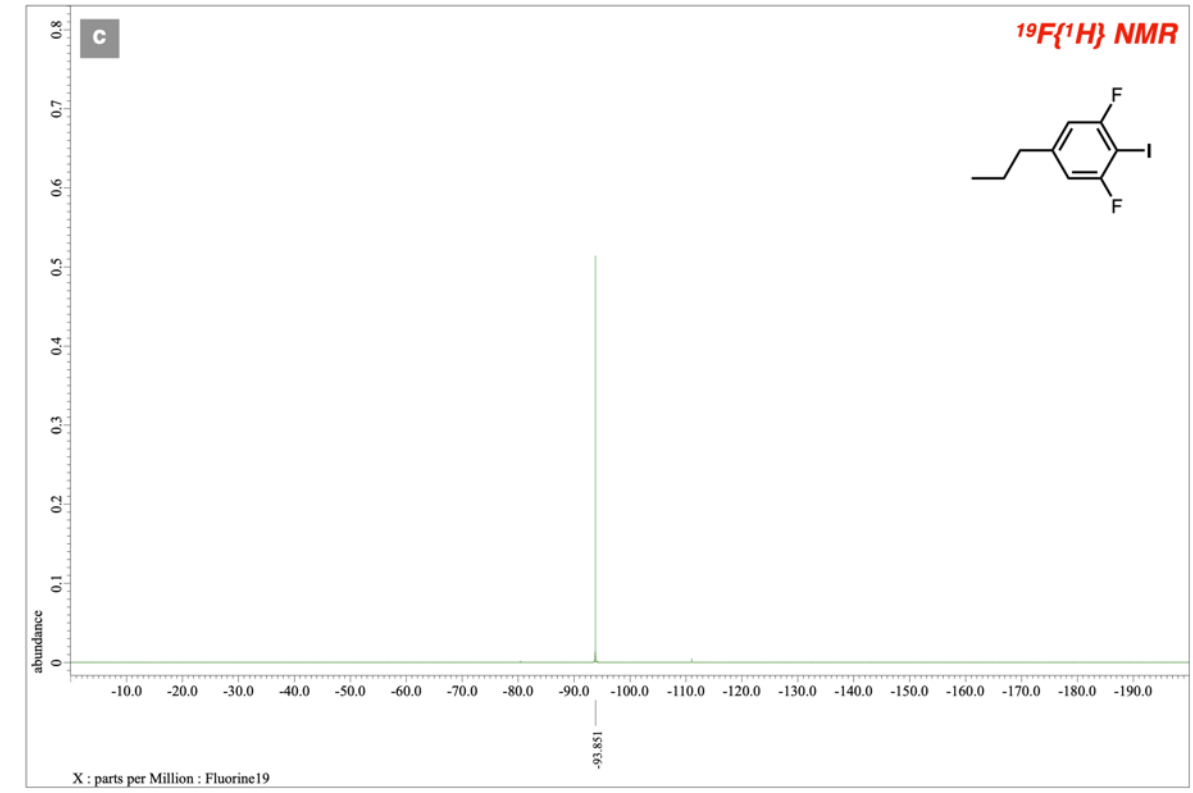

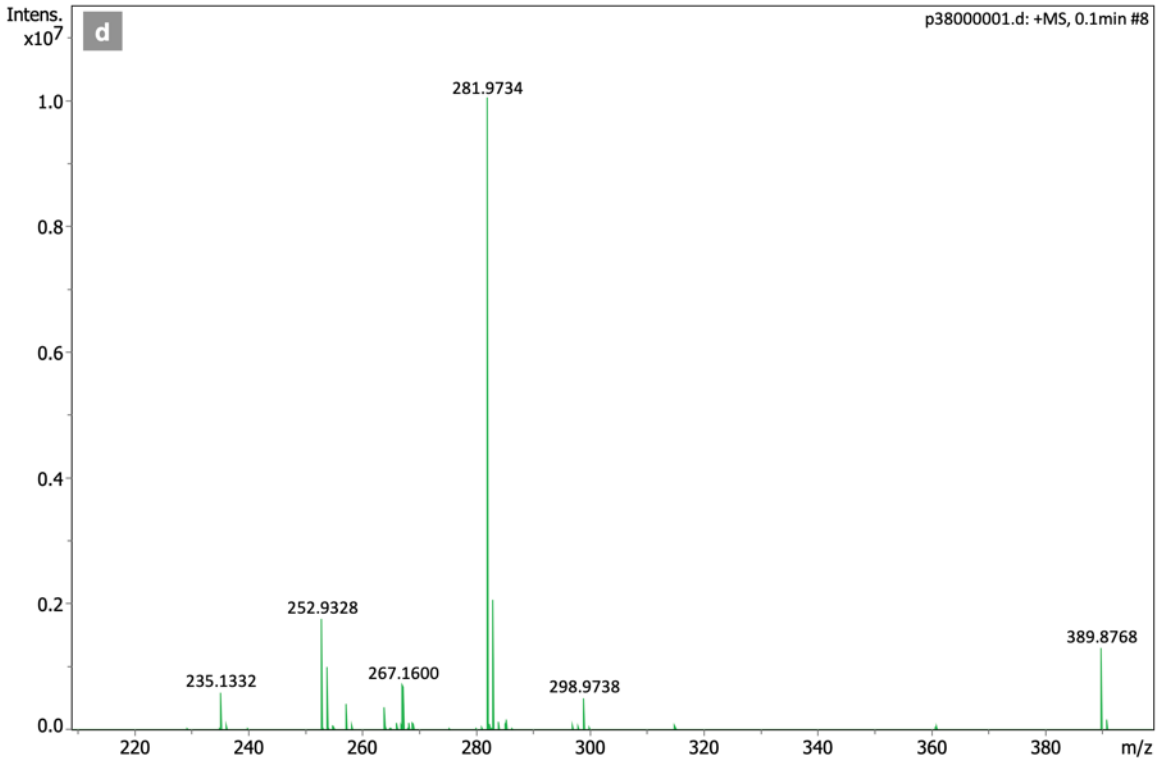

$^{1}H\{^{19}F\}$ NMR (a) and $^{13}C\{^{1}H,^{19}F\}$ NMR (b) spectra of compound ***12a***

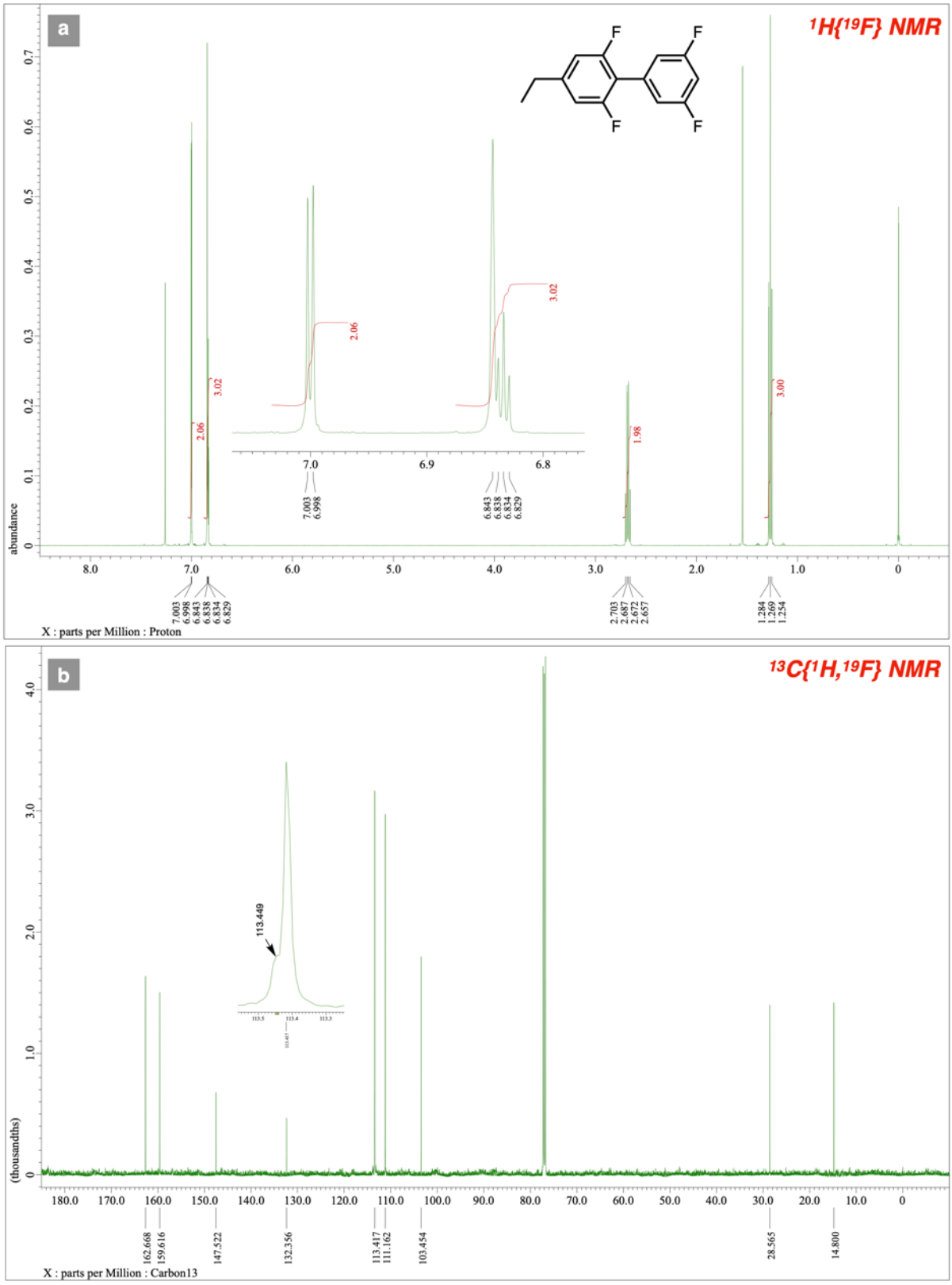

$^{19}F\{^{1}H\}$ NMR (a) and QTOF-HRMS (b) spectra of compound ***12a***

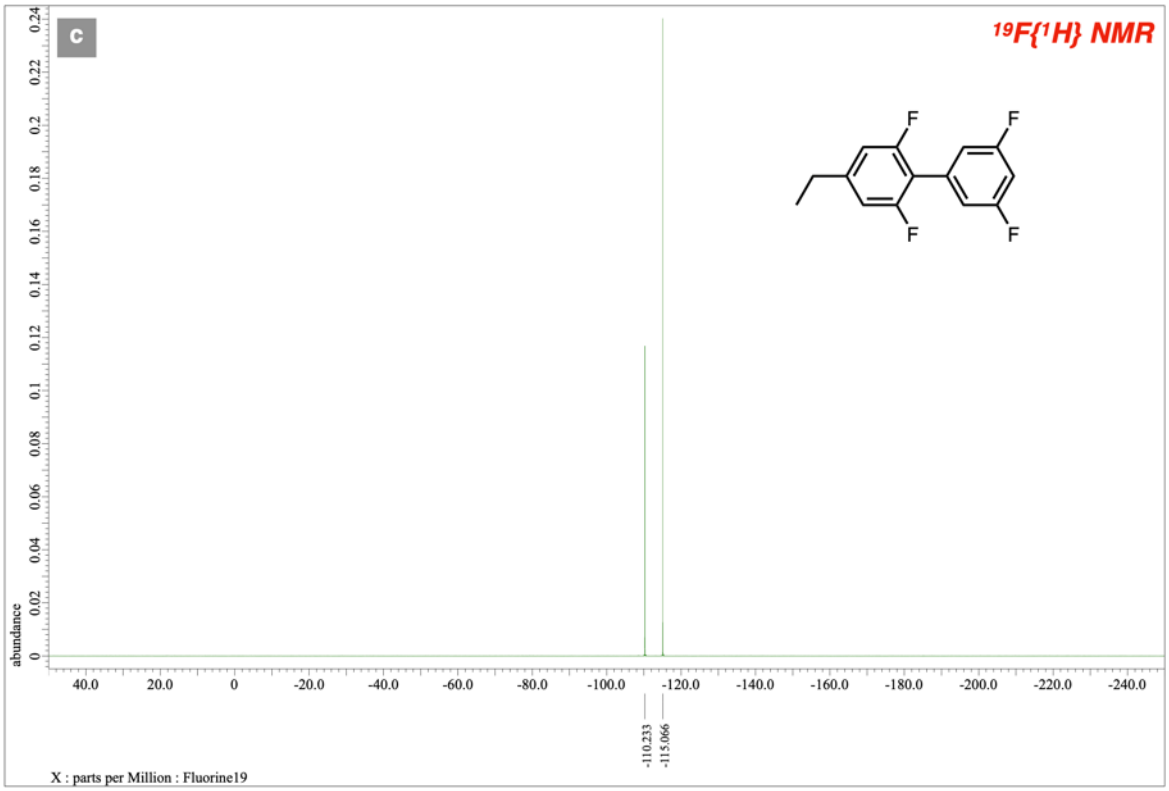

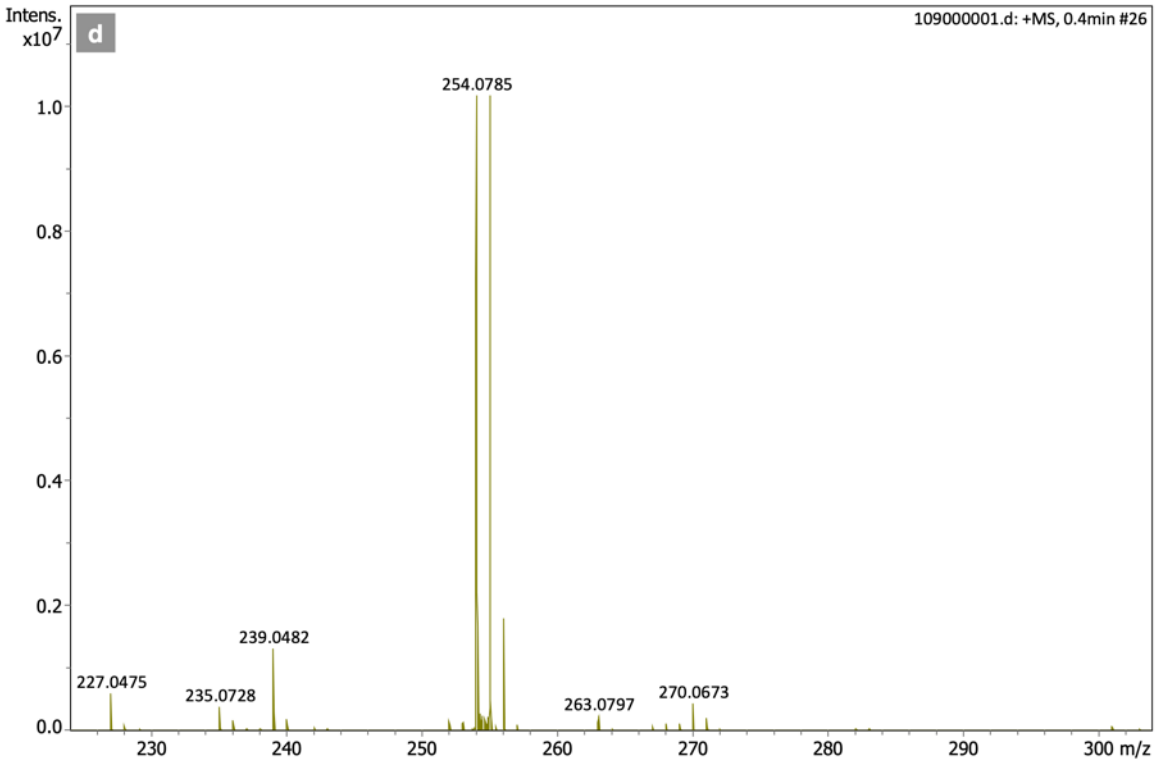

$^{1}H\{^{19}F\}$ NMR (a) and $^{13}C\{^{1}H,^{19}F\}$ NMR (b) spectra of compound ***12b***

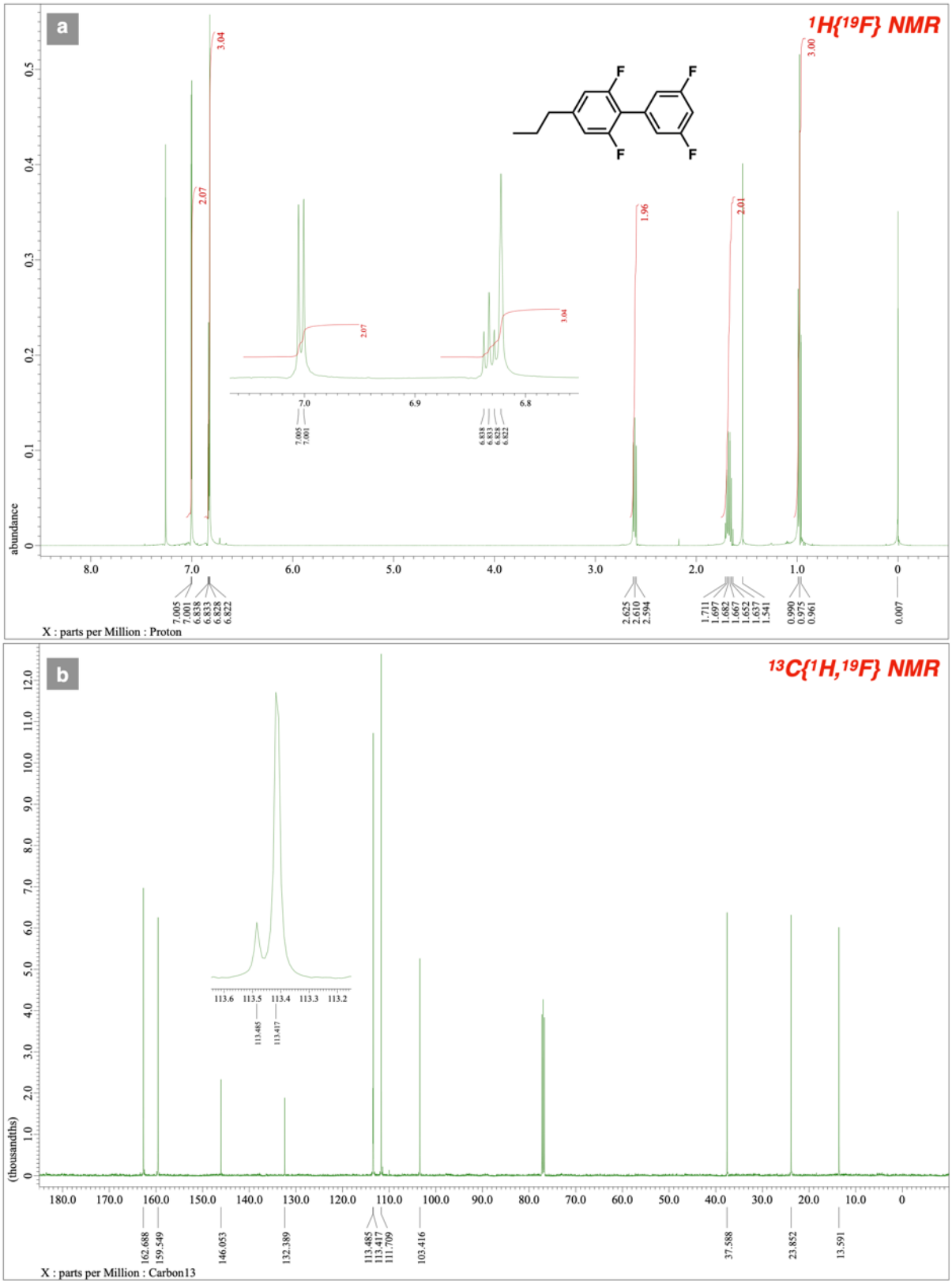

$^{19}F\{^{1}H\}$ NMR (a) and QTOF-HRMS (b) spectra of compound ***12b***

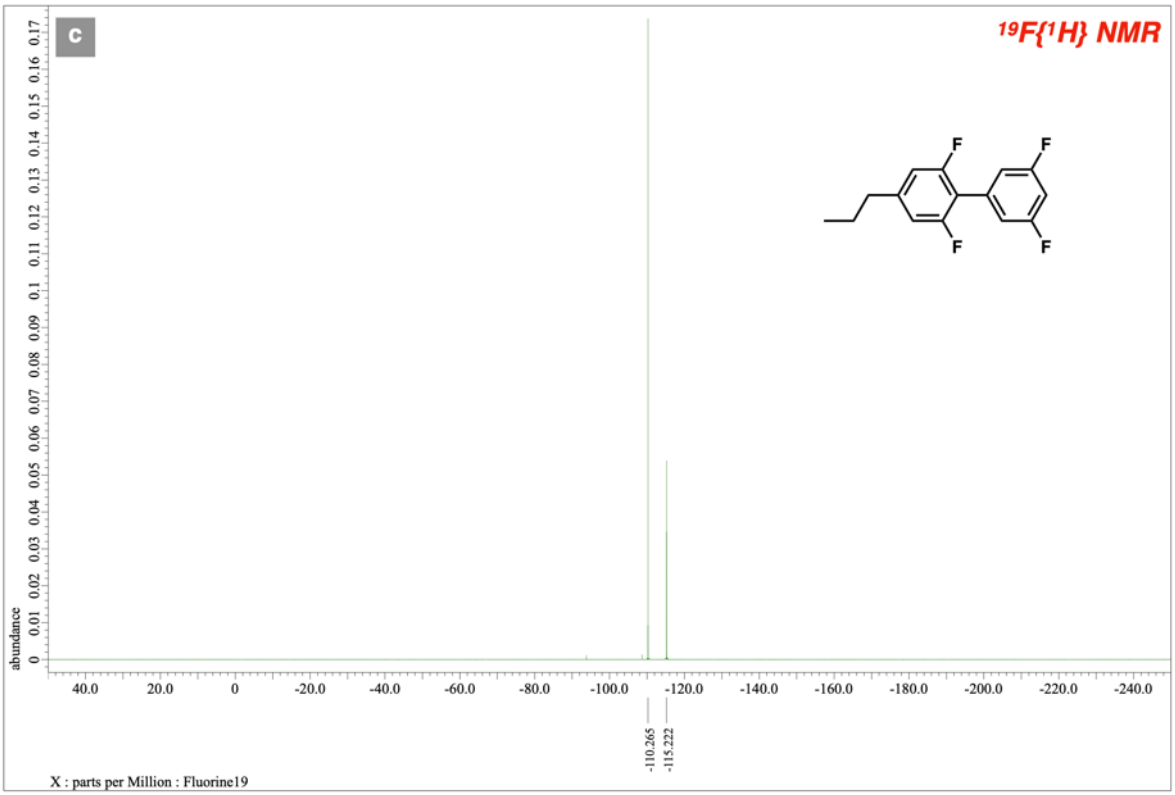

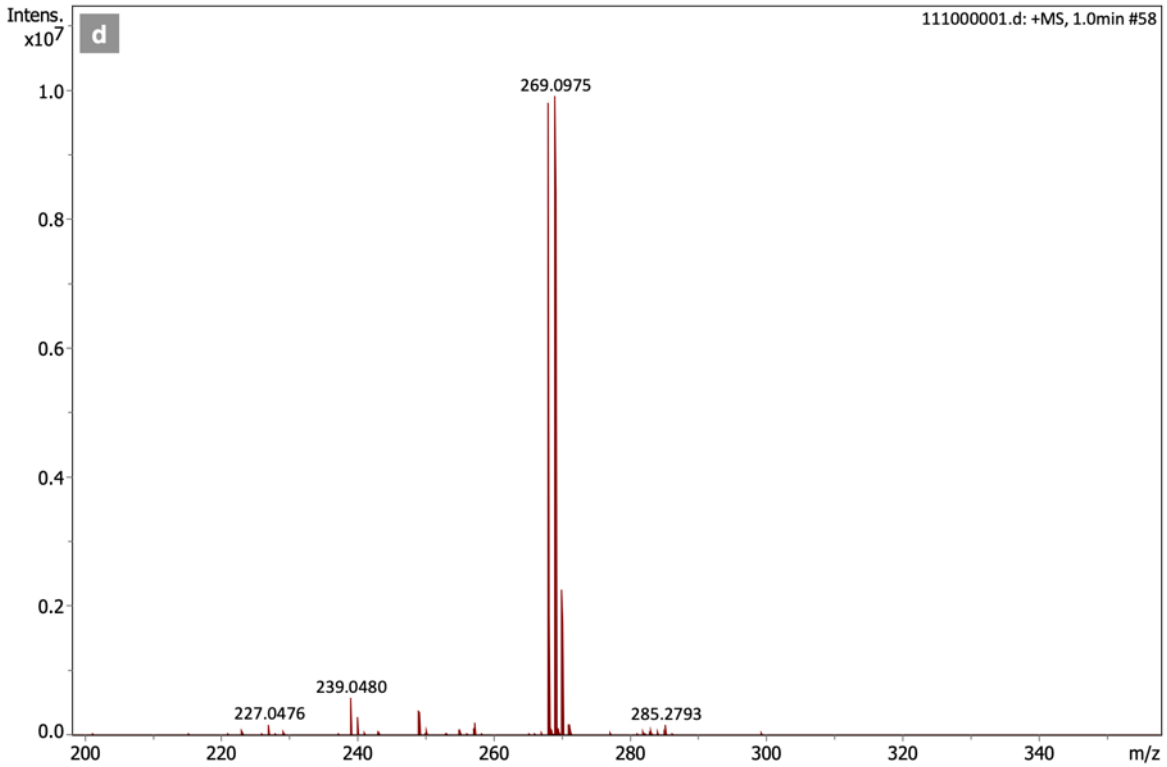

$^{1}H\{^{19}F\}$ NMR (a) and $^{13}C\{^{1}H,^{19}F\}$ NMR (b) spectra of compound ***13a***

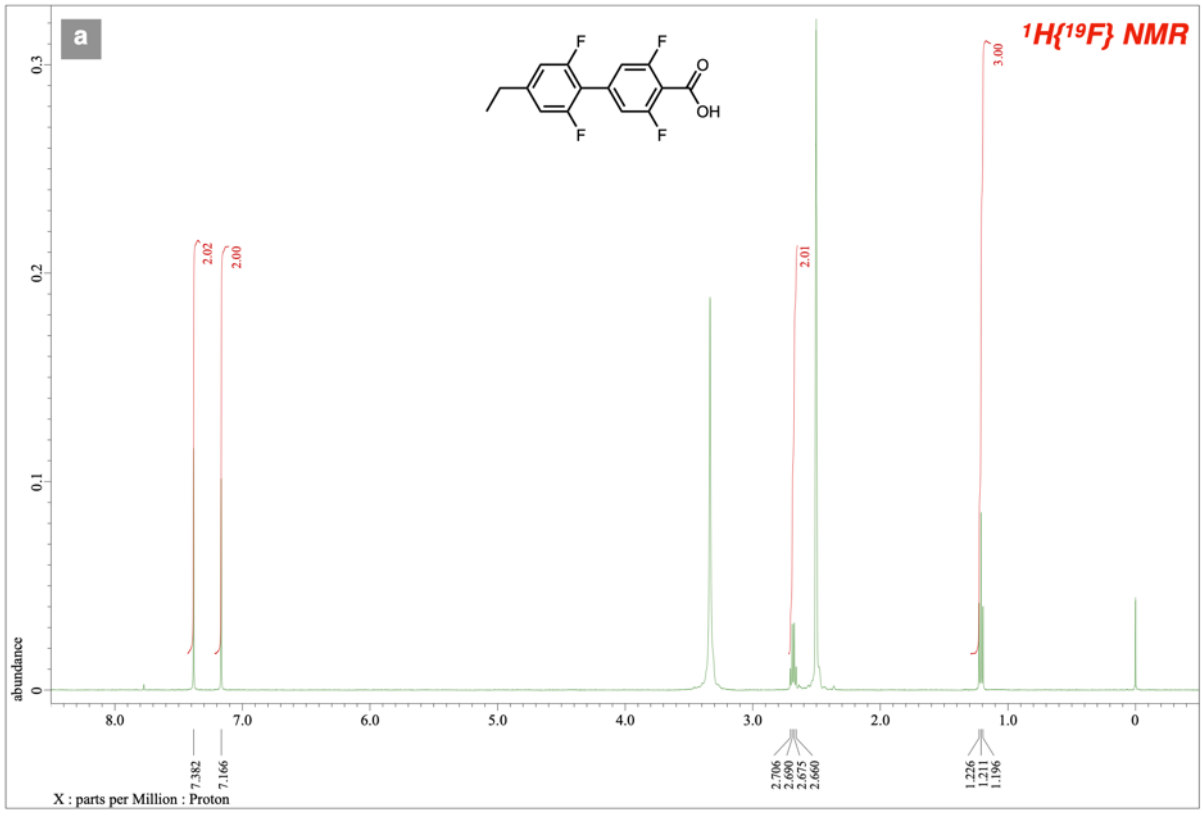

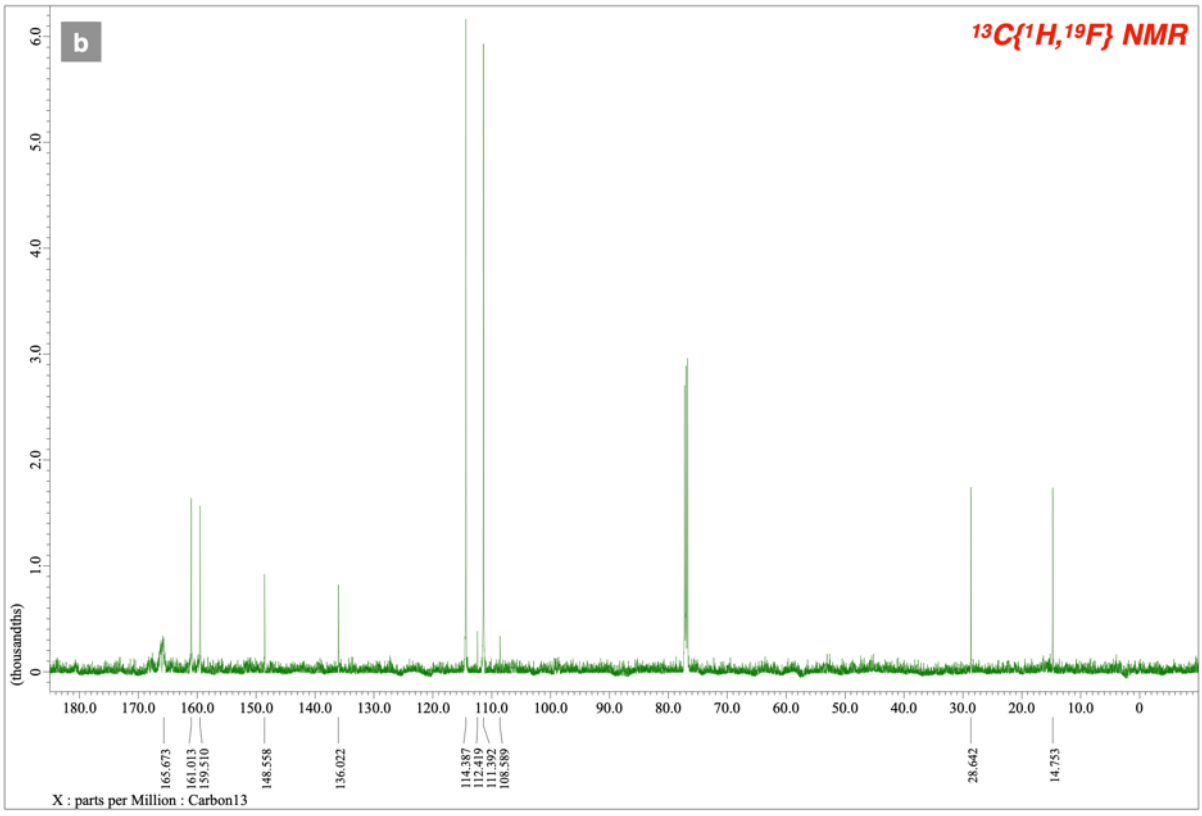

$^{19}F\{^{1}H\}$ NMR (a) and QTOF-HRMS (b) spectra of compound ***13a***

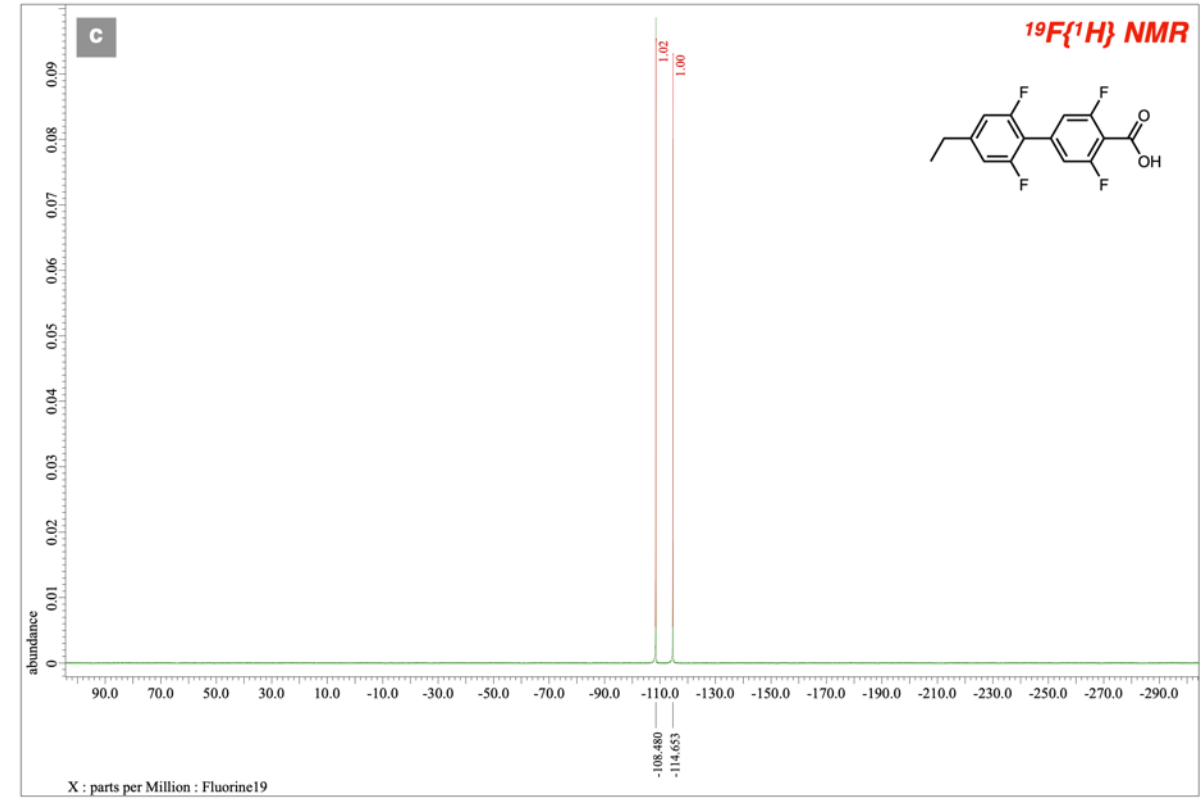

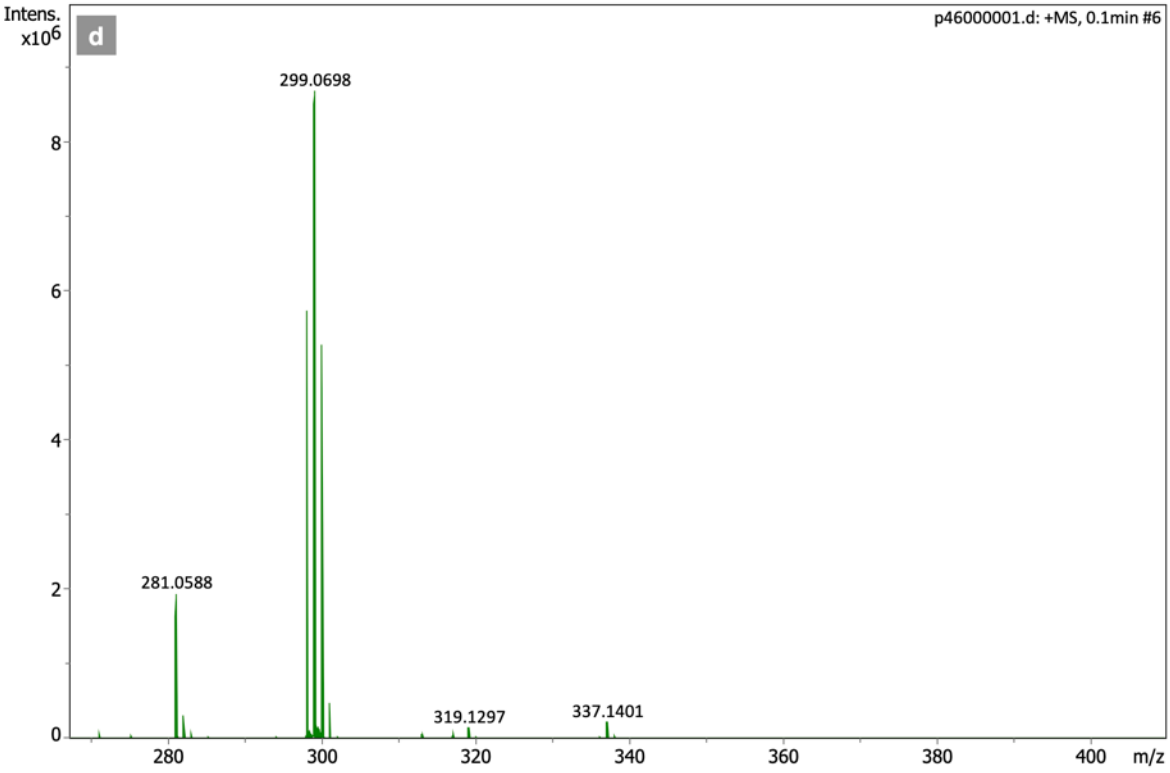

$^{1}H\{^{19}F\}$ NMR (a) and $^{13}C\{^{1}H,^{19}F\}$ NMR (b) spectra of compound ***13b***

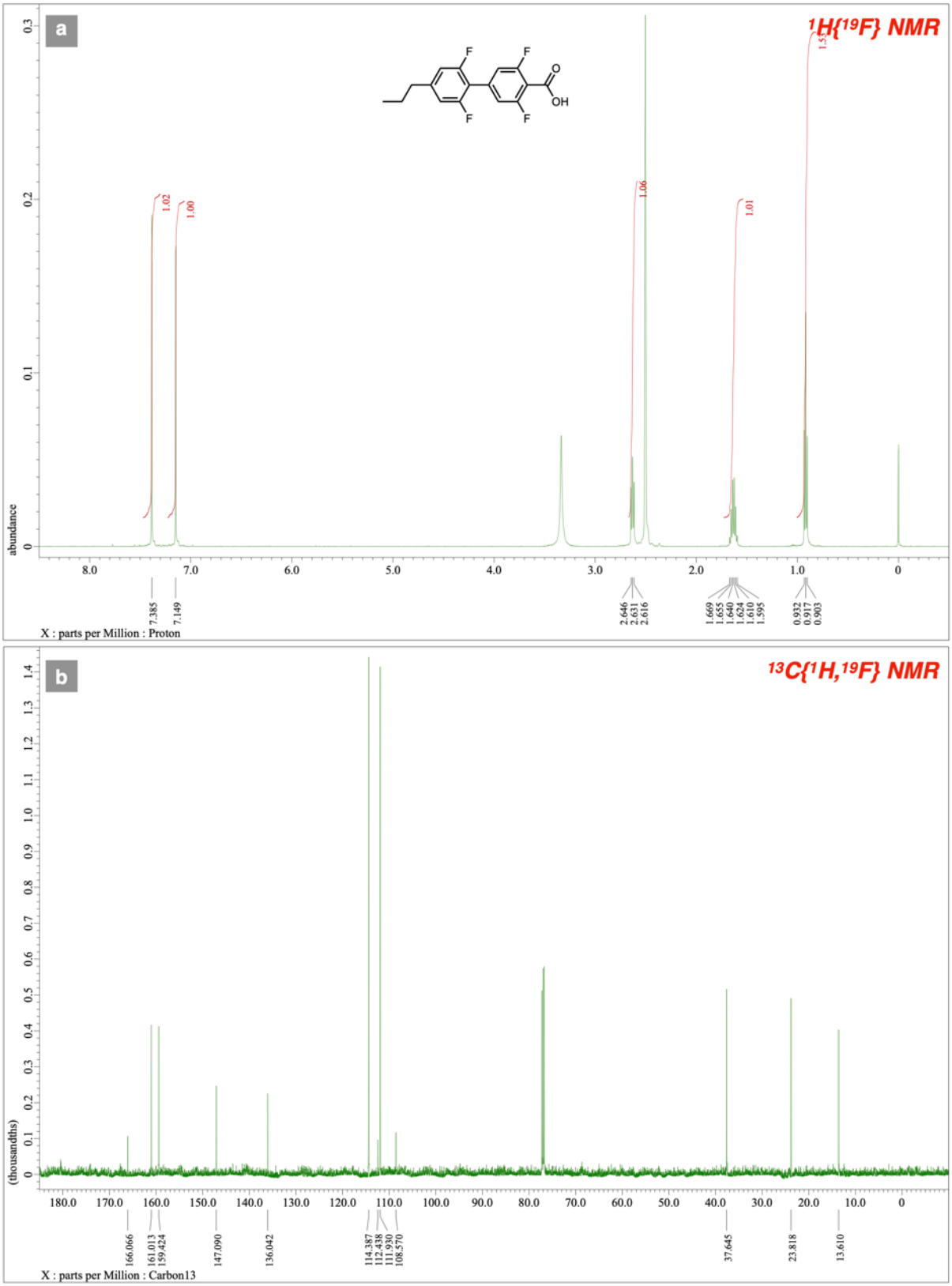

$^{19}F\{^{1}H\}$ NMR (a) and QTOF-HRMS (b) spectra of compound ***13b***

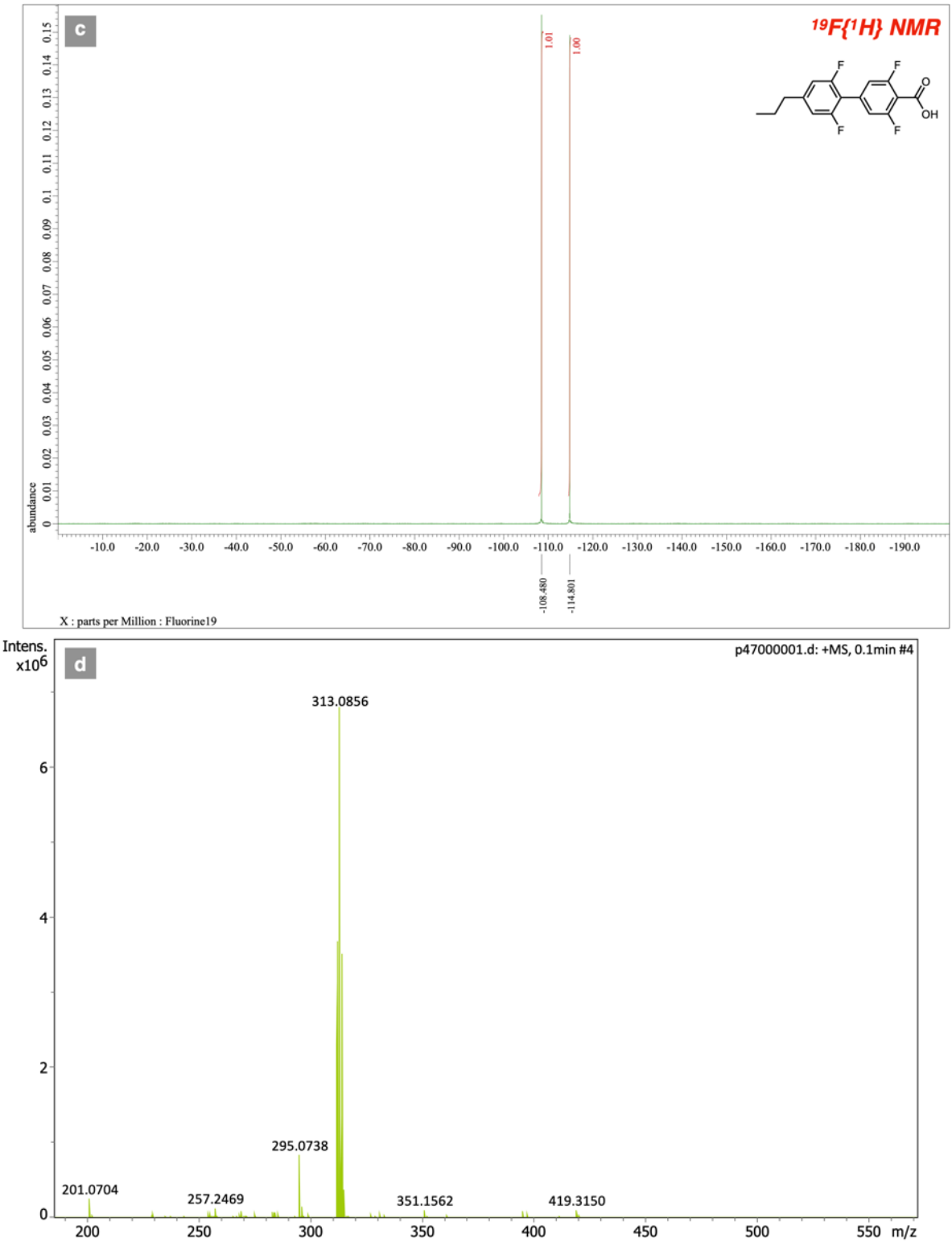

$^{1}H\{^{19}F\}$ NMR (a) and $^{13}C\{^{1}H,^{19}F\}$ NMR (b) spectra of compound ***14a***

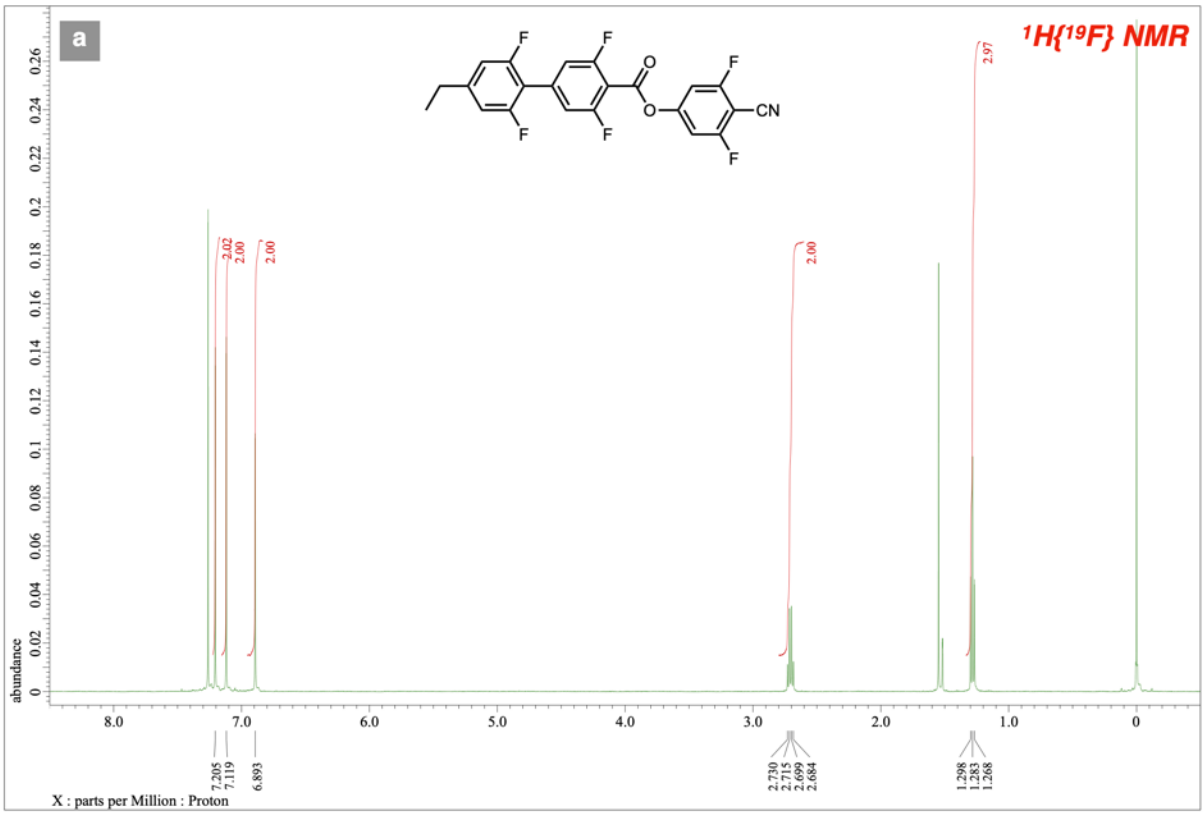

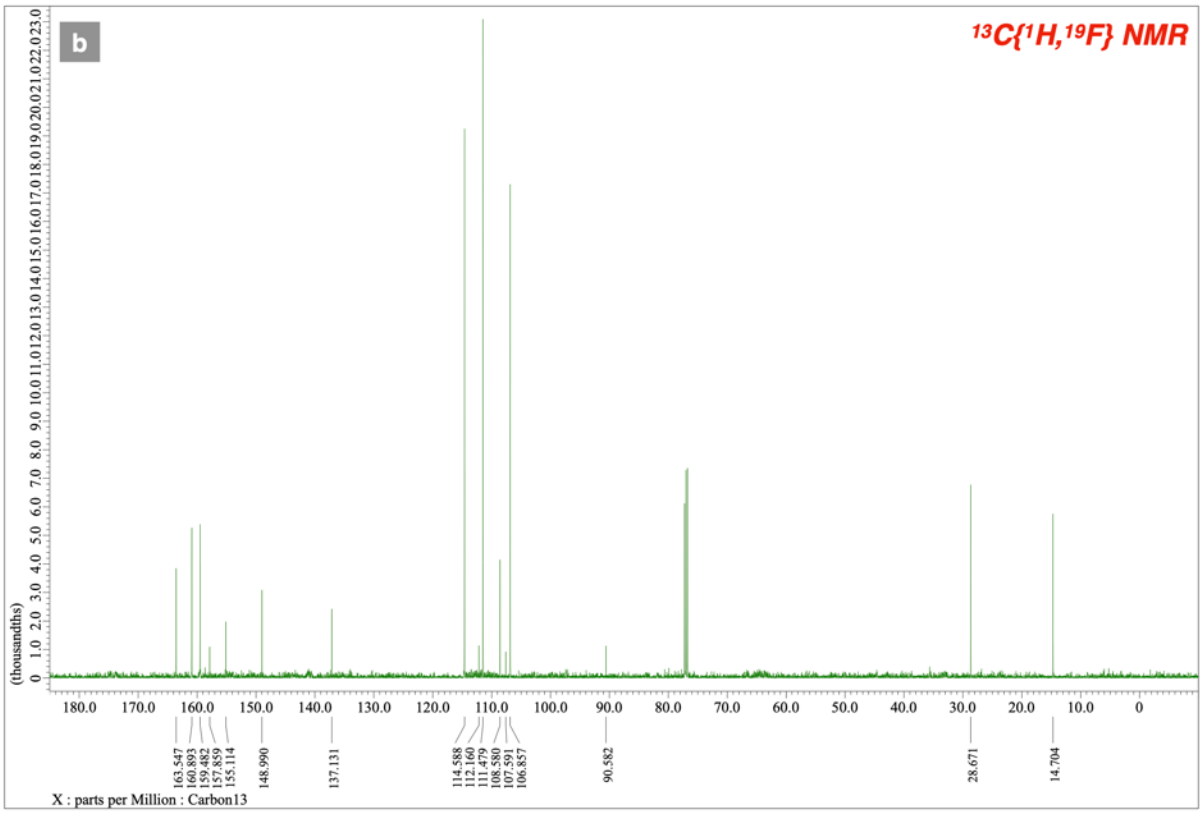

$^{19}F\{^{1}H\}$ NMR (a) and QTOF-HRMS (b) spectra of compound ***14a***

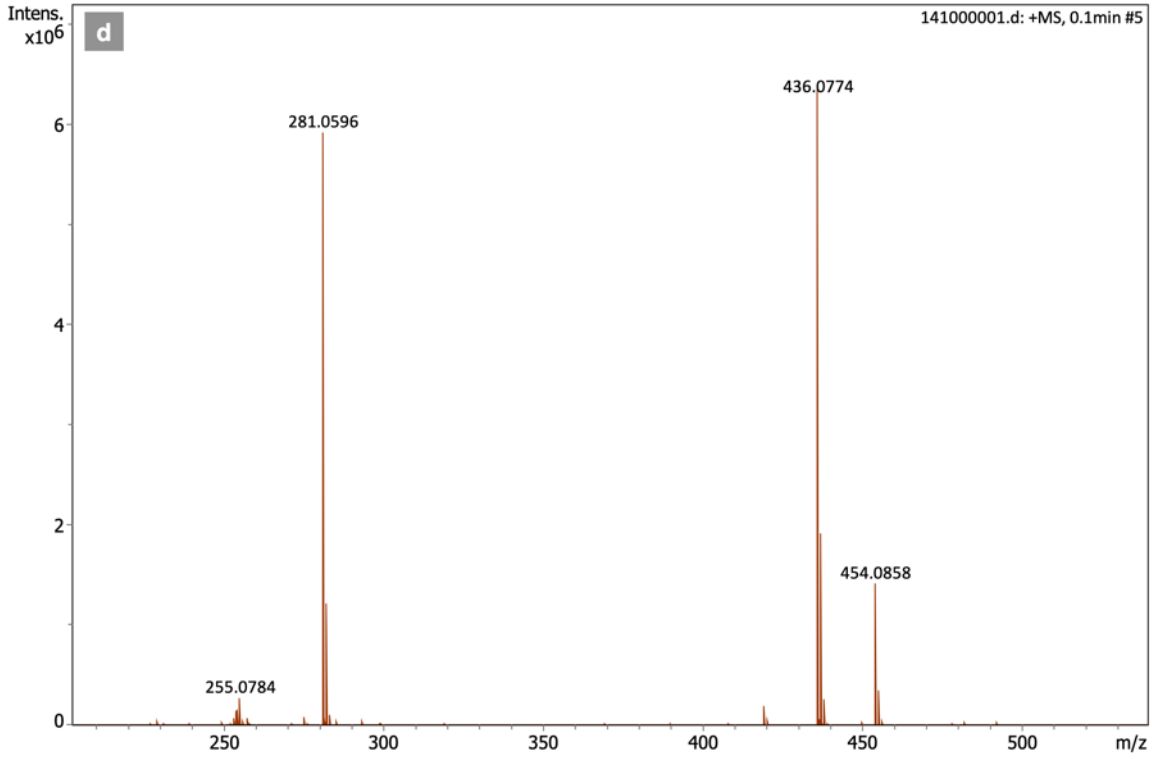

$^{1}H\{^{19}F\}$ NMR (a) and $^{13}C\{^{1}H,^{19}F\}$ NMR (b) spectra of compound ***14b***

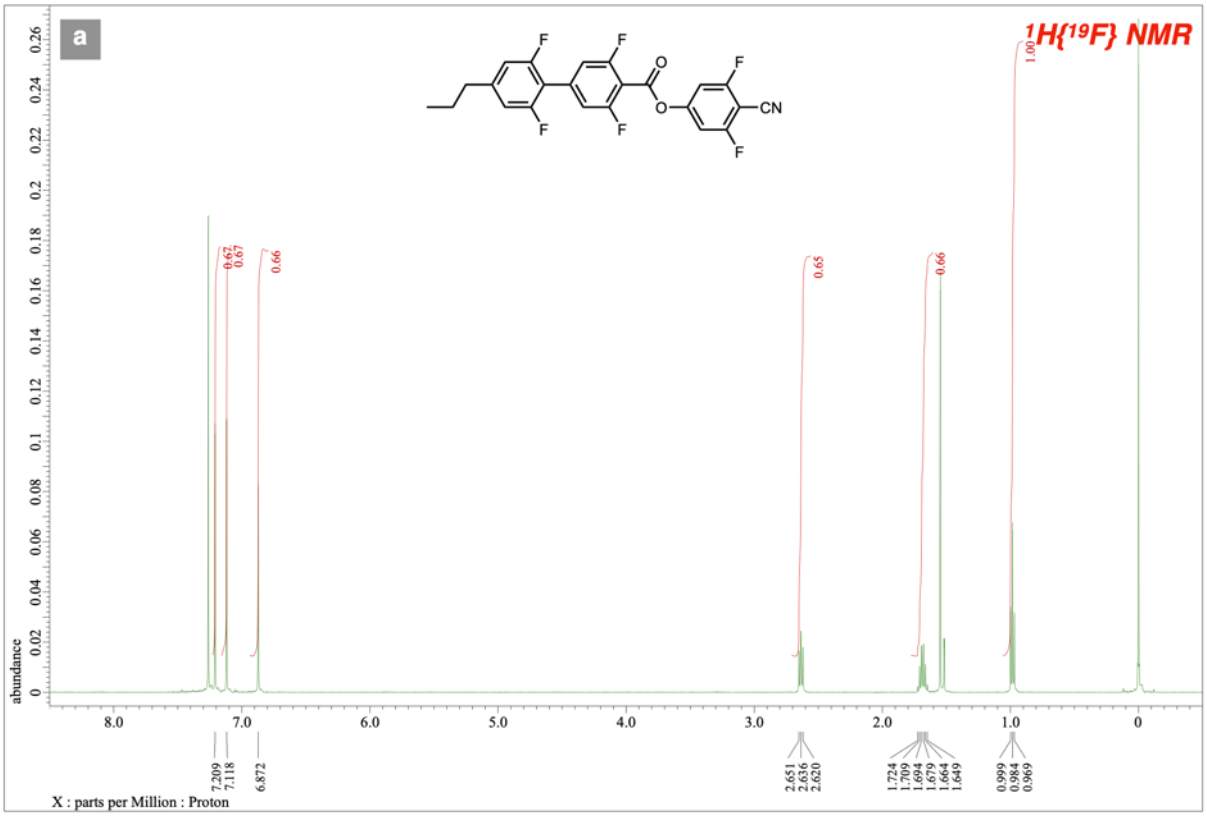

*$^{19}F\{^1H\}$ NMR (a) and QTOF-HRMS (b) spectra of compound **14b***

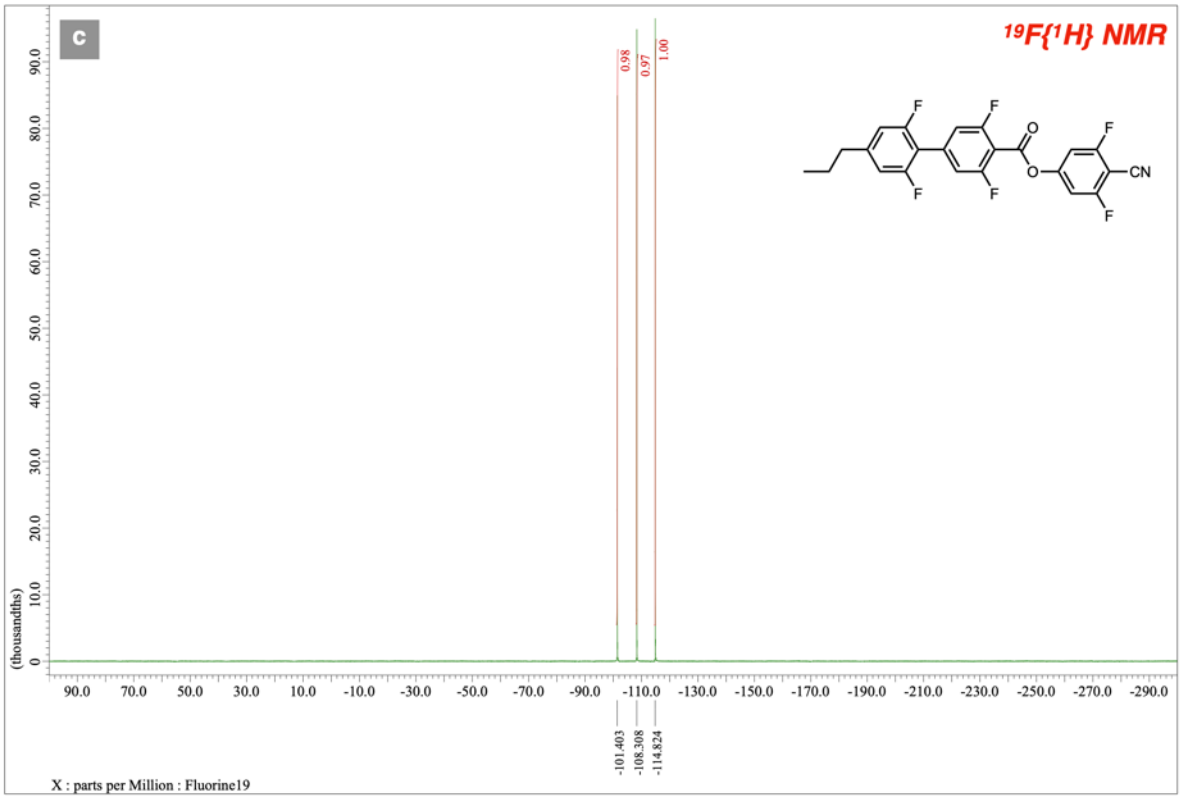

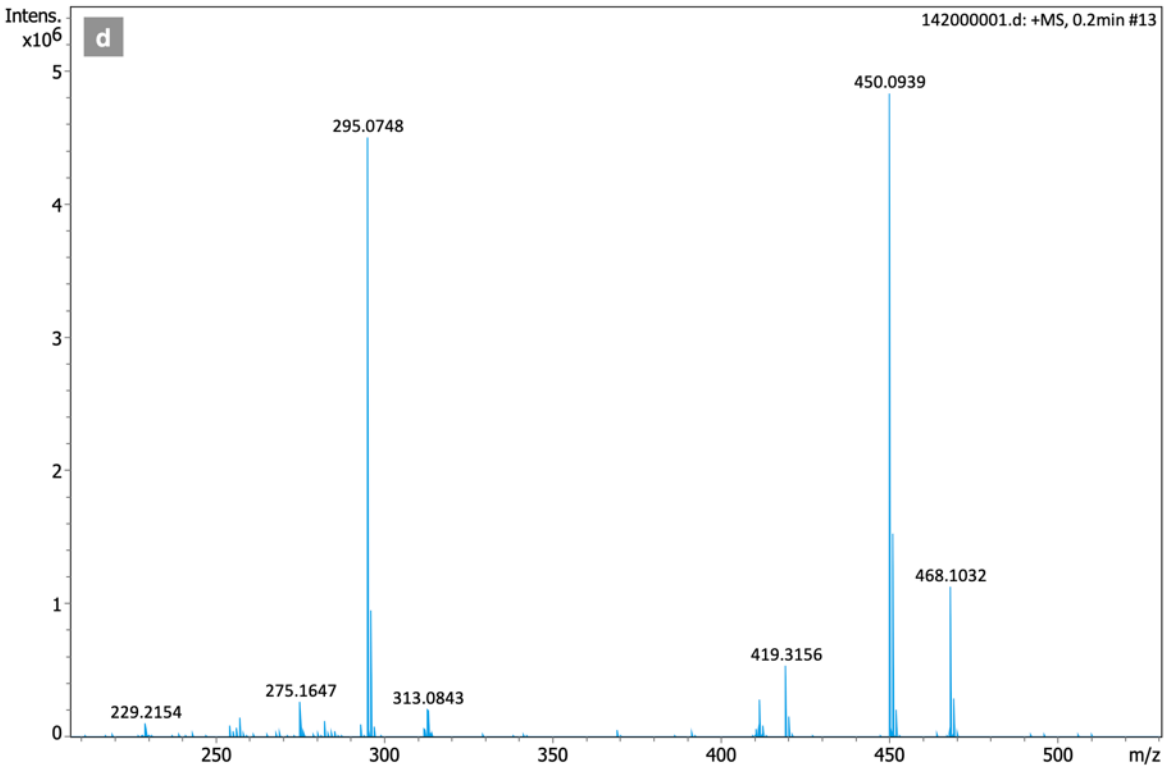

$^{1}H\{^{19}F\}$ NMR (a) and $^{13}C\{^{1}H,^{19}F\}$ NMR (b) spectra of compound ***15a***

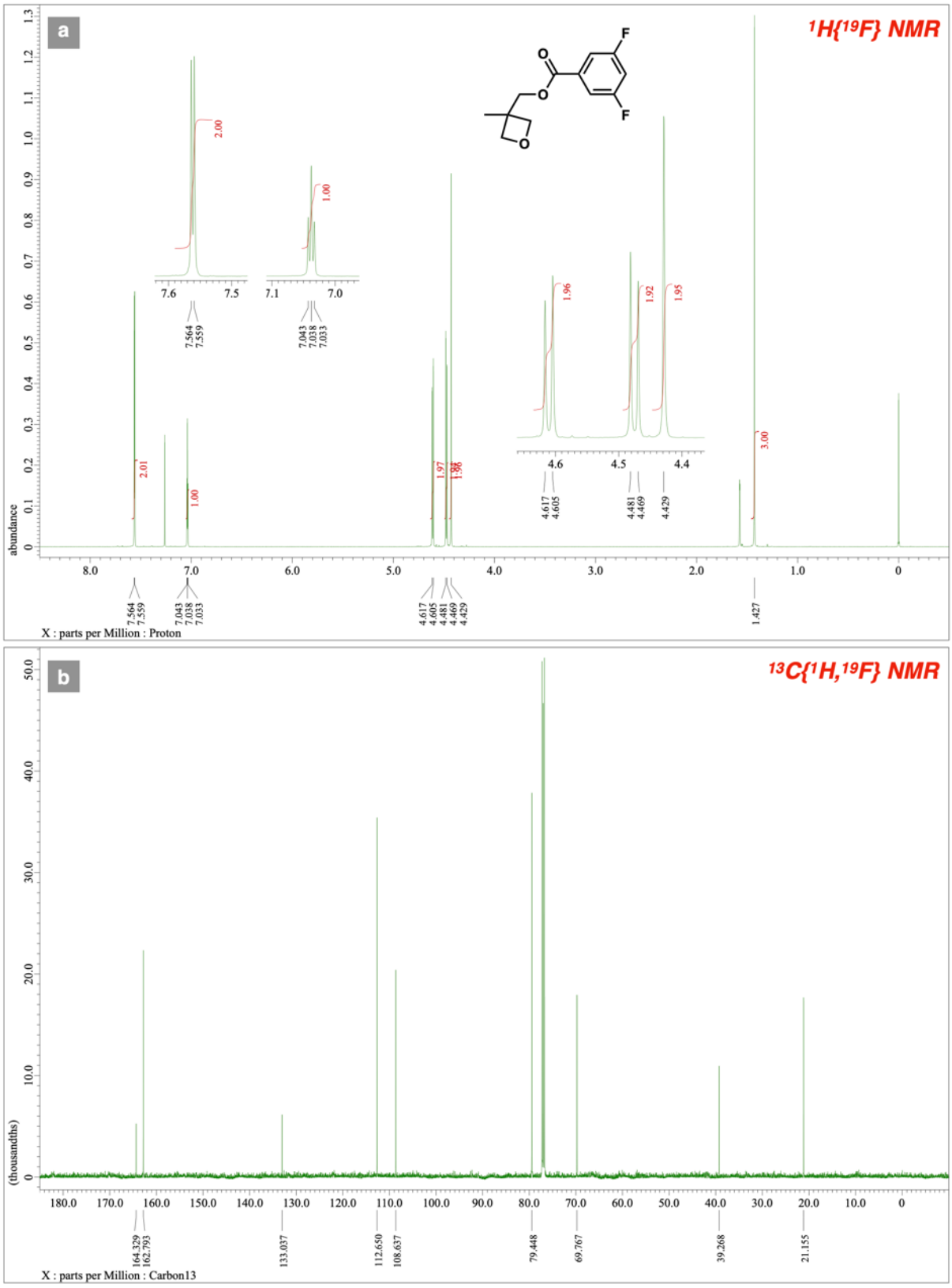

$^{19}F\{^{1}H\}$ NMR (a) and QTOF-HRMS (b) spectra of compound ***15a***

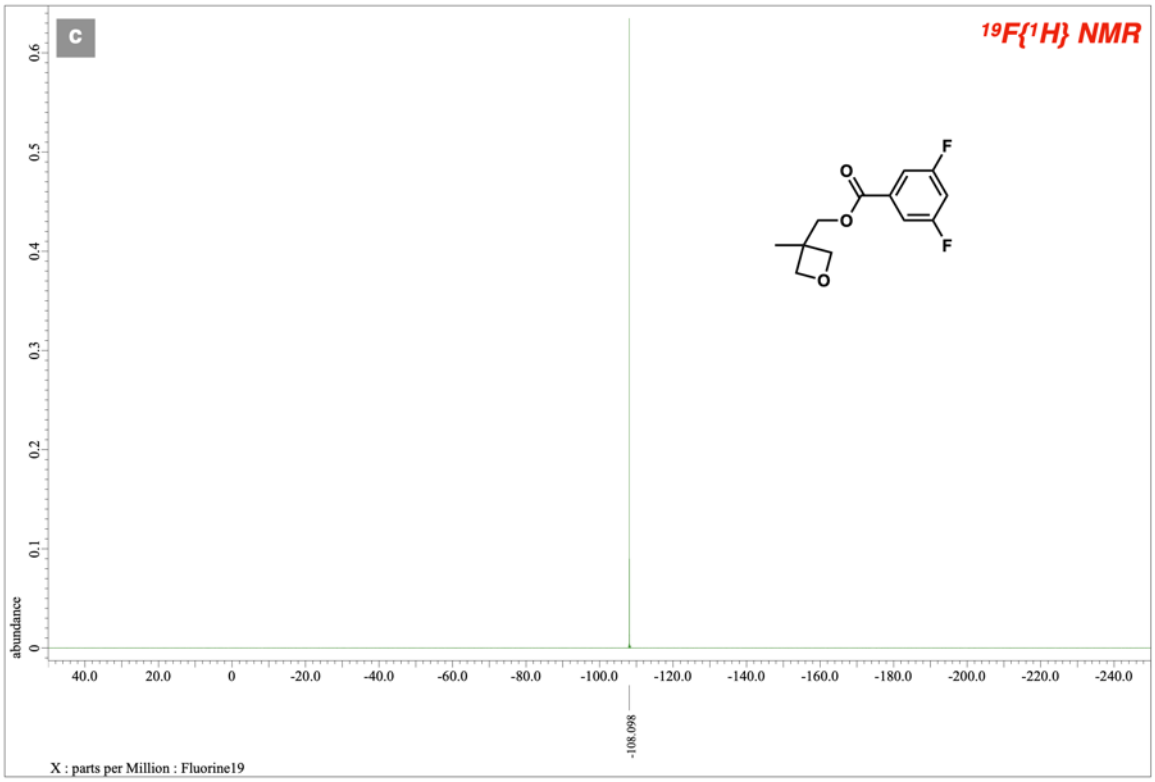

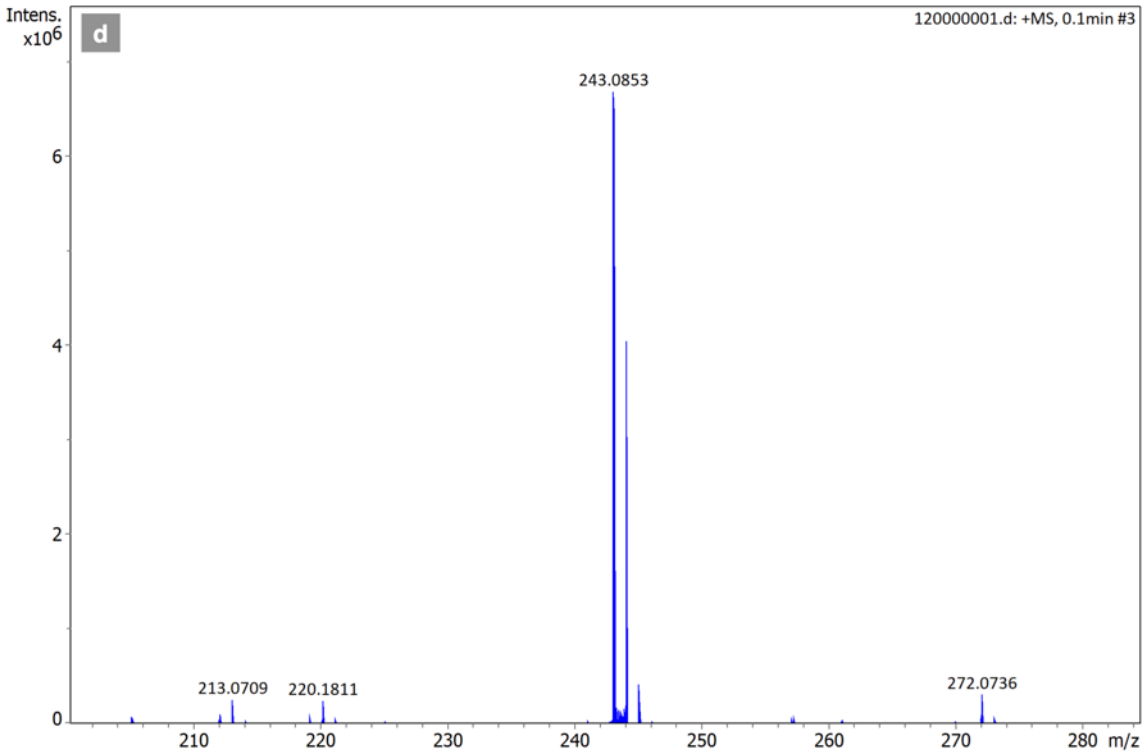

$^{1}H\{^{19}F\}$ NMR (a) and $^{13}C\{^{1}H,^{19}F\}$ NMR (b) spectra of compound ***15b***

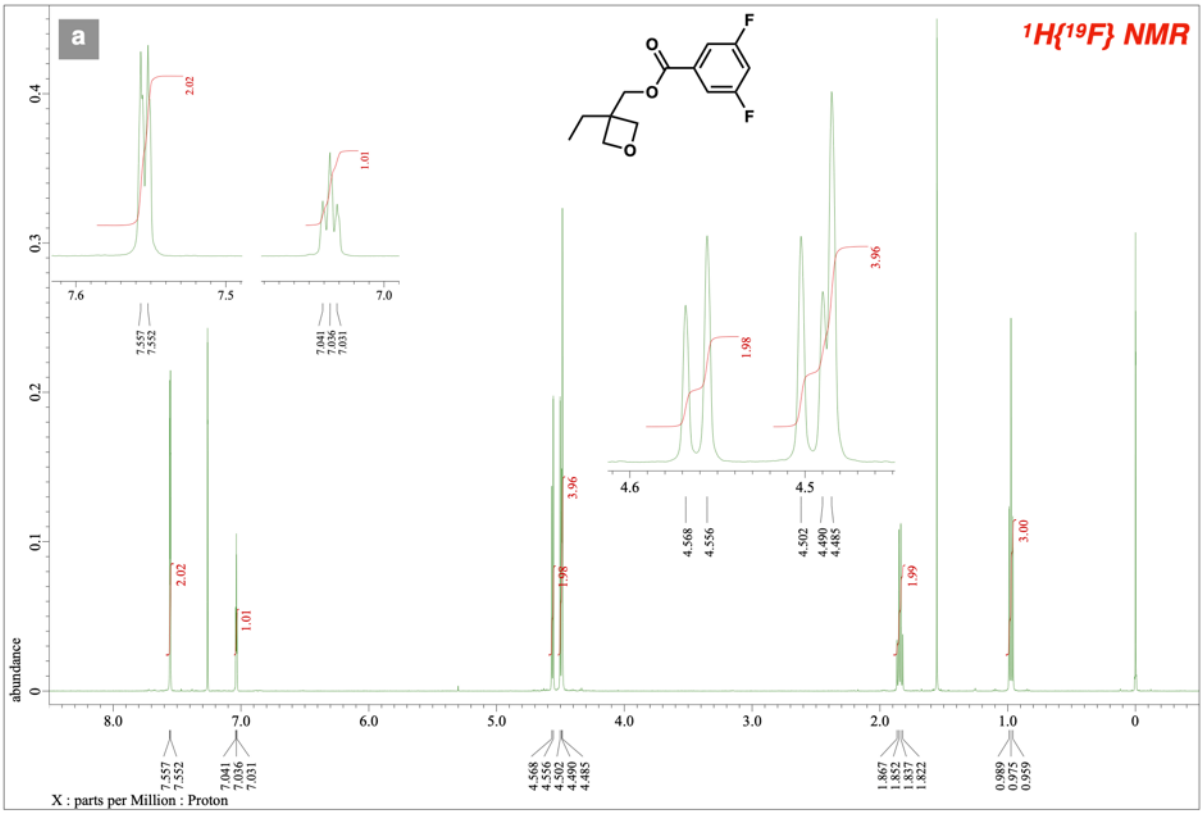

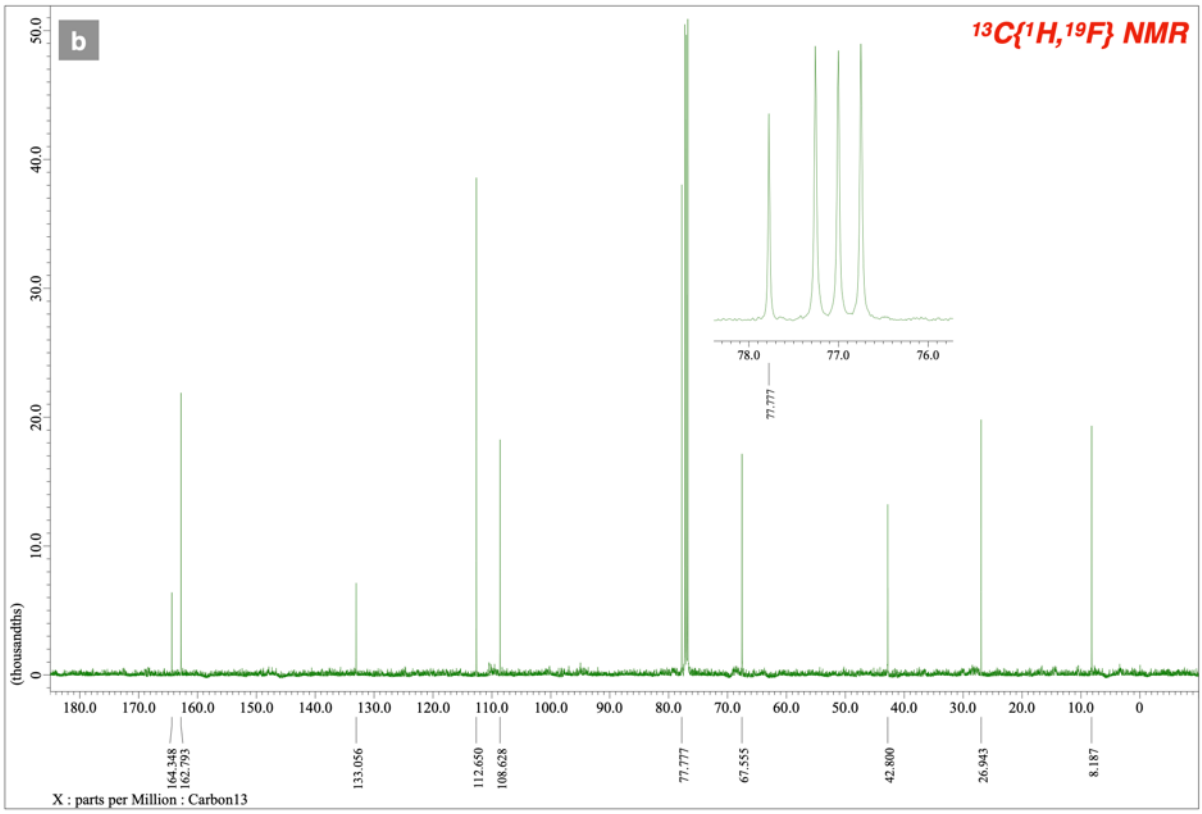

*$^{19}F\{^{1}H\}$ NMR (a) and QTOF-HRMS (b) spectra of compound **15b***

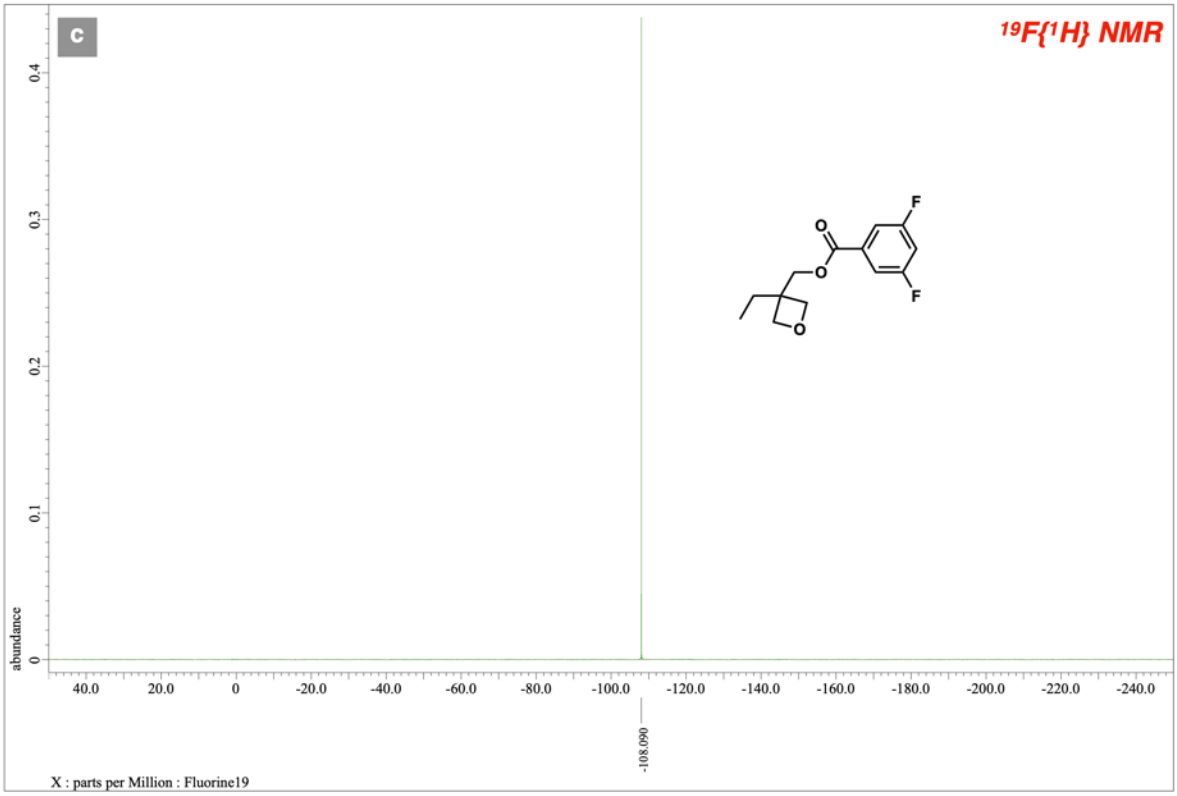

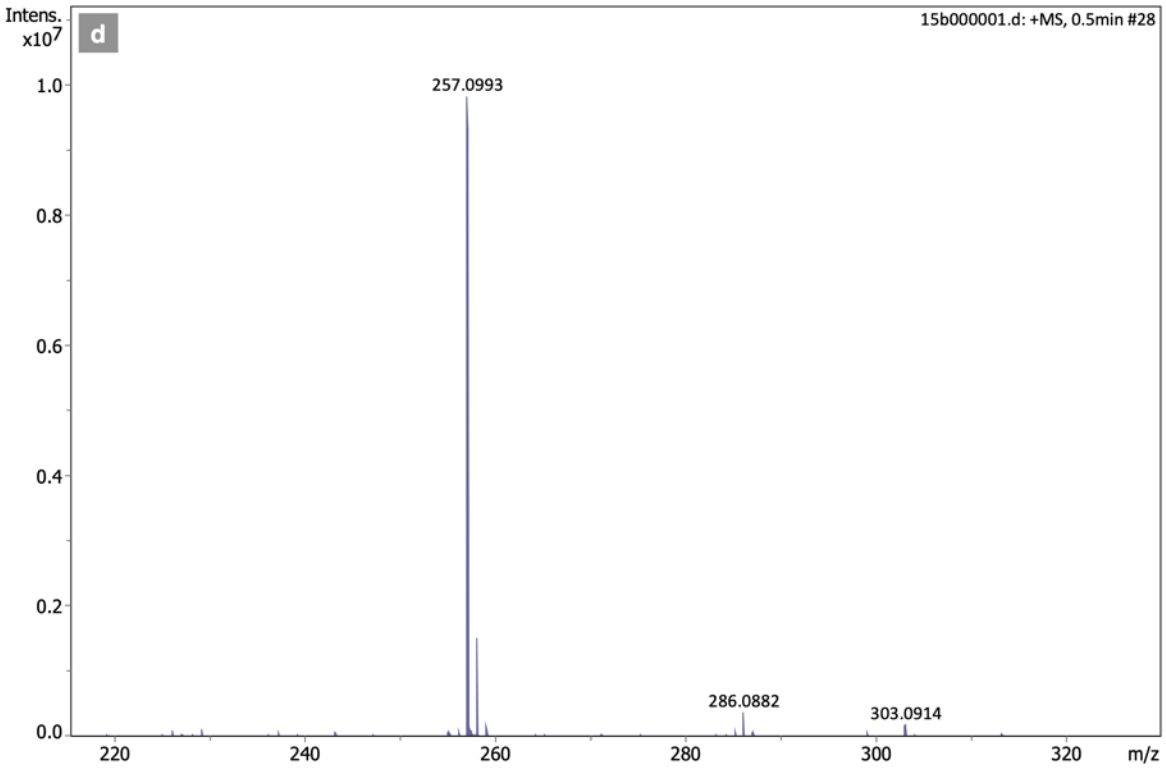

$^{1}H\{^{19}F\}$ NMR (a) and $^{13}C\{^{1}H,^{19}F\}$ NMR (b) spectra of compound ***16a***

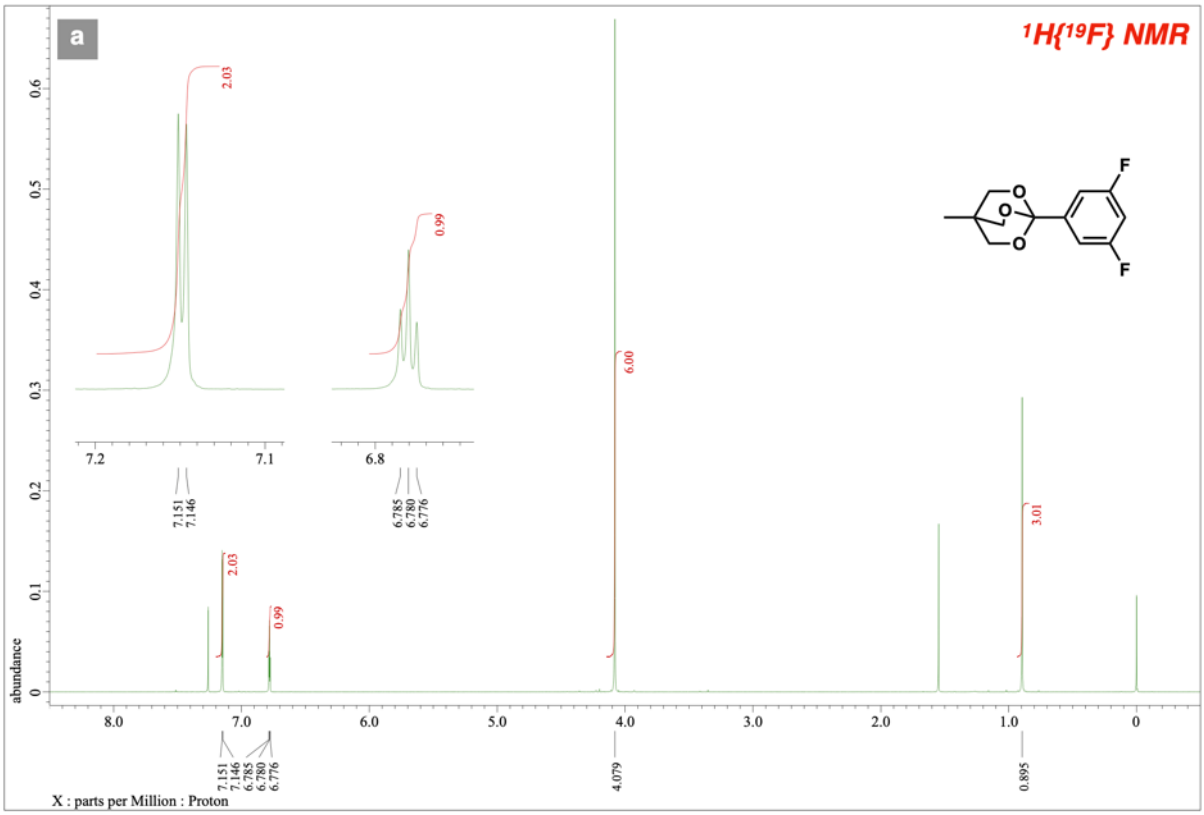

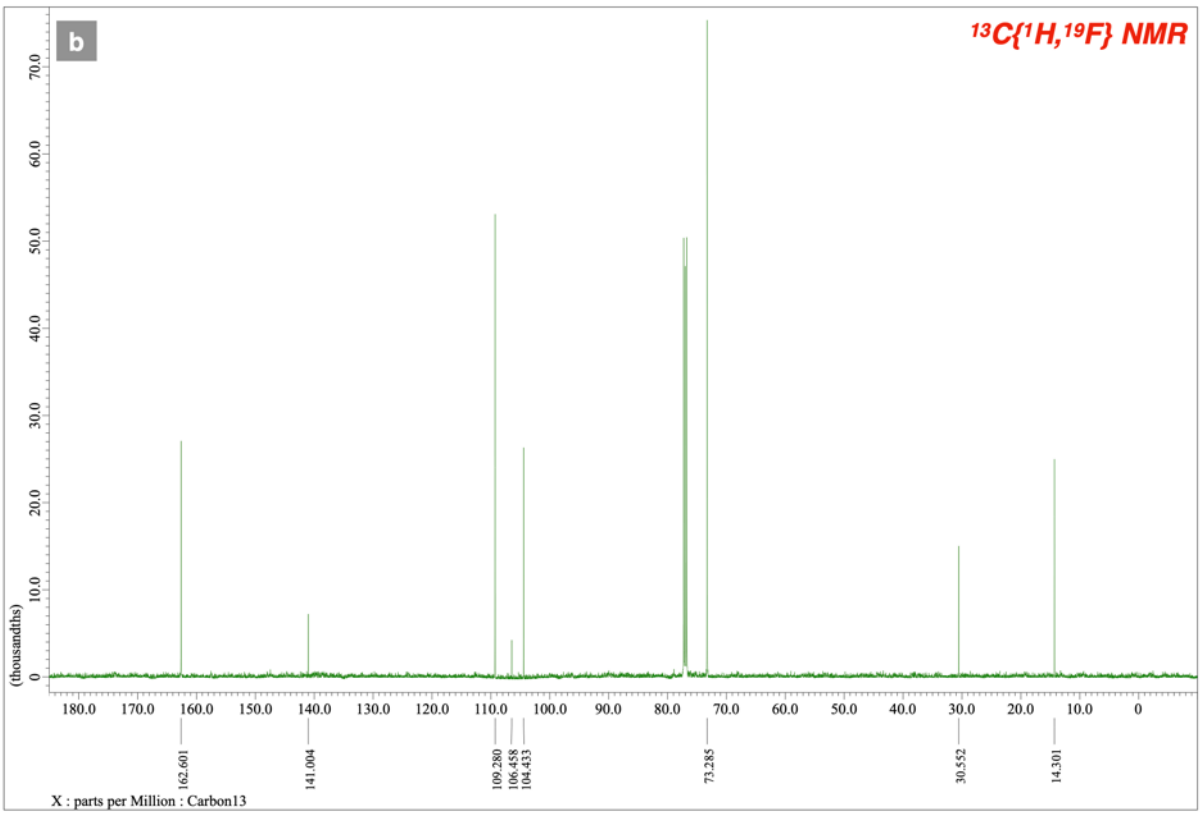

$^{19}F\{^{1}H\}$ NMR (a) and QTOF-HRMS (b) spectra of compound ***16a***

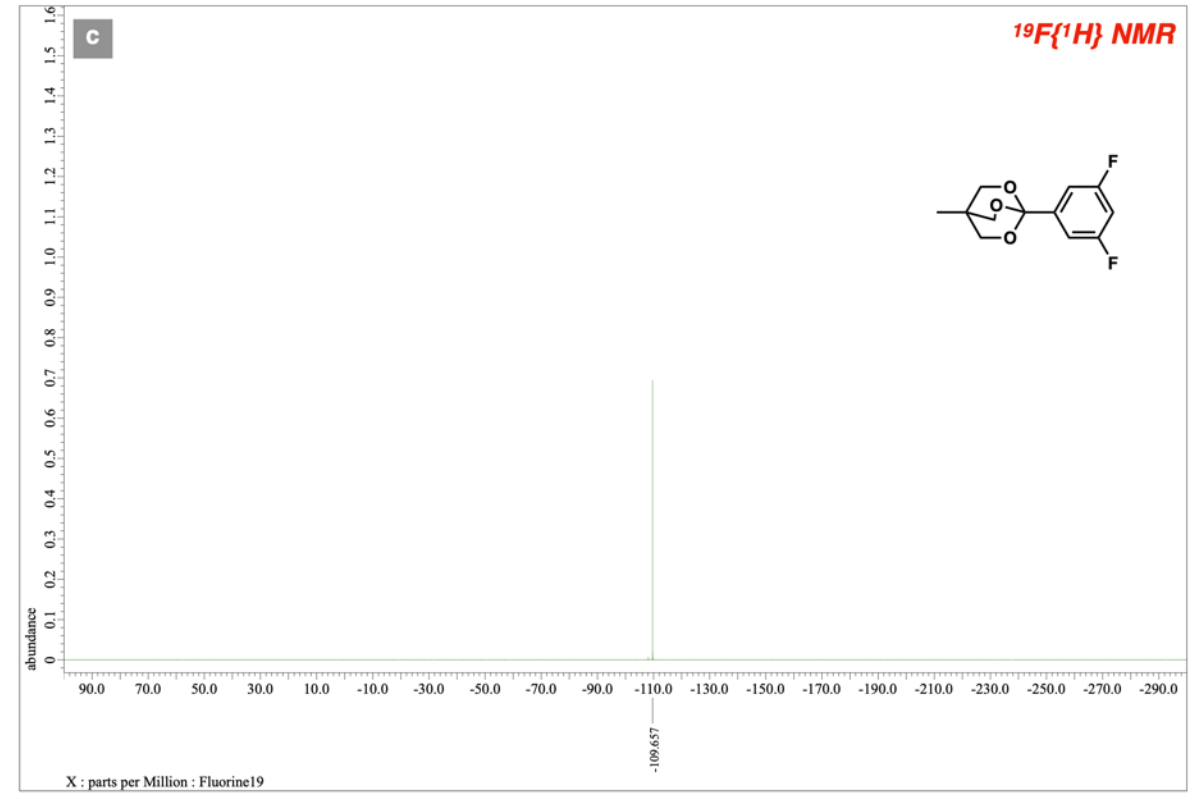

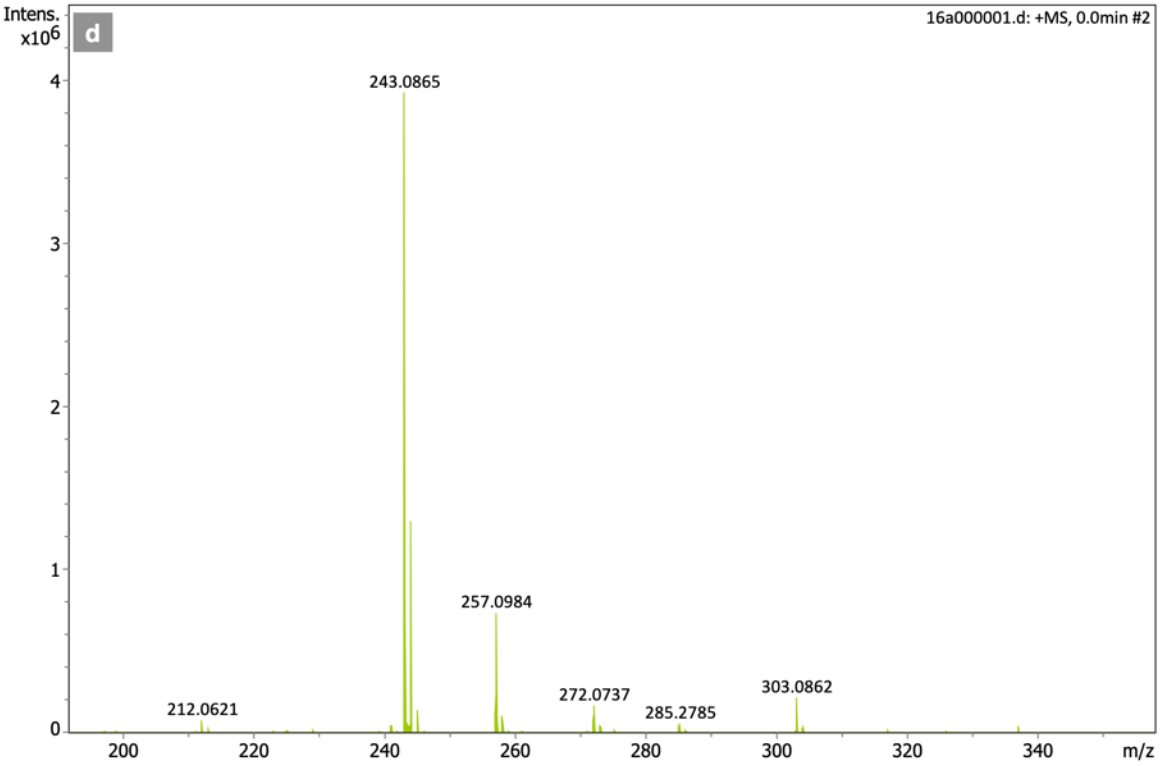

$^{1}H\{^{19}F\}$ NMR (a) and $^{13}C\{^{1}H,^{19}F\}$ NMR (b) spectra of compound ***16b***

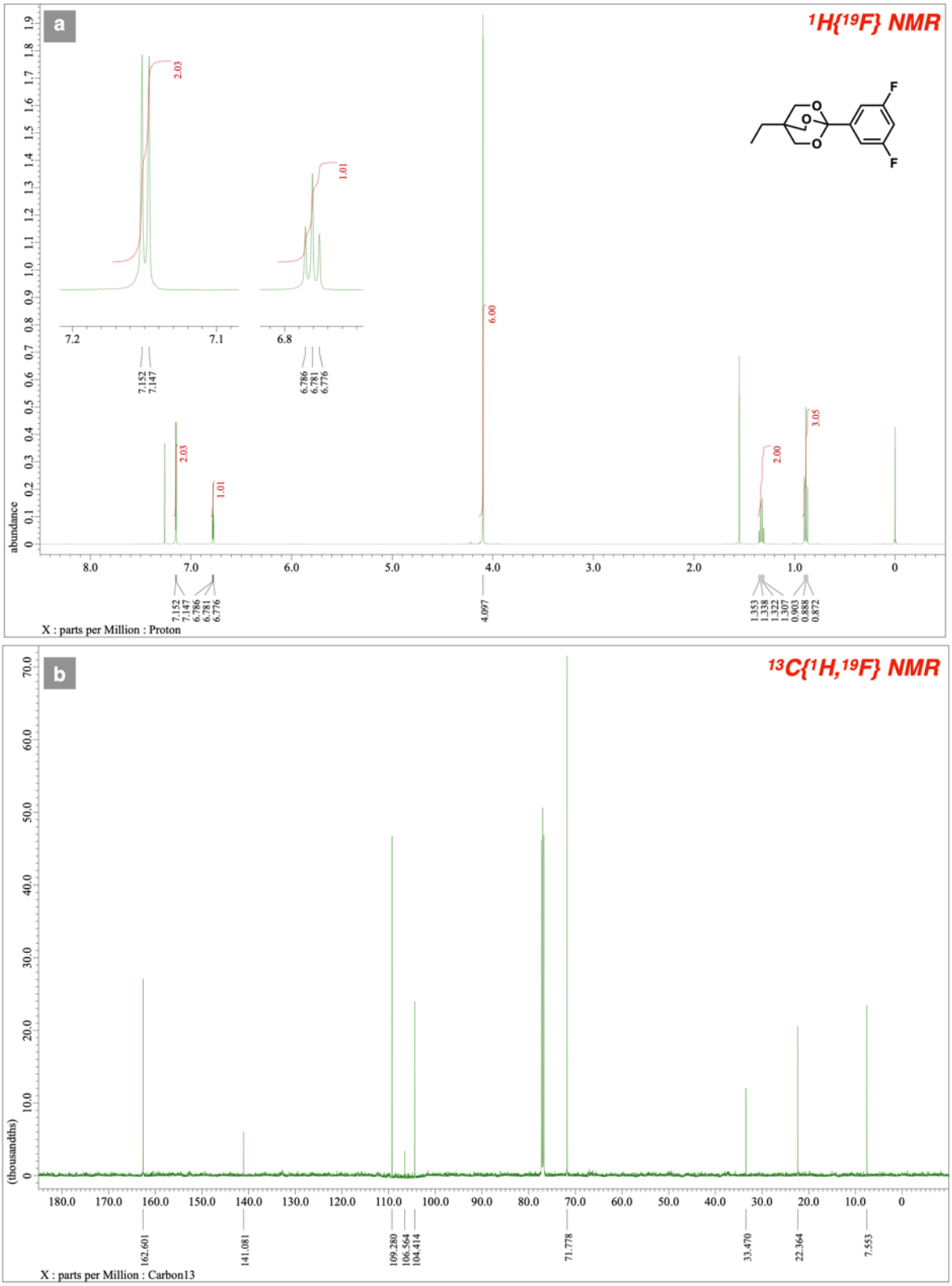

*$^{19}F\{^{1}H\}$ NMR (a) and QTOF-HRMS (b) spectra of compound **16b***

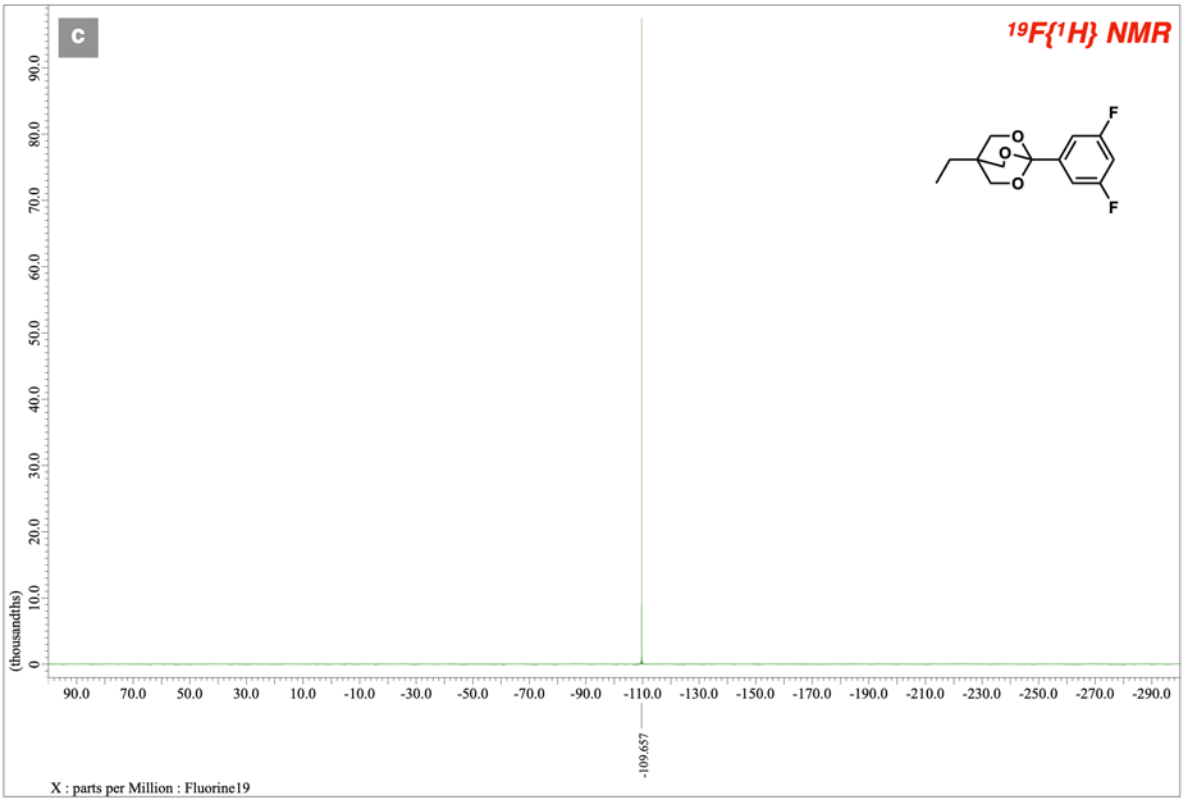

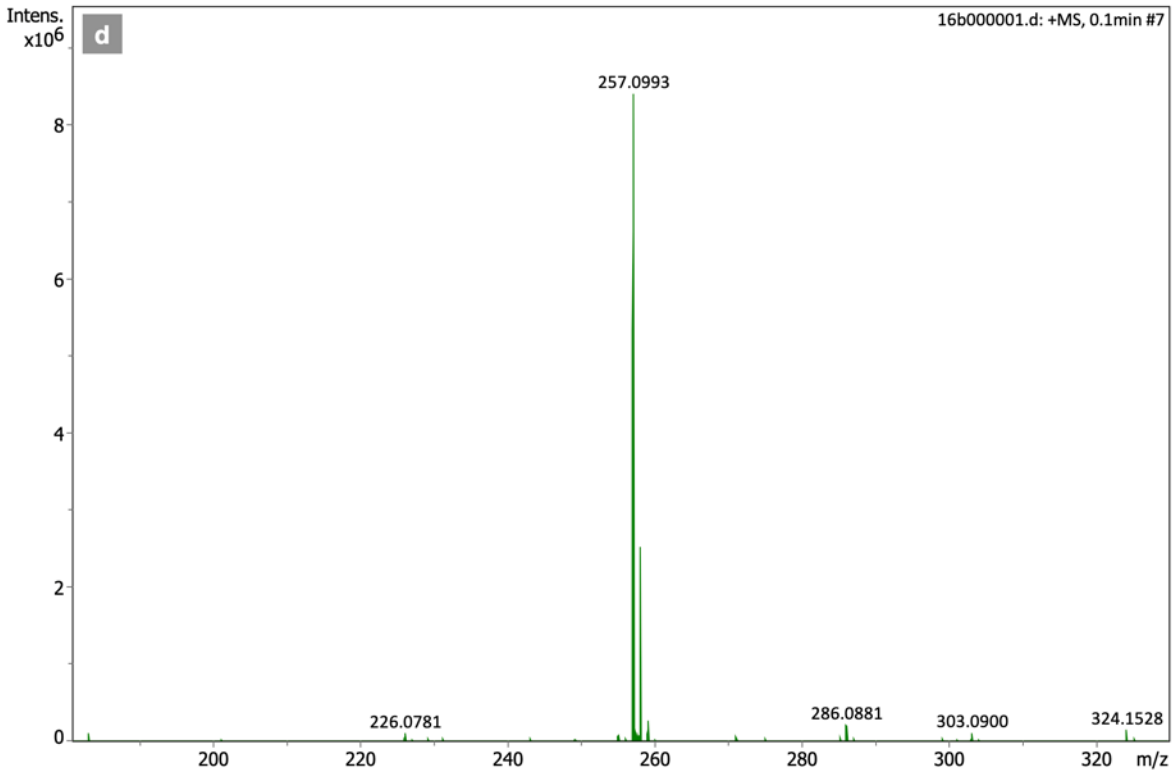

$^{1}H\{^{19}F\}$ NMR (a) and $^{13}C\{^{1}H,^{19}F\}$ NMR (b) spectra of compound ***18***

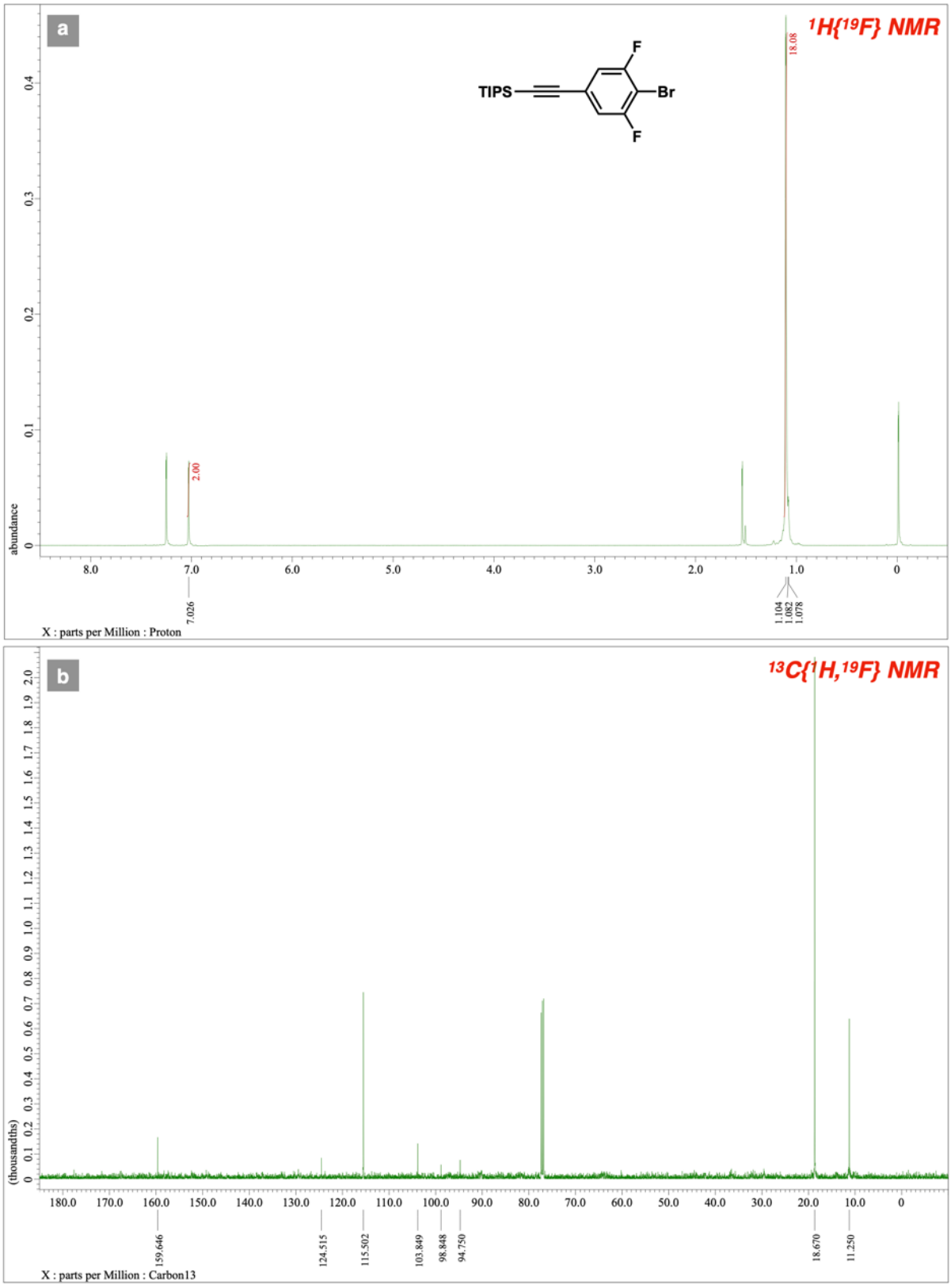

$^{19}F\{^{1}H\}$ NMR spectra of compound ***18***

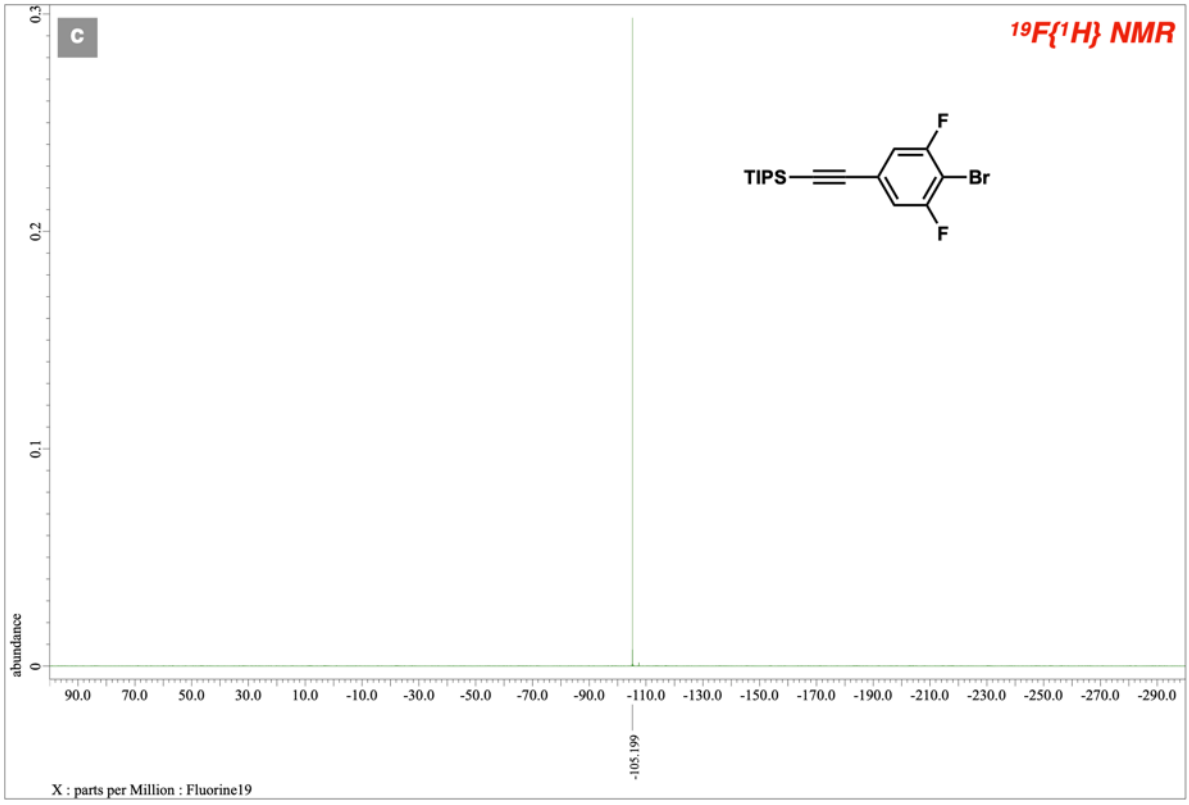

*$^{1}H\{^{19}F\}$ NMR (a) and $^{13}C\{^{1}H,^{19}F\}$ NMR (b) spectra of compound **19***

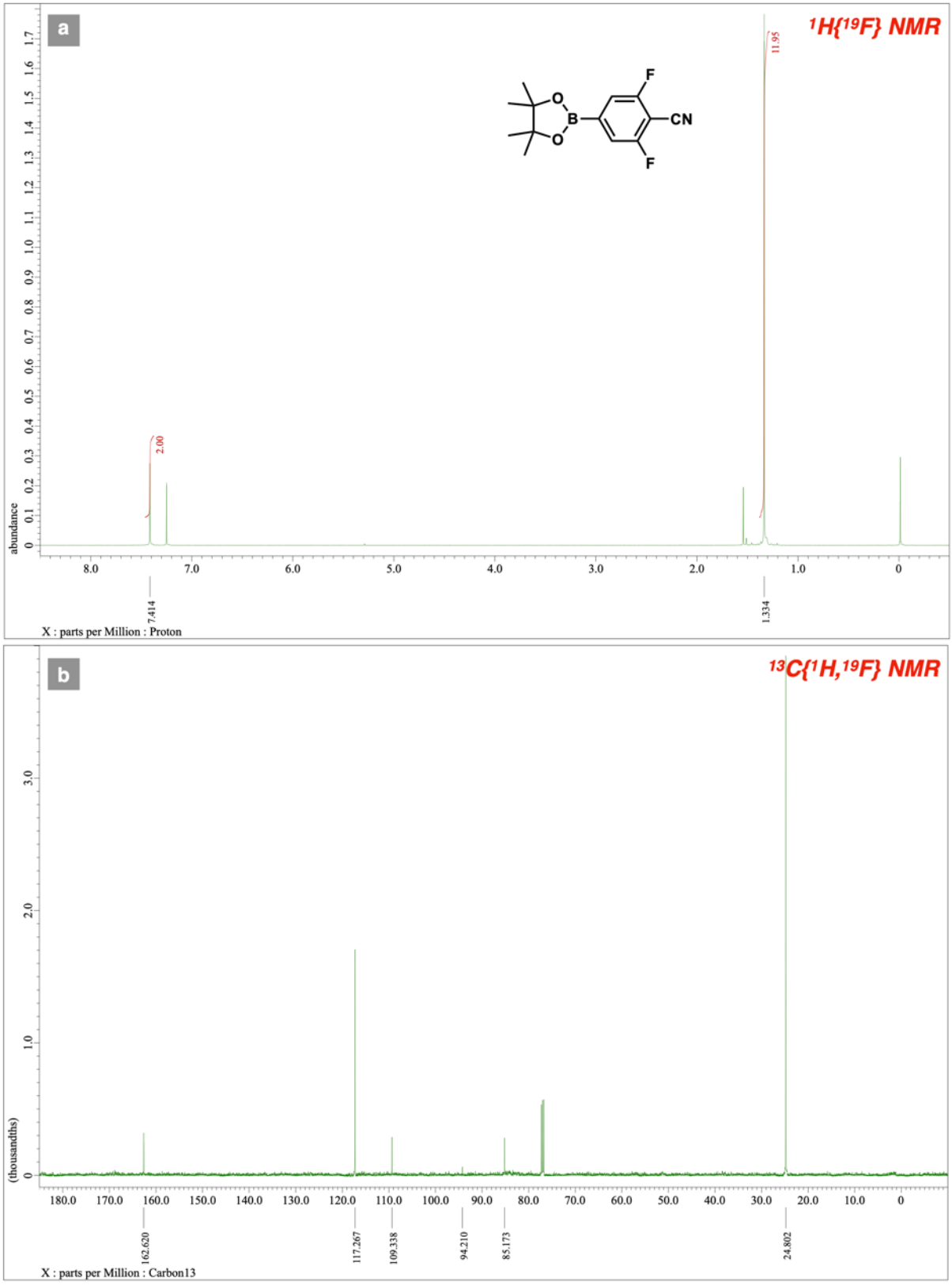

*$^{19}F\{^{1}H\}$ NMR (a) and QTOF-HRMS (b) spectra of compound **19***

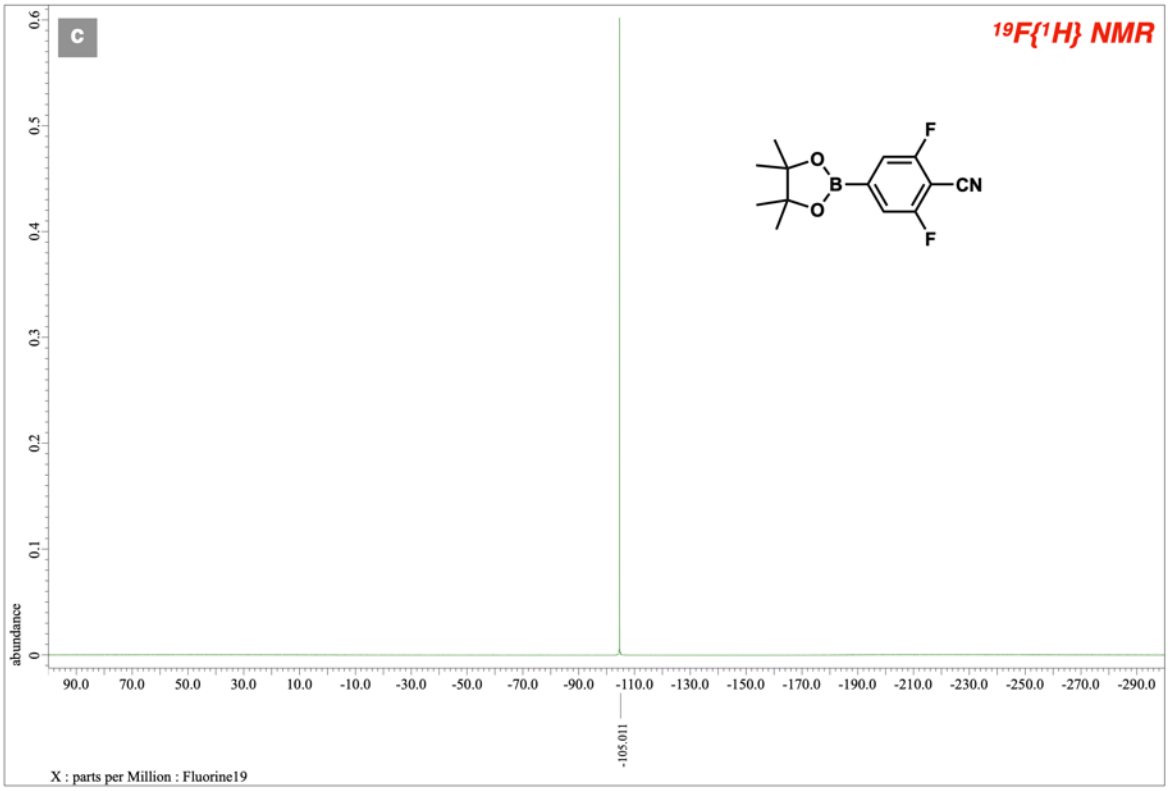

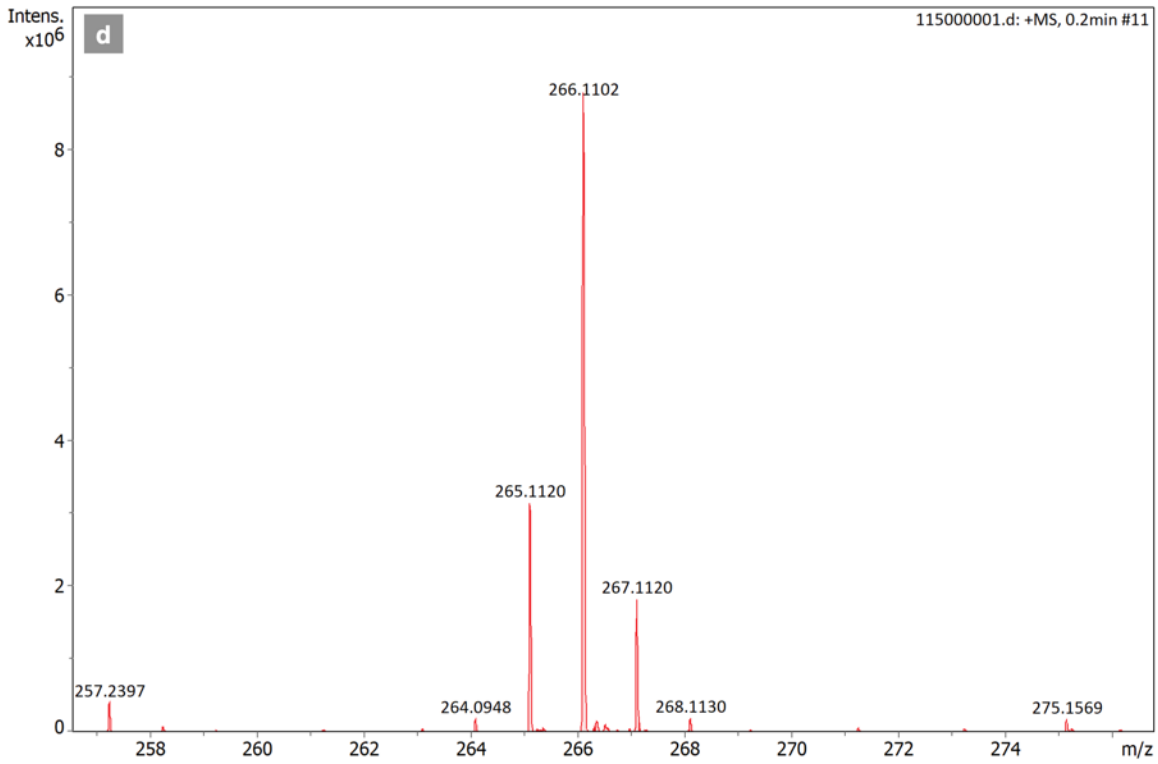

*$^{1}H\{^{19}F\}$ NMR (a) and $^{13}C\{^{1}H,^{19}F\}$ NMR (b) spectra of compound **20***

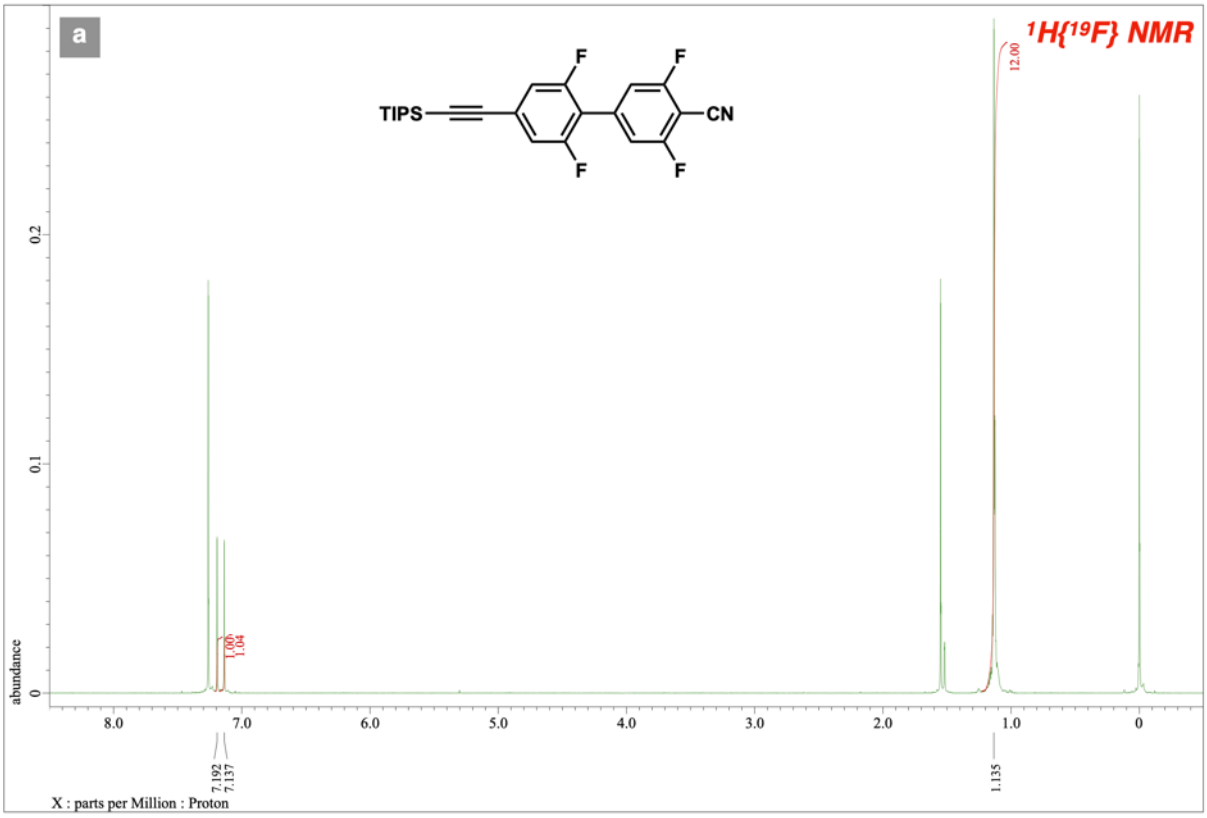

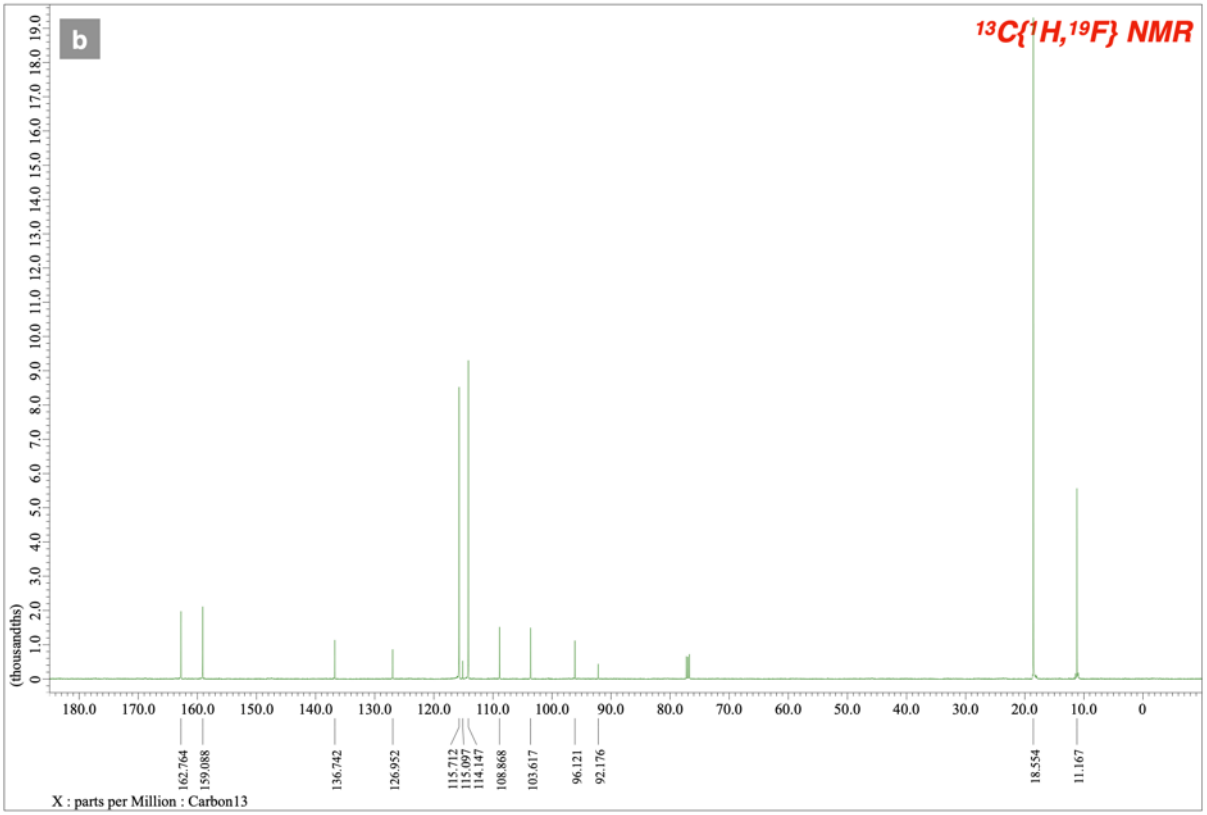

$^{19}F\{^{1}H\}$ NMR spectra of compound ***20***

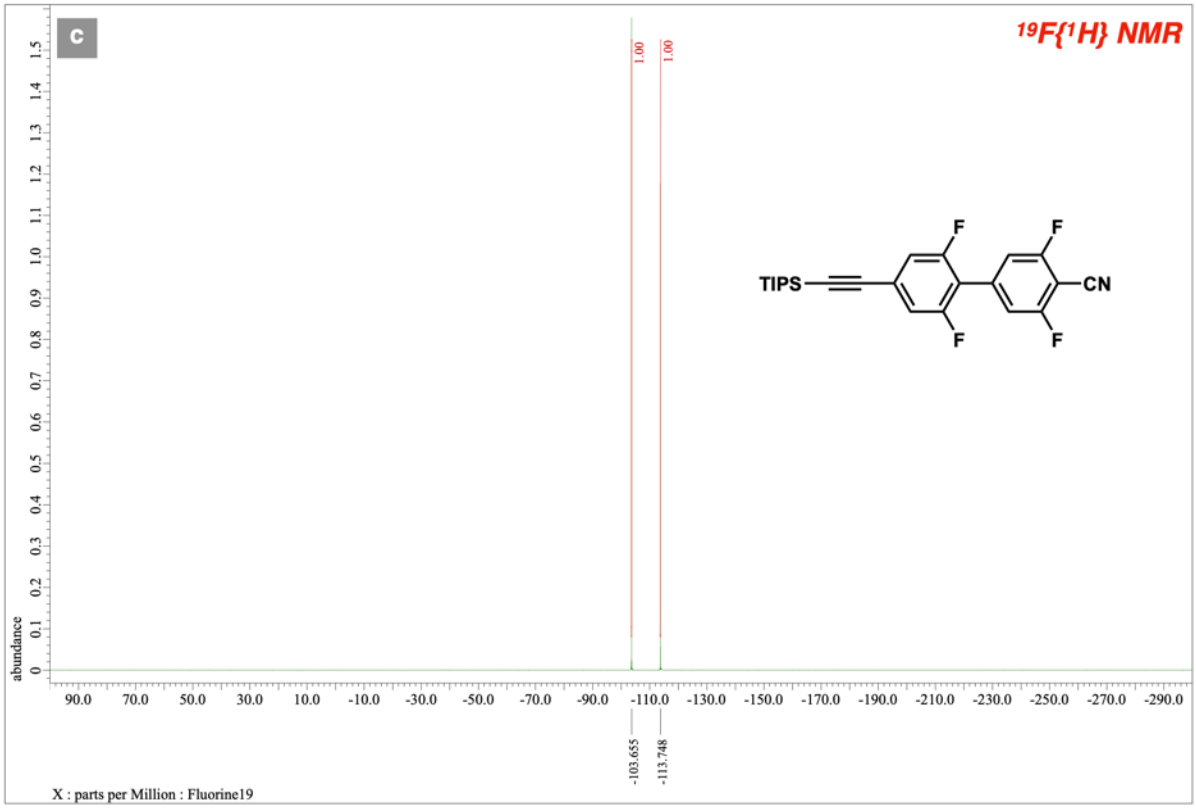

*$^{1}H\{^{19}F\}$ NMR (a) and $^{13}C\{^{1}H,^{19}F\}$ NMR (b) spectra of compound **21***

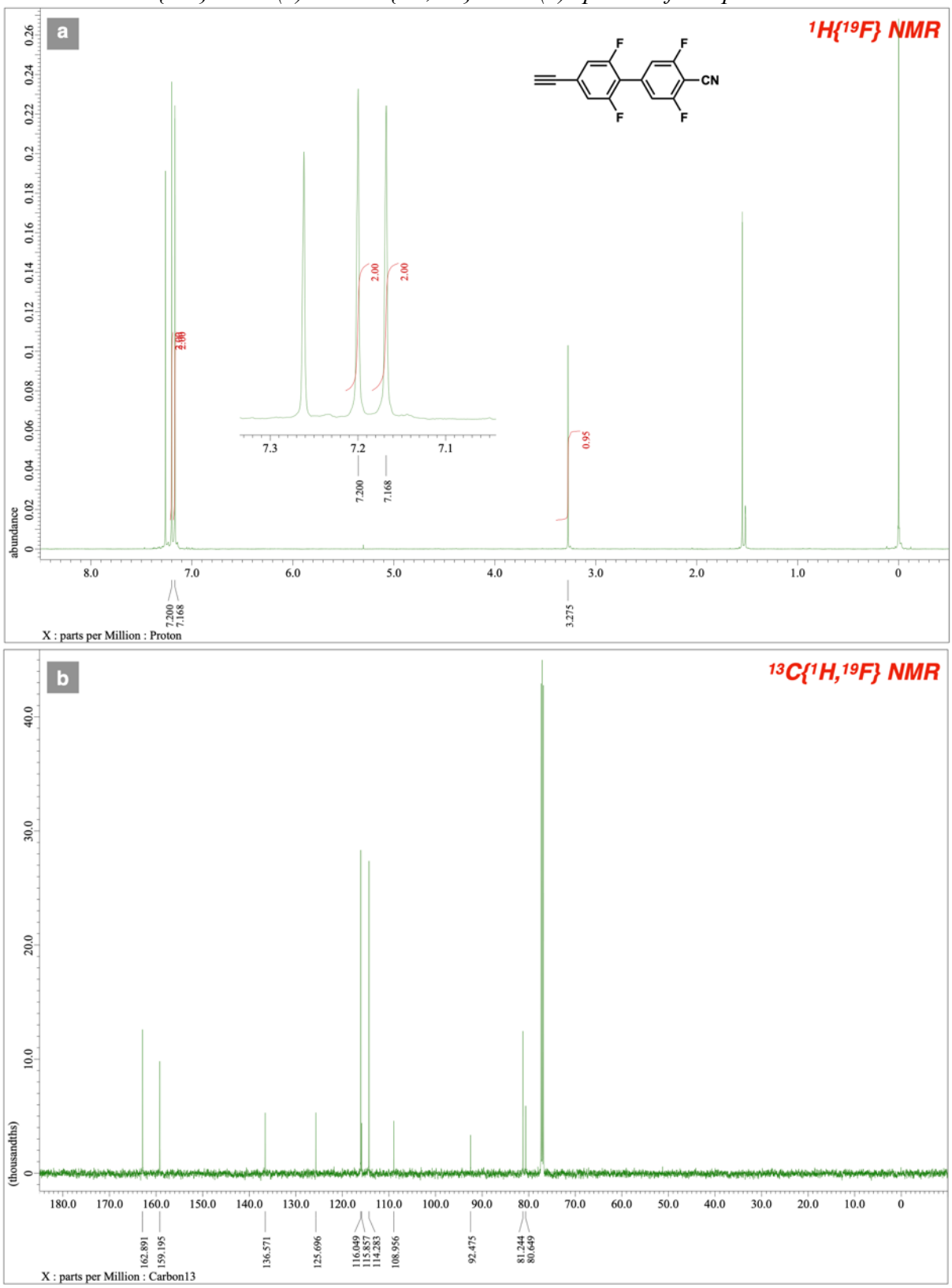

*$^{19}F\{^{1}H\}$ NMR (a) and QTOF-HRMS (b) spectra of compound **21***

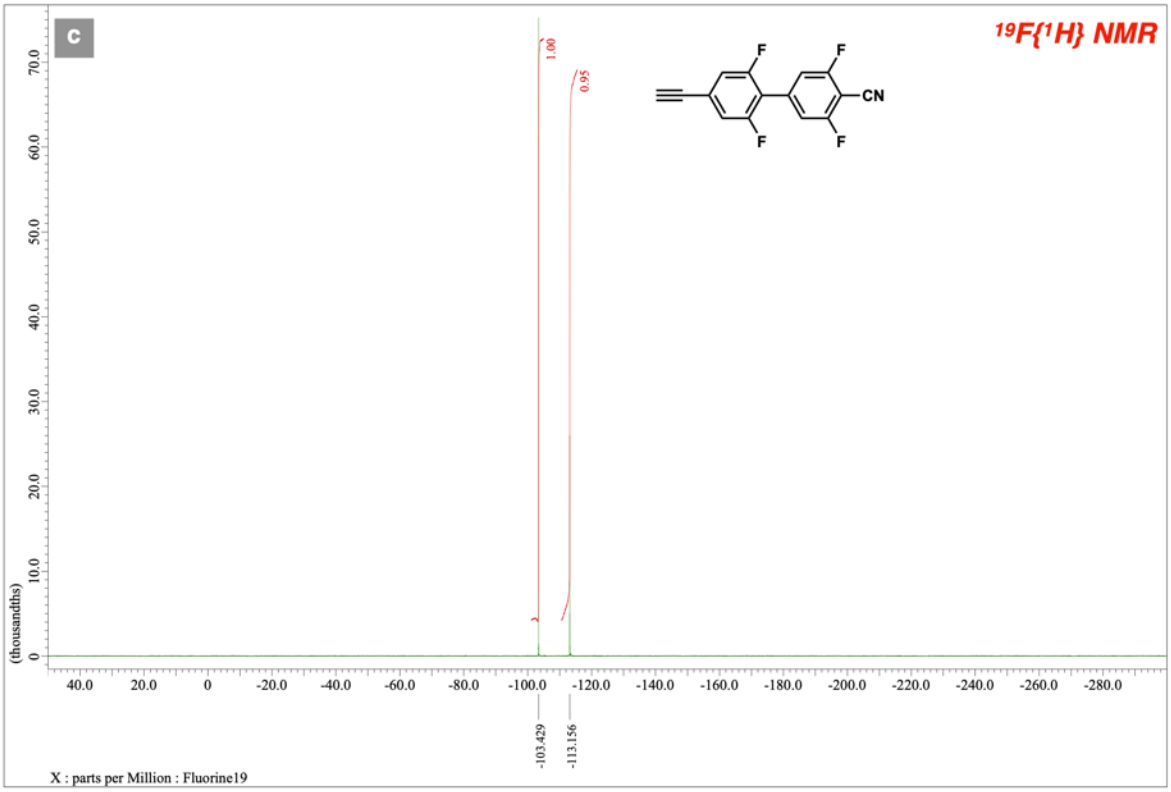

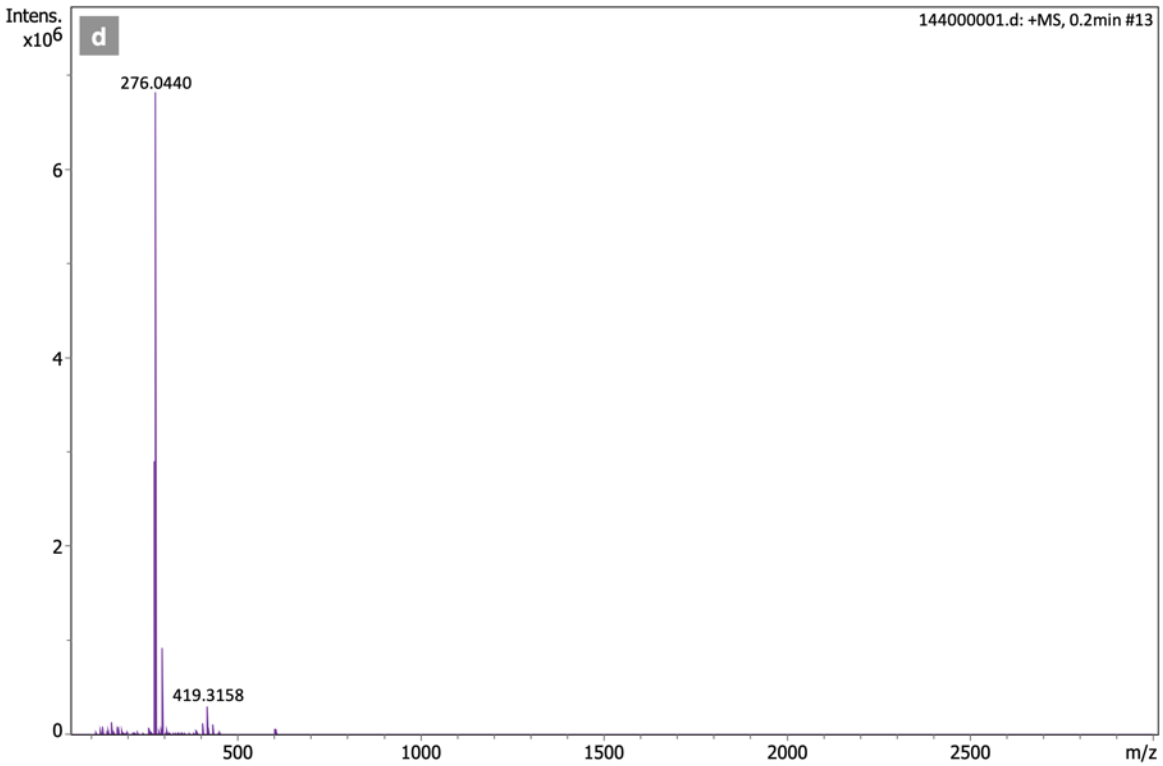

*$^{1}H\{^{19}F\}$ NMR (a) and $^{13}C\{^{1}H,^{19}F\}$ NMR (b) spectra of compound **22a***

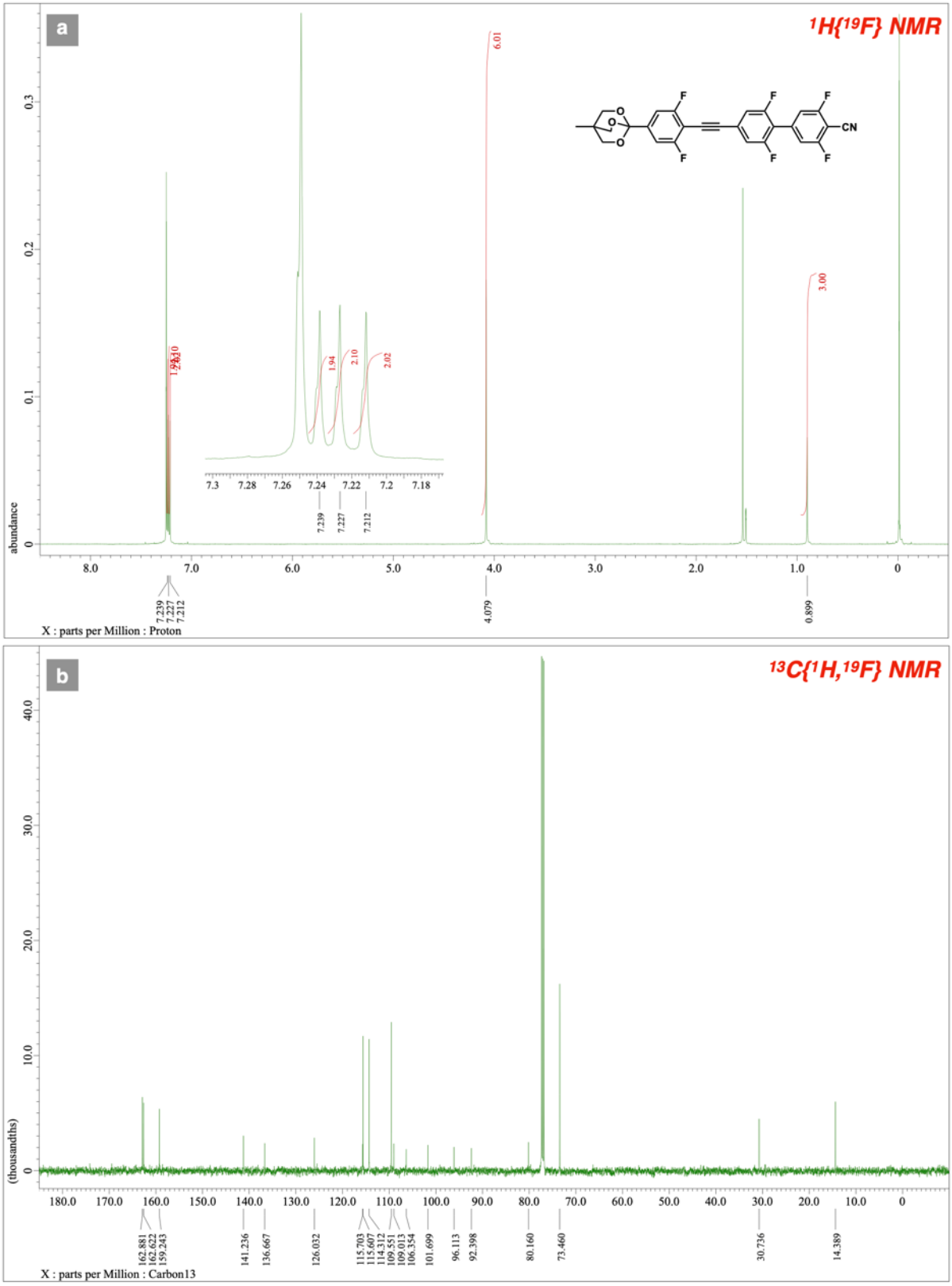

$^{19}F\{^{1}H\}$ NMR (a) and QTOF-HRMS (b) spectra of compound ***22a***

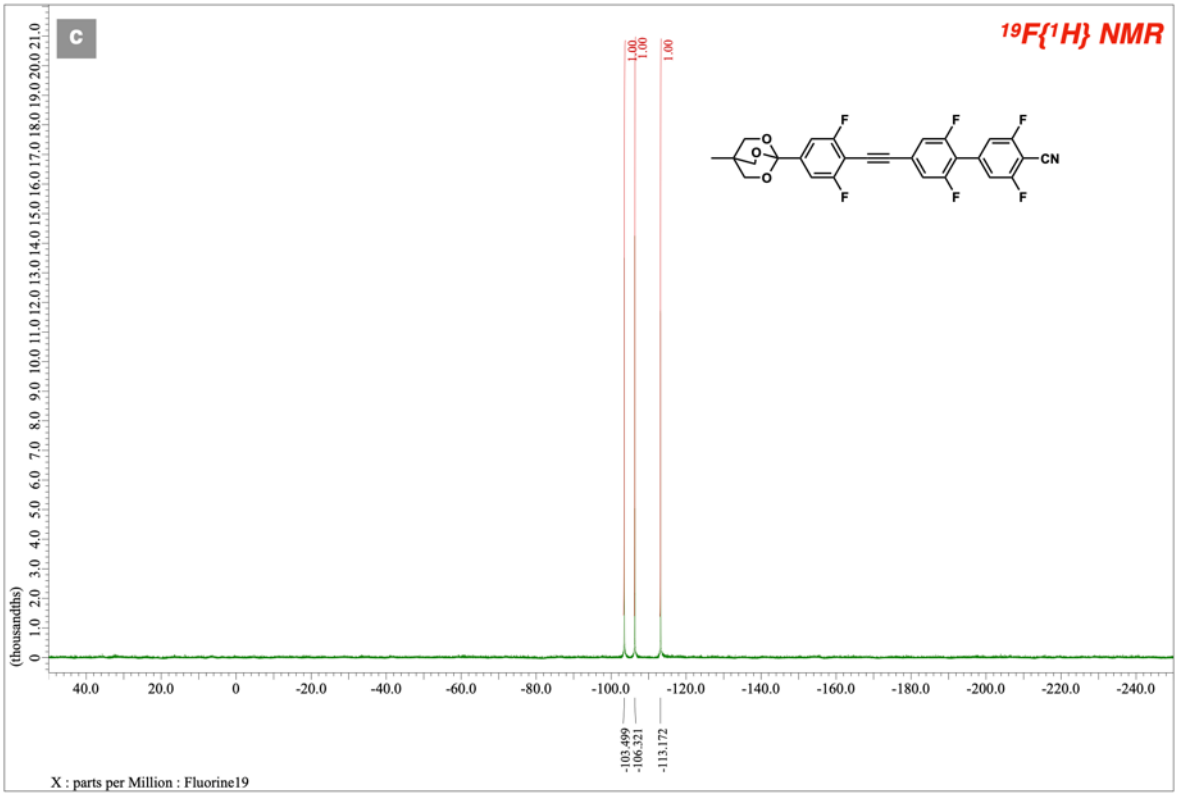

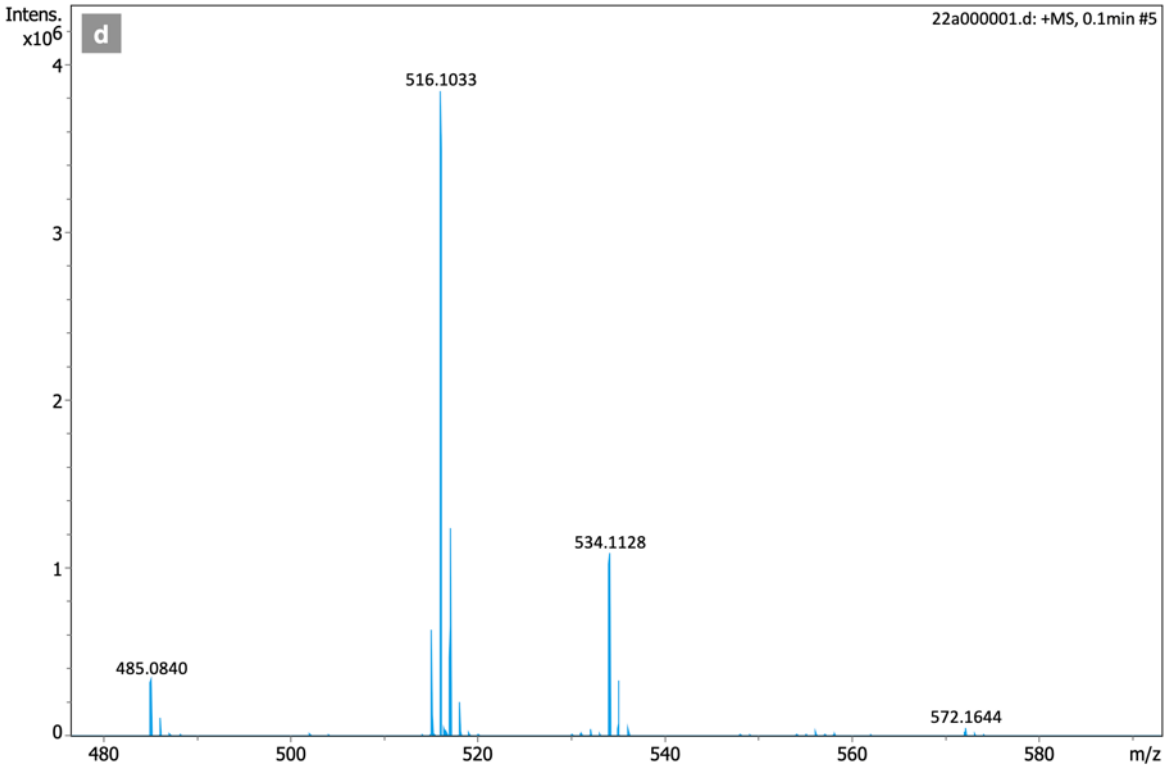

$^{1}H\{^{19}F\}$ NMR (a) and $^{13}C\{^{1}H,^{19}F\}$ NMR (b) spectra of compound ***22b***

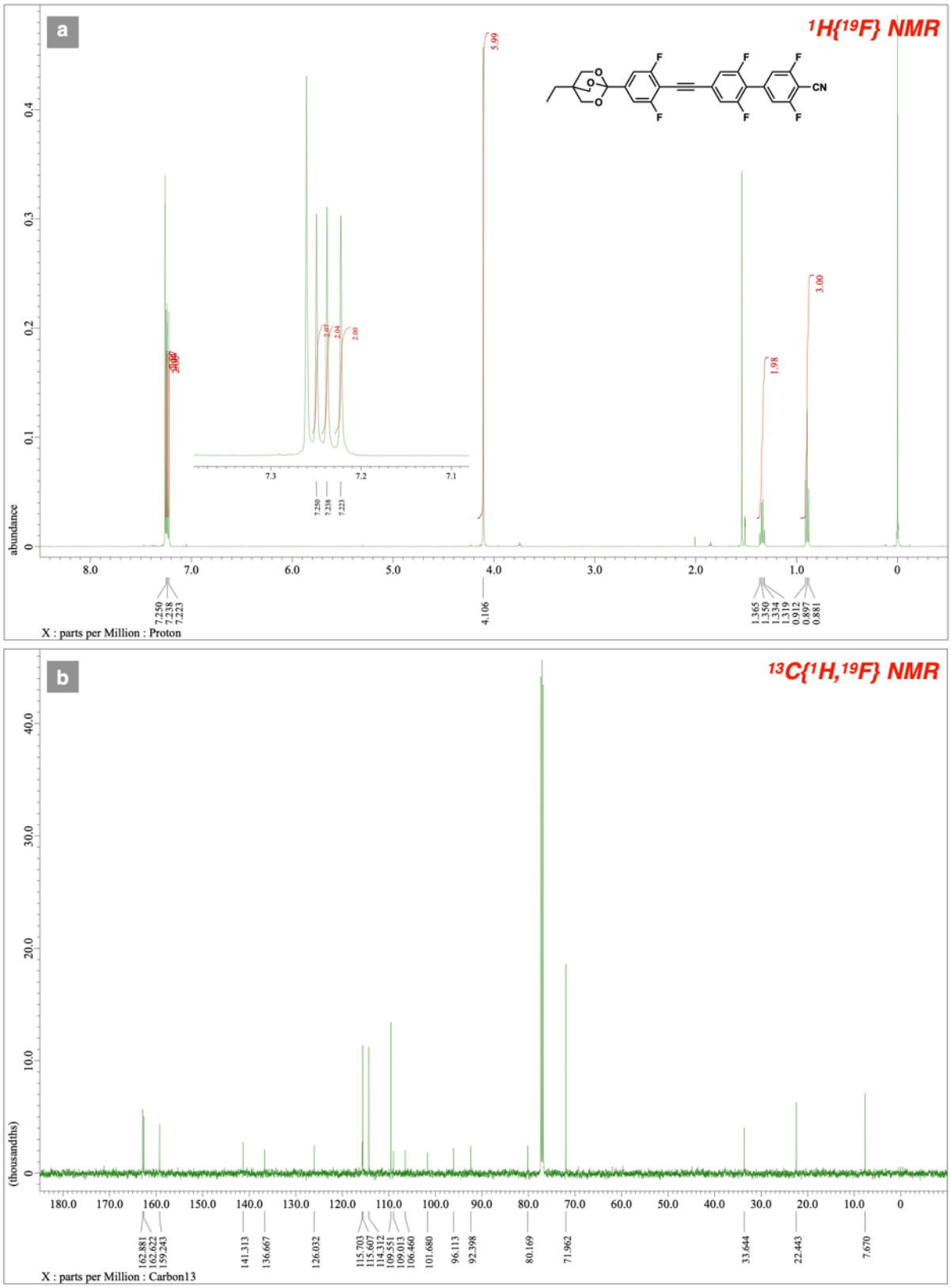

$^{19}F\{^{1}H\}$ NMR (a) and QTOF-HRMS (b) spectra of compound ***22b***